ISSN 1063-7796, Physics of Particles and Nuclei, 2020, Vol. 51, No. 1, pp. 1–106. © Pleiades Publishing, Ltd., 2020.
Russian Text © The Author(s), 2020, published in Fizika Elementarnykh Chastits i Atomnogo Yadra, 2020, Vol. 51, No. 1.

Quantum Field Theory of Neutrino Oscillations

D. V. Naumov[a], * and V. A. Naumov[a], **

[a] *Joint Institute for Nuclear Research, Dubna, Moscow oblast, 141980 Russia*

**e-mail: dnaumov@jinr.ru*

***e-mail: vnaumov@theor.jinr.ru*

Received July 10, 2019; revised August 14, 2019; accepted August 14, 2019

Abstract—The theory of neutrino oscillations in the framework of the quantum field perturbative theory with relativistic wave packets as asymptotically free in- and out-states is expounded. A covariant wave packet formalism is developed. This formalism is used to calculate the probability of the interaction of wave packets scattered off each other with a nonzero impact parameter. A geometric suppression of the probability of interaction of wave packets for noncollinear collisions is calculated. Feynman rules for the scattering of wave packets are formulated, and a diagram of a sufficiently general form with macroscopically spaced vertices (a "source" and a "detector") is calculated. Charged leptons ($\ell^{\pm}_{\alpha}$ in the source and $\ell^{\mp}_{\beta}$ in the detector) are produced in the space-time regions around these vertices. A neutrino is regarded as a virtual particle (propagator) connecting the macrodiagram vertices. An appropriate method of macroscopic averaging is developed and used to derive a formula for the number of events corresponding to the macroscopic Feynman diagram. The standard quantum-mechanical probability of flavor transitions is generalized by considering the longitudinal dispersion of an effective neutrino wave packet and finite time intervals of activity of the "source" and the "detector". A number of novel and potentially observable effects in neutrino oscillations is predicted.

DOI: 10.1134/S1063779620010050

CONTENTS

1. INTRODUCTION

A neutrino is a light fermion with zero electric charge that participates in weak interactions. This particle was proposed by Pauli in 1930 as a means to preserve the energy conservation law and explain the "incorrect" statistics in nuclear β-decays and was used shortly after by Fermi in the development of the first quantitative theory of β-decay [1]. Fermi had rightly assumed that a neutrino is produced in the decay of a nucleus together with a beta particle[1], while Pauli believed neutrinos to be constituents of nuclei. Three

[1] Pauli's famous letter was published in [2] with comments and insightful historical remarks. The preliminary report of Fermi was published in 1933 [3].

neutrino flavors $\nu_\alpha = (\nu_e, \nu_\mu, \nu_\tau)$ have been discovered since then. They are associated with the corresponding charged leptons $\ell_\alpha = (e, \mu, \tau)$: the production of lepton ℓ_α^+ in weak interactions is always accompanied by the production of neutrino ν_α of the same flavor α. This may be formulated as the law of conservation of lepton number L_α.

By analogy with oscillations of neutral kaons, $K^0 \leftrightarrow \bar{K}^0$, Bruno Pontecorvo hypothesized the existence of neutrino flavor oscillations [4, 5] in the late 1950s. The validity of this hypothesis was verified in experiments with solar [6–8], atmospheric [9, 10], accelerator [10, 11], and reactor [12–15] neutrinos and antineutrinos. Neutrino oscillations (or flavor transitions) are a quantum effect of quasi-periodic variations of neutrino flavor $\nu_\alpha \to \nu_\beta$ in time. This effect, which violates the conservation of lepton numbers, is attributable to the nonequivalence of eigenstates of neutrinos with a definite flavor $|\nu_\alpha\rangle$ and states with definite masses $|\nu_k\rangle$, $(k = 1, 2, 3)$, the nonzero difference in masses of the latter, and the hypothesis that a neutrino takes part in weak interactions as a coherent superposition of the mass eigenstates

$$|\nu_\alpha\rangle = \sum_{k=1}^{3} V_{\alpha k}^* |\nu_k\rangle. \quad (1)$$

Here, $V_{\alpha k}$ is an element of a unitary vacuum mixing matrix, which is also called the Pontecorvo–Maki–Nakagawa–Sakata (PMNS) matrix [5, 16]. The temporal evolution of state (1) leads to an oscillatory dependence of the probability of detection of a neutrino with a certain flavor β in time t after the production of state $|\nu_\alpha\rangle$. The simplest quantum-mechanical theory of oscillations based on the plane-wave approximation was formulated by Gribov and Pontecorvo [17]. This theory had a great influence on research in neutrino physics and was developed further in subsequent years by other physicists (see, e.g., [18–20] and reviews [21–31], where the advances in experimental studies and phenomenology of neutrino oscillations in vacuum and matter as well as various mechanisms of neutrino mass generation and mixing, which are not addressed in the present paper, were discussed in detail).

Although the plane-wave approximation is very efficient in characterizing the results of experiments, it is not self-consistent and leads to a number of paradoxes, which were discussed widely in literature. For those interested, we have compiled a list of studies [32–65] directly related to the subject of the present paper. Although this list is extensive, it is not exhaustive by any means. A systematic formulation of the theory itself, critical comments, generalizations, and references for further study are given, e.g., in [66].

The need to describe neutrino oscillations in a model with neutrino wave packets was noted in [67–72] (see also [63, 66, 73–79]). A wave packet (WP) is a coherent superposition of waves with momenta distributed about the most probable value with a certain "width" (dispersion). A WP is localized in the momentum and configuration spaces. The theory of neutrino oscillations in a model with WPs provides an opportunity to resolve some paradoxes of the plane-wave approximation and predicts several novel phenomena. Following the publication of pioneering studies [67–72], two distinct paths towards the development of this theory of oscillations have emerged. In the first approach, the formalism was developed within relativistic quantum mechanics, and the neutrino wave function was postulated (see, e.g., [45, 66, 80]). In the second approach, the theoretical apparatus of quantum field theory (QFT) with wave packets for all particles involved in the processes of production and detection of neutrinos (except for neutrinos themselves, which are regarded as virtual particles) was used [32–48, 51–58, 60–65]. The form of the neutrino wave packet follows from the formalism in this paradigm. Both approaches predicted novel potentially observable effects, which were related to the loss of coherence. The interest in decoherence in neutrino oscillations has been on the rise lately, since several recent (and future) experiments are potentially sensitive to these effects [81–95].

The aim of this work is to examine the theory of vacuum neutrino oscillations thoroughly and systematically within the QFT perturbative approach with relativistic WPs serving as external in- and out-states. This theory has been outlined earlier in [57, 58, 96]. We start with a brief discussion of the standard quantum-mechanical theory of neutrino oscillations in the plane-wave approximation (see Section 2). As was already noted, the quantum-mechanical theory of neutrino oscillations in the plane-wave approximation is incomplete and contradictory. The underlying factors are discussed in Section 2.3.

The model with a wave packet (see Section 3) solves some of the problems inherent in the theory with plane waves. This model introduces WP spreading and the procedure of macroscopic averaging, which allows one to derive a correct formula for the oscillation probability.

The focus of the paper is on the construction of the theory of neutrino oscillations within QFT. Conceptually, the mechanism of neutrino oscillations within QFT is the result of interference of diagrams with mass eigenfields ν_i $(i = 1, 2, 3)$ in the intermediate states. Let us highlight the key stages and features of our approach.

(1) The problem is formulated as follows. Two spatial regions with a macroscopically large interval between them are considered. Charged leptons (ℓ_α^+ and ℓ_β^-) are produced in these regions (the "source"

and the "detector," respectively). The source and the detector remain active within certain time intervals. This corresponds to the most general setup of an oscillation experiment. One needs to calculate the number of such events ($N_{\alpha\beta}$) within QFT.

(2) Naturally, number $N_{\alpha\beta}$ of events in the detector is independent of the reference frame (i.e., is a relativistic invariant). Therefore, quantum states corresponding to external particles should transform covariantly under Lorentz transformations. This implies that a WP corresponding to any external particle is required to be covariant. The theory of a covariant WP is constructed in Section 4; its properties are also examined in detail. Section 4.5 is focused on multipacket states for fermions and bosons. In particular, it is demonstrated that if WPs corresponding to identical particles are separated by sufficiently large space-time intervals, the system lacks the Bose–Einstein condensation for bosons and the Pauli Exclusion Principle is not valid for fermions. This intuitively obvious result is impossible to infer in the model with plane waves.

(3) The model of a relativistic Gaussian WP (RGP) is developed as a working model for further calculations in Section 5. It is demonstrated that a traditional Gaussian WP of the form $\propto e^{-(\mathbf{k}-\mathbf{p})^2/4\sigma_p^2}$ is a nonrelativistic approximation of an RGP. This is the key result presented in Section 5.

(4) The above formalism is applied in solving the problem of scattering of two WPs in Section 6. The general case of WP scattering with a nonzero impact parameter is considered. It is demonstrated that the number of interactions of two WPs may be presented as a product of three factors: the cross section (with the dimension of area), the luminosity (with the dimension of reciprocal area), and a dimensionless factor that suppresses interactions at large impact parameters. This result is intuitively expected and illustrates the predictive power of the theory.

(5) A "macroscopic" diagram with vertices (the neutrino source and the detector) separated by a macroscopic distance is examined in Sections 7 and 8. The initial and final particles are characterized by the constructed covariant WPs; and neutrinos are described by a propagator. Charged leptons ℓ^+_α and ℓ^-_β are produced in the source and the detector, respectively. The Feynman rules for such diagrams are formulated, and the amplitude of the process of interest is calculated. No form of the virtual neutrino WP is assumed; a causal fermion propagator, which emerges automatically in QFT, is used instead. It is demonstrated below that the asymptotic behavior of the propagator at large distances between vertices of the diagram reproduces the properties of the wave function of a free neutrino; in other words, a free neutrino at large distances from the source behaves, in a first approximation, as a free wave packet of a particle on the mass shell.

(6) Microscopic probability $|\mathfrak{A}_{\alpha\beta}|^2$ is calculated in Section 9. Once each external (in or out) WP is characterized by mean coordinate $\mathbf{x}_\kappa$ at time x^0_κ, mean 4-momentum p_κ, and momentum dispersion σ_κ, $|\mathfrak{A}_{\alpha\beta}|^2$ depends parametrically on the set of all these parameters $\{x_\kappa, p_\kappa, \sigma_\kappa\}$.

Macroscopic averaging over $\{\mathbf{x}_\kappa, \mathbf{p}_\kappa\}$ is performed in Section 10. This provides an opportunity to determine number $N_{\alpha\beta}$ of events with ℓ^+_α in the source and ℓ^-_β in the detector. The terms "source" and "detector" now acquire their meaning as space-time regions around the so-called impact points X_s and X_d defined by parameters $\{x_\kappa, p_\kappa, \sigma_\kappa\}$ at the vertices, where leptons ℓ^+_α and ℓ^-_β are produced. The conditions under which $N_{\alpha\beta}$ may be presented as an integral over the source and detector volumes of the product of three factors $\Phi_\nu(E_\nu, L)\times\mathcal{P}_{\alpha\beta}(E_\nu, L; \mathfrak{D})\times\sigma(E_\nu)$ are examined. Here, $\Phi_\nu(E_\nu, L)$ is the flux of massless neutrinos from the source to the detector (it is demonstrated that it behaves as $1/L^2$); $\sigma(E_\nu)$ is the cross section of scattering of a massless neutrino in the detector; and $\mathcal{P}_{\alpha\beta}$, which depends on flavor indices α and β, the neutrino energy, the effective distance between the source and the detector, and on neutrino energy-momentum dispersion $\mathfrak{D}$, is a generalization of the quantum-mechanical probability of neutrino oscillations. The obtained "probability" of oscillations is then examined in different experimental settings. Under certain conditions, the obtained formula for the oscillation probability is numerically close to that from the plane-wave model. However, the new formula predicts a number of novel effects such as the loss of coherence, the dependence on the temporal windows of activity of the source and the detector, and many others.

The decoherence function, which suppresses interference contributions to the oscillation probability, is discussed in detail in Section 11.

(7) The main results presented in this article are discussed in Section 12, and conclusions are drawn in Section 13.

For convenience, the details of cumbersome calculations are given in the appendices. A natural system of units, where $\hbar = c = 1$, is used. Abbreviations of the form of $\int dx\ldots$ instead of $\int d^4x\ldots$ in Minkowski space integrals (the Feynman metric is used throughout the paper) and $\int d\mathbf{x}\ldots$ instead of $\int d^3x\ldots$ in three-dimensional Euclidean space integrals are used in those cases where this does not lead to misunderstanding. Although the number of active flavors is not essential to our analysis, we assume that this number is three in the particular examples considered below.

2. QUANTUM-MECHANICAL THEORY OF NEUTRINO OSCILLATIONS IN THE PLANE-WAVE APPROXIMATION

2.1. Quantum States

Let us first recall the key concepts of quantum mechanics essential to the quantum-mechanical theory of neutrino oscillations and introduce the definitions that will be used in subsequent analysis. We start with the one-dimensional case and a free theory.

A quantum system in the Hilbert space is characterized by abstract time-dependent state $|\psi(t)\rangle$. Its evolution in time is given by the Schrödinger equation

$$i\frac{\partial|\psi(t)\rangle}{\partial t} = \hat{H}|\psi(t)\rangle, \tag{2}$$

where $\hat{H} = \hat{H}_0$ is the Hamiltonian. Let $|p\rangle$ be an eigenstate of the free Hamiltonian $\hat{H}_0$ with eigenvalue E_p:

$$\hat{H}_0|p\rangle = E_p|p\rangle. \tag{3}$$

Let $|x\rangle$ be an eigenstate of coordinate operator $\hat{X}$ with eigenvalue x:

$$\hat{X}|x\rangle = x|x\rangle. \tag{4}$$

The norms of these states are as follows: $\langle q|p\rangle = 2\pi\delta(p-q)$, $\langle y|x\rangle = \delta(x-y)$, where $\delta(x-y)$ is the common Dirac delta function. Quantum state $|\psi(t)\rangle$ may be characterized either by coordinate distribution $\psi_x(t,x)$ in the coordinate representation or by momentum distribution $\psi_p(t,p)$ in the momentum representation for a free or a full Hamiltonian:

$$|\psi(t)\rangle = \int dx\psi_x(t,x)|x\rangle = \int\frac{dp}{2\pi}\psi_p(t;p)|p\rangle. \tag{5}$$

States $|x\rangle$ and $|p\rangle$ are related in the following way:

$$|x\rangle = \int\frac{dp}{2\pi}e^{-ipx}|p\rangle, \quad |p\rangle = \int dxe^{+ipx}|x\rangle. \tag{6}$$

In view of (5) and (6), it is evident that

$$\begin{aligned}\psi_x(t,x) &= \int\frac{dp}{2\pi}e^{ipx}\psi_p(t,p),\\ \psi_p(t,p) &= \int dxe^{-ipx}\psi_x(t,x).\end{aligned} \tag{7}$$

The formal solution of (2)

$$|\psi(t)\rangle = e^{-i\hat{H}t}|\psi(0)\rangle \tag{8}$$

by using representation (5) yields:

$$\begin{aligned}|\psi(t)\rangle &= \int\frac{dp}{2\pi}e^{-iE_pt}\psi_p(0,p)|0,p\rangle\\ &= \int dx\psi_x(0,x)|t;x\rangle,\end{aligned} \tag{9}$$

where

$$|t;x\rangle = e^{-i\hat{H}_0t}|x\rangle. \tag{10}$$

Expressions (6) and (7) were used to derive (9):

$$\begin{aligned}\int\frac{dp}{2\pi}e^{-iE_pt}\psi_p(0,p)|p\rangle &= e^{-i\hat{H}_0t}\int\frac{dp}{2\pi}\psi_p(0,p)|p\rangle\\ &= e^{-i\hat{H}_0t}\int\frac{dpdx}{2\pi}e^{+ipx}\psi_p(0,p)|x\rangle\\ &= \int dx\psi_x(0,x)|t,x\rangle.\end{aligned} \tag{11}$$

If $\psi_p(0,p) = 2\pi\delta(p-k)$, where k is the momentum that can be considered as a parameter of function $\psi_p(0,p)$, solution (9) takes the well-known form

$$|\psi(t)\rangle = e^{-iE_kt}|k\rangle = \int dxe^{-iE_kt+ikx}|x\rangle, \tag{12}$$

that is, the temporal evolution of a state with a strictly defined momentum is characterized by factor e^{-iE_kt} multiplied by a state with a definite momentum $|k\rangle$ in the momentum representation or by a superposition of states with a definite coordinate $|x\rangle$ with weight factor e^{-iE_kt+ikx}. This solution is known as a plane wave.

2.2. Plane-Wave Theory of Neutrino Oscillations in Vacuum

Let us define a flavor state $|\nu_\alpha\rangle$ as a coherent superposition of mass states $|\nu_i(p)\rangle$:

$$|\nu_\alpha\rangle = \sum_i V^*_{\alpha i}|\nu_i(p)\rangle, \tag{13}$$

where each mass state is an eigenstate of a free Hamiltonian with eigenvalue p. The evolution of state (13) is given by

$$|\nu_\alpha(t)\rangle = e^{-i\hat{H}t}|\nu_\alpha\rangle = \sum_i V^*_{\alpha i}e^{-iE_it}|\nu_i(p)\rangle, \tag{14}$$

where $E_i = \sqrt{p^2+m_i^2}$. Let us assume that a coherent superposition of states with strictly defined momenta (13) was produced in a certain weak process. The projection of this state onto a state with arbitrary flavor $|\nu_\beta\rangle$ is not reduced to $\delta_{\alpha\beta}$:

$$\langle\nu_\beta|\nu_\alpha(t)\rangle = \sum_i V^*_{\alpha i}V_{\beta i}e^{-iE_it}. \tag{15}$$

The corresponding probability of flavor transition $\nu_\alpha \to \nu_\beta$ is

$$P_{\alpha\beta}(t) = \left|\langle\nu_\beta|\nu_\alpha(t)\rangle\right|^2 = \sum_{ij} V^*_{\alpha i}V_{\alpha j}V_{\beta i}V^*_{\beta j}e^{-i(E_i-E_j)t}. \tag{16}$$

Using ultrarelativistic approximations $E_i - E_j \simeq (m_i^2 - m_j^2)/2p$ and putting $t = L$, where L is

the distance travelled by a neutrino in the time t, we obtain the well-known formula

$$P_{\alpha\beta}(L) = \sum_{ij} V^*_{\alpha i} V_{\alpha j} V_{\beta i} V^*_{\beta j} e^{-i\Delta m^2_{ij} L/2p} = \sum_{ij} V^*_{\alpha i} V_{\alpha j} V_{\beta i} V^*_{\beta j} e^{-i2\pi L/L^{\rm osc}_{ij}}, \quad (17)$$

where

$$\Delta m^2_{ij} = m^2_i - m^2_j \ \text{ and } \ L^{\rm osc}_{ij} = 2\pi \frac{2p}{\Delta m^2_{ij}}.$$

The expanded form of (17) is

$$P_{\alpha\beta}(L) = \sum_j |V_{\alpha j}|^2 |V_{\beta j}|^2 + 2\sum_{j>i} \left[{\rm Re}\left(V^*_{\alpha j} V_{\beta j} V_{\alpha i} V^*_{\beta i}\right) \cos\left(\frac{2\pi L}{L^{\rm osc}_{ji}}\right) + {\rm Im}\left(V^*_{\alpha j} V_{\beta j} V_{\alpha i} V^*_{\beta i}\right) \sin\left(\frac{2\pi L}{L^{\rm osc}_{ji}}\right) \right]. \quad (18)$$

In the two-neutrino case, probability $P^{2\nu}_{\alpha\beta}(L)$ is a periodic function of distance L with a period equal to length $L^{\rm osc}_{12}$. The distance dependence $P^{2\nu}_{\alpha\beta}(L + L^{\rm osc}_{12}) = P^{2\nu}_{\alpha\beta}(L)$ is what justifies the term "neutrino oscillations." In the three-neutrino case, this term is not entirely correct, since oscillation probabilities may have no periodicity (except special cases with peculiar relations between the oscillation lengths $L^{\rm osc}_{12}$, $L^{\rm osc}_{23}$, $L^{\rm osc}_{13}$). In the general case, it would be better to call neutrino oscillations as quasi-periodic.

The unitary property of the vacuum mixing matrix gives rise to the expected probability conservation law:

$$\sum_\beta P_{\alpha\beta} = \sum_\alpha P_{\alpha\beta} = 1. \quad (19)$$

Note that although the energy of the state with definite flavor $|\nu_\alpha(t)\rangle$ is not defined, its mean energy

$$\langle E_\alpha(t)\rangle = \langle \nu_\alpha(t)|\hat{H}|\nu_\alpha(t)\rangle \quad (20)$$

is a well-defined and conserved quantity. Indeed,

$$\langle E_\alpha(t)\rangle = \sum_{ij} V_{\alpha i} V^*_{\alpha j} \langle \nu_i(p)|\hat{H}|\nu_j(p)\rangle = \sum_{ij} V_{\alpha i} V^*_{\alpha j} \langle \nu_i(p)|E_i|\nu_j(p)\rangle = \sum_i |V_{\alpha i}|^2 E_i \simeq p + \sum_i |V_{\alpha i}|^2 \frac{m^2_i}{2p},$$

$$\sum_\alpha \langle E_\alpha\rangle = \sum_i E_i \simeq 3\left(p + \sum_i \frac{m^2_i}{2p}\right).$$

The mean energy of an arbitrary entangled state characterized by a certain density matrix $\hat{\rho}(t)$ is also conserved. Indeed, let the initial state have the form

$$\hat{\rho}(0) = \sum_\alpha w_\alpha |\nu_\alpha(0)\rangle\langle\nu_\alpha(0)|, \quad (21)$$

where w_α is the probability of finding pure state $|\nu_\alpha(0)\rangle$ in this (mixed) state ($\sum_\alpha w_\alpha = 1$). The mean energy of the mixed state $\hat{\rho}(t)$ at arbitrary time instant t is then written as

$$\langle E(t)\rangle = {\rm Tr}\left(\hat{H}\hat{\rho}(t)\right) = {\rm Tr}\left(\hat{H} e^{-i\hat{H}t}\hat{\rho}(0) e^{i\hat{H}t}\right) = \sum_\alpha w_\alpha \sum_{ij} V^*_{\alpha i} V_{\alpha j} e^{-i(E_i - E_j)t} E_i {\rm Tr}|\nu_i(p)\rangle\langle\nu_j(p)| = \sum_\alpha w_\alpha \sum_i |V_{\alpha i}|^2 E_i = \sum_\alpha w_\alpha \langle E_\alpha(t)\rangle.$$

Naturally, $\langle E(t)\rangle = \langle E_\alpha(t)\rangle$ in the special case of a pure initial state $|\nu_\alpha(0)\rangle$. If all pure states in initial mixture (21) were equally probable, the mean energy

$$\langle E(t)\rangle = \frac{1}{3}\sum_\alpha \langle E_\alpha(t)\rangle = \frac{1}{3}\sum_i \langle E_i\rangle \simeq p + \sum_i \frac{m^2_i}{6p},$$

is independent of the mixing parameters.

2.3. Incompleteness and Paradoxes of the Plane-Wave Approximation: Review of the Proposed Solutions

The following crucial assumptions and approximations were used in derivation of the formula characterizing the probability of oscillations:

(i) A coherent superposition of states with definite masses m_i ($i = 1, 2, 3$), which is often called a state with definite flavor $|\nu_\alpha\rangle = \sum_i V^*_{\alpha i}|\nu_i\rangle$, where $V_{\alpha i}$ are elements of the unitary vacuum mixing matrix, interacts in the processes of neutrino production and detection.

(ii) States $|\nu_i\rangle$ have definite momenta $\mathbf{p}_i$.

(iii) All momenta $\mathbf{p}_i$ are the same ($\mathbf{p}_i = \mathbf{p}$).

(iv) Neutrinos are ultrarelativistic ($\mathbf{p}^2 \gg \max(m^2_i)$).

(v) The neutrino propagation time can be replaced by the distance travelled ($t = L$).

Let us scrutinize all these presumptions. At first glance, assumption (i), which states that a neutrino interacts as state $|\nu_\alpha\rangle$ in the production and detection processes, appears to be fairly natural. Moreover, in literature one can often find a mystic statement that neutrinos interact with matter as flavor eigenstates, $|\nu_\alpha\rangle = \sum_i V^*_{\alpha i}|\nu_i\rangle$, but between the interaction acts they evolve in space as mass eigenstates. Note, however, that the SM Lagrangian of interactions of massive neutrinos with charged leptons l_α ($\alpha = e, \mu, \tau$) can be written either in therms of fields $\nu_i(x)$ and $\ell_\alpha(x)$ or $\nu_\alpha(x)$ and $\ell_i(x) = \sum_\alpha V^*_{\alpha i}\ell_\alpha(x)$, since the charged lepton current $j^\mu_\ell(x) = \bar{\nu}_\alpha(x) O^\mu \ell_\alpha(x)$ can be represented in two fully equivalent forms: $\sum_{\alpha i} V^*_{\alpha i}\bar{\nu}_i(x) O^\mu \ell_\alpha(x)$ and $\sum_{\alpha i} V^*_{\alpha i}\bar{\nu}_\alpha(x) O^\mu \ell_i(x)$. It is then instructive to ponder

the question whether it is possible for a coherent superposition of states $|\ell_i\rangle = \sum_\alpha V_{\alpha i}^* |\ell_\alpha\rangle$ to be produced and interact and whether oscillations of charged leptons (similar to neutrino oscillations) are observable. Since there is no experimental evidence of such oscillations, one has to admit that charged leptons are produced (and interact) incoherently. Therefore, assumption (i) is not valid for charged leptons and, in the general case, requires a quantitative justification.

Let us now turn to assumption (ii) and discuss the $\pi^+ \to \mu^+\nu_\mu$ decay as an example. Since the state $|\nu_\mu\rangle$ does not have definite energy, the energy of at least one of the two final-state particles is also undefined. Since the pion and muon have definite masses, the momentum of one of them (or both particles) is also undefined. Therefore, the momentum of the final-state neutrino should be undefined, but this contradicts assumption (ii). Another argument against this assumption consists in the fact that the spatial coordinates of the regions of neutrino production and absorption (the source and the detector) and, consequently, the distance between these regions, involved in the formula for the flavor transition probability, are completely undefined if the momentum is completely defined.

It is worth noting here that an unstable particle cannot have definite 4-momentum only due to the fact that the spatial delocalization of such a particle is limited by its decay path length. In other words, the indeterminacy of the 4-momentum of a particle cannot be smaller than its decay width. Therefore, the momenta of neutrinos produced in particle decays should also be undefined; i.e., assumption (ii) is a mere approximation, and a more general theory is needed to verify its validity.

Assumption (iii), as well as the similar assumption of equality of energies found in certain studies, is at odds with relativistic invariance. Let us assume that (iii) holds true in laboratory frame K. Both energies E_i' and momenta $\mathbf{p}_i'$ are then not equal in frame K' moving with velocity $\mathbf{v}$ relative to K, since it follows from the Lorentz transformations that

$$\begin{aligned} E_i' - E_j' &= \Gamma_\mathbf{v}(E_i - E_j) \neq 0, \\ \mathbf{p}_i' - \mathbf{p}_j' &= \Gamma_\mathbf{v}(E_j - E_i)\mathbf{v} \neq 0, \quad \Gamma_\mathbf{v} = \frac{1}{\sqrt{1-\mathbf{v}^2}}. \end{aligned} \tag{22}$$

It is easy to see that $|\mathbf{p}_i' - \mathbf{p}_j'| \geq |E_i - E_j| \approx |m_i^2 - m_j^2|/(2|\mathbf{p}|)$ at $|\mathbf{v}| \geq 1/\sqrt{2}$. If the velocity of frame K' satisfies condition $\Gamma_\mathbf{v} \ll \min(E_i'/m_i)$, neutrinos remain ultrarelativistic in K'; i.e., condition (iv) is satisfied, but condition (iii) is violated. Naturally, this violation is infinitesimal if velocity $\mathbf{v}$ is low (more precisely, if $|\mathbf{vp}| \ll |\mathbf{p}|$). In the general case, regarding the Lorentz transformation as an active one, we conclude that condition (iii) cannot be simultaneously satisfied for two neutrino beams emitted by identical sources moving with different velocities.

Condition (iv) states that (a) the masses of known neutrinos are infinitesimal (much below 1–2 eV) and (b) modern current detection techniques are not sensitive to neutrinos with energies below ~100 keV; thus, only ultrarelativistic neutrinos are probed in experiments. However, this condition is not satisfied for relic neutrinos.

Finally, let us turn to condition (v). This condition is not equivalent to and does not follow from (iv), which allows for expansion $E_i \simeq p + m_i^2/2p + \ldots$, since the second expansion term (and, in certain studies, the third) is preserved in (iv) together with the first term $E = p$. By contrast, condition (v) utilizes only the first expansion term $t = L$. The elementary expression reproducing the exact relation between time t and the distances travelled by states $|\nu_k\rangle$ and $|\nu_j\rangle$ is

$$t = \frac{L_k}{v_k} = \frac{L_j}{v_j},$$

which allows one to rewrite oscillation phase $(E_k - E_j)t$ in the following form:

$$\begin{aligned} (E_k - E_j)t &= \frac{E_k L_k}{v_k} - \frac{E_j L_j}{v_j} \\ &= \frac{E_k^2 L_k}{p} - \frac{E_j^2 L_j}{p} \approx \frac{(E_k^2 - E_j^2)L}{p} = \frac{\Delta m_{kj}^2}{p}, \end{aligned}$$

where approximation $L_k \approx L_j \approx L$ was used to obtain the second-to-last expression. The resulting oscillation phase is two times larger compared to (17). This disconcerting fact is the result of voluntary treatment of orders of smallness of $\frac{\Delta m_{kj}^2}{p^2}$, which is inherent in both the above "alternative derivation" and condition (v) itself. One may ask oneself, why the difference between the times of neutrino detection and production is equated to distance L? The time of production of the neutrino is unknown in the majority of experiments; therefore, one should integrate over it. Having performed this integration, we find that all interference terms vanish, since $\int dt \exp[-i(E_k - E_j)t] \propto \delta(E_k - E_j)$; i.e.,

$$\langle P_{\alpha\beta}(t)\rangle_t \propto \sum_k |V_{\alpha k}|^2 |V_{\beta k}|^2. \tag{23}$$

The theory of neutrino oscillations is based on assumptions (i)–(v). Only condition (iv) is satisfied in current experiments (although it is violated for relic

neutrinos). Conditions (ii) and (iii) are evidently nonphysical. Condition (i) requires a quantitative justification. Condition (v) is unjustified. Small corrections to it induce significant changes in the resultant formula for the probability of neutrino oscillations.

3. QUANTUM-MECHANICAL THEORY OF NEUTRINO OSCILLATIONS IN THE MODEL WITH A WAVE PACKET

3.1. General Properties of a Wave Packet

Let us consider a WP at $t = 0$:

$$|\psi(0)| = \int \frac{d\mathbf{p}}{(2\pi)^3}\psi_{\mathrm{p}}(\mathbf{p})|\mathbf{p}\rangle, \tag{24}$$

where $\langle\mathbf{q}|\mathbf{p}\rangle = (2\pi)^3\delta^3(\mathbf{q}-\mathbf{p})$. The evolution of state in (24) with time is given by

$$|\psi(t)\rangle = e^{-i\hat{H}_0 t}|\psi(0)\rangle = \int \frac{d\mathbf{p}}{(2\pi)^3}e^{-iE_{\mathbf{p}}t}\psi_{\mathrm{p}}(\mathbf{p})|\mathbf{p}\rangle, \tag{25}$$

which corresponds to the following wave function in the coordinate space:

$$\psi_{\mathrm{x}}(t,\mathbf{x}) = \int \frac{d\mathbf{p}}{(2\pi)^3}e^{-iE_{\mathbf{p}}t+i\mathbf{p}\mathbf{x}}\psi_{\mathrm{p}}(\mathbf{p}). \tag{26}$$

Let us normalize the state in (25) to unity:

$$\langle\psi(t)|\psi(t)\rangle = \int \frac{d\mathbf{p}}{(2\pi)^3}\left|\psi_{\mathrm{p}}(\mathbf{p})\right|^2 = 1. \tag{27}$$

The mean energy, momentum, and velocity of a packet are defined as follows:

$$\begin{aligned}\langle E\rangle &= \langle\psi(t)|\hat{H}_0|\psi(t)\rangle = \int \frac{d\mathbf{p}}{(2\pi)^3}\left|\psi_{\mathrm{p}}(\mathbf{p})\right|^2 E_{\mathbf{p}},\\ \langle\mathbf{P}\rangle &= \langle\psi(t)|\hat{\mathbf{P}}|\psi(t)\rangle = \int \frac{d\mathbf{p}}{(2\pi)^3}\left|\psi_{\mathrm{p}}(\mathbf{p})\right|^2 \mathbf{p},\\ \langle\mathbf{v}\rangle &= \langle\psi(t)|\hat{\mathbf{V}}|\psi(t)\rangle = \int \frac{d\mathbf{p}}{(2\pi)^3}\left|\psi_{\mathrm{p}}(\mathbf{p})\right|^2 \mathbf{v}_{\mathbf{p}},\end{aligned} \tag{28}$$

where the one-particle velocity operator is defined using

$$\hat{\mathbf{V}} = \int \frac{d\mathbf{p}}{(2\pi)^3}\mathbf{v}_{\mathbf{p}}|\mathbf{p}\rangle\langle\mathbf{p}|. \tag{29}$$

A quantum WP is similar in some respects to a classical object; in particular, its energy and momentum are conserved, and it moves (on average) along a classical trajectory. Let us establish the latter assertion by performing explicit calculations.

3.2. Mean Trajectory of a Wave Packet

By definition, the mean WP coordinate is

$$\langle\mathbf{x}(t)\rangle = \langle\psi(t)|\hat{\mathbf{X}}|\psi(t)\rangle. \tag{30}$$

Expressing $|\psi(t)\rangle$ in accordance with (25) and making use of relations $|\mathbf{p}\rangle = \int d\mathbf{x}e^{+i\mathbf{p}\mathbf{x}}|\mathbf{x}\rangle$ and $\hat{\mathbf{X}}|\mathbf{x}\rangle = \mathbf{x}|\mathbf{x}\rangle$, we determine the right-hand part of (30) by explicit calculations:

$$\begin{aligned}\langle\psi(t)|\hat{\mathbf{X}}|\psi(t)\rangle &= \int \frac{d\mathbf{k}d\mathbf{q}}{(2\pi)^6}\psi^*_{\mathrm{p}}(\mathbf{q})\psi_{\mathrm{p}}(\mathbf{k})e^{-i(E_{\mathbf{k}}-E_{\mathbf{q}})t}\\ &\times\langle\mathbf{q}|\int d\mathbf{x}\mathbf{x}e^{+ikx}|\mathbf{x}\rangle\\ &= \int \frac{d\mathbf{k}d\mathbf{q}}{(2\pi)^6}\psi^*_{\mathrm{p}}(\mathbf{q})\psi_{\mathrm{p}}(\mathbf{k})e^{-i(E_{\mathbf{k}}-E_{\mathbf{q}})t}\int d\mathbf{x}\mathbf{x}e^{+i(\mathbf{k}-\mathbf{q})x},\end{aligned} \tag{31}$$

where $\langle\mathbf{q}|\mathbf{x}\rangle = e^{-i\mathbf{q}\mathbf{x}}$ was used. The $\int d\mathbf{x}$ integral may be removed:

$$\begin{aligned}\int d\mathbf{x}\mathbf{x}e^{i(\mathbf{k}-\mathbf{q})\mathbf{x}} &= \frac{1}{2i}\left(\frac{\partial}{\partial\mathbf{k}}-\frac{\partial}{\partial\mathbf{q}}\right)\int d\mathbf{x}e^{i(\mathbf{k}-\mathbf{q})\mathbf{x}}\\ &= \frac{1}{2i}\left(\frac{\partial}{\partial\mathbf{k}}-\frac{\partial}{\partial\mathbf{q}}\right)(2\pi)^3\delta^3(\mathbf{k}-\mathbf{q}).\end{aligned} \tag{32}$$

Then,

$$\begin{aligned}\langle\mathbf{x}(t)\rangle &= \frac{1}{2i}\int \frac{d\mathbf{k}d\mathbf{q}}{(2\pi)^3}\psi^*_{\mathrm{p}}(\mathbf{q})\psi_{\mathrm{p}}(\mathbf{k})e^{-i(E_{\mathbf{k}}-E_{\mathbf{q}})t}\\ \times\left(\frac{\partial}{\partial\mathbf{k}}-\frac{\partial}{\partial\mathbf{q}}\right)\delta^3(\mathbf{k}-\mathbf{q}) &= -\frac{1}{2i}\int \frac{d\mathbf{k}d\mathbf{q}}{(2\pi)^3}\delta^3(\mathbf{k}-\mathbf{q})\\ &\times\left(\frac{\partial}{\partial\mathbf{k}}-\frac{\partial}{\partial\mathbf{q}}\right)\psi^*_{\mathrm{p}}(\mathbf{q})\psi_{\mathrm{p}}(\mathbf{k})e^{-i(E_{\mathbf{k}}-E_{\mathbf{q}})t}\\ &= \int \frac{d\mathbf{k}}{(2\pi)^3}\left|\psi_{\mathrm{p}}(\mathbf{k})\right|^2\mathbf{v}_{\mathbf{k}}t = \langle\mathbf{v}\rangle t,\end{aligned} \tag{33}$$

where $\langle\mathbf{v}\rangle$ is given by the third expression from (28). Integration by parts was performed in the transition from the first line in (33) to the second. Thus, it was proven that, on average, the WP coordinate follows a classical trajectory:

$$\langle\mathbf{x}(t)\rangle = \langle\mathbf{v}\rangle t. \tag{34}$$

It was explicitly assumed in this proof that the mean WP coordinate is zero at $t = 0$.

3.3. Spreading of a Wave Packet in the Configuration Space

Let us demonstrate by direct calculations that a WP spreads with time. By definition, the spatial coordinate dispersion is

$$\sigma_x^2(t) = \langle\mathbf{x}^2(t)\rangle - \langle\mathbf{x}(t)\rangle^2. \tag{35}$$

The mean value of the coordinate squared is

$$\begin{aligned}\langle\mathbf{x}^2(t)\rangle &\equiv \langle\psi(t)|\hat{\mathbf{X}}^2|\psi(t)\rangle\\ &= \int d\mathbf{x}\mathbf{x}^2\int \frac{d\mathbf{k}d\mathbf{q}}{(2\pi)^6}\psi^*_{\mathrm{p}}(\mathbf{q})\psi_{\mathrm{p}}(\mathbf{k})e^{-i(E_{\mathbf{k}}-E_{\mathbf{q}})t+i(\mathbf{k}-\mathbf{q})\mathbf{x}}.\end{aligned} \tag{36}$$

Using the approach similar to (32)

$$\int d\mathbf{x}\mathbf{x}^2 e^{+i(\mathbf{k}-\mathbf{q})\mathbf{x}} = -\frac{1}{2}\left(\frac{\partial^2}{\partial\mathbf{k}^2}+\frac{\partial^2}{\partial\mathbf{q}^2}\right)\int d\mathbf{x}e^{+i(\mathbf{k}-\mathbf{q})\mathbf{x}}$$
$$= -\frac{1}{2}\left(\frac{\partial^2}{\partial\mathbf{k}^2}+\frac{\partial^2}{\partial\mathbf{q}^2}\right)(2\pi)^3\delta^3(\mathbf{k}-\mathbf{q}),$$

and, following (33), integrating by parts in (36), we arrive at

$$\langle\mathbf{x}^2\rangle = -\frac{1}{2}\int\frac{d\mathbf{k}d\mathbf{q}}{(2\pi)^3}\delta^3(\mathbf{k}-\mathbf{q})\left(\frac{\partial^2}{\partial\mathbf{k}^2}+\frac{\partial^2}{\partial\mathbf{q}^2}\right)$$
$$\times\,\psi_{\mathrm{p}}^*(\mathbf{q})\psi_{\mathrm{p}}(\mathbf{k})e^{-i(E_{\mathbf{k}}-E_{\mathbf{q}})t}$$
$$= \langle\mathbf{v}^2\rangle t^2 - \mathrm{Re}\int\frac{d\mathbf{k}}{(2\pi)^3}\frac{\psi_{\mathrm{p}}^*(\mathbf{k})\partial^2\psi_{\mathrm{p}}(\mathbf{k})}{\partial\mathbf{k}^2}.$$

Thus,

$$\sigma_x^2(t) = \left(\langle\mathbf{v}^2\rangle - \langle\mathbf{v}\rangle^2\right)t^2 - \mathrm{Re}\int\frac{d\mathbf{k}}{(2\pi)^3}\frac{\psi_{\mathrm{p}}^*(\mathbf{k})\partial^2\psi_{\mathrm{p}}(\mathbf{k})}{\partial\mathbf{k}^2}.$$

Setting $t = 0$, we find that

$$\sigma_x^2(0) = -\mathrm{Re}\int\frac{d\mathbf{k}}{(2\pi)^3}\frac{\psi_{\mathrm{p}}^*(\mathbf{k})\partial^2\psi_{\mathrm{p}}(\mathbf{k})}{\partial\mathbf{k}^2}$$

is the coordinate dispersion at the initial time. Thus,

$$\sigma_x^2(t) = \sigma_x^2(0) + \left(\langle\mathbf{v}^2\rangle - \langle\mathbf{v}\rangle^2\right)t^2 = \sigma_x^2(0) + \sigma_{\mathbf{v}}^2t^2, \quad (37)$$

where $\sigma_{\mathbf{v}}^2 = \langle\mathbf{v}^2\rangle - \langle\mathbf{v}\rangle^2$ is the WP velocity dispersion. This is the general dispersion law of a nonrelativistic WP, which has already been obtained earlier in [97].

Let us examine how the WP spreading rate depends on relativistic effects. We write $\sigma_{\mathbf{v}}^2$ in the following form:

$$\sigma_{\mathbf{v}}^2 = \langle\mathbf{v}^2\rangle - \langle\mathbf{v}\rangle^2 = \langle\mathbf{v}_T^2\rangle + \langle\mathbf{v}_L^2\rangle - \langle\mathbf{v}\rangle^2$$
$$= \langle\mathbf{v}_T^2\rangle + \langle(\mathbf{v}_L - \langle\mathbf{v}\rangle)^2\rangle, \quad (38)$$

where $\langle\mathbf{v}_T^2\rangle$ and $\langle\mathbf{v}_L^2\rangle$ are the mean squares of longitudinal and transverse projections of the WP velocity with respect to mean velocity vector $\langle\mathbf{v}\rangle$, respectively. Let us rewrite $\langle\mathbf{v}_T^2\rangle$ and $\langle(\mathbf{v}_L - \langle\mathbf{v}\rangle)^2\rangle$ in terms of variables in the intrinsic frame of reference of the WP

$$E_{\mathbf{k}} = \overline{\Gamma}(E_{\mathbf{k}}^* + \langle\mathbf{v}\rangle\mathbf{k}_L^*), \quad (39)$$

$$\mathbf{k}_L = \overline{\Gamma}(\mathbf{k}_L^* + \langle\mathbf{v}\rangle E_{\mathbf{k}^*}), \quad \mathbf{k}_T = \mathbf{k}_T^*, \quad (40)$$

$$\mathbf{v}_{\mathbf{k}L} = \frac{\mathbf{v}_{\mathbf{k}L}^* + \langle\mathbf{v}\rangle}{1 + \mathbf{v}_{\mathbf{k}L}^*\langle\mathbf{v}\rangle}, \quad \overline{\Gamma} \equiv \Gamma_{\langle\mathbf{v}\rangle} = \frac{1}{\sqrt{1-\langle\mathbf{v}\rangle^2}} \quad (41)$$

in the following way:

$$\langle\mathbf{v}_T^2\rangle = \int\frac{d\mathbf{k}}{(2\pi)^3}\left|\psi_{\mathrm{p}}(\mathbf{k})\right|^2\mathbf{v}_{\mathbf{k}T}^2$$
$$= \frac{1}{\overline{\Gamma}^2}\int\frac{d\mathbf{k}^*}{(2\pi)^3}\left|\psi_{\mathrm{p}}(\mathbf{k}^*)\right|^2\frac{\mathbf{v}_{\mathbf{k}T}^{*2}}{(1+\langle\mathbf{v}\rangle\mathbf{v}_{\mathbf{k}L}^*)^2}, \quad (42)$$

and

$$\langle(\mathbf{v}_L - \langle\mathbf{v}\rangle)^2\rangle = \int\frac{d\mathbf{k}}{(2\pi)^3}\left|\psi_{\mathrm{p}}(\mathbf{k})\right|^2(\mathbf{v}_{\mathbf{k}L} - \langle\mathbf{v}\rangle)^2$$
$$= \frac{1}{\overline{\Gamma}^4}\int\frac{d\mathbf{k}^*}{(2\pi)^3}\left|\psi_{\mathrm{p}}(\mathbf{k}^*)\right|^2\frac{\mathbf{v}_{\mathbf{k}L}^{*2}}{\left(1+\langle\mathbf{v}\rangle\mathbf{v}_{\mathbf{k}L}^*\right)^2}. \quad (43)$$

Comparing (42) and (43), one may note that the following is true in the first order for WPs that are sufficiently narrow in the momentum space:

$$\langle\mathbf{v}_T^2\rangle = \langle\mathbf{v}_T^{*2}\rangle/\overline{\Gamma}^2, \quad \langle(\mathbf{v}_L - \langle\mathbf{v}\rangle)^2\rangle = \langle\mathbf{v}_L^{*2}\rangle/\overline{\Gamma}^4.$$

Thus, using (37) and considering that $\langle\mathbf{v}_L^{*2}\rangle = \frac{1}{2}\langle\mathbf{v}_T^{*2}\rangle = \frac{1}{3}\langle\mathbf{v}^{*2}\rangle$ in the intrinsic frame of the WP, we obtain the following in the full spreading regime:

$$\sigma_{xL}^2(t) = \frac{1}{3}\langle\mathbf{v}^{*2}\rangle t^2/\overline{\Gamma}^4, \quad \sigma_{xT}^2(t) = \frac{2}{3}\langle\mathbf{v}^{*2}\rangle t^2/\overline{\Gamma}^2,$$
$$\sigma_{xL}^2(t) = \frac{1}{2}\sigma_{xT}^2(t)/\overline{\Gamma}^2. \quad (44)$$

The rate of longitudinal WP spreading is $\overline{\Gamma}$ times lower than the rate of transverse spreading. It is evident that

$$\sigma_x^2(t) = \sigma_{xL}^2(t) + \sigma_{xT}^2(t) = \langle\mathbf{v}^{*2}\rangle t^2.$$

in the intrinsic frame of reference of the WP.

3.4. Transverse Spreading of a Wave Packet Leads to an Inverse Square Law

Any WP spreads with time. In other words, the spatial dispersion of a WP increases with time, while its amplitude decreases. This well-known and inherent property of WPs is often considered to be their "drawback." This stimulated the search for temporally stable solutions needed to associate a WP with a particle. In particular, although a consistent scattering theory is known to be impossible to construct without WPs [98, 99], it is not uncommon to come across such assertions that the decay of the amplitude with time makes WPs not fully adequate objects to describe the initial and final states, which are defined formally at $t = -\infty$ and $t = +\infty$, respectively. However, as will be shown below , and this is a new result, WP spreading is not critical for the S-matrix formalism, since it has a clear interpretation. This is a novel result. Just as in an ensemble of classical particles, WP spreading results in suppression (proportional to $1/|\mathbf{x}|^2$) of the time-inte-

grated probability of finding a particle at distance $\mathbf{x}$ from the point of its production. Thus, the result leads to simple normalization factors for the initial and final states taken at sufficiently long (but finite) times.

The assertion regarding the nature of the inverse square law was proven in [96] in three different ways:

(i) For two explicit examples of $\psi_p(\mathbf{p})$: a Gaussian function that is invariant or not invariant with respect to relativistic transformations.

(ii) For a WP of an arbitrary form.

(iii) Based on the continuity equation.

In the present study, we utilize the simplest and fairly general approach based on the continuity equation, which agrees with both relativistic and nonrelativistic equations of motion.

Let us write the continuity equation for an arbitrary quantum state with scalar function $\rho(t, \mathbf{x}')$, which is the probability density of finding a particle at point $\mathbf{x}'$ at time t, and vector function $\mathbf{j}(t, \mathbf{x}')$, which is the flux density:

$$\frac{\partial \rho(t, \mathbf{x}')}{\partial t} + \nabla \mathbf{j}(t, \mathbf{x}') = 0. \quad (45)$$

This equation may be rewritten in equivalent form

$$\frac{\partial}{\partial t} \int\limits_{|\mathbf{x}'| \le |\mathbf{x}|} d\mathbf{x}' \rho(t, \mathbf{x}') = -\int\limits_S d\mathbf{S}\mathbf{j}(t, \mathbf{x}'), \quad (46)$$

where integration is bounded by sphere S with radius $|\mathbf{x}|$. If this radius is sufficiently large and the time is too short for a WP to spread (both conditions are satisfied if $|\mathbf{x}| \gg \sigma_x(t)$), the integral is expected to be equal to unity based on the normalization condition

$$\int\limits_{|\mathbf{x}'| \le |\mathbf{x}|} d\mathbf{x}' \rho(t, \mathbf{x}') \approx 1;$$

therefore, the time derivative of the integral at the left-hand side of this equality is negligible, and the right-hand side of (46) is also negligible. This implies that the flux density should decrease faster than $1/|\mathbf{x}|^2$. The example of a Gaussian WP considered below is in agreement with this assertion.

Let us now integrate over time the right- and left-hand sides of (46) from zero to infinity:

$$\int\limits_{|\mathbf{x}'| \le |\mathbf{x}|} d\mathbf{x}' \rho(\infty, \mathbf{x}') - \int\limits_{|\mathbf{x}'| \le |\mathbf{x}|} d\mathbf{x}' \rho(0, \mathbf{x}') = -\int\limits_S d\mathbf{S}\mathbf{\Phi}(\mathbf{x}'), \quad (47)$$

where $\mathbf{\Phi}(\mathbf{x}') = \int_0^\infty dt \mathbf{j}(t, \mathbf{x}')$ is the time integral of the flux density. By definition,

$$P(t, |\mathbf{x}|) \equiv \int\limits_{|\mathbf{x}'| \le |\mathbf{x}|} d\mathbf{x}' \rho(t, \mathbf{x}') \quad (48)$$

is the probability of finding a particle inside a sphere with radius $|\mathbf{x}|$ at the time instant t. Naturally, owing to the WP dispersion, the probability of finding a particle within an arbitrary finite volume tends to zero as $t \to \infty$, since the WP leaves this volume. On the other hand, if $|\mathbf{x}|$ is much larger than the WP size, $P(0, |\mathbf{x}|)$ is very close to unity, since the WP initially was localized almost completely within a sufficiently large volume. Under these conditions, (47) turns into

$$\int\limits_{|\mathbf{x}'| \le |\mathbf{x}|} d\mathbf{x}' \rho(0, \mathbf{x}') = \int\limits_S d\mathbf{S}\mathbf{\Phi}(\mathbf{x}') \simeq 1. \quad (49)$$

The modulus of vector $\mathbf{\Phi}(\mathbf{x}')$ in the intrinsic frame of reference of the WP is independent of the direction of vector $\mathbf{x}'$. Therefore,

$$|\mathbf{\Phi}(|\mathbf{x}|)| \simeq \frac{1}{4\pi |\mathbf{x}|^2}$$

in this frame.

Thus, inverse square law $1/|\mathbf{x}|^2$ is true for any solutions of the Klein–Gordon and/or Dirac equations with finite normalizations but is not valid for plane waves with a singular normalization. At any given time, flux density $\nabla \mathbf{j}(t, \mathbf{x}')$ decreases faster than $1/|\mathbf{x}|^2$.

3.5. Noncovariant Gaussian Wave Packet

Let us examine the useful example of a well-known noncovariant Gaussian WP with a wave function of the following form in the momentum space:

$$\psi_p(\mathbf{k}) = \left(\frac{2\pi}{\sigma_p^2}\right)^{3/4} e^{-\frac{(\mathbf{k}-\mathbf{p})^2}{4\sigma_p^2}}, \quad (50)$$

where σ_p is the *constant* dispersion of the Gaussian distribution, or the "width" of the momentum distribution in a WP. The wave function in the coordinate representation may be obtained by assuming that dispersion σ_p is sufficiently small to calculate accurately the integral with expansion

$$E_\mathbf{k} = E_\mathbf{p} + \mathbf{v}_\mathbf{p}(\mathbf{k} - \mathbf{p}) + \frac{m^2}{2E_\mathbf{p}^3}(\mathbf{k} - \mathbf{p})^2 + \frac{(\mathbf{p} \times \mathbf{k})^2}{2E_\mathbf{p}^3} + \ldots, \quad (51)$$

where $\mathbf{v} = \mathbf{p}/E_\mathbf{p}$. Integration reduces to a Gaussian quadrature, which provides an opportunity to calculate

$$\psi_x(t, \mathbf{x}) = \frac{\exp\left[-ipx - \frac{(\mathbf{x}_L - \mathbf{v}t)^2}{4\sigma_x^2(1 + it/\tau_L)} - \frac{\mathbf{x}_T^2}{4\sigma_x^2(1 + it/\tau_T)}\right]}{(2\pi\sigma_x^2)^{3/4}\sqrt{(1 + it/\tau_L)}(1 + it/\tau_T)}, \quad (52)$$

where $p = (E_\mathbf{p}, \mathbf{p})$, $\sigma_x^2 = 1/4\sigma_p^2$,

$$\tau_L = \Gamma_\mathbf{p}^3 \tau, \quad \tau_T = \Gamma_\mathbf{p} \tau, \quad \tau = 2\sigma_x^2 m, \quad \Gamma_\mathbf{p} = \frac{E_\mathbf{p}}{m}. \quad (53)$$

Here, $\mathbf{x}_L$ and $\mathbf{x}_T$ are the components of vector $\mathbf{x}$ that are parallel and perpendicular to mean velocity vector $\mathbf{v}$, respectively. Expression (52) shows clearly that the WP spreads with time. For greater clarity, we write down the modulus of function (52):

$$|\psi_x(t,\mathbf{x})| = \frac{\exp\left[-\frac{(\mathbf{x}_L-\mathbf{v}t)^2}{4\sigma_x^2(1+t^2/\tau_L^2)} - \frac{\mathbf{x}_T^2}{4\sigma_x^2(1+t^2/\tau_T^2)}\right]}{(2\pi\sigma_x^2)^{3/4}\left(1+t^2/\tau_L^2\right)^{1/4}\sqrt{1+t^2/\tau_T^2}}.$$

Thus, a Gaussian WP characterized at $t = 0$ by a wave function in the configuration space

$$\psi_x(0,\mathbf{x}) = \frac{1}{(2\pi\sigma_x^2)^{3/4}}\exp\left(i\mathbf{p}\mathbf{x} - \frac{\mathbf{x}^2}{4\sigma_x^2}\right)$$

spreads with time in the longitudinal and transverse directions. The squares of longitudinal $\sigma_{xL}^2(t)$ and transverse $\sigma_{xT}^2(t)$ dispersions are

$$\begin{aligned}\sigma_{xL}^2(t) &= \sigma_x^2(1+t^2/\tau_L^2),\\ \sigma_{xT}^2(t) &= \sigma_x^2(1+t^2/\tau_T^2),\end{aligned} \tag{54}$$

where τ_L and τ_T given by (53) are related as $\tau_L = \Gamma_\mathbf{p}^2\tau_T$. Parameters τ_L and τ_T have the physical meaning of longitudinal and transverse spreading times, respectively. Parameter τ is the WP dispersion time in the intrinsic frame, where $\tau_L = \tau_T = \tau$.

Note that the spreading rate of a noncovariant Gaussian packet in the longitudinal direction is $\Gamma_\mathbf{p}^2$ times lower than in the transverse one. A Gaussian WP has two spreading regimes: transverse ($t \gg \tau_T$) and longitudinal ($t \gg \tau_L$). In the case of full spreading in all directions,

$$\begin{aligned}\sigma_{xL}(t) &= \sigma_x\frac{t}{\tau}\frac{1}{\Gamma_\mathbf{p}^3}, \quad t \gg \tau_L,\\ \sigma_{xT}(t) &= \sigma_x\frac{t}{\tau}\frac{1}{\Gamma_\mathbf{p}}, \quad t \gg \tau_T.\end{aligned}$$

Comparing the obtained rates of longitudinal and transverse spreading with the results of calculations that make use of relativistic relations (44), we find that the spreading rate of a noncovariant Gaussian packet is $\Gamma_\mathbf{p}$ times lower. The covariant Gaussian packet considered in the next section agrees with general formula (44).

Let us verify that the Gaussian WP spreading leads to $1/|\mathbf{x}|^2$ in suppression of the time-integrated flux. The flux density is calculated in accordance with the standard formula

$$\mathbf{j}(t,\mathbf{x}) = -\frac{i}{2m} \times\left[\psi_x^*(t,\mathbf{x})\nabla\psi_x(t,\mathbf{x}) - \psi_x(t,\mathbf{x})\nabla\psi_x^*(t,\mathbf{x})\right].$$

Let us perform calculations in the intrinsic frame of reference of the WP. The flux density is then

$$\mathbf{j}(t,\mathbf{x}) = \frac{\mathbf{x}(t/\tau)\exp\left[-\frac{\mathbf{x}^2}{2\sigma_x^2(1+(t/\tau)^2)}\right]}{(2\pi)^{3/2}2m\sigma_x^5\left[1+(t/\tau)^2\right]^{5/2}}. \tag{55}$$

The time integral may be calculated exactly:

$$\begin{aligned}\mathbf{\Phi}(\mathbf{x}) = \int_0^\infty dt\mathbf{j}(t,\mathbf{x}) &= \frac{\mathbf{x}}{4\pi|\mathbf{x}|^3}\,\mathrm{erf}\left(\sqrt{\frac{\mathbf{x}^2}{2\sigma_x^2}}\right)\\ &- \frac{\mathbf{x}}{(2\pi)^{3/2}|\mathbf{x}|^2\,\sigma_x}e^{-\mathbf{x}^2/2\sigma_x^2}.\end{aligned} \tag{56}$$

The following formula is then obtained at distances much larger than the packet size, $|\mathbf{x}|^2 \gg \sigma_x^2$:

$$\mathbf{\Phi}(\mathbf{x}) \simeq \frac{\mathbf{x}}{4\pi|\mathbf{x}|^3}. \tag{57}$$

3.6. Theory of Vacuum Neutrino Oscillations in the Wave Packet Model

Let us apply the above WP theory to neutrino oscillations. It was demonstrated in the previous section that the transverse WP spreading introduces suppression factor $\frac{1}{4\pi|\mathbf{x}|^2}$ to the probability of finding a particle at distance $\mathbf{x}$ from the point of its production in infinite observation time. Let us assume that the transverse degrees of freedom do not exert any significant influence on the oscillation pattern (with the exception of the above suppression factor). In what follows, we will dispense with this hypothesis and perform a complete three-dimensional calculation, which will verify the validity of the assumption.

3.6.1. Neutrino state in the wave packet model and amplitude of the transition from the source to the detector. Let us consider a one-dimensional neutrino WP with mean coordinate x_s at time t_s:

$$\left|\nu_\alpha^s\right\rangle = \sum_k V_{\alpha i}^*\int\frac{dk}{2\pi}\psi_\mathrm{p}^s(k)e^{-iE_it_s+ikx_s}\left|\nu_i(k)\right\rangle, \tag{58}$$

where $E_i = \sqrt{k^2+m_i^2}$, the state $\left|\nu_i(k)\right\rangle$ with the normalization in accordance with $\left\langle\nu_j(q)\middle|\nu_i(k)\right\rangle = 2\pi\delta(q-k)$, and

$$\psi_\mathrm{p}^s(k) = \left(\frac{2\pi}{\sigma_s^2}\right)^{\frac{1}{4}}e^{-\frac{(k-p_s)^2}{4\sigma_s^2}}. \tag{59}$$

The state norm in (59) is $\left\langle\nu_\alpha^s\middle|\nu_\alpha^s\right\rangle = 1$. The detected state should also be characterized by a WP with mean

coordinate x_d at the time instant t_d. In principle, the state in the detector may differ in flavor:

$$\left|\nu_\beta^d\right\rangle = \sum_i V_{\beta i}^* \int \frac{dk}{2\pi} \psi_{\mathrm{p}}^d(k) e^{-iE_i t_d + ikx_d} \left|\nu_i(k)\right\rangle, \qquad (60)$$

where $\psi_{\mathrm{p}}^d(k)$ is defined as in (59) with obvious substitutions $s \to d$. The projection of state $\left|\nu_\alpha^s\right\rangle$ onto $\left|\nu_\beta^d\right\rangle$ yields the transition amplitude:

$$A_{\alpha\beta}(t, L) \equiv \left\langle \nu_\beta^d \middle| \nu_\alpha^s \right\rangle = \sum_j V_{\alpha j}^* V_{\beta j} \int_{-\infty}^{+\infty} \frac{dk}{2\pi} \psi_{\mathrm{p}}^s(k) \psi_{\mathrm{p}}^{d*}(k) e^{-iE_j t + ikL}, \qquad (61)$$

where $L = |x_d - x_s|$ is the distance between the mean positions of neutrino WPs in the source and the detector and $t = (t_d - t_s)$. The product of Gaussian form factors in (61) may be presented as a Gaussian function in (59) with momentum

$$p = \frac{p_s \sigma_d^2 + p_d \sigma_s^2}{\sigma_s^2 + \sigma_d^2} = \sigma_p^2 \left(\frac{p_s}{\sigma_s^2} + \frac{p_d}{\sigma_d^2} \right), \qquad (62)$$

and dispersion σ_p defined by

$$\frac{1}{\sigma_p^2} = \frac{1}{\sigma_s^2} + \frac{1}{\sigma_d^2}. \qquad (63)$$

The amplitude in (61) takes the following form:

$$A_{\alpha\beta}(t, L) = \sum_j V_{\alpha i}^* V_{\beta i} \sqrt{\frac{2\pi}{\sigma_s \sigma_d}} \int_{-\infty}^{+\infty} \frac{dk}{2\pi} \times \exp\left[-iE_j t + ikL - \frac{(k-p)^2}{4\sigma_p^2} - \frac{(p_s - p_d)^2}{4(\sigma_s^2 + \sigma_d^2)} \right]. \qquad (64)$$

The momentum integral may be calculated in the approximation of a small width of the effective WP[2] ($\sigma_p \ll p$) by considering of the one-dimensional equivalent of the expansion in (51)

$$E_{kj} \simeq E_{pj} + v_{pj}(k - p) + \frac{m_j^2}{2E_{pj}^3}(k - p)^2, \qquad (65)$$

where $v_{pj} = dE_j/dp = p/E_{pj}$ is the group velocity of the WP state with mass m_j. This allows one to calculate the amplitude:

$$A_{\alpha\beta}(t, L) = \frac{\left[2\pi\tilde{\delta}(p_s - p_d)\right]^{1/2}}{\left(2\pi\sigma_x^2\right)^{1/4}} \sum_j V_{\alpha j}^* V_{\beta j} \times \frac{\exp\left[-iE_{pj}t - \frac{(L - v_{pj}t)^2}{4\sigma_x^2(1 + it/\tau_{Lj})} \right]}{(1 + it/\tau_{Lj})^{1/2}}, \qquad (66)$$

where

$$2\pi\tilde{\delta}(p_s - p_d) = \left(\frac{2\pi}{\sigma_s^2 + \sigma_d^2} \right)^{1/2} \exp\left[-\frac{(p_s - p_d)^2}{2(\sigma_s^2 + \sigma_d^2)} \right] \qquad (67)$$

is the "spread" equivalent of the $2\pi\delta(p_s - p_d)$ function, which exercises the momentum conservation law, $\tau_{Lj} = E_{pj}^3 / 2m_j^2 \sigma_p^2$ is the characteristic time of longitudinal spreading of a neutrino WP with m_j in strict accordance with (53), and $\sigma_x = 1/2\,\sigma_p$.

3.7. Macroscopic Averaging of the Transition Probability

How does one determine the probability of neutrino oscillations in the model with a WP? The probability density corresponding to the amplitude $A_{\alpha\beta}(t, L)$ from (64) depends both on distance $L = x_d - x_s$ and time difference $t = (t_d - t_s)$ and on the mean neutrino WP momenta in the source and the detector. Importantly, all these parameters are completely arbitrary; i.e., we do not impose constraints such as $t = L$ and $p_s = p_d$. The macroscopic number of "events" averaged over nonobservables (production time t_s and mean momentum p_s at production) is the observable quantity:

$$\int dt_s dp_s \frac{d^2 n_\nu}{dt_s dp_s} \left| A_{\alpha\beta}(t_d - t_s, p_s, p_d) \right|^2 \simeq \left\langle \frac{d^2 n_\nu}{dt_s dp_s} \right\rangle P_{\alpha\beta}(L), \qquad (68)$$

where $d^2 n_\nu(t_s, p_s)/dt_s dp_s$ is the number density of neutrinos at the source in unit time dt_s and unit momentum dp_s. Brackets $\langle ... \rangle$ denote averaging over time and momentum within the intervals where $\left|A_{\alpha\beta}(t - t_s, p_s - p_d)\right|^2$ decreases rapidly. The probability of flavor transition $\nu_\alpha \to \nu_\beta$ averaged over time and momentum at the source is

$$P_{\alpha\beta}(L) = \int dt_s dp_s \left| A_{\alpha\beta}(t - t_s; p_s, p_d) \right|^2. \qquad (69)$$

Using (67), one may easily integrate over momentum p_s. In order to perform integration over time, one should consider that terms of the t/τ_{Lj} form are varying slowly compared to the exponential suppression occurring at times $(L - v_j t)^2 / 4\sigma_x^2 \gtrsim 1$, since relation

$$\frac{t}{\tau_{Lj}} \lesssim \frac{(L - 2\sigma_x) m_j^2}{p^2 E_{pj} \sigma_x^2} \ll 1 \qquad (70)$$

holds true in a wide range of neutrino masses $m_j \lesssim 1$ eV and spatial dispersions σ_x. Thus, the integral over time t_s reduces to a Gaussian one. This provides an oppor-

[2] A WP is called "effective," since it incorporates the processes of neutrino production and detection.

tunity to determine the oscillation probability in the WP model:

$$P_{\alpha\beta}(L) = \sum_{i,j} \frac{V_{\beta i} V^*_{\alpha i} V_{\alpha j} V^*_{\beta j}}{\sqrt[4]{1 + \left(L/L^{\rm d}_{ij}\right)^2}} \times \exp\left[-i(\varphi_{ij} + \varphi^{\rm d}_{ij} - \mathcal{A}^2_{ij} - \mathcal{B}^2_{ij}\right], \quad (71)$$

where

$$\mathcal{A}^2_{ij} = \frac{1}{1 + \left(L/L^{\rm d}_{ij}\right)^2}\left(\frac{L}{L^{\rm coh}_{ij}}\right)^2 \quad \text{and} \quad \mathcal{B}^2_{ij} = \left(\frac{\sqrt{2}\pi\sigma_x}{L^{\rm osc}_{ij}}\right)^2. \quad (72)$$

The probability of oscillations in (71) depends on the following parameters with a dimension of length:

$$L^{\rm osc}_{ij} = 2\pi\frac{2p}{\Delta m^2_{ij}}, \quad (73a)$$

$$L^{\rm coh}_{ij} = \frac{2\sqrt{2}p^2}{\sigma_{\rm p}\Delta m^2_{ij}} = \frac{1}{\sqrt{2}\pi\sigma_{\rm rel}} L^{\rm osc}_{ij}, \quad (73b)$$

$$L^{\rm d}_{ij} = \frac{p^3}{\sigma^2_{\rm p}\Delta m^2_{ij}} = \frac{1}{2\sqrt{2}\sigma_{\rm rel}} L^{\rm coh}_{ij}, \quad (73c)$$

$$\sigma_x = \frac{1}{2\sigma_p}, \quad (73d)$$

where dimensionless parameter $\sigma_{\rm rel} \equiv \sigma_p/p$. Phase $\varphi_{ij}(L)$ depends linearly on distance L:

$$\varphi_{ij}(L) = 2\pi\frac{L}{L^{\rm osc}_{ij}},$$

and is inversely proportional to oscillation length $L^{\rm osc}_{ij}$, which turned out to be the same as in the plane-wave case. However, the following addition emerged in the WP model in the standard phase:

$$\varphi^{\rm d}_{ij}(L) = -\frac{1}{1 + \left(L/L^{\rm d}_{ij}\right)^2}\left(\frac{L}{L^{\rm coh}_{ij}}\right)^2 \frac{L}{L^{\rm d}_{ij}} + \frac{1}{2}\arctan\frac{L}{L^{\rm d}_{ij}}. \quad (74)$$

Let us discuss the obtained results qualitatively.

3.8. Qualitative Discussion of the Formula for the Oscillation Probability in the Wave Packet Model

It follows from (71) that neutrino oscillations in the WP model depend on several parameters with a dimension of length:

(i) Oscillation length $L^{\rm osc}_{ij}$.

(ii) Coherence length $L^{\rm coh}_{ij}$.

(iii) Dispersion length $L^{\rm d}_{ij}$.

(iv) Effective spatial size σ_x of a neutrino WP, which may differ by many orders of magnitude. Let us discuss the physical meaning of these scales. Coherence length $L^{\rm coh}_{ij}$ corresponds to the distance at which two WPs with masses m_i and m_j travelling with different group velocities $v_i \simeq 1 - m^2_i/2p^2$ and $v_j \simeq 1 - m^2_j/2p^2$ cease to overlap spatially. This occurs at time t, when $(v_i - v_j)t \simeq \sigma_x$, where σ_x is the spatial size of the neutrino WP. The estimate of time $t \simeq 2\sigma_x p^2/\Delta m^2_{ij}$ agrees to within a numerical factor with the definition of coherence length $L^{\rm coh}_{ij}$ from (73b). Note that the coherence length is proportional to oscillation length $L^{\rm osc}_{ij}$ and is inversely proportional to relative dispersion $\sigma_{\rm rel}$ of the WP momentum. Therefore, the lower the relative dispersion of the WP momentum, the longer is the time interval of preservation of the WP coherence. Factor $\left(\frac{L}{L^{\rm coh}_{ij}}\right)^2$ in the exponential function in (71) represents the suppression related to the coherence length.

Dispersion length $L^{\rm d}_{ij}$ emerges as a result of expansion of energy up to the second order (see (65)). This corresponds to WP spreading in the configuration space as demonstrated in Section 3.5. Note that $L^{\rm d}_{ij}$ is inversely proportional to $\sigma_{\rm rel}$ squared. The spatial size of WPs increases after spreading, which compensates partially the loss of overlap of WPs ν_i and ν_j due to the difference in their group velocities. The characteristic time of longitudinal spreading of a WP of a neutrino with mass m_j (parameter $\tau_{Lj} = E^3_{pj}/2m^2_j\sigma^2_p$) turned out to be the same as in (53). The time derivative of spatial WP dispersion parameter $\sigma_x(t)$ defined in accordance with (54) may be interpreted as the spreading rate:

$$\frac{d|\sigma_{x,j}(t)|}{dt} = \frac{\sigma_x t/(\tau_{Lj})^2}{\sqrt{1 + (t/\tau_{Lj})^2}} = \begin{cases} \sigma_x t/(\tau_{Lj})^2, & t \ll \tau_{Lj}, \\ \sigma_x/\tau_{Lj} = \dfrac{m^2_j}{E^2_p}\dfrac{\sigma_p}{E_p} \ll 1, & t \gg \tau_{Lj}. \end{cases} \quad (75)$$

It can be seen that $d\sigma_{x,j}(t)/dt$ grows linearly with time until it reaches the asymptotic value of spreading rate σ_x/τ_{Lj}. The spreading rate is much lower than the velocity of neutrinos but is not necessarily lower than the difference between their group velocities $v_i - v_j$. Indeed,

$$v_i - v_j = \frac{\Delta m^2_{ij}}{2E^2_p} \simeq \frac{\Delta m^2_{ij}}{2m^2_{\max}}\frac{E_p}{\sigma_p}\frac{d\sigma_{x,j}(t)}{dt}, \quad (76)$$

where $m_{\max}$ is the maximum neutrino mass. With the cosmological constraint ($m_{\max} \lesssim 0.2$ eV) factored in and taking $\Delta m_{ij}^2 = 2.45\times10^{-3}$ eV^2 as an estimate, we find that $v_i - v_j$ is comparable to WP spreading rate $d\sigma_{x,j}(t)/dt$ if $\sigma_p \simeq 0.03E_p$. The spreading rate for packets with much smaller spatial dispersions is much lower than $v_i - v_j$. At much higher values of σ_{rel} (still satisfying the $\sigma_{\mathrm{rel}} \ll 1$ condition), the spreading of packets will compensate (partially) the loss of their overlap more efficiently. For example, at distances $L = L_{ij}^{\mathrm{osc}}/2$ from the source, where it is reasonable to install detectors to maximize the sensitivity to neutrino oscillations, the maximum suppression of interference terms in (71) is $e^{-\pi/8}$ at $\sigma_{\mathrm{rel}} = 1/\sqrt{2\pi} \simeq 0.4$.

In the $L \to \infty$ limit,

$$\lim_{L\to\infty} \frac{1}{1+\left(L/L_{ij}^{\mathrm{d}}\right)^2}\left(\frac{L}{L_{ij}^{\mathrm{coh}}}\right)^2 = \left(\frac{L_{ij}^{\mathrm{d}}}{L_{ij}^{\mathrm{coh}}}\right)^2 = \frac{p^2}{8\sigma_p^2} \gg 1, \quad (77)$$

and spreading does not compensate completely the loss of coherence in (71). Thus, oscillations are *strongly suppressed* at distances that are much greater than the coherence and dispersion lengths. Apparently, one may state that neutrinos from astrophysical and cosmological sources are noncoherent and do not oscillate.

It may seem surprising that the partial restoration of coherence due to WP spreading is sensitive to the *difference* between spreading rates rather than to their *sum*, which is to be expected for WPs with their spatial widths increasing with time. In fact, it is indeed easy to demonstrate that the coherence loss compensation for real Gaussian widths depends on the sum of spreading rates. The explanation is that the spreading effect manifests itself as complex-valued function $\sigma_x^2(1 + it/\tau_{Lj})$, which is characterized both by its absolute value and its phase. Therefore, just as the oscillation length depends on energy difference $(E_i - E_j)t$, the WP spreading effect, which depends on it/τ_{Lj}, should depend on phase difference $\propto it(1/\tau_{Lj} - 1/\tau_{Li})$ in the interference terms of the amplitude modulus squared in (66).

Since the WP spatial width is complex-valued function $\sigma_x^2(1 + it/\tau_{Lj})$, the spreading of WPs both affects their overlap and produces a correction to the interference phase. Therefore, the oscillation phase acquires addition $\varphi_{ij}^{\mathrm{d}}(L)$ defined in (74).

Additional suppression factor $\mathcal{B}_{ij}^2$ defined in (72) is independent of distance. This suppression is substantial if the spatial width of a neutrino WP is comparable in order of magnitude to oscillation length $L = L_{ij}^{\mathrm{osc}}$ (or exceeds it). In the mathematical sense, this corresponds to the plane-wave limit, wherein the spatial width of a neutrino packet tends to infinity. This has a trivial interpretation: the interference terms are averaged over distances of the order of the packet size. Formula (71) may be rewritten in the following form:

$$\mathcal{B}_{kj}^2 = \frac{1}{4}\left(\frac{\Delta m_{kj}^2}{\sigma_{m^2}}\right)^2, \quad (78)$$

which allows one to interpret the suppression of interference of states $|\nu_i\rangle$ and $|\nu_j\rangle$ if $\Delta m_{ij}^2 \gg \sigma_{m^2}$, where $\sigma_{m^2} = 2\sqrt{2}p\sigma_p$ may be interpreted formally as the uncertainty of the neutrino mass squared [68]. This is the factor that explains why charged leptons do not oscillate. Actually, the theory developed above may formally be applied to the oscillations of charged leptons by substituting ν_1, ν_2, ν_3 with e, μ, τ under the assumption that all charged leptons are ultrarelativistic. However, all interference terms are suppressed very strongly in this case, since quantities $|\Delta m_{e\mu}^2| \equiv |m_\mu^2 - m_e^2|$ are much larger than any realistic value of σ_p due to the factor $\exp\left[-\mathcal{B}_{e\mu}^2\right] \ll 1$. Note that the interference terms in (71) are also suppressed by numerator

$$q_{kj} = \sqrt[4]{1+\left(L/L_{kj}^{\mathrm{d}}\right)^2}. \quad (79)$$

Interference vanishes at $\sigma_p \to 0$ and $\sigma_p \to \infty$ in (71), and the oscillation probability becomes a noncoherent sum

$$P_{\alpha\beta} = \sum_k |V_{\alpha k}|^2 |V_{\beta k}|^2, \quad (80)$$

which is independent of energy, distance, and neutrino masses.

Note finally that the $\sigma_p \to 0$ limit, which corresponds formally to the plane-wave limit, predicts, in contrast to the plane-wave model itself, the lack of neutrino oscillations. Although this result is obvious *post factum*, it may seem paradoxical at first glance, since WPs turn into states with definite momentum at $\sigma_p \to 0$, which is a throwback to the model with plane waves. However, one more important step is made in the WP model: integration over the neutrino emission time is performed instead of the unjustified use of equality $t = L$ in the plane-wave model. If one is to act consistently in the plane-wave model, one should also perform integration over time (as a nonobservable). The plane-wave model then also yields a probability in the form of a noncoherent sum in (80). Luckily, this step was omitted in the pioneering works on oscillations. Thus, it is evident that the "obvious" substitution $t = L$ is far from being innocuous.

Let us now examine whether the assumptions (discussed in Section 2.3) made in the derivation of for-

mula (17) for the probability of flavor transitions are valid.

Assumption (i), which states that a coherent superposition of states with masses m_i $(i = 1,2,3)$ $|\nu_\alpha\rangle = \sum_i V_{\alpha i}^* |\nu_i\rangle$ interacts in the processes of neutrino production and detection, may be erroneous if $\exp\left[-\mathcal{B}_{ij}^2\right] \lesssim 1$. In particular, this hypothesis is definitely not valid for charged leptons, which is why their oscillations are infeasible.

Condition (ii) that states $|\nu_i\rangle$ have definite momenta $\mathbf{p}_i$ is violated, since it corresponds to an infinite spatial width $\sigma_x = (2\sigma_p)^{-1}$, which yields $\exp\left[-\mathcal{B}_{ij}^2\right] \to 0$. This leads to (80).

Hypothesis (III) states that all momenta $\mathbf{p}_i$ are the same ($\mathbf{p}_i = \mathbf{p}$). This contradicts relativistic invariance. The noncovariant theory of neutrino oscillations in the WP model, which was discussed above, did not address this deficiency.

Approximation (iv) of ultrarelativistic neutrinos ($\mathbf{p}^2 \gg \max(m_i^2)$) was also used in the theory of neutrino oscillations in the WP model.

Hypothesis (v), which states that neutrino propagation time $t = L$, is not valid. In fact, a consistent calculation requires integrating over time, which was done in (68). The largest contribution to the time integral is produced by times of the order of L/v_{ij}, where

$$\frac{1}{v_{ij}} = \frac{v_i + v_j}{v_i^2 + v_j^2},$$

which corresponds to the time instant of the maximum overlap of two WPs representing states ν_i and ν_j.

4. RELATIVISTIC WAVE PACKET

4.1. Definitions

Let $|\mathbf{k}\rangle$ be the eigenstate of the operator of 4-momentum $\hat{P} = (\hat{P}_0, \hat{\mathbf{P}})$ of a particle with mass m:

$$\hat{P}_\mu |\mathbf{k}\rangle = k_\mu |\mathbf{k}\rangle \quad (\mu = 0,1,2,3). \tag{81}$$

$k \mapsto k' = \Lambda k$ transforms state $|\mathbf{k}\rangle$ to $|\mathbf{k}'\rangle$. States $|\mathbf{k}\rangle$ are normalized in a relativistically invariant way: $\langle \mathbf{q}|\mathbf{k}\rangle = (2\pi)^3 2E_\mathbf{k} \delta^3(\mathbf{q} - \mathbf{k})$. In what follows, $k_0 = E_\mathbf{k} = \sqrt{\mathbf{k}^2 + m^2}$. The completeness relation takes the form

$$\int \frac{d\mathbf{k}}{(2\pi)^3 2E_\mathbf{k}} |\mathbf{k}\rangle\langle\mathbf{k}| = 1.$$

An arbitrary "single-particle" spin-free state $|a\rangle$ may be presented as an expansion in the full set of states $|\mathbf{k}\rangle$ (i.e., as a *wave packet*):

$$|a\rangle = \int \frac{d\mathbf{k}}{(2\pi)^3 \sqrt{2E_\mathbf{k}}} \psi_\mathrm{p}(\mathbf{k}) |\mathbf{k}\rangle, \quad \psi_\mathrm{p}(\mathbf{k}) = \frac{\langle \mathbf{k}|a\rangle}{\sqrt{2E_\mathbf{k}}}. \tag{82}$$

State $|a\rangle$ may be expanded in eigenstates of any other self-adjoint operator (e.g., 3-dimensional coordinate operator $\hat{\mathbf{X}} = (\hat{X}_1, \hat{X}_2, \hat{X}_3)$ $(\hat{X}_i |\mathbf{x}\rangle = x_i |\mathbf{x}\rangle$, $i = 1,2,3)$). Choosing the $\langle \mathbf{y}|\mathbf{x}\rangle = \delta(\mathbf{y} - \mathbf{x})$ norm for $|\mathbf{x}\rangle$, which gives $\int d\mathbf{x} |\mathbf{x}\rangle\langle\mathbf{x}| = 1$, we write

$$|a\rangle = \int d\mathbf{x} \psi_\mathrm{x}(\mathbf{x}) |\mathbf{x}\rangle, \quad \psi_\mathrm{x}(\mathbf{x}) = \langle \mathbf{x}|a\rangle. \tag{83}$$

Since operator $\hat{\mathbf{P}}$ acting on state $\langle \mathbf{x}|$ is written as $-i\nabla_\mathbf{x}$,

$$\mathbf{k}\langle \mathbf{x}|\mathbf{k}\rangle = \langle \mathbf{x}|\hat{\mathbf{P}}|\mathbf{k}\rangle = -i\nabla_\mathbf{x} \langle \mathbf{x}|\mathbf{k}\rangle.$$

Taking into consideration the chosen norms, we find that $\langle \mathbf{x}|\mathbf{k}\rangle = \sqrt{2E_\mathbf{k}} e^{i\mathbf{kx}}$. Therefore,

$$|\mathbf{x}\rangle = \int \frac{d\mathbf{k} e^{-i\mathbf{kx}}}{(2\pi)^3 \sqrt{2E_\mathbf{k}}} |\mathbf{k}\rangle, \quad |\mathbf{k}\rangle = \sqrt{2E_\mathbf{k}} \int d\mathbf{x} e^{+i\mathbf{kx}} |\mathbf{x}\rangle. \tag{84}$$

Thus, functions $\psi_\mathrm{p}(\mathbf{k})$ and $\psi_\mathrm{x}(\mathbf{x})$ are the Fourier transforms of each other:

$$\begin{aligned} \psi_\mathrm{x}(\mathbf{x}) &= \int \frac{d\mathbf{k}}{(2\pi)^3} e^{+i\mathbf{kx}} \psi_\mathrm{p}(\mathbf{k}), \\ \psi_\mathrm{p}(\mathbf{k}) &= \int d\mathbf{x} e^{-i\mathbf{kx}} \psi_\mathrm{x}(\mathbf{x}). \end{aligned} \tag{85}$$

The following relations will also be of use in subsequent analysis:

$$\begin{aligned} \frac{\partial |\mathbf{x}\rangle}{\partial \mathbf{x}} &= -i \int \frac{d\mathbf{k} e^{-i\mathbf{kx}}}{(2\pi)^3 \sqrt{2E_\mathbf{k}}} \mathbf{k} |\mathbf{k}\rangle, \\ \frac{\partial |\mathbf{k}\rangle}{\partial \mathbf{k}} &= \frac{\mathbf{v}_\mathbf{k}}{2E_\mathbf{k}} |\mathbf{k}\rangle + i\sqrt{2E_\mathbf{k}} \int d\mathbf{x} e^{+i\mathbf{kx}} \mathbf{x} |\mathbf{x}\rangle. \end{aligned} \tag{86}$$

The norm of state $|a\rangle$ takes the form

$$\langle a|a\rangle = \int \frac{d\mathbf{k}}{(2\pi)^3} |\psi_\mathrm{p}(\mathbf{k})|^2 = \int d\mathbf{x} |\psi_\mathrm{x}(\mathbf{x})|^2. \tag{87}$$

If $\psi_\mathrm{x}(\mathbf{x})$ is a real function, WP $|a\rangle$ has mean coordinate $\langle \mathbf{x}_a \rangle = 0$ at $t = 0$. A WP with three-dimensional coordinate $\langle \mathbf{x}_a \rangle$, which is, in the general case, nonzero, at time t_a is needed for further calculations. To obtain it, one just needs to apply translation operator $e^{i\hat{P}x_a}$ to state $|a\rangle$:

$$\begin{aligned} |a\rangle \to |\mathbf{p}_a, x_a\rangle &= e^{i\hat{P}x_a} |a\rangle \\ &= \int \frac{d\mathbf{k}}{(2\pi)^3 \sqrt{2E_\mathbf{k}}} e^{ikx_a} \psi_\mathrm{p}(\mathbf{k}, \mathbf{p}_a) |\mathbf{k}\rangle, \end{aligned} \tag{88}$$

where wave function $\psi_{\rm p}(\mathbf{k}, \mathbf{p}_a)$ depends both on a variable (vector $\mathbf{k}$) and on a parameter (mean momentum vector $\mathbf{p}_a$). Function $\psi_{\rm p}(\mathbf{k}, \mathbf{p}_a)$ is also characterized by dispersion parameter σ in the momentum space. For convenience, we require that the WP evolve into a state with definite momentum at $\sigma \to 0$: $\lim_{\sigma\to 0}|\mathbf{p}_a, x_a\rangle = |\mathbf{p}_a\rangle$. This implies that factor $e^{-ip_a x_a}$ is present in wave function $\psi_{\rm p}(\mathbf{k})$ to compensate factor e^{ikx_a}. In what follows, the presence of this factor is assumed for a unique transition to the plane-wave limit to exist. However, since this factor is constant, it exerts no influence on the predicted number of interactions. Therefore, to avoid overcomplicating the formulas, we omit such factors.

It is convenient to rewrite wave function $\psi_{\rm p}(\mathbf{k}, \mathbf{p}_a)$ in the $\psi_{\rm p}(\mathbf{k}, \mathbf{p}_a) = \phi(\mathbf{k}, \mathbf{p}_a)/\sqrt{2E_{\mathbf{k}}}$ form to determine its transformation properties. Using the transformation properties of the state $|\mathbf{k}\rangle = \sqrt{2E_{\mathbf{k}}}a^{\dagger}_{\mathbf{k}}|0\rangle$ in responce of the Lorentz transformation

$$|\mathbf{k}\rangle \to U(\Lambda)|\mathbf{k}\rangle = |\Lambda\mathbf{k}\rangle, \quad k \to \Lambda k, \tag{89}$$

where $U(\Lambda)$ is a unitary operator, one readily sees that function $\phi(\mathbf{k}, \mathbf{p}_a)$ is a relativistic invariant:

$$\phi(\mathbf{k}', \mathbf{p}'_a) = \phi(\mathbf{k}, \mathbf{p}_a) \quad (k' = \Lambda k, p'_a = \Lambda p_a). \tag{90}$$

The state in (88) may be expressed in terms of Lorentz-invariant function $\phi(\mathbf{k}, \mathbf{p}_a)$ (form factor):

$$|\mathbf{p}_a, x_a\rangle = \int \frac{d\mathbf{k}}{(2\pi)^3 2E_{\mathbf{k}}} e^{-ikx_a}\phi(\mathbf{k}, \mathbf{p}_a)|\mathbf{k}\rangle. \tag{91}$$

The wave function in the configuration space corresponding to the state in (88) is

$$\begin{aligned}\psi_{{\rm x},a}(\mathbf{x}) &\equiv \psi_{\rm x}(\mathbf{x}, x_a, \mathbf{p}_a)\\ &= \int \frac{d\mathbf{k}}{(2\pi)^3} e^{-i\left[\mathbf{k}(\mathbf{x}+\mathbf{x}_a)-k^0 x_a^0\right]}\psi_{\rm p}(\mathbf{k}, \mathbf{p}_a).\end{aligned} \tag{92}$$

We prefer not to equate the norm of state

$$\begin{aligned}\langle a|a\rangle \equiv \langle \mathbf{p}_a, x_a|\mathbf{p}_a, x_a\rangle &= \int \frac{d\mathbf{k}}{(2\pi)^3}\left|\psi_{\rm p}(\mathbf{k}, \mathbf{p}_a)\right|^2\\ &= \int \frac{d\mathbf{k}}{(2\pi)^3 2E_{\mathbf{k}}}|\phi(\mathbf{k}, \mathbf{p}_a)|^2\end{aligned} \tag{93}$$

to unity in the present study, although this appears to be natural. The theoretical model with a WP in quantum theory, where a limiting transition to the ordinary state with definite momentum and norm $\langle \mathbf{q}|\mathbf{k}\rangle = (2\pi)^3 2E_{\mathbf{k}}\delta^3(\mathbf{q}-\mathbf{k})$ exists, is considered here. This norm is often substituted in handbooks with $2E_{\mathbf{k}}V$, where V is a "certain infinitely large spatial volume." In order to obtain a correct limiting transition of our formalism to the common plane-wave one, we define the Lorentz-invariant norm of state in (93) as $\langle a|a\rangle = 2m\mathrm{V}_\star$, where $\mathrm{V}_\star$ is a finite quantity with a dimension of volume, which is defined uniquely by the WP form factor. Its explicit form is derived in Section 4.2.

Note on "hidden variables." If WP $|\mathbf{p}, x\rangle$ is treated as a physical quantum state produced in collisions or decays of other particles, function $\phi(\mathbf{k}, \mathbf{p})$ is expected to depend parametrically on 4-momenta $Q_\varkappa$ of the primary and, possibly, secondary particles involved in the process of WP production[3]. In the most general case, the set of parent and accompanying daughter particles includes particles from the *entire chain* of reactions and decays leading to the production of state $|\mathbf{p}, x\rangle$ (see Fig. 1). "Hidden variables" $Q_\varkappa$ may enter scalar function $\phi(\mathbf{k}, \mathbf{p})$ only in the form of scalar products $(Q_\varkappa k)$, $(Q_\varkappa p)$, and $(Q_\varkappa Q_{\varkappa'})$. If one considers the expected properties of function $\phi(\mathbf{k}, \mathbf{p})$, it should be positively defined around $\mathbf{k} = \mathbf{p}$ and satisfy the following conditions:

$$\begin{aligned}\left[\frac{\partial\phi(\mathbf{k}, \mathbf{p})}{\partial k_l}\right]_{\mathbf{k}=\mathbf{p}} &= \left[\frac{\partial(k-p)^2}{\partial k_l}\frac{\partial\phi(\mathbf{k}, \mathbf{p})}{\partial(k-p)^2}\right]_{\mathbf{k}=\mathbf{p}}\\ &+ \sum_\varkappa\left[\frac{\partial(Q_\varkappa k)}{\partial k_l}\frac{\partial\phi(\mathbf{k}, \mathbf{p})}{\partial(Q_\varkappa k)}\right]_{\mathbf{k}=\mathbf{p}}\\ = \sum_\varkappa Q^0_\varkappa\left(\frac{p_l}{p^0} - \frac{Q_l}{Q^0_\varkappa}\right)&\left[\frac{\partial\phi(\mathbf{k}, \mathbf{p})}{\partial(Q_\varkappa k)}\right]_{\mathbf{k}=\mathbf{p}} = 0 \quad (l = 1, 2, 3).\end{aligned}$$

The last equations are satisfied *identically* only in the nonphysical case when the most probable velocities of all packets $\varkappa$ are the same ($\mathbf{Q}_\varkappa/Q^0_\varkappa = \mathbf{p}/E_{\mathbf{p}}$). In view of this fact and the arbitrariness of configurations of 4-momenta $\{Q_\varkappa\}$, we conclude that $\left[\partial\phi(\mathbf{k}, \mathbf{p})/\partial(Q_\varkappa k)\right]_{\mathbf{k}=\mathbf{p}} = 0$. In much the same fashion, we find that $\left[\partial\phi(\mathbf{k}, \mathbf{p})/\partial(Q_\varkappa p)\right]_{\mathbf{p}=\mathbf{k}} = 0$. Thus, the dependence of $\phi(\mathbf{k}, \mathbf{p})$ on scalar products $(Q_\varkappa k)$ and $(Q_\varkappa p)$ should vanish at least near the maximum of function $\phi(\mathbf{k}, \mathbf{p})$. Postulating analyticity of function $\phi(\mathbf{k}, \mathbf{p})$ in the vicinity of its maximum ($\mathbf{k} = \mathbf{p}$), we find that $\phi(\mathbf{k}, \mathbf{p})$ in the neighborhood of this point may depend on 4-momenta $Q_\varkappa$ only via invariants

$$\begin{gathered}g^{\mu\nu}(k-p)_\mu(k-p)_\nu, \quad G_2^{\mu\nu}(k-p)_\mu(k-p)_\nu,\\ G_3^{\mu\nu\lambda}(k-p)_\mu(k-p)_\nu(k-p)_\lambda, \ldots,\end{gathered} \tag{94}$$

where g is the metric tensor and G_2, G_3, G_4, etc. are tensors constructed from the components of 4-vectors $Q_\varkappa$. Since we consider only very narrow packets ("smoothed" δ-functions), the behavior of $\phi(\mathbf{k}, \mathbf{p})$ in the vicinity of the maximum is of interest. Thus, this function should include only "building blocks" (94).

[3] The packet evolution under the influence of external fields is incorporated into this representation, since any interaction in the S-matrix QFT formalism should be regarded as a local interaction of real or virtual fields.

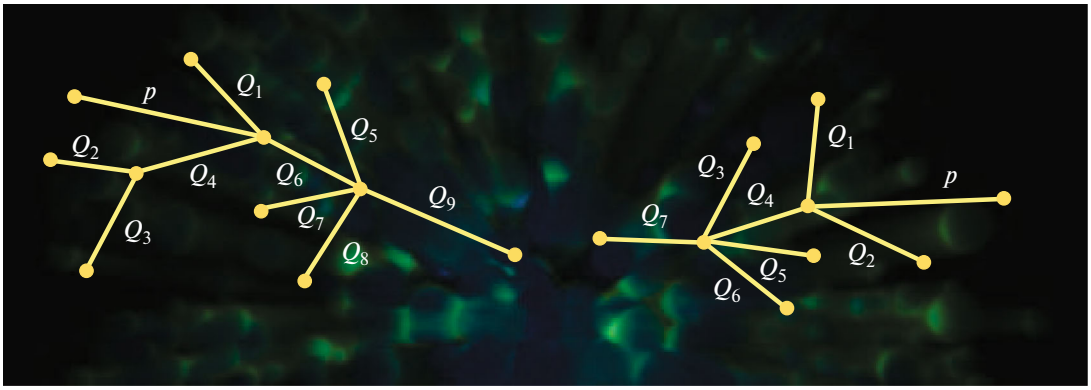

Fig. 1. Schematic illustration of chains of WP production processes.

The remaining scalar products $(Q_\varkappa Q_{\varkappa'})$ may be incorporated into the definition of scalar parameters σ_i, which determine the explicit form of $\phi(\mathbf{k}, \mathbf{p})$; in other words, these parameters, in the general case, may be not just constants, but scalar functions of 4-momenta of particles $\varkappa$ involved in the processes forming the WP. Therefore, WPs produced in different reactions and decays (or chains of reactions and decays) and constructed from identical single-particle states $|\mathbf{p}\rangle$ *are, strictly speaking, not identical.* As a result, the quantum statistics of such "packets with memory" may differ greatly from the statistics of their elementary components (states with definite momenta).

To avoid unnecessary (though by no means fatal) overcomplication of the formalism, we sacrifice generality and assume that parameters σ_i are effective constants. In addition, we limit ourselves to the simplest "memoryless"[4] WPs, which are independent of tensors G_i and, consequently, of hidden variables. Undoubtedly, the issue outlined here is not specific to our approach, but is often disregarded or intentionally ignored in postulating the WP properties.

Correspondence principle and normalization of a wave packet. We require that the state in (91) turn into $|\mathbf{p}\rangle$ in the plane-wave limit. This condition is called here the correspondence principle:

$$\lim_{\sigma\to 0}\phi(\mathbf{k},\mathbf{p}) = (2\pi)^3 2E_{\mathbf{p}}\delta^3(\mathbf{k}-\mathbf{p}).$$

Note that the dimensionless Lorentz-invariant integral

$$\int\frac{d\mathbf{k}\phi(\mathbf{k},\mathbf{p})}{(2\pi)^3 2E_{\mathbf{k}}} = \int\frac{d\mathbf{k}'\phi(\mathbf{k}',\mathbf{p}')}{(2\pi)^3 2E_{\mathbf{k}'}}$$

is independent of $\mathbf{p}$ and, consequently, may depend only on parameter σ and mass m. However, in accordance with the condition in (4.3), the considered integral tends to unity in the $\sigma = 0$ limit. Therefore, it is also natural to set it equal to unity at a finite small σ:

$$\int\frac{d\mathbf{k}\phi(\mathbf{k},\mathbf{p})}{(2\pi)^3 2E_{\mathbf{k}}} = \int\frac{d\mathbf{k}\phi(\mathbf{k},0)}{(2\pi)^3 2E_{\mathbf{k}}} = 1. \qquad (95)$$

Although this technical condition is not required, it provides a practically convenient norm of form factors $\phi(\mathbf{k}, \mathbf{p})$.

Certain general properties of a wave packet. **The following are the key properties of a WP:**

(1) Since the invariance of $\phi(\mathbf{k}, \mathbf{p}_a)$ with respect to rotations $\mathbf{k} \mapsto \mathbf{k}' = \mathbf{O}\mathbf{k}$, $\mathbf{p}_a \mapsto \mathbf{p}'_a = \mathbf{O}\mathbf{p}_a$ is a special case of (90), functions $\psi_{\mathrm{p}}(\mathbf{k}, \mathbf{p}_a)$ and $\psi_{\mathrm{x}}(\mathbf{x}, x_a, \mathbf{p}_a)$ are also rotationally invariant.

(2) The modulus of function $\psi_{\mathrm{x}}(\mathbf{x}, x_a, \mathbf{p}_a)$ is also invariant with respect to spatial translations but is not invariant with respect to temporal ones.

(3) It follows from (92) that $|\psi_{\mathrm{x}(}\mathbf{x}, x_a, \mathbf{p}_a)| \to 0$ at $|x_a^0| \to \infty$; i.e., a WP spreads with time in the configuration space.

(4) Since $|\psi_{\mathrm{x}}(\mathbf{x}, x_a, \mathbf{p}_a)|$ is independent of $\mathbf{x}_a$, one can conclude that $\mathbf{x}_a$ is the center of spherical symmetry of a packet. In what follows, we call this point the packet center.

(5) It follows from (90) that function $\phi(\mathbf{k}, \mathbf{p})$ may depend only on Lorentz-invariant quantity kp. Therefore, function $\phi(\mathbf{k}, \mathbf{p})$ is symmetric with respect to permutation of its arguments; i.e., $\phi(\mathbf{k}, \mathbf{p}) = \phi(\mathbf{p}, \mathbf{k})$.

(6) It is also evident that $\phi(\mathbf{k}, 0) = \phi(0, \mathbf{k}) = \tilde{\phi}(k_0)$, where $\tilde{\phi}(k_0)$ is the rotationally invariant function of a single variable $k_0 = E_{\mathbf{k}}$.

(7) Another simple and important corollary of (90) is the independence of norm (93) of both space-time coordinate x_a and momentum $\mathbf{p}_a$.

[4] A more complex WP model was examined in [100].

4.2. Mean Four-Momentum

Let us now find the mean values of components of 4-momentum $\langle P\rangle = (\langle P_0\rangle, \langle \mathbf{P}\rangle)$ of a packet, which are defined by the standard quantum-mechanical rule

$$\langle P_\mu\rangle = \langle P_\mu(\mathbf{p}_a)\rangle = \frac{\langle \mathbf{p}_a, x_a|\hat{P}_\mu|\mathbf{p}_a, x_a\rangle}{\langle \mathbf{p}_a, x_a|\mathbf{p}_a, x_a\rangle}.$$

Inserting (88) into this equation, we find

$$\langle P_\mu(\mathbf{p})\rangle = \frac{1}{2m\mathrm{V}_\star}\int \frac{d\mathbf{k}\,|\phi(\mathbf{k},\mathbf{p})|^2}{(2\pi)^3 2E_\mathbf{k}} k_\mu, \tag{96}$$

where denominator $2m\mathrm{V}_\star$ is equal to the norm of state $|\mathbf{p}_a, x_a\rangle$:

$$\begin{aligned} 2m\mathrm{V}_\star &= \int \frac{d\mathbf{k}|\phi(\mathbf{k},\mathbf{p})|^2}{(2\pi)^3 2E_\mathbf{k}} = \int \frac{d\mathbf{k}|\phi(\mathbf{k},0)|^2}{(2\pi)^3 2E_\mathbf{k}} \\ &= \frac{1}{4\pi^2}\int_m^\infty dk_0\sqrt{k_0^2-m^2}\,|\tilde{\phi}(k_0)|^2. \end{aligned} \tag{97}$$

Here and elsewhere, index a of variables $\mathbf{p}_a$ and x_a is omitted for brevity (if this does not lead to misunderstanding). Formulas (96) and (97) demonstrate that mean 4-momentum $\langle P\rangle$ is an integral of motion, and quantity $\mathrm{V}_\star$, which has the dimension of spatial volume, is completely independent of the momentum and the space-time coordinate.

In view of the $\phi(\mathbf{k},0)$ function's parity, it follows from (96) that $\langle \mathbf{P}(0)\rangle = 0$; in other words, the mean momentum turns to zero in the intrinsic frame of reference of the packet[5], which is defined by condition $\mathbf{p} = 0$. Therefore, the mean (effective) mass of a packet, $\langle m\rangle$, is equal to its mean energy (the zeroth component of 4-vector $\langle P\rangle$ in this frame):

$$\begin{aligned} \langle m\rangle &= \langle P_0(0)\rangle = \int \frac{d\mathbf{k}\,|\phi(\mathbf{k},0)|^2}{4(2\pi)^3 m\mathrm{V}_\star} \\ &= \frac{1}{8\pi^2 m\mathrm{V}_\star}\int_m^\infty dk_0 k_0\sqrt{k_0^2-m^2}\,|\tilde{\phi}(k_0)|^2. \end{aligned} \tag{98}$$

Using (97) and writing (88) as

$$\frac{\langle m\rangle}{m} = \frac{\int_m^\infty dk_0 k_0\sqrt{k_0^2-m^2}\,|\tilde{\phi}(k_0)|^2}{\int_m^\infty dk_0 m\sqrt{k_0^2-m^2}\,|\tilde{\phi}(k_0)|^2}, \tag{99}$$

we find that $\langle m\rangle \geq m$ with equality $\langle m\rangle = m$ attained only in the plane-wave limit; i.e., WP $|\mathbf{p}, x\rangle$ is "heavier" than its component states with definite momenta. This effect is of a general nature and is a manifestation of mass nonadditivity. In the case under consideration, it is attributable to the fact that the components of momenta of Fock states $|\mathbf{k}\rangle$ transverse to vector $\mathbf{p}$, which are constituent parts of the WP, do not contribute to the mean momentum value $(\mathbf{p}\times\bar{\mathbf{P}} = 0)$, but produce a nonnegative contribution to the mean packet energy[6]. Note that the mean value of the mass *squared* is m^2; thus, $\langle P\rangle^2 \geq \langle P^2\rangle = m^2$.

Let us demonstrate that the packet is, on the average, on the mass shell. It follows from the dimensional considerations mentioned above that $\langle P_0\rangle = \kappa E_\mathbf{p}$ and $\langle \mathbf{P}\rangle = \kappa'\mathbf{p}$, where κ and κ' are certain dimensionless quantities independent of $\mathbf{p}$. We then obtain from (96) the following relation:

$$\begin{aligned} p^\mu\langle P_\mu\rangle &= \kappa E_\mathbf{p}^2 - \kappa'\mathbf{p}^2 \\ &= \kappa m^2 + (\kappa-\kappa')\mathbf{p}^2 = \frac{1}{2m\mathrm{V}_\star}\int \frac{d\mathbf{k}(pk)|\phi(\mathbf{k},\mathbf{p})|^2}{(2\pi)^3 2E_\mathbf{k}}. \end{aligned} \tag{100}$$

Since the left-hand and the right-hand expressions in (100) are Lorentz-invariant, $\kappa = \kappa'$. Setting $\mathbf{p} = 0$ in (100) and using the definition in (98) we find $\kappa = \langle m\rangle/m \geq 1$. This proves that

$$\langle P\rangle = (\langle P_0\rangle, \langle \mathbf{P}\rangle) = (\langle m\rangle/m)(\mathbf{p}, E_\mathbf{p})$$
$$\text{and}\quad \langle P\rangle^2 = \langle P_\mu\rangle\langle P^\mu\rangle = \langle m\rangle^2.$$

It follows from these relations that group velocity $\nabla_{\langle\mathbf{P}\rangle}\langle P_0\rangle = \langle\mathbf{P}\rangle/\langle P_0\rangle$ of the packet is the same as its most probable velocity $\mathbf{v}_\mathbf{p} = \mathbf{p}/E_\mathbf{p}$.

4.3. Wave Packet for a Fermion

Wave packets of fermions with single-particle Fock states of the form $|\mathbf{k}, s\rangle = \sqrt{2E_\mathbf{k}}a^\dagger_{\mathbf{k}s}|0\rangle$ with Lorentz-invariant norm $\langle \mathbf{q}, r|\mathbf{k}, s\rangle = (2\pi)^3 2E_\mathbf{k}\delta_{sr}\delta(\mathbf{k}-\mathbf{q})$ are needed for further calculations within the S-matrix QFT formalism. Operators $a^\dagger_{\mathbf{k}s}$ and $a_{\mathbf{k}s}$ are standard creation and annihilation operators for a particle with mass $m > 0$, 3-momentum $\mathbf{k}$, and spin projection s. They satisfy the following anticommutation relations:

$$\{a_{\mathbf{q}r}, a_{\mathbf{k}s}\} = \{a^\dagger_{\mathbf{q}r}, a^\dagger_{\mathbf{k}s}\} = 0,$$
$$\{a_{\mathbf{q}r}, a^\dagger_{\mathbf{k}s}\} = (2\pi)^3\delta_{sr}\delta(\mathbf{k}-\mathbf{q}).$$

Let us construct a relativistic fermion WP, which is a state localized in the configuration and momentum spaces that features transformation properties similar to those of Fock states and evolves into a Fock state in the plane-wave limit. Similar to a scalar particle, a WP

[5] This also follows from simple dimensional considerations: since 3-vector $\bar{\mathbf{P}}$ depends on just a single vector quantity $\mathbf{p}$, $\langle\mathbf{P}\rangle \propto \mathbf{p}$.

[6] This is similar in certain respects to the following well-known relativistic effect: the mass of gas in a vessel increases in the process of its (uniform) heating. The vessel acquires no additional momentum, but the internal energy and, consequently, the mass of gas increase.

is characterized here by the most probable 3-momentum $\mathbf{p}$ and spin projection s. The most general construction of this type at a fixed point in time takes the form

$$\int \frac{d\mathbf{k}}{(2\pi)^3 2E_{\mathbf{k}}} \sum_r \Phi_{sr}(\mathbf{k},\mathbf{p};\sigma)|\mathbf{k},r\rangle, \qquad (101)$$

where functions $\Phi_{sr}(\mathbf{k},\mathbf{p};\sigma)$ depend both on momentum and discrete spin variables and on a set (finite or infinite) parameters $\boldsymbol{\sigma} = \{\sigma_1, \sigma_2, \ldots\}$, which are independent of these variables and specify the properties of the packet. By definition, momenta $\mathbf{p}$ and $\mathbf{k}$ lie on the mass shell; i.e., $E_{\mathbf{p}}^2 - \mathbf{p}^2 = E_{\mathbf{k}}^2 - \mathbf{k}^2 = m^2$. We require that state (101) evolve into $|\mathbf{p},s\rangle$ in the plane-wave limit. Since one can always define parameters σ_i in such a way that they satisfy this limit at $\sigma_i \to 0$ $(\forall i)$, we may formulate a simple correspondence principle:

$$\lim_{\sigma\to 0} \Phi_{sr}(\mathbf{k},\mathbf{p};\sigma) = (2\pi)^3 2E_{\mathbf{p}} \delta_{sr} \delta(\mathbf{k}-\mathbf{p}).$$

Since the right-hand side of this equation is a relativistic scalar, it is natural to assume that functions Φ_{sr} are also scalars and $|\Phi_{sr}| \ll |\Phi_{ss}|$ at $r \neq s$. Assuming that parameters σ_i are sufficiently small, one may summarize these requirements using the following simple *ansatz*:

$$\Phi_{sr}(\mathbf{k},\mathbf{p};\boldsymbol{\sigma}) = \delta_{sr}\phi(\mathbf{k},\mathbf{p};\boldsymbol{\sigma}),$$

where $\phi(\mathbf{k},\mathbf{p};\boldsymbol{\sigma})$ is a spin-independent function such that

$$\phi(\mathbf{k}',\mathbf{p}';\boldsymbol{\sigma}) = \phi(\mathbf{k},\mathbf{p};\boldsymbol{\sigma}) \quad (p' = \Lambda p, k' = \Lambda k),$$

and

$$\lim_{\sigma\to 0} \phi(\mathbf{k},\mathbf{p};\boldsymbol{\sigma}) = (2\pi)^3 2E_{\mathbf{p}} \delta(\mathbf{k}-\mathbf{p}). \qquad (102)$$

Thus, if at least some parameters σ_i in set $\boldsymbol{\sigma}$ are nonzero (and all of them are sufficiently small), function $\phi(\mathbf{k},\mathbf{p};\boldsymbol{\sigma})$ is (to within a factor) a "smeared" δ-function in the momentum space. More precisely, as in the quantum-mechanical case, we assume that $|\phi(\mathbf{k},\mathbf{p};\boldsymbol{\sigma})|$ has a peak at $\mathbf{k} = \mathbf{p}$ and decreases rapidly outside the small neighborhood of this point. In order to simplify notation, we do not specify the explicit dependence of $\phi(\mathbf{k},\mathbf{p};\boldsymbol{\sigma})$ on parameter set $\boldsymbol{\sigma}$ in subsequent analysis and write expression (101) in the form

$$\int \frac{d\mathbf{k}}{(2\pi)^3 2E_{\mathbf{k}}} \phi(\mathbf{k},\mathbf{p})|\mathbf{k},s\rangle. \qquad (103)$$

The WP in (103) characterizes a state with spin projection s, the most probable momentum $\mathbf{p}$, and a mean three-dimensional coordinate of the packet center that is equal to zero at time $t = 0$. To set the initial state of a WP, one just needs to define its mean coordinate at an arbitrary fixed time point. It makes no difference whether this point is located in the future or past relative to $t = 0$, since the temporal evolution of a WP allows one to reconstruct its trajectory at any time point. For visual convenience (more specifically, for objects emerging in the formalism to have an explicitly translation-invariant form [$\psi(x-y)$ rather than $\psi(x+y)$]), we set the initial condition for a WP with mean three-dimensional coordinate $(-\mathbf{x})$ at a certain time point $(-x^0)$ located in a sufficiently distant past; i.e., we use transformation $|\mathbf{p},s\rangle \mapsto e^{+i\hat{P}x}|\mathbf{p},s\rangle$, which yields the following expression for a WP at an arbitrary space-time point x:

$$|\mathbf{p},s,x\rangle = \int \frac{d\mathbf{k}}{(2\pi)^3 2E_{\mathbf{k}}} e^{+ikx} \phi(\mathbf{k},\mathbf{p})|\mathbf{k},s\rangle. \qquad (104)$$

Coordinate representation. Let us consider a free fermion field with spin $\frac{1}{2}$ and a field operator of the following form:

$$\Psi(y) = \int \frac{d\mathbf{k}}{(2\pi)^3 \sqrt{2E_{\mathbf{k}}}} \sum_s \left[a_{\mathbf{k}s} u_s(\mathbf{k}) e^{-iky} + b^\dagger_{\mathbf{k}s} v_s(\mathbf{k}) e^{iky}\right].$$

State $\langle 0|\Psi(y)$ is often called the state of a fermion with definite coordinate. This is suggested by the following elementary calculation:

$$\langle 0|\Psi(y)|\mathbf{p},s\rangle = u_s(\mathbf{p}) e^{-ipy}, \qquad (105)$$

yielding a plane wave e^{-ipy} multiplied by spinor $u_s(\mathbf{p})$. In much the same fashion, we define coordinate wave function

$$\langle 0|\Psi(y)|\mathbf{p},s,x\rangle = \int \frac{d\mathbf{k}}{(2\pi)^3 2E_{\mathbf{k}}} u_s(\mathbf{k}) e^{-ik(y-x)} \times \phi(\mathbf{k},\mathbf{p}) \simeq u_s(\mathbf{p})\psi(\mathbf{p}, y-x), \qquad (106)$$

where the approximate equality corresponds to narrow packets. The condition of applicability of this approximation may be written as

$$|i\nabla_{\mathbf{y}} \ln \psi(\mathbf{p}, x-y) + \mathbf{p}| \ll 2E_{\mathbf{p}}. \qquad (107)$$

Lorentz-invariant function ψ is defined as follows:

$$\psi(\mathbf{p},x) \equiv \psi(\mathbf{p},x_0,\mathbf{x}) = \int \frac{d\mathbf{k}}{(2\pi)^3 2E_{\mathbf{k}}} \phi(\mathbf{k},\mathbf{p}) e^{-ikx}. \qquad (108)$$

It is evident that the function in (108) satisfies (at any $\mathbf{p}$) the Klein–Gordon equation

$$(\partial^2 + m^2)\psi(\mathbf{p},x) = 0,$$

i.e., it is a relativistic WP in terms of the standard QFT scattering theory. It is also clear that, under the assumptions made above, function $\psi(\mathbf{p},x)$ depends only on two independent scalar variables x^2 and (px).

Scalar function ψ remains unchanged after the transition to the intrinsic frame of reference of a packet ($\mathbf{p}_\star = 0$); i.e.,

$$\psi(\mathbf{p}, x) = \int \frac{d\mathbf{k}}{(2\pi)^3 2E_\mathbf{k}} \varphi(\mathbf{k}, 0) e^{-ikx_\star} = \psi(0, x_\star), \quad (109)$$

where 4-vector $x_\star = (x^0_\star, \mathbf{x}_\star)$ is related to $x = (x^0, \mathbf{x})$ by the Lorentz transformation along the $-\mathbf{p}$ direction (from the laboratory frame to the intrinsic frame),

$$\begin{aligned} x^\star_0 &= \Gamma_\mathbf{p}(x_0 - \mathbf{v}_\mathbf{p}\mathbf{x}), \\ \mathbf{x}^\star &= \mathbf{x} + \Gamma_\mathbf{p}\left[\frac{\Gamma_\mathbf{p}(\mathbf{v}_\mathbf{p}\mathbf{x})}{\Gamma_\mathbf{p} + 1} - x_0\right]\mathbf{v}_\mathbf{p}, \end{aligned} \quad (110a)$$

and $\Gamma_\mathbf{p} = E_\mathbf{p}/m = 1/\sqrt{1 - \mathbf{v}^2_\mathbf{p}}$ is the Lorentz factor of the packet. Since $\psi(0, x_\star)$ is an even function of variable $\mathbf{x}_\star$, it can depend only on variables $x^0_\star$ and $|\mathbf{x}_\star|$, which are expressed in terms of invariants (px) and x^2 in the following way:

$$\begin{aligned} x^0_\star &= \frac{(px)}{m}, \quad |\mathbf{x}_\star|^2 = (x^0_\star)^2 - x^2 \\ &= \frac{1}{m^2}\left[(px)^2 - m^2x^2\right]. \end{aligned} \quad (110b)$$

Using (110a) and (110b), one can easily verify that

$$\begin{aligned} |\mathbf{x}^\star| &= \Gamma_\mathbf{p}\sqrt{(\mathbf{x} - \mathbf{v}_\mathbf{p}x_0)^2 - (\mathbf{v}_\mathbf{p} \times \mathbf{x})^2} \\ &= \frac{1}{m}\sqrt{(E_\mathbf{p}\mathbf{x} - \mathbf{p}x_0)^2 - (\mathbf{p} \times \mathbf{x})^2}. \end{aligned} \quad (111)$$

Effective volume of a wave packet. According to the adopted WP normalization in (95), dimensionless function $\psi(\mathbf{p}, x)$ is not a normalized wave function. This allows one to interpret

$$\mathrm{V}(\mathbf{p}) \overset{\text{def}}{=} \int d\mathbf{x}|\psi(\mathbf{p}, x)|^2 = \int \frac{d\mathbf{k}}{(2\pi)^3}\frac{|\phi(\mathbf{k}, \mathbf{p})|^2}{(2E_\mathbf{k})^2} = \frac{\mathrm{V}(0)}{\Gamma_\mathbf{p}} \quad (112)$$

as a three-dimensional volume in space occupied by the WP. The narrower the WP in the momentum space, the more accurate the above interpretation. The state norm in this approximation may be written as

$$\begin{aligned} \langle p, x|\, p, x\rangle &= \int \frac{d\mathbf{k}|\phi(\mathbf{k}, \mathbf{p})|^2}{(2\pi)^3 2E_\mathbf{k}} \\ &\simeq 2\langle E_\mathbf{p}\rangle \int \frac{d\mathbf{k}|\phi(\mathbf{k}, \mathbf{p})|^2}{(2\pi)^3 (2E_\mathbf{k})^2} = 2\langle E_\mathbf{p}\rangle \mathrm{V}(\mathbf{p}). \end{aligned} \quad (113)$$

Note that $\mathrm{V}_\star \neq \mathrm{V}(0)$ in the general case.

4.4. Commutator Function

It is convenient to introduce an auxiliary WP creation operator:

$$A^\dagger_{\mathbf{p}s}(x) = \int \frac{d\mathbf{k}\phi(\mathbf{k}, \mathbf{p})e^{ikx}}{(2\pi)^3\sqrt{2E_\mathbf{k}2E_\mathbf{p}}} a^\dagger_{\mathbf{k}r}, \quad (114)$$

which provides an opportunity to rewrite the state in (103) in the form similar to the plane-wave limit,

$$|\mathbf{p}, s, x\rangle = \sqrt{2E_\mathbf{p}} A^\dagger_{\mathbf{p}s}(x)|0\rangle. \quad (115)$$

Naturally, $A^\dagger_{\mathbf{p}s}(x)$ turns into $a^\dagger_{\mathbf{p}s}$ in the $\sigma \to 0$ limit.

The following (anti)commutation relations are easy to derive from the definition of operators $A_{\mathbf{p}s}(x)$ and $A^\dagger_{\mathbf{p}s}(x)$:

$$\left\{a_{\mathbf{q}r}, A^\dagger_{\mathbf{p}s}(x)\right\} = \delta_{sr}\left(4E_\mathbf{q}E_\mathbf{p}\right)^{-1/2} e^{iqx}\phi(\mathbf{q}, \mathbf{p}), \quad (116a)$$

$$\left\{A_{\mathbf{q}r}(y), A_{\mathbf{p}s}(x)\right\} = \left\{A^\dagger_{\mathbf{q}r}(y), A^\dagger_{\mathbf{p}s}(x)\right\} = 0, \quad (116b)$$

$$\left\{A_{\mathbf{q}r}(y), A^\dagger_{\mathbf{p}s}(x)\right\} = \delta_{sr}\left(4E_\mathbf{q}E_\mathbf{p}\right)^{-1/2} \mathscr{D}(\mathbf{p}, \mathbf{q}; x - y). \quad (116c)$$

Lorentz- and translation-invariant commutator function

$$\mathscr{D}(\mathbf{p}, \mathbf{q}; x - y) = \int \frac{d\mathbf{k}}{(2\pi)^3 2E_\mathbf{k}} \phi(\mathbf{k}, \mathbf{p})\phi^*(\mathbf{k}, \mathbf{q})e^{ik(x-y)}, \quad (117)$$

was introduced here. It follows from (104) and (116c) that

$$\langle \mathbf{q}, r, y|\, \mathbf{p}, s, x\rangle = \delta_{sr}\mathscr{D}(\mathbf{p}, \mathbf{q}; x - y). \quad (118)$$

Certain properties of the commutator function in (117) become especially clear in the center-of-inertia frame of two packets. We denote quantities in this frame by an asterisk subscript or (when it cannot be mistaken for the complex conjugation sign) superscript. Since $\mathbf{p}_* + \mathbf{q}_* = 0$ in the center-of-inertia frame, we have

$$\begin{aligned} &\mathscr{D}(\mathbf{p}_*, -\mathbf{p}_*; x_* - y_*) \\ &= \int \frac{d\mathbf{k}}{(2\pi)^3 2E_\mathbf{k}} \phi(\mathbf{k}, \mathbf{p}_*)\phi^*(\mathbf{k}, -\mathbf{p}_*)e^{ik(x_* - y_*)}. \end{aligned} \quad (119)$$

The characteristic behavior of form factor $\phi(\mathbf{k}, \mathbf{p})$ in the vicinity of $\mathbf{k} = \mathbf{p}$ suggests that the modulus of function $\mathscr{D}(\mathbf{p}_*, -\mathbf{p}_*; x_* - y_*)$ has a sharp maximum at $\mathbf{p}_* = 0$ and vanishes rapidly at larger $|\mathbf{p}_*|$ values, since the maxima of factors $|\phi(\mathbf{k}, \mathbf{p}_*)|$ and $|\phi(\mathbf{k}, -\mathbf{p}_*)|$ in the expression under the integral sign in (119) are widely separated in this case; therefore, their product is small for *any* values of integration variable $\mathbf{k}$. This is illustrated schematically in Fig. 2. It is easy to see that the integral in (119) becomes vanishingly small if points x_* and y_* are widely separated in space (i.e., when the value of $|\mathbf{x}_* - \mathbf{y}_*|$ is large). This is attributable to rapidly oscillating factor $e^{-i\mathbf{k}(\mathbf{x}_* - \mathbf{y}_*)}$ in the integrand in (119).

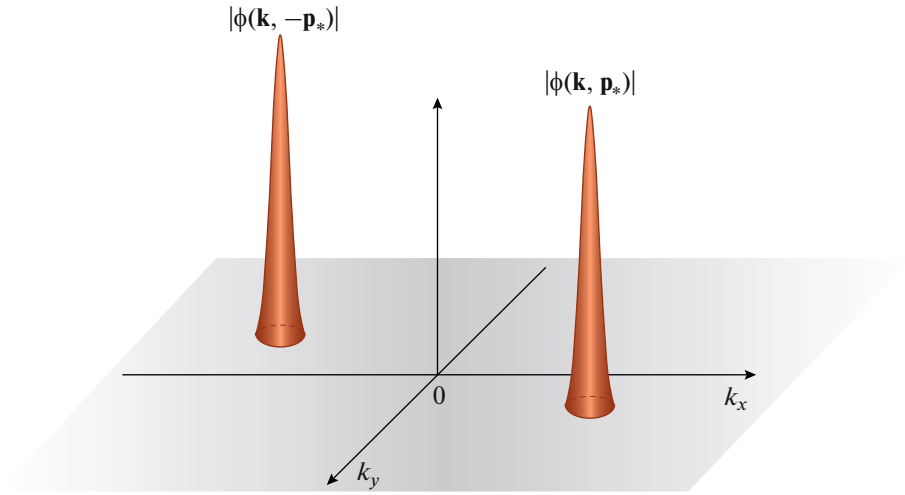

Fig. 2. Schematic illustration of the smallness of the integrand in (119) at large values of momentum $|\mathbf{p}_*|$ in the center-of-inertia of wave packets.

In order to return to the laboratory (or any other) frame, one needs to express variables in the center-of-inertia frame in terms of variables in the frame of interest. The corresponding Lorentz transformation takes the form

$$x_*^0 = \Gamma(x^0 - \mathbf{vx}),$$
$$\mathbf{x}_* = \mathbf{x} + \Gamma\left[\frac{\Gamma}{\Gamma+1}(\mathbf{vx}) - x^0\right]\mathbf{v}$$

(the same goes for y_* and $x_* - y_*$), where

$$\mathbf{v} = \frac{\mathbf{p}+\mathbf{q}}{E_\mathbf{p} + E_\mathbf{q}} \quad \text{and} \quad \Gamma = \frac{1}{\sqrt{1-\mathbf{v}^2}} = \frac{E_\mathbf{p} + E_\mathbf{q}}{E_{\mathbf{p}_*} + E_{\mathbf{q}_*}}$$

denote the velocity and the Lorentz factor of the center-of-inertia frame in the laboratory frame; the energy and the momentum in the center-of-inertia frame are given by

$$E_{\mathbf{p}_*} = E_{\mathbf{q}_*} = \frac{1}{2}\sqrt{(p+q)^2} \equiv E_*,$$
$$|\mathbf{p}_*| = |\mathbf{q}_*| = \frac{1}{2}\sqrt{-(p-q)^2} \equiv P_*.$$

The latter equality demonstrates that P_* decreases at $\mathbf{p} \to \mathbf{q}$ and increases as $|\mathbf{p} - \mathbf{q}|$ grows larger. Therefore, it follows from the above considerations that function $|\mathcal{D}(\mathbf{p}, \mathbf{q}; x - y)|$ reaches its maximum at $\mathbf{p} = \mathbf{q}$ and decreases at large values of $|\mathbf{p} - \mathbf{q}|$.

To conclude this section, we write kinematic identities

$$2E_*x_*^0 = (p+q)x, \quad 2\mathbf{p}_*\mathbf{x}_* = (q-p)x,$$
$$\mathbf{vx}_* = (\mathbf{vx} - \mathbf{v}^2x^0), \tag{120a}$$

$$\mathbf{x}_*^2 = \frac{[(p+q)x]^2}{(p+q)^2} - x^2 = ^2\left(|\mathbf{x} - \mathbf{v}x^0|^2 - |\mathbf{v}\times\mathbf{x}|^2\right), \tag{120b}$$

which will be used often in subsequent analysis. It follows from the last identity that

$$\mathbf{x}_* = 0 \Leftrightarrow \mathbf{x} = \mathbf{v}x^0.$$

4.5. Multipacket States

Multipacket states are crucial for the theory of neutrino oscillations in matter when one considers the effects of coherent neutrino scattering off matter particles. We assume that identical WPs, which correspond to states of one and the same quantum field but have different momenta and spin projection, are characterized by identical sets of parameters $\boldsymbol{\sigma} = \{\sigma_1, \sigma_2, \ldots\}$. Therefore, the dependence on σ is not stated explicitly. Ket state n of identical WPs is defined as

$$|\mathbf{p}_1, s_1, x_1; \mathbf{p}_2, s_2, x_2; \ldots; \mathbf{p}_n, s_n, x_n\rangle$$
$$= \left(\prod_{i=1}^n \sqrt{2E_{\mathbf{p}_i}}\right)\left|A^\dagger_{\mathbf{p}_1 s_1}(x_1)A^\dagger_{\mathbf{p}_2 s_2}(x_2)\cdots A^\dagger_{\mathbf{p}_n s_n}(x_n)\right|0\rangle. \tag{121}$$

The corresponding bra state is derived from (121) using Hermitian conjugation. It is evident that state (121) is completely symmetric (antisymmetric) for bosons (fermions) with respect to permutations $(\mathbf{p}_i, s_i, x_i) \leftrightarrow (\mathbf{p}_j, s_j, x_j)$ for any pair of indices i, j $(1 \le i, j \le n,\ i \ne j)$. The general symmetry relation takes the form

$$|\mathbf{p}_1, s_1, x_1; \mathbf{p}_2, s_2, x_2; \ldots; \mathbf{p}_n, s_n, x_n\rangle$$
$$= (\pm 1)^{\eta_P}\left|\mathbf{p}_{i_1}, s_{i_1}, x_{i_1}; \mathbf{p}_{i_2}, s_{i_2}, x_{i_2}; \ldots; \mathbf{p}_{i_n}, s_{i_n}, x_{i_n}\right\rangle.$$

Here and elsewhere, the upper and the lower signs correspond to bosons and fermions, respectively, and η_P is the parity of permutation

$$\mathcal{P} = \begin{pmatrix} 1 & 2 & \ldots & n \\ i_1 & i_2 & \ldots & i_n \end{pmatrix}.$$

In order to find the norm of states (121), we introduce an $n\times n$ matrix

$$\mathbb{D}_n \equiv \mathbb{D}\left(\{\mathbf{q}, r, y\}_n, \{\mathbf{p}, s, x\}_n\right) = \left\|\delta_{s_i r_j}(\mp 1)^{i+j}\mathscr{D}(\mathbf{p}_i, \mathbf{q}_j; x_i - y_j)\right\|.$$

Let us prove that

$$M_n \equiv \langle \mathbf{q}_1, r_1, y_1; \mathbf{q}_2, r_2, y_2; \ldots; \mathbf{q}_n, r_n, y_n | \mathbf{p}_1, s_1, x_1; \mathbf{p}_2, s_2, x_2; \ldots; \mathbf{p}_n, s_n, x_n\rangle = |\mathbb{D}_n|. \quad (122)$$

This relation is trivial if $n = 1$. It is easy to verify by direct calculations that

$$M_2 \equiv \langle \mathbf{q}_1, r_1, y_1; \mathbf{q}_2, r_2, y_2 | \mathbf{p}_1, s_1, x_1; \mathbf{p}_2, s_2, x_2\rangle = \left[\delta_{s_1 r_1}\delta_{s_2 r_2}\mathscr{D}(\mathbf{p}_1, \mathbf{q}_1; x_1 - y_1)\mathscr{D}(\mathbf{p}_2, \mathbf{q}_2; x_2 - y_2) \pm \delta_{s_1 r_2}\delta_{s_2 r_1}\mathscr{D}(\mathbf{p}_1, \mathbf{q}_2; x_1 - y_2)\mathscr{D}(\mathbf{p}_2, \mathbf{q}_1; x_2 - y_1)\right] = |\mathbb{D}_2|.$$

Therefore, equality (122) also holds true at $n = 2$. Let us now consider matrix element M_{n+1} at $n \geq 2$. According to (121) and (116b),

$$M_{n+1} = \left(\prod_{i=1}^{n+1} 4E_{\mathbf{q}_i}E_{\mathbf{p}_i}\right)^{1/2} \times \langle 0| A_{\mathbf{q}_1 r_1}(y_1)\cdots A_{\mathbf{q}_n r_n}(y_n)A_{\mathbf{q}_{n+1} r_{n+1}}(y_{n+1}) \times A^{\dagger}_{\mathbf{p}_{n+1} s_{n+1}}(x_{n+1})A^{\dagger}_{\mathbf{p}_n s_n}(x_n)\cdots A^{\dagger}_{\mathbf{p}_1 s_1}(x_1)|0\rangle.$$

Following successive permutations of operator $A^{\dagger}_{\mathbf{p}_{n+1} s_{n+1}}(x_{n+1})$ with operators $A_{\mathbf{q}_n r_n}(y_n)$, ..., $A_{\mathbf{q}_1 r_1}(y_1)$ with the use of (122) for n-packet matrix elements and with (anti) commutation relations (116c) factored in, we than find

$$M_{n+1} = \left(\prod_{i=1}^{n+1} 4E_{\mathbf{q}_i}E_{\mathbf{p}_i}\right)^{1/2} \sum_{j=1}^{n+1}(\pm 1)^{n+j+1}\delta_{s_{n+1} r_j} \times \left(4E_{\mathbf{q}_j}E_{\mathbf{p}_{n+1}}\right)^{-1/2}\mathscr{D}\left(\mathbf{p}_{n+1}, \mathbf{q}_j; x_{n+1} - y_j\right) \times \langle 0| A_{\mathbf{q}_1 r_1}(y_1)\cdots A_{\mathbf{q}_{j-1} r_{j-1}}(y_{j-1})A_{\mathbf{q}_{j+1} r_{j+1}}(y_{j+1})\cdots \cdots A_{\mathbf{q}_n r_n}(y_n)A_{\mathbf{q}_{n+1} r_{n+1}}(y_{n+1})A^{\dagger}_{\mathbf{p}_n s_n}(x_n)\cdots A^{\dagger}_{\mathbf{p}_1 s_1}(x_1)|0\rangle.$$

The right-hand side of this relation may be rearranged in compact form

$$\sum_{j=1}^{n+1}(\pm 1)^{n+j+1}\delta_{s_{n+1} r_j}\mathscr{D}\left(\mathbf{p}_{n+1}, \mathbf{q}_j; x_{n+1} - y_j\right)\left|\mathbb{D}^{(j)}_{n+1}\right|,$$

where $\left|\mathbb{D}^{(j)}_{n+1}\right|$ is the nth-order minor of determinant $|\mathbb{D}_{n+1}|$ arising from elimination of the $(n+1)$th row and the jth column from $|\mathbb{D}_{n+1}|$. The sum over j of the latter expression is nothing but the minor expansion of determinant $|\mathbb{D}_{n+1}|$ over the $(n+1)$-th row. Therefore, $M_{n+1} = |\mathbb{D}_{n+1}|$, which completes the inductive proof.

Thus, according to (122), n-boson (n-fermion) matrix element M_n is proportional to the $\left\|\delta_{s_i r_j}\mathscr{D}(\mathbf{p}_i, \mathbf{q}_j; x_i - y_j)\right\|$ matrix permanent (determinant). Let us now turn to the normalization problem. Since

$$\mathscr{D}(\mathbf{p}, \mathbf{q}; x - y) = \mathscr{D}^*(\mathbf{q}, \mathbf{p}; y - x),$$

matrix $\mathbb{D}\left(\{\mathbf{p}, s, x\}_n, \{\mathbf{p}, s, x\}_n\right)$ is Hermitian. Therefore, n-packet matrix element

$$\langle \mathbf{p}_1, s_1, x_1; \mathbf{p}_2, s_2, x_2; \ldots; \mathbf{p}_n, s_n, x_n | \mathbf{p}_1, s_1, x_1; \mathbf{p}_2, s_2, x_2; \ldots; \mathbf{p}_n, s_n, x_n\rangle \equiv {}_n\langle \mathbf{p}, s, x | \mathbf{p}, s, x\rangle_n \quad (123)$$

is a real polynomial combination of order n of commutator functions $\mathscr{D}$ with different arguments. For example, the following is obtained for $n = 1$, 2, and 3:

$$\begin{aligned} {}_1\langle \mathbf{p}, s, x | \mathbf{p}, s, x\rangle_1 &= 2m\mathrm{V}_\star, \\ {}_2\langle \mathbf{p}, s, x | \mathbf{p}, s, x\rangle_2 &= (2m\mathrm{V}_\star)^2 \pm \delta_{s_1 s_2}\left|\mathscr{D}(\mathbf{p}_1, \mathbf{p}_2; x_1 - x_2)\right|^2, \\ {}_3\langle \mathbf{p}, s, x | \mathbf{p}, s, x\rangle_3 &= (2m\mathrm{V}_\star)^3 \pm 2m\mathrm{V}_\star \times \sum_{1\leq i<j\leq 3}\delta_{s_i s_j}\left|\mathscr{D}(\mathbf{p}_i, \mathbf{p}_j; x_i - x_j)\right|^2 \\ &\quad + 2\mathrm{Re}\prod_{1\leq i<j\leq 3}\left[\delta_{s_i s_j}\mathscr{D}(\mathbf{p}_i, \mathbf{p}_j; x_i - x_j)\right]. \end{aligned} \quad (124)$$

The properties of the commutator function, discussed in Section 4.4, provide an opportunity to analyze these results in two simple limiting cases. If all space-time points $x_1, x_2, \ldots, x_n$ ($n \geq 2$) are sufficiently separated and/or 3-momenta $\mathbf{p}_1, \mathbf{p}_2, \ldots, \mathbf{p}_n$ differ strongly in amplitude or direction (nonintersection mode), it follows from (122) that

$${}_n\langle \mathbf{p}, s, x | \mathbf{p}, s, x\rangle_n \approx (2m\mathrm{V}_\star)^n = \langle \mathbf{p}, s, x | \mathbf{p}, s, x\rangle^n.$$

In the opposite case, when packets with identical spin projections intersect strongly both in the momentum space and in the configuration space,

$${}_n\langle \mathbf{p}, s, x | \mathbf{p}, s, x\rangle_n \approx \begin{cases} n!(2m\mathrm{V}_\star)^n & \text{for bosons,} \\ 0 & \text{for fermions.} \end{cases}$$

A matrix element is independent of momenta, coordinates, and spin projections in both limiting cases. The behavior of an n-packet matrix element in the intersection regime is just the manifestation of Bose attraction and Pauli blocking for identical bosons and fermions, respectively. Much less trivial is the fact that the WP formalism validates the intuitive expectations that free identical bosons (fermions) with the same momenta and spin projections do not condense (may coexist freely) if they are separated by sufficiently large space-time intervals. This physically understandable result is incomprehensible within the plane-wave QFT formalism. In fact, the Pauli principle is sometimes formulated in the following categorical form: "the probability of finding two identical fermions with the same momenta and spin projections is zero." We see that, strictly speaking, this is not true,

unless particles with definite momenta (idealized mathematical objects existing in the entire infinite space-time) are considered instead of WPs, which are localized in finite space-time regions and characterized by the most probable momentum values. We will revisit this conceptually important issue in Section 5.5 and clarify the meaning of words "sufficiently large space-time interval" using a simple model of a relativistic WP.

5. RELATIVISTIC GAUSSIAN PACKETS

5.1. Function $\phi_G(\mathbf{k},\mathbf{p})$

This section is focused on the simple (but important for the considered formalism) model of a relativistic Gaussian packet that is applicable in characterizing sufficiently narrow (in the momentum space) wave packets that are spherically symmetric in the intrinsic frame of reference and have a single maximum[7]. Since function $\phi(\mathbf{k},\mathbf{p})$ for such packets is essentially (to within a known positively defined factor) a smeared δ-function, we may assume that $\phi(\mathbf{k},\mathbf{p}) > 0$ without loss of generality. It is also assumed that form factor $\phi(\mathbf{k},\mathbf{p})$ depends on a single scalar variable $(k-p)^2$. It is easy to see that $(k-p)^2 \le 0$. Since $E_{\mathbf{k}_\star} \ge m$, we obtain the following in the intrinsic frame of reference of the packet ($\mathbf{p}_\star = 0$):

$$(k-p)^2 = (k_\star - p_\star)^2 = -2m\left(E_{\mathbf{k}_\star} - m\right) \le 0.$$

Note also that $(k-p)^2 \approx -(\mathbf{k}-\mathbf{p})^2 + \left[\mathbf{v}_\mathbf{p}(\mathbf{k}-\mathbf{p})\right]^2$ at $\mathbf{k} \sim \mathbf{p}$. Since function $\phi(\mathbf{k},\mathbf{p})$ has its maximum at point $\mathbf{k} = \mathbf{p}$, one can apply a natural additional constraint

$$\left.\frac{d\ln\phi(\mathbf{k},\mathbf{p})}{d(k-p)^2}\right|_{\mathbf{k}=\mathbf{p}} \equiv \frac{1}{4\sigma^2} > 0, \quad \sigma = \text{const}.$$

Function $\phi(\mathbf{k},\mathbf{p})$ may then be approximated in a sufficiently small neighborhood of the maximum by the following expression:

$$\phi(\mathbf{k},\mathbf{p}) \approx N_\sigma \exp\left[\frac{(k-p)^2}{4\sigma^2}\right] \stackrel{\text{def}}{=} \phi_G(\mathbf{k},\mathbf{p}). \qquad (125)$$

[7] The RGP model was proposed in [57]. It was thoroughly analyzed mathematically and generalized in [101]. Intriguing applications of the RGP (apart from neutrino physics) were discussed in [102]. Another class of models (covariant asymmetric WP, AWP) was proposed in [100]. It was demonstrated that an AWP is never the same as an RGP, although it features all the properties needed for a covariant description of localized "particle-like" quantum states. It was also demonstrated that the WP considered below is the only relativistic "memoryless" packet (i.e., a packet independent of 4-momenta of "parent" states (particles) involved in the reactions or decays producing the WP; see Section 4.1). We follow the logic of [57], which is sufficient for our purpose.

We call the states with such form factors RGPs by analogy with noncovariant (nonrelativistic) Gaussian packets in (50) (NGPs) with form factor

$$\varphi_G(\mathbf{k}-\mathbf{p}) = \left(\frac{2\pi}{\sigma^2}\right)^{3/4} \exp\left[-\frac{(\mathbf{k}-\mathbf{p})^2}{4\sigma^2}\right],$$

which is normalized by condition

$$\int \frac{d\mathbf{k}}{(2\pi)^3}\left|\varphi_G(\mathbf{k})\right|^2 = 1.$$

It will be demonstrated below that the properties of RGPs differ considerably from those of NGPs. Normalization constant N_σ in (125) may be derived from condition (95), which states that

$$\frac{1}{N_\sigma} = \int_0^\infty \frac{d|\mathbf{k}|}{(2\pi)^2}\frac{\mathbf{k}^2}{E_\mathbf{k}}\exp\left(\frac{m^2 - mE_\mathbf{k}}{2\sigma^2}\right)$$
$$= \left(\frac{m}{2\pi}\right)^2 \int_1^\infty d\Gamma\sqrt{\Gamma^2-1}\exp\left[-\frac{m^2}{2\sigma^2}(\Gamma-1)\right].$$

Thus, we obtain

$$N_\sigma = \phi_G(\mathbf{p},\mathbf{p}) = \frac{2\pi^2\exp\left(-m^2/2\sigma^2\right)}{\sigma^2 K_1(m^2/2\sigma^2)}, \qquad (126)$$

where

$$K_1(z) = z\int_1^\infty dt e^{-zt}\sqrt{t^2-1} \quad \left(|\arg z| < \frac{\pi}{2}\right)$$

denotes the modified Bessel function of the third kind of order 1. We can now rewrite (125) in the following form:

$$\phi_G(\mathbf{k},\mathbf{p}) = \frac{2\pi^2}{\sigma^2 K_1(m^2/2\sigma^2)}\exp\left(-\frac{E_\mathbf{k}E_\mathbf{p} - \mathbf{kp}}{2\sigma^2}\right). \qquad (127)$$

Imposing the natural (assumed by default in what follows) requirement that

$$\sigma^2 \ll m^2, \qquad (128)$$

and making use of the known asymptotic expansion of function $K_1(z)$, which is true at large $|z|$ [103],

$$K_1(z) \sim \sqrt{\frac{\pi}{2z}}e^{-z}\left[1 + \frac{3}{8z} + \frac{15}{2(8z)^2} + \mathbb{O}\left(\frac{1}{z^3}\right)\right] \qquad (129)$$
$$\left(|\arg z| < \frac{3\pi}{2}\right),$$

we can rewrite expression (127) as follows:

$$\phi_G(\mathbf{k},\mathbf{p}) = \frac{2\pi^{3/2}}{\sigma^2}\frac{m}{\sigma}\exp\left[\frac{(k-p)^2}{4\sigma^2}\right] \qquad (130)$$
$$\times\left[1 + \frac{3\sigma^2}{4m^2} + \mathbb{O}\left(\frac{\sigma^4}{m^4}\right)\right].$$

The following is obtained from (130) in the nonrelativistic case ($(|\mathbf{k}|+|\mathbf{p}|)^2 \ll 4m^2$):

$$\phi_G(\mathbf{k},\mathbf{p}) \approx \frac{2\pi^{3/2}}{\sigma^2}\frac{m}{\sigma}\exp\left[-\frac{(\mathbf{k}-\mathbf{p})^2}{4\sigma^2}\right] \equiv \phi_G^{\mathrm{NR}}(\mathbf{k},\mathbf{p}). \quad (131)$$

This agrees, to within a normalization, with NGP form factor $\varphi_G(\mathbf{k}-\mathbf{p})$. However, the difference between $\phi_G(\mathbf{k},\mathbf{p})$ and $\varphi_G(\mathbf{k}-\mathbf{p})$ may be arbitrarily large (irrespective of the difference in normalizations) at relativistic momenta. For example, function (130) behaves in the following way in the ultrarelativistic limit ($\mathbf{p}^2 \gg m^2$, $\mathbf{k}^2 \gg m^2$):

$$\phi_G(\mathbf{k},\mathbf{p}) \approx \frac{2\pi^{3/2}}{\sigma^2}\frac{m}{\sigma} \times \exp\left[-\frac{m^2(|\mathbf{k}|-|\mathbf{p}|)^2}{4\sigma^2|\mathbf{k}||\mathbf{p}|} - \frac{(1-\cos\vartheta)|\mathbf{k}||\mathbf{p}|}{2\sigma^2}\right] \equiv \phi_G^{\mathrm{UR}}(\mathbf{k},\mathbf{p}),$$

where ϑ is the angle between vectors $\mathbf{k}$ and $\mathbf{p}$. In particular, we obtain the following at $\vartheta = 0$ and $\pi/2$:

$$\phi_G^{\mathrm{UR}}\big|_{\vartheta=0} \propto \exp\left[-\frac{(\mathbf{k}-\mathbf{p})^2}{4\sigma^2\Gamma_{\mathbf{k}}\Gamma_{\mathbf{p}}}\right]$$
$$\text{and} \quad \phi_G^{\mathrm{UR}}\big|_{\vartheta=\pi/2} \propto \exp\left[-\frac{|\mathbf{k}||\mathbf{p}|}{2\sigma^2}\right].$$

In the first example, the relativistic effect is limited to packet broadening (compared to the nonrelativistic case) in the momentum space ($\sigma \mapsto \sigma\sqrt{\Gamma_{\mathbf{k}}\Gamma_{\mathbf{p}}}$). This effect is significant for all processes of neutrino production and absorption (scattering) involving relativistic particles.

If one needs to illustrate the significance of correct normalization, it is instructive to verify explicitly that the $\phi_G(\mathbf{k},\mathbf{p})$ limit at $\sigma \to 0$ is indeed given by equality (4.3).To this end, it is sufficient to prove that

$$\lim_{\sigma\to 0}\int \frac{d\mathbf{k}\varphi_G(\mathbf{k},0)}{(2\pi)^3 2E_{\mathbf{k}}}F(\mathbf{k}) = F(0), \quad (132)$$

for any smooth function $F(\mathbf{k})$.

The left-hand side of (132) may be rearranged in the following way:

$$\lim_{\sigma\to 0}\frac{m}{(4\pi)^{3/2}\sigma^3}\int d\Omega_{\mathbf{k}}\int_0^\infty d|\mathbf{k}|\frac{\mathbf{k}^2}{E_{\mathbf{k}}} \times \exp\left[-\frac{m^2}{2\sigma^2}\left(\frac{E_{\mathbf{k}}}{m}-1\right)\right]F(\mathbf{k})$$
$$= \lim_{\sigma\to 0}\left(\frac{m^2}{4\pi\sigma^2}\right)^{3/2}\int d\Omega_{\mathbf{n}}\int_0^\infty dt \times \exp\left(-\frac{m^2 t}{2\sigma^2}\right)\sqrt{t(t+2)}F\left(m\sqrt{t(t+2)}\mathbf{n}\right),$$

where $\mathbf{n} = \mathbf{k}/|\mathbf{k}|$. The obtained integral over t may be estimated using the well-known asymptotic formula (see, e.g., [104])

$$\int_0^\infty dt t^{a-1}e^{-\nu t}f(t) \sim \nu^{-a}\Gamma(a)f(0)[1+o(1)] \quad (a>0, \nu\to\infty), \quad (133)$$

which holds true for an arbitrary continuous function $f(t)$, $t \in [0,\infty)$. Since

$$a = \frac{3}{2}, \quad \nu = \frac{m^2}{2\sigma^2}$$
$$\text{and} \quad f(t) = \sqrt{t+2}F\left(m\sqrt{t(t+2)}\mathbf{n}\right)$$

in the case under consideration, the equality in (132) becomes evident.

Thus, we see that function $\phi_G(\mathbf{k},\mathbf{p})$ is the simplest model of a form factor that satisfies all the requirements imposed on function $\phi(\mathbf{k},\mathbf{p})$ of the general form. Let us derive explicit formulas for the mean and root-mean-square velocities of an RGP to understand its properties better.

5.2. Mean and Root-Mean-Square Velocities

Let us start with definitions

$$\langle\mathbf{v}\rangle = \frac{1}{2m\mathrm{V}_\star}\int\frac{d\mathbf{k}\mathbf{k}|\phi(\mathbf{k},\mathbf{p})|^2}{(2\pi)^3 2E_{\mathbf{k}}^2},$$
$$\langle\mathbf{v}^2\rangle = \frac{1}{2m\mathrm{V}_\star}\int\frac{d\mathbf{k}\mathbf{k}^2|\phi(\mathbf{k},\mathbf{p})|^2}{(2\pi)^3 2E_{\mathbf{k}}^3}. \quad (134)$$

Evidently, $\langle\mathbf{v}\rangle \propto \mathbf{v}_{\mathbf{p}} \propto \mathbf{p}$; therefore, it is sufficient to determine the projection of the mean velocity onto the momentum direction ($\mathbf{n}_{\mathbf{p}} = \mathbf{p}/|\mathbf{p}|$). Integrating in angular variables, we find

$$\langle\mathbf{v}\rangle\mathbf{n}_{\mathbf{p}} = \frac{\pi^2\lambda^2}{4m^5\mathrm{V}_\star K_1^2(\lambda/2)}\int_0^\infty\frac{d|\mathbf{k}||\mathbf{k}|^3}{E_{\mathbf{k}}^2} \times \int_{-1}^1 d\cos\theta\cos\theta\exp\left[-\frac{\lambda(pk)}{m^2}\right]$$
$$= \frac{m^2}{2\lambda|\mathbf{p}|^2K_1(\lambda)}\int_{-\infty}^\infty\frac{|\mathbf{k}||\mathbf{k}|}{E_{\mathbf{k}}^2}\left(\lambda\frac{|\mathbf{p}||\mathbf{k}|}{m^2}-1\right) \times \exp\left[-\frac{\lambda(E_{\mathbf{p}}E_{\mathbf{k}}-|\mathbf{p}||\mathbf{k}|)}{m^2}\right],$$

($\lambda = \mathbf{m}^2/\sigma^2$); it is assumed here that $|\mathbf{p}| > 0$ because the $|\mathbf{p}| = 0$ case is trivial. The saddle-point method is

used in subsequent calculations; we utilize the well-known theorem of asymptotic integral expansion

$$F(\lambda) = \int_{-\infty}^{\infty} dt f(t) \exp[-\lambda S(t)], \quad f(t), S(t) \in \mathbb{C}(-\infty, \infty) \tag{135}$$

(see, e.g., [104], p. 41), which states that

$$F(\lambda) \sim \exp[-\lambda S(t_0)] \sum_{n=0}^{\infty} \Gamma\left(n + \frac{1}{2}\right) \times \frac{b_{2n}(\lambda)}{(2n)!} \left[\frac{2}{\lambda S''(t_0)}\right]^{n+1/2}, \quad \lambda \to \infty, \tag{136}$$

where

$$b_n(\lambda) = \frac{d^n}{dt^n}\{f(t)\exp[\lambda h(t, t_0)]\}\Big|_{t=t_0},$$
$$h(t, t_0) = S(t_0) - S(t) + \frac{1}{2}(t - t_0)^2 S''(t_0),$$

t_0 is the only stationary point of function $S(t)$ $(-\infty < t_0 < \infty)$, $S''(t_0) > 0$, and $f(t), S(t) \in \mathbb{C}^{\infty}$ in the neighborhood of t_0. All these conditions are evidently satisfied in our special case[8]. The result is

$$\langle \mathbf{v} \rangle = \mathbf{v}_\mathbf{p}\left[1 - \frac{1}{\Gamma_\mathbf{p}^2\lambda} + \frac{7 - 6\mathbf{v}_\mathbf{p}^2}{2\Gamma_\mathbf{p}^2\lambda^2} + \mathbb{O}(\lambda^{-3})\right]. \tag{137}$$

As expected, the mean velocity is always lower than the most probable. In the nonrelativistic case, $\mathbf{v}_\mathbf{p} - \langle \mathbf{v} \rangle \approx \mathbf{v}_\mathbf{p}/\lambda$; in the ultrarelativistic one, $\mathbf{v}_\mathbf{p} - \langle \mathbf{v} \rangle \approx \mathbf{n}_\mathbf{p}/\left(\Gamma_\mathbf{p}^2\lambda\right)$. Similar calculations for the root-mean-square velocity and its longitudinal and transverse components yield the following:

$$\langle \mathbf{v}^2 \rangle = \mathbf{v}_\mathbf{p}^2 + \frac{3}{\Gamma_\mathbf{p}^4\lambda} - \frac{3(7 - 10\mathbf{v}_\mathbf{p}^2)}{2\Gamma_\mathbf{p}^4\lambda^2} + \mathbb{O}(\lambda^{-3}), \tag{138a}$$

$$\langle \mathbf{v}_L^2 \rangle = \langle (\mathbf{v}\mathbf{n}_\mathbf{p})^2 \rangle = \mathbf{v}_\mathbf{p}^2 + \frac{1 - 3\mathbf{v}_\mathbf{p}^2}{\Gamma_\mathbf{p}^2\lambda} - \frac{7 - 39\mathbf{v}_\mathbf{p}^2 + 30\mathbf{v}_\mathbf{p}^4}{2\Gamma_\mathbf{p}^2\lambda^2} + \mathbb{O}(\lambda^{-3}), \tag{138b}$$

$$\langle \mathbf{v}_T^2 \rangle = \langle (\mathbf{v} \times \mathbf{n}_\mathbf{p})^2 \rangle = \frac{2}{\Gamma_\mathbf{p}^2\lambda} - \frac{7 - 6\mathbf{v}_\mathbf{p}^2}{\Gamma_\mathbf{p}^2\lambda^2} + \mathbb{O}(\lambda^{-3}). \tag{138c}$$

In the nonrelativistic case, $\langle \mathbf{v}^2 \rangle - \mathbf{v}_\mathbf{p}^2 \approx 3/\lambda$; i.e., jitters are observed in the WP, although the jitters are negligible. In the ultrarelativistic case, they vanish completely, and a WP behaves as a classical particle. The following is obtained from (137) and (138a):

$$\langle \mathbf{v}^2 \rangle - \langle \mathbf{v} \rangle^2 = \frac{3}{\Gamma_\mathbf{p}^2\lambda}\left[1 - \frac{\mathbf{v}_\mathbf{p}^2}{3} - \left(7 - \frac{35\mathbf{v}_\mathbf{p}^2}{3} + \frac{16\mathbf{v}_\mathbf{p}^4}{3}\right)\frac{1}{2\lambda} + \mathbb{O}(\lambda^{-2})\right]. \tag{139}$$

Thus, difference (139) assumes the value of $3/\lambda$ in the nonrelativistic limit and tends to zero as $2/(\Gamma_\mathbf{p}^2\lambda)$ in the ultrarelativistic limit. The RGP model allows one to study the properties of the wave and commutator functions in detail.

5.3. Wave Function $\psi_G(\mathbf{p}, x)\psi_G$

Inserting (127) into (109), integrating over the direction of vector $\mathbf{k}$, and performing simple transformations, we obtain the following:

$$\psi(0, x_\star) = \int_m^{\infty} dE \exp\left[-\frac{E}{m}\left(\frac{m^2}{2\sigma^2} + imx_\star^0\right)\right] \times \frac{\sin\left(|\mathbf{x}_\star|\sqrt{E^2 - m^2}\right)}{2\sigma^2|\mathbf{x}_\star| K_1(m^2/2\sigma^2)}.$$

This integral is calculated using the known representation for function K_1

$$\int_a^{\infty} dt e^{-bt} \sin\left(c\sqrt{t^2 - a^2}\right) = \frac{ac}{\sqrt{b^2 + c^2}} K_1\left(a\sqrt{b^2 + c^2}\right), \tag{140}$$

which holds true for $a > 0$ and $\mathrm{Re}\, b > |\mathrm{Im}\, c|$ (see, e.g., [105, (2.5.42.3), p. 460]). Thus, we arrive at a compact expression

$$\psi(\mathbf{p}, x) = \frac{K_1(\zeta m^2/2\sigma^2)}{\zeta K_1(m^2/2\sigma^2)} \overset{\text{def}}{=} \psi_G(\mathbf{p}, x), \tag{141}$$

which features a dimensionless Lorentz-invariant variable

$$\zeta = |\zeta| e^{i\varphi} = \sqrt{1 - \frac{4\sigma^2}{m^2}\left[\sigma^2 x_\star^2 - imx_\star^0\right]} = \sqrt{1 - \frac{4\sigma^2}{m^2}\left[\sigma^2 x^2 - i(px)\right]}. \tag{142}$$

Here and elsewhere, the square root sign is understood in the sense of its principal value, and $x_\star^2 = (x_\star^0)^2 - \mathbf{x}_\star^2$.

It is instructive to verify that function (141) satisfies the Klein–Gordon equation. Considering that $K_0(z) = -K_1(z)$ and $K_1'(z) = -K_0(z) - K_1(z)/z$, we find

$$\partial_\mu\left[\frac{K_1(z)}{z}\right] = -\left[K_0(z) + \frac{2}{z}K_1(z)\right]\frac{\partial_\mu z}{z},$$

[8] The linear dependence of function $f(t)$ on parameter λ does not preclude one from applying the theorem.

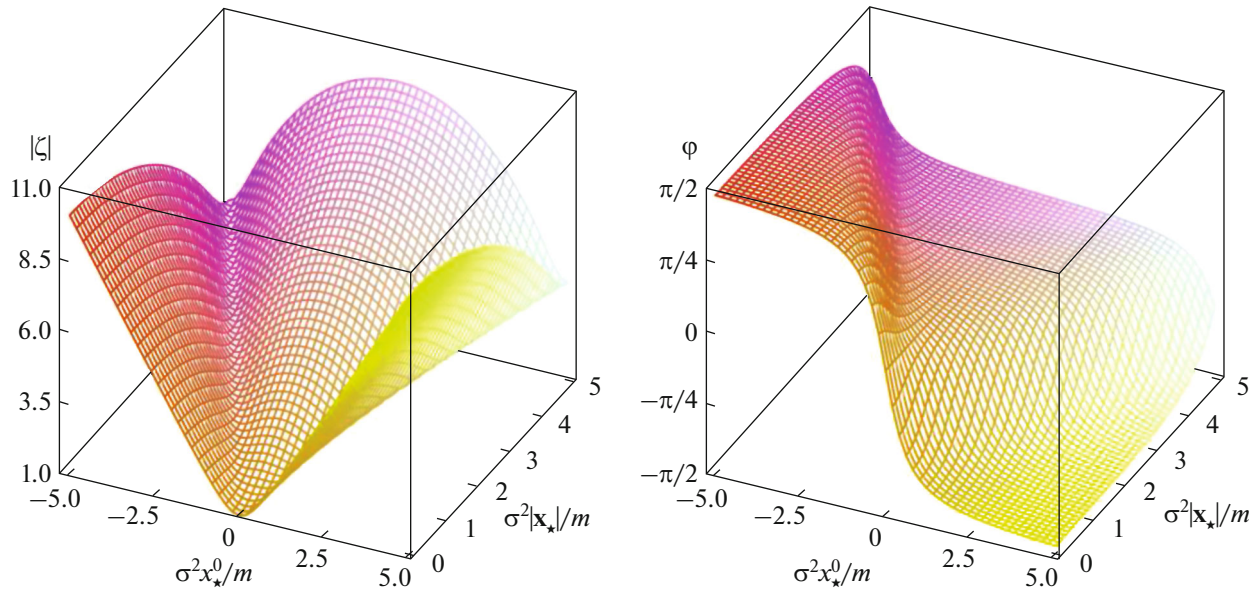

Fig. 3. Three-dimensional plots of functions $|\zeta|$ and φ in variables $\sigma^2 x^0_\star/m$ and $\sigma^2|\mathbf{x}_\star|/m$.

where $z = m^2\zeta/(2\sigma^2)$. Therefore,

$$\Box\left[\frac{K_1(z)}{z}\right] = -\left[K_0(z) + \frac{2}{z}K_1(z)\right]\frac{\Box z}{z} - \left[\frac{3}{z}K_0(z) + \left(1 + \frac{6}{z^2}\right)K_1(z)\right]\frac{(\partial_\mu z)(\partial^\mu z)}{z}. \quad (143)$$

Since

$$\partial_\mu z = -\frac{m^2}{\sigma^2 z}\left(\sigma^2 x_\mu - \frac{i}{2}p_\mu\right),$$

it follows that

$$\Box z = -\partial_\mu\partial^\mu z = \frac{3m^2}{z}, \quad (\partial_\mu z)(\partial^\mu z) = -m^2.$$

Inserting these identities into (143) and using (141) we make sure that

$$(\partial^2 + m^2)\psi_G = 0.$$

The modulus and the phase of variable (142) are given by

$$|\zeta|^4 = \left(1 - \frac{4\sigma^4 x_\star^2}{m^2}\right)^2 + \left(\frac{4\sigma^2 x^0_\star}{m}\right)^2 = 1 + \frac{8\sigma^4}{m^2}\left[(x^0_\star)^2 + \mathbf{x}_\star^2\right] + \left(\frac{4\sigma^4 x_\star^2}{m^2}\right)^2, \quad (144)$$

$$\sin 2\varphi = \frac{4\sigma^2 x^0_\star}{m|\zeta|^2}, \quad \cos 2\varphi = \frac{m^2 - 4\sigma^4 x_\star^2}{m^2|\zeta|^2}. \quad (145)$$

It follows from the last equality in (144) that, for any x_*,

$$|\zeta| \geq 1, \quad (146)$$

with equality holding true only at the packet center ($x^0_\star = 0$, $|\mathbf{x}_\star| = 0$). Relying on (145) and analyticity considerations, one may easily demonstrate that

$$|\varphi| < \pi/2. \quad (147)$$

Indeed, it follows from (145) that $\varphi \to \mp 0$ at $x^0_\star \to \pm 0$. Since this is the only zero of phase φ at $|\zeta| < \infty$, the continuity of φ implies that $2\varphi \to \mp\pi$ at $x^0_\star \to \pm\infty$.

Figure 3 illustrates the behavior of $|\zeta|$ and φ as a function of two independent dimensionless variables $\sigma^2 x^0_\star/m$ and $\sigma^2|\mathbf{x}_\star|/m$. It can be demonstrated that function $\psi_G(\mathbf{p}, x)$ has no zeros at $1 \leq |\zeta| < \infty$ and tends to unity (zero) at $\zeta \to 1$ ($\zeta \to \infty$) in sector (147). It follows from the properties of parameter ζ that $\psi_G(\mathbf{0}, x_\star) \to 0$ if $|x^0_\star| \to \infty$ (at fixed $\mathbf{x}_\star$) or $|\mathbf{x}_\star| \to \infty$ (at fixed $x^0_\star$).

The behavior of wave function $\psi_G(\mathbf{0}, x_\star)$ depends strongly on the value of ratio σ/m. Figure 4 presents the profile of the modulus of function $\psi_G(\mathbf{0}, x_\star)$ (left panel) and an enlarged fragment of this function in the neighborhood of its maximum (right panel) as examples. Calculations were performed with $\sigma/m = 0.1$ in terms of dimensionless variables $\sigma^2 x^0_\star/m$ and $\sigma^2 x^3_\star/m$, and the reference frame was chosen so that vector $\mathbf{x}_\star$ is directed along the third axis. Note that the

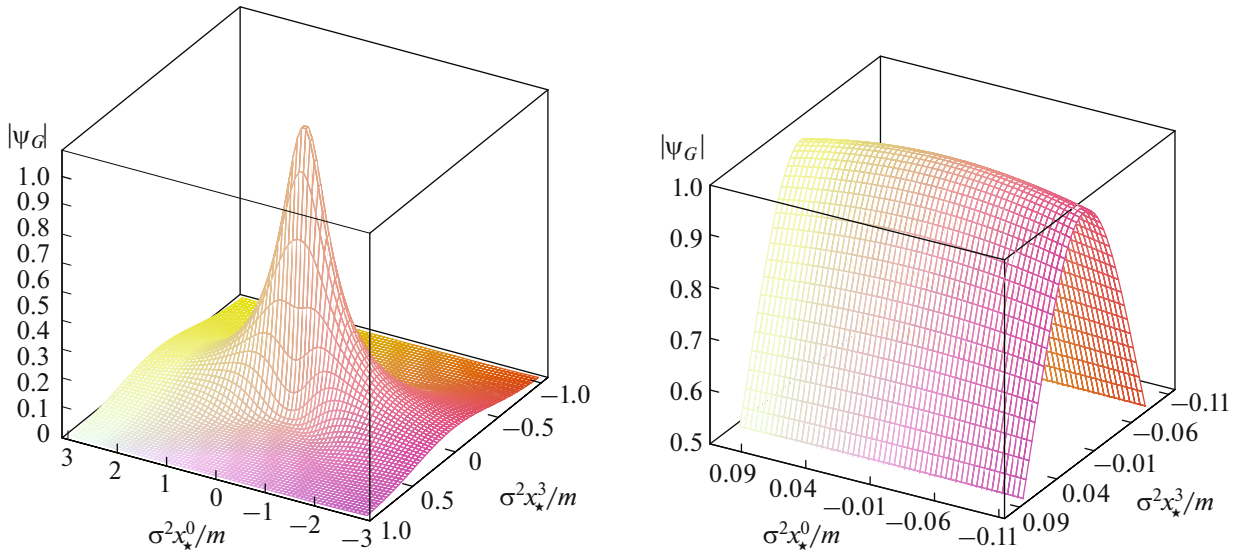

Fig. 4. Three-dimensional plot of function $|\psi_G(\mathbf{0}, x_\star)|$ in variables $\sigma^2 x^0_\star/m$ and $\sigma^2 x^3_\star/m$ (left) and its zoomed fragment in the neighborhood of the maximum (right). It is assumed that $\mathbf{x}_\star = (0,0,x^3_\star))$. Calculations were performed for $\sigma = 0.1m$.

value of σ/m is entirely unrealistic and was chosen only for illustrative purposes, since the fine features of behavior of $|\psi_G(\mathbf{0}, x_\star)|$ would be indiscernible at $\sigma/m \ll 0.1$. Naturally, $|\psi_G(\mathbf{0}, x_\star)|$ is an even function of both variables; this explains the symmetry of the $|\psi_G(\mathbf{0}, x_\star)|$ profile in Fig. 4. In a sufficiently small neighborhood of the $|\psi_G(\mathbf{0}, x_\star)|$ maximum and as the σ/m value decreases, the profile of function $|\psi_G(\mathbf{0}, x_\star)|$ changes relatively slightly along the time axis, but flattens rapidly along the space axis. Figure 4 provides an insight as to why the effective packet volume defined in accordance with (97) is independent of time, although wave function $|\psi_G(\mathbf{0}, x_\star)|$ itself tends asymptotically to zero at $|x^0_\star| \to \infty$. The reason is that the packet spreads with time in such a manner that this spreading compensates accurately the $|\psi_G(\mathbf{0}, x_\star)|$ reduction. This compensation preserves the norm of the packet. Thus, contrary to the claims made in certain textbooks on quantum mechanics, the spreading of a relativistic WP does not imply that it vanishes.

5.4. Commutator Function $\mathcal{D}_G(\mathbf{p}, \mathbf{q}; x)$

Inserting (127) into the definition of commutator function (117) written in the intrinsic frame of reference of the packet and integrating in angular variables, we obtain

$$\frac{\mathcal{D}(\mathbf{p}_*, -\mathbf{p}_*; x_*)}{2m\mathrm{V}_\star} = \int_m^\infty dE \exp\left[-\frac{E}{m}\left(\frac{mE_*}{\sigma^2} + imx^0_*\right)\right] \times \frac{\sin\left(|\mathbf{x}_*|\sqrt{E^2 - m^2}\right)}{\sigma^2 |\mathbf{x}_*| K_1(m^2/\sigma^2)}.$$

Expression (140) allows one to calculate the remaining integral over E easily; we find [cf. (141)]

$$\mathcal{D}(\mathbf{p}, \mathbf{q}; x) = 2m\mathrm{V}_\star \frac{K_1(zm^2/\sigma^2)}{zK_1(m^2/\sigma^2)} \overset{\text{def}}{=} \mathcal{D}_G(\mathbf{p}, \mathbf{q}; x). \quad (148)$$

Invariant dimensionless variable z is defined as

$$z = \frac{E_*}{m}\sqrt{1 - \frac{\sigma^2}{E^2_*}\left[\sigma^2 x^2_* - 2iE_* x^0_*\right]} = \frac{1}{2m}\sqrt{(p+q)^2 - 4\sigma^2\left[\sigma^2 x^2 - i(p+q)x\right]}. \quad (149)$$

The relations between kinematic variables in the intrinsic frame of reference and the laboratory frame (see the end of Section 4.4) were used in deriving the last equality. The modulus and the phase of variable z are given by

$$|z|^4 = \frac{1}{4}\left(1 + \frac{pq - 2\sigma^4 x^2}{m^2}\right)^2 + \left[\frac{\sigma^2(p+q)x}{m^2}\right]^2,$$

$$\arg z = -\frac{1}{2}\arcsin\left[\frac{\sigma^2(p+q)x}{m^2|z|^2}\right].$$

Using these relations, one can prove that

$$|z| \geq E_*/m \geq 1 \quad \text{and} \quad |\arg z| < \pi/2. \quad (150)$$

The obtained formulas for the wave and commutator functions provide an opportunity to examine the properties of WPs and multipacket states in detail. However, the calculation of macroscopic Feynman diagrams of interest to us is a rather technically complicated task even in such a simple model as the RGP because one needs to calculate multidimensional integrals of products of Bessel functions of complex vari-

ables. In addition, for most practically important scenarios, the regime is interestig in which the WP spreading can be neglected. This regime is typical, e.g., of particles of a not too rarefied gas if the mean time between two successive collisions of a particle is much shorter than the effective spreading time of the packet that characterizes its state between the collisions. The case is similar for unstable particles with their lifetimes being short relative to the packet spreading time. The corresponding approximation in the RGP model is considered below.

5.5. Approximation of Nonspreading Packets

Let us determine the physical conditions under which the RGP spreading may be neglected[9].

Owing to inequalities (128), (146), and (147), one can use asymptotic equation (129), which yields

$$\psi_G(\mathbf{p},x)=\frac{1}{\zeta^{3/2}}\exp\left[\frac{m^2(1-\zeta)}{2\sigma^2}\right]\left[1-\frac{3\sigma^2}{4m^2}\left(1-\frac{1}{\zeta}\right)+\frac{3\sigma^4}{32m^4}\left(1-\frac{1}{\zeta}\right)\left(11+\frac{5}{\zeta}\right)+\mathbb{O}\left(\frac{\sigma^6}{m^6}\right)\right]. \tag{151}$$

This formula holds true for any $\mathbf{p}$ and x, but it is still too complicated for our purpose. Imposing additional constraints, one may simplify expression (151) considerably by expanding variable ζ in powers of small parameter σ^2/m^2. In the intrinsic frame of reference of a packet,

$$\ln\left[\psi_G(\mathbf{0},x_\star)\right]=-imx_\star^0\left[1+\frac{3\sigma^2}{m^2}-\frac{\sigma^4}{m^4}\left(2m^2\mathbf{x}_\star^2-\frac{3}{2}\right)\right]-\sigma^2\mathbf{x}_\star^2-\frac{3\sigma^4}{m^2}\left[(x_\star^0)^2+\mathbf{x}_\star^2\right]+\mathbb{O}\left(\frac{\sigma^6}{m^6}\right). \tag{152}$$

Elementary analysis suggests that one may limit this asymptotic series to the leading σ^2/m^2 corrections if the following (necessary and sufficient) conditions are satisfied:

$$\sigma^2(x_\star^0)^2\ll m^2/\sigma^2 \quad\text{and}\quad \sigma^2\mathbf{x}_\star^2\ll m^2/\sigma^2. \tag{153}$$

It is evident that the space-time region defined by these conditions becomes arbitrarily wide at $\sigma\to 0$. If (153) is satisfied, formula (152) evolves into a simple and physically transparent expression:

$$\psi_G(\mathbf{0},x_\star)=\exp\left(-imx_\star^0-\sigma^2|\mathbf{x}_\star|^2\right). \tag{154}$$

[9] It is clear that nonspreading WPs are easier to associate with (quasi) stable particles (i.e., localized objects) and to use as asymptotically free states of in- and out-fields in the S-matrix QFT formalism instead of common plane waves, which occupy the entire spacetime and are thus unable to serve as an adequate mathematical model of particles.

It is evident that, in the intrinsic frame of reference of a packet,

(i) $\psi_G(\mathbf{0},x_\star)$ behaves as a plane wave at $\mathbf{x}_\star^2\ll 1/\sigma^2$ (i.e., in the vicinity of the packet center).

(ii) $|\psi_G(\mathbf{0},x_\star)|$ is independent of time variable $x_\star^0$ (as required, RGP (154) does not spread).

(iii) $|\psi_G(\mathbf{0},x_\star)|$ decreases in accordance with the Gaussian law at large distances from the packet center, $|\mathbf{x}_\star|\gtrsim 1/\sigma$; note that the last inequality does not contradict the second one from (153).

Using kinematic relations (110a) and (111), we write function ψ_G in the laboratory frame:

$$\psi_G(\mathbf{p},x)=\exp\left\{-iE\left(x_0-\mathbf{v}_\mathbf{p}\mathbf{x}\right)-\sigma^2\Gamma_\mathbf{p}^2\left[\left(\mathbf{x}-\mathbf{v}_\mathbf{p}x_0\right)^2-\left(\mathbf{v}_\mathbf{p}\times\mathbf{x}\right)^2\right]\right\} \tag{155a}$$

$$=\exp\left[-iE\left(x_0-\mathbf{v}_\mathbf{p}\mathbf{x}\right)-\sigma^2\Gamma_\mathbf{p}^2\left(\mathbf{x}_\parallel-\mathbf{v}_\mathbf{p}x_0\right)^2-\sigma^2\mathbf{x}_\perp^2\right], \tag{155b}$$

where $\mathbf{x}_\parallel$ and $\mathbf{x}_\perp$ are the components of vector $\mathbf{x}$ ($\mathbf{x}=\mathbf{x}_\parallel+\mathbf{x}_\perp$) that are parallel and perpendicular to velocity vector $\mathbf{v}_\mathbf{p}$, respectively. It follows from (155b) that an RGP undergoes relativistic compression in the direction of velocity in the configuration space. This agrees with the abovementioned relativistic packet broadening in the momentum space for Fock components with momenta codirectional with vector $\mathbf{p}$ (see Section 5.1).

It follows from (155a) that function $|\psi_G(\mathbf{p},x)|$ is invariant with respect to a one-parameter group of transformations $x\mapsto x+p\theta/E_\mathbf{p}$ with $|\theta|<\infty$ (or, in the component-wise notation, $x_0\mapsto x_0+\theta$, $\mathbf{x}\mapsto\mathbf{x}+\mathbf{v}_\mathbf{p}\theta$). It follows that $|\psi_G(\mathbf{p},x_0,\mathbf{x})|=|\psi_G(\mathbf{p},0,\mathbf{x}-\mathbf{v}_\mathbf{p}x_0)|$. It is also evident that $|\psi_G(\mathbf{p},x)|=1$ and $\arg\left[\psi_G(\mathbf{p},x)\right]=mx_0/\Gamma_\mathbf{p}$ along classical world line $\mathbf{x}=\mathbf{v}_\mathbf{p}x_0$, but $|\psi_G(\mathbf{p},x)|<1$ for any deviation from it. The probability of quantum deviation $\delta\mathbf{x}=\mathbf{x}-\mathbf{v}_\mathbf{p}x_0$ from classical motion is suppressed by factor

$$\exp\left\{-2\sigma^2\left[(\delta\mathbf{x})^2+\Gamma_\mathbf{p}^2\left(\mathbf{v}_\mathbf{p}\delta\mathbf{x}\right)^2\right]\right\}.$$

It can be seen that transverse (with respect to velocity vector $\mathbf{v}_\mathbf{p}$) deviations are less suppressed than longitudinal ones. Moreover, the ultrarelativistic packets can deviate from classical trajectories exclusively in the transverse direction; i.e., the quantum motion of packets is confined to classical light cones.

The nonrelativistic limit corresponding to approximation (131) for function $\phi_G(\mathbf{k},\mathbf{p})$ is given by

$$\psi_G(\mathbf{p},x)\approx\exp\left[-im\left(x_0-\mathbf{v}_\mathbf{p}\mathbf{x}\right)-\sigma^2\left|\mathbf{x}-\mathbf{v}_\mathbf{p}x_0\right|^2\right]\equiv\psi_G^{\mathrm{NR}}(\mathbf{p},x),\quad |\mathbf{v}_\mathbf{p}|^2\ll 1.$$

The phase of the nonrelativistic wave function ψ_G^{NR} is independent of velocity ($x_0 - \mathbf{v_p}\mathbf{x} = x_0/\Gamma^2 \approx x_0$ at $\mathbf{x} = \mathbf{v_p}x_0$ and $\mathbf{v_p}^2 \ll 1$).

Using relation (110b), one may rewrite inequalities (153) and expression (154) in an explicitly relativistically invariant form:

$$(px)^2 \ll m^4/\sigma^4 \quad \text{and} \quad (px)^2 - m^2x^2 \ll m^4/\sigma^4, \quad (156)$$

$$\psi_G(\mathbf{p}, x) = \exp\left\{-i(px) - \frac{\sigma^2}{m^2}\left[(px)^2 - m^2x^2\right]\right\}. \quad (157)$$

Condition $\sigma^2|x^2| \ll m^2/\sigma^2$ follows from (156). In what follows, we call the considered approximation a stable relativistic Gaussian packet (SRGP). Applying the Klein–Gordon operator to (157), we obtain

$$\left[\partial^2 + m^2(1-\Delta)\right]\psi_G(\mathbf{p}, x) = 0,$$
$$\Delta = 6\frac{\sigma^2}{m^2} - \frac{4\sigma^4}{m^4}\left[(px)^2 - m^2x^2\right].$$

Thus, function ψ_G approximately satisfies the Klein–Gordon equation (i.e., $|\Delta| \ll 1$) if conditions (128) and (158), which define the domain of applicability of the SRGP approximation, are fulfilled. It will be demonstrated below that this region is sufficiently wide for our purpose.

Note that the inclusion of contributions $\mathbb{O}\left(\sigma^4/m^4\right)$ into (152) results in an even more rapid reduction in $|\psi_G|$ with distance at $\sigma^2\mathbf{x}_\star^2 \gtrsim m^2/\sigma^2$ and reduction in $|\psi_G|$ with time at $\sigma^2(x_\star^0)^2 \gtrsim m^2/\sigma^2$. One of the technical corollaries of this $|\psi_G|$ behavior, which is useful in amplitude calculations, consists in the fact that the SRGP approximation may be extended to the entire space-time integration region in integrals of the following type:

$$\int dx f(x)\prod_\varkappa \psi_\varkappa(\mathbf{p}_\varkappa, x - x_\varkappa),$$

where functions $\psi_\varkappa$ correspond to relativistic WPs characterizing the states of particles $\varkappa$, and $f(x)$ is an arbitrary smooth function of x without sharp extrema. Integrals of this type are found in formulas for the macroscopic amplitudes of scattering and decay of relativistic WPs.

Direct (and rather cumbersome) calculations of mean packet position $\langle\mathbf{x}\rangle$ with the use of (157) demonstrate that, as expected, a WP follows a classical trajectory. Thus, an SRGP reproduces completely the general properties of a relativistic WP.

The SRGP model allows one to verify the fulfillment of condition (107) needed for approximate formula (106), which is a significant element of the formalism, to be applicable. It follows from (157) that

$$i\nabla_{\mathbf{x}} \ln\psi_G(\mathbf{p}, x) = \mathbf{p} - 2i\frac{\sigma^2}{m^2}\left[(px)\mathbf{p} - m^2\mathbf{x}\right].$$

Therefore, condition (107) may be rewritten as

$$\left|(pX)\mathbf{p} - m^2\mathbf{X}\right| \ll \left(m^2/\sigma^2\right)E_{\mathbf{p}}, \quad (158)$$

where $X = (X_0, \mathbf{X}) = (y_0 - x_0, \mathbf{y} - \mathbf{x})$. Elementary algebra gives

$$\begin{aligned}&\left|(pX)\mathbf{p} - m^2\mathbf{X}\right|^2\\ &= (pX)^2\mathbf{p}^2 - 2m^2(pX)(\mathbf{pX}) + m^4\mathbf{X}^2\\ &= (pX)^2E_{\mathbf{p}}^2 + m^2\left[(\mathbf{pX})^2 + m^2\mathbf{X}^2 - E_{\mathbf{p}}^2X_0^2\right]\\ &\le (pX)^2E_{\mathbf{p}}^2 + m^2\left(\mathbf{p}^2\mathbf{X}^2 + m^2\mathbf{X}^2 - E_{\mathbf{p}}^2X_0^2\right).\end{aligned}$$

Thus, we have proven that

$$\left|(pX)\mathbf{p} - m^2\mathbf{X}\right| \le E_{\mathbf{p}}\sqrt{(pX)^2 - m^2X^2}.$$

Therefore, inequality (158) is not an independent condition and follows from the second constraint from (156), which defines the domain of applicability of the SRGP approximation.

Let us now examine the properties of commutator function (148) in the SRGP approximation. Using inequalities (150) and condition (128), we may write an asymptotic expansion for it [cf. (151)]:

$$\begin{aligned}\mathcal{D}_G(\mathbf{p}, \mathbf{q}; x) &= \frac{2m\mathrm{V}_\star}{z^{3/2}}\exp\left[\frac{m^2(1-z)}{\sigma^2}\right]\\ &\times\left[1 - \frac{3\sigma^2}{8m^2}\left(1 - \frac{1}{z}\right) + \frac{3\sigma^4}{128m^4}\right.\\ &\left.\times\left(1 - \frac{1}{z}\right)\left(11 + \frac{5}{z}\right) + \mathbb{O}\left(\frac{\sigma^6}{m^6}\right)\right].\end{aligned} \quad (159)$$

For self-consistency, one should rewrite this formula in an approximation satisfying the SRGP approximation conditions for function $\psi_G(\mathbf{p}, x)$. We use the truncated series for z for this purpose:

$$\begin{aligned}z &= \frac{E*}{m}\left(1 + \frac{\sigma^4\mathbf{x}_*^2}{2E_*^2}\right)\\ &+ i\frac{\sigma^2x_*^0}{m}\left(1 - \frac{\sigma^4\mathbf{x}_*^2}{2E_*^2}\right) + \mathbb{O}\left(\frac{\sigma^8}{m^8}\right).\end{aligned}$$

Inserting it into (159) and expanding the logarithm of ratio $\mathcal{D}_G/(2m\mathrm{V}_\star)$ (written in the center-of-inertia

frame) in powers of small parameter σ^2/m^2, we arrive at the following relation:

$$\ln\left[\frac{D_G(\mathbf{p}_*,-\mathbf{p}_*;x_*)}{2m\mathrm{V}_\star}\right] = -imx_*^0\left\{1+\frac{3\sigma^2}{2mE_*}\times\left[1+\frac{\sigma^2}{4mE_*}\left(1-\frac{4}{3}m^2\mathbf{x}_*^2\right)\right]\right\} - \frac{3}{2}\ln_* - \frac{m^2(\Gamma_*-1)}{\sigma^2} - \frac{\sigma^2\mathbf{x}_*^2}{2\Gamma_*} + \frac{3\sigma^2(\Gamma_*-1)}{8mE_*} - \frac{3\sigma^4}{4m^2E_*^2}\left\{m^2\left[(x_*^0)^2+\mathbf{x}_*^2\right]-\frac{P_*^2}{4m^2}\right\} + \mathbb{O}\left(\frac{\sigma^6}{m^6}\right),$$

where $\Gamma_* = E_*/m$. It can be seen that, if conditions

$$\sigma^2(x_*^0)^2 \ll E_*^2/\sigma^2 \quad \text{and} \quad \sigma^2\mathbf{x}_*^2 \ll E_*^2/\sigma^2, \qquad (160)$$

are satisfied, it is sufficient to use just four principal terms of the expansion in σ^2/m^2. The resultant formula in this approximation is

$$\mathscr{D}_G(\mathbf{p}_*,-\mathbf{p}_*;x_*) = \frac{2m\mathrm{V}_\star}{\Gamma_*^{3/2}} \times \exp\left[-imx_*^0 - \frac{m^2(\Gamma_*-1)}{\sigma^2} - \frac{\sigma^2\mathbf{x}_*^2}{2\Gamma_*}\right], \qquad (161)$$

where one should set $\mathrm{V}_\star = [\pi/(2\sigma^2)]^{3/2}$ (see the next section).

As expected, $\mathscr{D}_G(\mathbf{p}_*,-\mathbf{p}_*;x_*)$ decreases rapidly if $|\mathbf{p}_*|$ or $|\mathbf{x}_*|$ (or both quantities) are sufficiently large. The formal conditions for this, examined qualitatively in Section 4.4 for a WP of the general form, now become evident. In addition, commutator function (161) has certain properties that were not obvious in advance. It can be seen, e.g., that the dependence of $|\mathscr{D}_G|$ on variables x_0 and $\mathbf{x}$ vanishes on classical trajectories, while ratio $|D_G|/(2m\mathrm{V}_\star)$ is exponentially small even at subrelativistic energies ($\Gamma_* - 1 \sim 1$) and tends to zero at ultrarelativistic energies ($\Gamma_* \gg 1$) almost independently of $|\mathbf{x}_*|$. It is easy to demonstrate that

$$\frac{|\mathscr{D}_G(\mathbf{p}_*,-\mathbf{p}_*;x_*)|}{2m\mathrm{V}_\star} \le \exp\left[-\sqrt{2\left(1-\frac{1}{\Gamma_*}\right)}m|\mathbf{x}_*|\right],$$

at any σ.

Transforming (161) to the laboratory frame and switching to nonrelativistic energies, we obtain

$$\mathscr{D}_G(\mathbf{p},\mathbf{q};x) \approx 2m\mathrm{V}_\star \exp\left[-im(x_0-\mathbf{vx}) - \frac{m^2}{8\sigma^2}\times|\mathbf{v}_\mathbf{p}-\mathbf{v}_\mathbf{q}|^2 - \frac{\sigma^2}{2}|\mathbf{x}-\mathbf{v}x_0|^2\right]. \qquad (162)$$

Here, $\mathbf{v}_\mathbf{p} = \mathbf{p}/m$ and $\mathbf{v}_\mathbf{q} = \mathbf{q}/m$ are the group velocities of packets in the laboratory frame, $\mathbf{v} = \frac{1}{2}(\mathbf{v}_\mathbf{p}+\mathbf{v}_\mathbf{q})$, and it is assumed that $\mathbf{v}_\mathbf{p}^2 \ll 1$ and $\mathbf{v}_\mathbf{q}^2 \ll 1$. Note that the contribution $\propto (m^2/\sigma^2)$ in (162) may be large if $\mathbf{v}_\mathbf{p} \neq \mathbf{v}_\mathbf{q}$ and parameter σ is sufficiently small.

The transition to the plane-wave limit in (161) is not entirely trivial. In order to find this limit, we use asymptotic formula (133) (see Section 5.1), which provides an opportunity to prove that the following relation holds true for an arbitrary smooth function $F(\mathbf{p})$:

$$\lim_{\sigma\to 0}\int\frac{d\mathbf{p}_*}{(2\pi)^3 2E_{\mathbf{p}_*}}\mathscr{D}_G(\mathbf{p}_*,-\mathbf{p}_*;x_*)F(\mathbf{p}_*) = \frac{1}{8}e^{-imx_*^0}F(0).$$

Therefore,

$$\lim_{\sigma\to 0}\mathscr{D}_G(\mathbf{p},\mathbf{q};x) = (2\pi)^3 2E_*\delta(2\mathbf{p}_*)e^{-imx_*^0} = (2\pi)^3 2E_\mathbf{p}\delta(\mathbf{p}-\mathbf{q})e^{-ipx}.$$

Using kinematic relations (120a), one may rewrite inequalities (160) in an explicitly relativistically invariant (although somewhat less clear) form:

$$[(p+q)x]^2 \ll \left[(p+q)^2/\sigma^2\right]^2, \quad (p+q)^2|x^2| \ll \left[(p+q)^2/\sigma^2\right]^2. \qquad (163)$$

It is easy to demonstrate that conditions (163) agree completely with conditions (156), which define the domain of SRGP applicability. In much the same way, one may also rewrite expression (161) in an explicitly Lorentz-invariant form. We do not cite the corresponding formula, since it is rather cumbersome and not very useful in practice. It is often easier to operate in the center-of-inertia frame of two packets and boost to the laboratory frame only in the resultant expressions.

Let us examine n-packet matrix elements (123) with equal momenta ($\mathbf{p}_i = \mathbf{p}$, $\forall i$) as an important application of formula (161). The general case, which was discussed briefly in Section 4.5, is illustrated well by the simplest examples with $n = 2$ and 3. Rewriting relations (124) in the center-of-inertia frame, which is the same as the intrinsic frame of reference (the same for all one-packet "substates") in this case, and inserting (161), we find:

$${}_2\langle\mathbf{p},s,x|\,\mathbf{p},s,x\rangle_2 = (2m\mathrm{V}_\star)^2\times\left[1\pm\delta_{s_1s_2}\exp\left(-\sigma^2\left|\mathbf{x}_1^\star-\mathbf{x}_2^\star\right|^2\right)\right],$$

$${}_3\langle\mathbf{p},s,x|\,\mathbf{p},s,x\rangle_3 = (2m\mathrm{V}_\star)^3\times\left[1\pm\sum_{i<j}\delta_{s_is_j}\exp\left(-\sigma^2\left|\mathbf{x}_i^\star-\mathbf{x}_j^\star\right|^2\right) + 2\delta_{s_1s_2}\delta_{s_2s_3}\delta_{s_3s_1}\exp\left(-\frac{\sigma^2}{2}\sum_{i<j}\left|\mathbf{x}_i^\star-\mathbf{x}_j^\star\right|^2\right)\right],$$

where plus and minus signs correspond to bosons and fermions, respectively. It can be seen that the Bose–Einstein attraction and the Fermi repulsion, which are found at $s_i = s_j$ for any pair of particles (i, j), are significant only at short distances between the centers of packets i and j satisfying condition

$$\sigma^2 \left|\mathbf{x}_i^\star - \mathbf{x}_j^\star\right|^2 \lesssim 1. \tag{164}$$

In other words, both effects become significant when the spatial distance between identical packets (measured in their common rest frame) is comparable to the size of packets (i.e., precisely when it becomes necessary to consider the dynamic interaction of packets). At sufficiently large distances between packets, the difference in quantum statistics is irrelevant. This conclusion remains valid for states with an arbitrary number of noninteracting identical packets and is crucial to constructing the quantum WP statistics.

5.6. Effective Size and Mass of a Packet

It is easy to find an explicit form of volume $\mathrm{V}_\star$, which is defined by (97), in the RGP approximation:

$$\mathrm{V}_\star = \frac{\pi^2 \lambda K_1(\lambda)}{2m^3\left[K_1(\lambda/2)\right]^2} = \left(\frac{\pi}{2\sigma^2}\right)^{3/2} \times \left[1 - \frac{9}{8\lambda} + \frac{249}{128\lambda^2} + \mathbb{O}\left(\frac{1}{\lambda^3}\right)\right], \quad \lambda = \frac{m^2}{\sigma^2}. \tag{165}$$

The explicit formula for mean mass $\langle m\rangle$ may also be derived as an asymptotic expansion in parameter $1/\lambda$. It is convenient to use Watson's lemma, which states that the term-wise Laplace transform for the power expansion of function $f(t)$ is the expansion of the Laplace transform of this function, for this purpose. In the case under consideration,

$$\int_0^\infty dt t^{a-1} e^{-\lambda t} f(t) \sim \sum_{n=0}^\infty \frac{\Gamma(n+a) f^{(n)}(0)}{n!\lambda^{n+a}} \quad (a > 0, \lambda \gg 1).$$

Applying this asymptotic formula to the numerator and the denominator in (99) and inserting the expansion for the normalization constant from (126)

$$N_\sigma = \frac{2(\pi\lambda)^{3/2}}{m^2}\left[1 - \frac{3}{4\lambda} + \frac{33}{32\lambda^2} + \mathbb{O}\left(\frac{1}{\lambda^3}\right)\right],$$

we find the ratio of the mean packet mass to the field mass:

$$\frac{\langle m\rangle}{m} = 1 + \frac{3}{2\lambda} - \frac{3}{8\lambda^2} + \mathbb{O}\left(\frac{1}{\lambda^3}\right).$$

Thus, the mean (effective) mass of a WP exceeds the mass of its constituent Fock states by $\delta m \approx 1.5\sigma^2/m$.

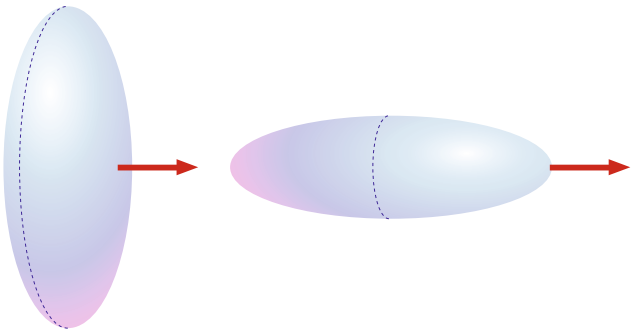

Fig. 5. SRGP in the configuration space (left) and the momentum space (right). Arrows denote the direction of the packet momentum.

Let us now turn to the SRGP model:

$$\mathrm{V}_\star \approx \left(\frac{\pi}{2\sigma^2}\right)^{3/2} \approx \frac{1.969}{\sigma^3}. \tag{166}$$

One may define (with the same accuracy) the effective WP size in the intrinsic frame of reference as diameter $d_\star$ of a sphere with volume $\mathrm{V}_\star$; i.e.,

$$d_\star = \left(\frac{6\mathrm{V}_\star}{\pi}\right)^{1/3} \approx \left(\frac{9\pi}{2}\right)^{1/6}\frac{1}{\sigma} \approx \frac{1.555}{\sigma}. \tag{167}$$

Evidently, the effective size of a packet in the laboratory frame in the direction of its momentum $\mathbf{p}$ is $d_\parallel = d_\star/\Gamma_\mathbf{p}$. An oblate spheroid with a cross diameter of $\sim 1.555/\sigma$ and an angular eccentricity of $\arccos(\Gamma_\mathbf{p})$ may serve as an illustration of a packet in the configuration space (see Fig. 5, left panel). Volumetric density $\rho(\mathbf{p}, x)$ of a packet at its center exceeds the density at the (nominal) boundary by a factor of more than three. To be more precise, this density ratio in the intrinsic frame is

$$\exp\left(\sigma^2 d_\star^2 / 2\right) = \exp\left[\left(9\pi/16\right)^{1/3}\right] \approx e^{1.21} \approx 3.35.$$

5.7. Energy and Momentum Uncertainties of a Packet

Let us examine the relation between parameter σ and quantum uncertainties of the WP energy and momentum in the SRGP approximation. Using the mean-value theorem and conditions (95), we obtain the following identity:

$$2m\mathrm{V}_\star = \varphi_G(\mathbf{p} + \delta\mathbf{p}, \mathbf{p})\int \frac{d\mathbf{k}}{(2\pi)^3 2E_\mathbf{k}}\phi_G(\mathbf{k}, \mathbf{p}) = \phi_G(\mathbf{p} + \delta\mathbf{p}, \mathbf{p}),$$

where $\delta\mathbf{p}$ is the vector to be determined with a small absolute value. This vector has a clear physical meaning: the WP momentum uncertainty. It is natural to

assume that $|\delta\mathbf{p}| \ll E_\mathbf{p}$[10]. This condition allows one to perform the expansion

$$E_{\mathbf{p}+\delta\mathbf{p}} \approx E_\mathbf{p}\left[1 + \frac{\delta\mathbf{p}\cdot\mathbf{p}}{E_\mathbf{p}^2} + \frac{|\delta\mathbf{p}|^2}{2E_\mathbf{p}^2} - \frac{(\delta\mathbf{p}\cdot\mathbf{p})^2}{2E_\mathbf{p}^4}\right],$$

which yields

$$E_{\mathbf{p}+\delta\mathbf{p}}E_\mathbf{p} - (\mathbf{p}+\delta\mathbf{p})\mathbf{p} \approx m^2 + \frac{|\delta\mathbf{p}|^2}{2} - \frac{(\delta\mathbf{p}\cdot\mathbf{p})^2}{2E_\mathbf{p}^2} = m^2 + \frac{|\delta\mathbf{p}_\parallel|^2}{2_\mathbf{p}^2} + \frac{|\delta\mathbf{p}_\perp|^2}{2},$$

where $\delta\mathbf{p}_\parallel$ and $\delta\mathbf{p}_\perp$ are the longitudinal and transverse (with respect to momentum vector $\mathbf{p}$) components of sought-for vector $\delta\mathbf{p}$. In accordance with (130), we have

$$\mathrm{V}_\star \approx \left(\frac{\pi}{\sigma^2}\right)^{3/2}\exp\left(-\frac{|\delta\mathbf{p}_\parallel|^2 + \Gamma_\mathbf{p}^2|\delta\mathbf{p}_\perp|^2}{4\sigma^2\Gamma_\mathbf{p}^2}\right) = \left(\frac{\pi}{\sigma^2}\right)^{3/2}\exp\left(-\frac{|\delta\mathbf{p}_\star|^2}{4\sigma^2}\right), \quad (168)$$

where $\delta\mathbf{p}_\star$ denotes vector $\delta\mathbf{p}$ written in the intrinsic frame of reference of the packet. Comparing relations (168) and (166) (derived in the same approximation), we find

$$|\delta\mathbf{p}_\star|^2 \approx 6\ln 2\sigma^2 \approx 4.159\sigma^2. \quad (169)$$

Formulas (167) and (166) yield "uncertainty relation"

$$d_\star\,|\delta\mathbf{p}_\star| \approx 3\sqrt{(4\pi/3)^{1/3}\ln 2} \approx 3.171. \quad (170)$$

To illustrate this, we consider a hadron WP. Its effective size obviously cannot be smaller than the natural size of the hadron itself (i.e., $d_* \gtrsim 1$ fm). It then follows from (169) and (170) that $|\delta\mathbf{p}_*| \lesssim 600$ MeV; therefore, $\sigma \approx 0.5|\delta\mathbf{p}_*| \lesssim 300$ MeV. Thus, 300 MeV is the maximum possible value of σ for a hadron WP. We will discuss the extreme allowed values σ in the SRGP model in Section 5.8.

Owing to the spherical packet symmetry in the intrinsic frame of reference,

$$|\delta\mathbf{p}_\perp|^2 = \frac{2}{3}|\delta\mathbf{p}_\star|^2 \approx 4\ln 2\sigma^2 \quad \text{and} \quad |\delta\mathbf{p}_\parallel|^2 = \frac{1}{3}|\delta\mathbf{p}_\star|^2\Gamma_\mathbf{p}^2 \approx 2\ln 2\sigma^2\Gamma_\mathbf{p}^2, \quad (171a)$$

from which it follows that

$$|\delta\mathbf{p}| \approx \sqrt{2\ln 2\left(\Gamma_\mathbf{p}^2 + 2\right)}\sigma, \quad |\delta\mathbf{p}_\parallel|/|\delta\mathbf{p}_\perp| \approx \Gamma_\mathbf{p}/\sqrt{2}. \quad (171b)$$

Relations (171) allow one to estimate the momentum uncertainty and the effective WP (half) width in the momentum space. We can see that the relative momentum uncertainty, $|\delta\mathbf{p}|/|\mathbf{p}|$, is small for ultrarelativistic momenta, but becomes arbitrarily large as $|\mathbf{p}| \to 0$:

$$\frac{|\delta\mathbf{p}|}{|\mathbf{p}|} \to \begin{cases}\sqrt{2\ln 2}\,\sigma/m & \text{for } |\mathbf{p}| \to \infty,\\ \sqrt{6\ln 2}\,\sigma/|\mathbf{p}| & \text{for } |\mathbf{p}| \to 0.\end{cases}$$

The corresponding energy uncertainty is

$$\delta E_\mathbf{p} \approx \delta\mathbf{p}\cdot\mathbf{p}/E_\mathbf{p} \approx |\delta\mathbf{p}_\parallel||\mathbf{v}_\mathbf{p}| \approx \sqrt{2\ln 2}\,|\mathbf{p}|\,\sigma/m.$$

Therefore, the relative energy uncertainty is always small, and the ultrarelativistic asymptotics, $\delta E_\mathbf{p}/E_\mathbf{p} \approx |\delta\mathbf{p}|/|\mathbf{p}| \approx \sqrt{2\ln 2}\,\sigma/m$, defines the upper limit of this ratio.

5.8. SRGP Applicability Domain

Depending on the WP production mode (i.e., the chain of reactions producing it), the effective WP sizes may vary from microscopically small to macroscopically large. The latter possibility should come as no surprise if one recalls that the "size" of a plane is infinite. Let us stress once again that the effective WP size is a characteristic of the quantum state of a field rather than an internal property of this field. This size naturally depends on the field properties, but not exclusively on them. The "natural" and, probably, practically unreachable upper limit, $d_\star^{\max}$, for the effective size of a WP characterizing an unstable particle should be of the order of its own lifetime τ (macroscopic for long-lived particles such as a neutron or a muon), while the "lower limit", $d_\star^{\min}$, is set by the inherent particle size, which is on the order of 1 fm for hadrons (compound particles) and on the order of the Compton wavelength ($\sim 1/m$) for leptons and gauge bosons (structureless particles). Whatever the case, owing to the general $\sigma^2 \ll m^2$ restriction, the packet size allowed by the formalism should be much larger than $d_\star^{\min}$.

In the case of unstable particles, conditions (153) of applicability of the SRGP approximation impose an additional tight constraint on the value of parameter σ. For these conditions to be satisfied at $0 \le |x_\star^0| \lesssim \tau$ (i.e., to avoid substantial WP spreading within the state lifetime), the $\sigma^4\tau^2 \ll m^2$ inequality should hold true. Therefore, $\sigma_{\max} = \sqrt{m/\tau}$ sets the absolute upper limit[11] for values of σ allowed in the SRGP model. Thus,

$$d_\star^{\min} = \left(\frac{9\pi}{2}\right)^{1/6}\frac{1}{\sigma_{\max}} = \left(\frac{9\pi}{2}\right)^{1/6}\left(\frac{\tau}{m}\right)^{1/2}$$

[10] This assumption is verified a posteriori by relation (171).

[11] In the physical (rather than in the formally mathematical) sense.

Table 1. The maximum allowed value of parameter σ ($\sigma_{\max} = \sqrt{m\Gamma}$) and ratio $\Gamma/\sigma_{\max} = \sqrt{\Gamma/m}$, and the minimum allowed effective size of wave packets ($d_*^{\min} \approx 1.55/\sqrt{m\Gamma}$) for some unstable particles in the SRGP approximation

Particle	$\sigma_{\max}$, eV	$\Gamma/\sigma_{\max}$	$d_\star^{\min}$, cm
$\mu^\pm$	1.78×10^{-1}	1.68×10^{-9}	1.72×10^{-4}
$\tau^\pm$	2.01×10^{3}	1.13×10^{-6}	1.53×10^{-8}
$\pi^\pm$	1.88	1.35×10^{-8}	1.63×10^{-5}
π^0	3.25×10^{4}	2.41×10^{-4}	0.94×10^{-9}
$K^\pm$	5.12	1.04×10^{-8}	5.99×10^{-6}
K_S^0	6.05×10^{1}	1.22×10^{-7}	5.07×10^{-7}
K_L^0	2.53	5.08×10^{-9}	1.21×10^{-5}
$D^\pm$	1.09×10^{3}	5.82×10^{-7}	2.82×10^{-8}
D^0	1.73×10^{3}	9.28×10^{-7}	1.77×10^{-8}
$D_s^\pm$	1.61×10^{3}	8.18×10^{-7}	1.91×10^{-8}
$B^\pm$	1.46×10^{3}	2.76×10^{-7}	2.11×10^{-8}
B^0	1.51×10^{3}	2.86×10^{-7}	2.03×10^{-8}
B_s^0	1.55×10^{3}	2.89×10^{-7}	1.98×10^{-8}
n	2.64×10^{-5}	2.81×10^{-14}	1.16
Λ	5.28×10^{1}	4.74×10^{-7}	5.81×10^{-7}
$\Lambda_c^\pm$	2.74×10^{3}	1.87×10^{-6}	1.12×10^{-8}

sets the lower limit for the effective spatial size of a WP characterizing an unstable particle in the SRGP approximation.

Since WPs are not related in any way to natural decay width $\Gamma = 1/\tau$ in the considered formalism, it is applicable only to states with $\sigma \gg \Gamma$ (more precisely, $\sigma^2 \gg \Gamma^2$), that is, to packets with spatial sizes $d_\star \ll d_\star^{\max} \sim \tau$. The lifetime of a particle needs to be sufficiently large to reconcile this constraint with conditions (153). Since $\Gamma \ll m$ for all known long-lived elementary particles and atomic nuclei, $\sigma_{\max} = \sqrt{m/\tau} = \sqrt{\Gamma m} \gg \Gamma$ and, naturally, $\sigma_{\max} \ll m$. Therefore, the SRGP approximation is expected to be applicable both to stable and unstable long-lived particles (neutrons, muons, τ-leptons, charged pions, etc.) and nuclei, but inapplicable to broad hadronic resonances, gauge bosons, and other particles that do not satisfy the $\sigma_{\max} \gg \Gamma$ condition. Note also that the maximum value of $\delta m = \langle m\rangle - m$ allowed in the SRGP model is $\delta m_{\max} \approx 1.5\sigma_{\max}^2/m = 1.5\Gamma$. Therefore, the "weighting effect" is substantial for the nucleon and baryon resonances, while its impact to physical observables needs dedicated investigation.

The values of $\sigma_{\max}$, $\Gamma/\sigma_{\max}$, and $d_\star^{\min}$ for a number of unstable elementary particles are presented for illustrative purposes in Table 1. The masses and lifetimes of particles used in the calculation were taken from [106]. The particles to be listed in Table 1 were chosen for the following reasons: the decays of $\pi^\pm$, $K^\pm$, K_L^0, and $\mu^\pm$ are the dominant sources of atmospheric and accelerator neutrinos and antineutrinos with energies $E_\nu \lesssim 1$ TeV; the decays of short-lived K_S^0, D, D_s, B, and B_s mesons and Λ, Λ_c hyperons become the dominant sources of (anti) neutrinos at $E_\nu \gg 1$ TeV (see, e.g., [107]); τ leptons, which emerge as rare events in interactions of (anti) neutrino beams with matter, serve an important purpose in oscillation experiments as "indicators" of flavor transitions $\nu_\mu \to \nu_\tau$. A neutral pion and a neutron are listed to illustrate two extreme cases (very small and very large values of $\sigma_{\max}$, respectively). In addition, the decays of free neutrons are sources of low-energy astrophysical electron antineutrinos [108].

Numerous $\beta^\pm$-active radionuclides, which act as decay sources of ν_e and $\bar\nu_e$ in reactor experiments and future experiments with β beams [109–111]; heavy

ions, which emit ν_e in the process of capture of orbital electrons from low-lying electron shells and regarded as candidate sources of monochromatic neutrino beams [112]; as well as excited ions moving along circular orbits and coherently emitting $\nu\bar{\nu}$ pairs of all flavors [113, 114] are not listed in Table 1. The value of $d_\star^{\min}$ for all such ions and nuclei is of the order of either the nucleus size or the K-orbit diameter, and their half-life period $T_{1/2}$ is long. Therefore, $\Gamma/\sigma_{\max} \sim d_\star^{\min}/T_{1/2} \lll 1$; i.e., the SRGP approximation conditions are definitely fulfilled.

It follows from Table 1 that the typical $d_\star^{\min}$ values are "mesoscopic" (i.e., span the range from an angstrom to a micrometer) and are much smaller than the widths of tracks of charged particles in detectors. Ratios $\Gamma/\sigma_{\max}$ are no greater than $\approx 2\times10^{-6}$ for all the mentioned particles (except for a neutral pion), thus allowing for a fairly wide "spectrum" of σ values satisfying the SRGP applicability conditions:

$$\Gamma^2 \ll \sigma^2 \ll \sigma_{\max}^2 \ll m^2.$$

It should be noted that hadronic resonances and other short-lived particles are also of interest in the context of neutrino oscillations, since neutrinos and antineutrinos may be produced in their decays and, what is probably even more important, may produce short-lived particles in interactions with matter. The inapplicability of the SRGP approximation to short-lived particles does not imply that the processes involving them cannot be considered within the S-matrix formalism, since resonances may be regarded as virtual particles (i.e., internal lines of Feynman diagrams). It is then not necessary to construct WPs for resonances. The same approach is actually applicable to processes involving neutral pions with a relatively large $\Gamma/\sigma_{\max}$ ratio, since the events of π^0-meson production are identified in neutrino experiments based on gamma quanta produced in their decays[12]. That said, the generalization of this formalism to particles with arbitrary decay widths is of a methodological interest, if for no other reason than because a more general approach would allow one to define more accurately the domain of applicability of the theory outlined here and provide a way to simplify the calculations for specific processes with the use of known phenomenological models for the resonance neutrino production of mesons.

[12] It is worth noting here that the states of gamma quanta emerging in processes involving (anti) neutrinos (real or virtual) may be considered in the plane-wave limit, although a rigorous substantiation of this statement is outside the bounds of the present study. See [115, 116] for a thorough discussion of the theory of photon WPs.

6. SCATTERING OF WAVE PACKETS

Let us apply the above formalism in calculating the probability of interaction of covariant WPs. Although the results are similar in part to those discussed by Peskin and Schroeder [117], some of them are novel and intriguing. For example, the explicit form of suppression of the interaction probability of WPs (in the SRGP model) scattering with a nonzero impact parameter was calculated. This result is conceptually and practically important.

The cross section for certain processes (e.g., $e^+e^- \to e^+e^-\gamma$) calculated in the plane-wave approximation does indeed contradict experimental data. This has been observed for the first time at the VEPP-4 collider in Novosibirsk in the MD-1 detector data [118]. The measured cross section turned out to be ~30% lower than the calculated one at low photon energies. It was demonstrated in [119] that impact parameters ρ up to 5 cm produce a considerable contribution to the cross section of the $e^+e^- \to e^+e^-\gamma$ process calculated in the plane-wave approximation, while transverse size a of the colliding beams did not exceed $\approx10^{-3}$ cm. If the impact parameters are limited as $\rho \le a$, the observed number of photons decreases. The theory in which the finite size of colliding beams are considered is developed in [120].

The results of our calculation are similar to the ones obtained in pioneering study [120], although the formalism developed here differs considerably from the formalism used in [120]. Let us discuss these differences. The definition (Eq. (4.1)) and the normalization condition (Eq. (4.2)) of WPs used in [120] demonstrate that they are noncovariant. Statistical averaging over the states of particles (Eq. (4.7)) was performed to pass to the density matrix in the momentum representation, which is a Fourier transform of Wigner function $n(\mathbf{r},\mathbf{p},t)$ (a fine introduction to the theory of Wigner functions and Weyl transformations may be found in [121]). Integrals $\int d\mathbf{r} n(\mathbf{r},\mathbf{p},t) = n(\mathbf{p},t)$ and $\int d\mathbf{p}/(2\pi)^3\, n(\mathbf{r},\mathbf{p},t) = n(\mathbf{r},t)$ of the Wigner function yield the particle number densities in the momentum and coordinate representations, respectively. The relative velocity of two particles was introduced ad hoc into the resulting formula for the number of interactions (e.g., Eq. (4.23)). The following approximation was also used: final-state particles were regarded as plane waves.

We deal with covariant WPs in the initial and final states and do not use the Wigner function formalism, performing calculations for a collision of WPs defined by arbitrary mean 4-coordinates x_a, x_b and 4-momenta p_a, p_b. The application of this simpler approach is made possible by the assumption of a weak dependence of the matrix element upon a momentum change within the interval of the order of the WP

momentum dispersion. This assumption, however, is not universally valid. For example, both the modulus and the phase of the matrix element are of interest in certain problems (e.g., *pp* scattering). The matrix element variation on a scale of the momentum variation in a WP should not then be neglected. Factoring this variation in as a correction at the σ/p level, one may calculate the correction to the plane-wave cross section as a function of phase of the matrix element. This is a novel and potentially interesting method for measuring this phase by varying the impact parameter of the particle collision [122]. The case of a strong momentum dependence of the matrix element is another important exception. A strong dependence is expected if an intermediate state relating the sets of initial and final particles with a 4-momentum on the mass shell exists. By virtue of the singular propagator of the intermediate state, the strong dependence of the matrix element on the combination of momenta corresponding to the 4-momentum of the intermediate state is then evident. This is the case corresponding to a virtual neutrino in the quantum-field theory of neutrino oscillations discussed in the next section.

Thus, limiting ourselves to weak variations of the matrix element on a scale of the momentum variation in a WP, we calculate the probability of interaction of two WPs. The formula reveals the suppression of the interaction probability at a nonzero impact parameter of colliding packets. We also demonstrate explicitly how the dimensionless interaction probability is expressed in terms of the product of the plane-wave cross section (with a dimension of area) and the microscopic luminosity (with a dimension of reciprocal area). Macroscopic averaging over the impact parameter leads to the well-known expression for the event number expressed in terms of the product of the plane-wave cross section and the flux.

6.1. Scattering Amplitude

Let us consider the interaction of two colliding particles a and b. Final state X and the process dynamics are arbitrary. For definiteness, each initial and final state is assumed a fermion WP. The quantum particle statistics is irrelevant in this case. We are interested in process amplitude $\mathfrak{A} = \langle\{\mathbf{p}_f, x_f\}|\mathbb{S}-1|\{\mathbf{p}_i, x_i\}\rangle$, where the curly bracket denotes a set of WPs with mean momenta $\mathbf{p}_i$ and mean coordinates $\mathbf{x}_i$ at time points x_i^0 for the initial (index i) and final (index f) states. This process amplitude takes the form

$$\mathfrak{A} = \frac{1}{\mathcal{N}}\left[\prod_{i,f}\int\frac{d\mathbf{q}_i\phi(\mathbf{q}_i,\mathbf{p}_i)e^{iq_ix_i}}{(2\pi)^3 2E_{\mathbf{q}_i}}\frac{d\mathbf{k}_f\phi^*(\mathbf{k}_f,\mathbf{p}_f)e^{-ik_fx_f}}{(2\pi)^3 2E_{\mathbf{k}_f}}\right] \times i\widetilde{\mathcal{M}}(\{\mathbf{q}_i,\mathbf{k}_f,r_i,s_f\}), \quad (172)$$

where

$$\begin{aligned} &i\widetilde{\mathcal{M}}(\{\mathbf{q}_i,\mathbf{k}_f,r_i,s_f\}) \\ &= \langle\mathbf{k}_1,s_1,\dots\mathbf{k}_{n_f},s_{n_f}|\mathbb{S}-1|\mathbf{q}_1,r_1,\dots\mathbf{q}_{n_f},r_{n_f}\rangle \\ &= (2\pi)^4\delta^4\left(\sum_i q_i-\sum_f k_f\right)i\mathcal{M}(\{\mathbf{q}_i,\mathbf{k}_f,r_i,s_f\}) \end{aligned} \quad (173)$$

is the standard plane-wave S-matrix element involving singular factor $(2\pi)^4\delta^4(\sum_i q_i-\sum_f k_f)$, which considers the conservation law of energy and momentum and the regular matrix element $i\mathcal{M}(\{\mathbf{q}_i,\mathbf{k}_f,r_i,s_f\})$.

Factor N, which corresponds to the normalization of the initial and final states, is given by

$$\begin{aligned} \mathcal{N}^2 &= \langle\{\mathbf{p}_f,x_f\}|\{\mathbf{p}_f,x_f\}\rangle\langle\{\mathbf{p}_i,x_i\}|\{\mathbf{p}_i,x_i\}\rangle \\ &= \prod_i 2m_i\mathrm{V}_{\bigstar,i}\prod_i 2m_f\mathrm{V}_{\bigstar,f} \\ &\simeq \prod_i 2\bar{E}_{\mathbf{p}_i}\mathrm{V}(\mathbf{p}_i)\prod_i 2\bar{E}_{\mathbf{p}_f}\mathrm{V}(\mathbf{p}_f). \end{aligned} \quad (174)$$

Let us rewrite the δ-function in the form of an integral over four-dimensional space:

$$(2\pi)^4\delta^4(\sum_i q_i-\sum_f k_f) = \int d^4x e^{-i\left(\sum_i q_i-\sum_f k_f\right)}.$$

This provides an opportunity to rewrite (172) as

$$\begin{aligned} \mathfrak{A} &= \frac{1}{N}\int d^4x\left[\prod_{i,f}\int\frac{d\mathbf{q}\phi(\mathbf{q}_i,\mathbf{p}_i)e^{+iq_i(x_i-x)}}{(2\pi)^3 2E_{\mathbf{q}_i}}\right. \\ &\left.\times\frac{d\mathbf{k}_f\phi^*(\mathbf{k}_f,\mathbf{p}_f)e^{-ik_f(x_f-x)}}{(2\pi)^3 2E_{\mathbf{k}_f}}\right]i\mathcal{M}(\{\mathbf{q}_i,\mathbf{k}_f,r_i,s_f\}) \\ &\simeq \frac{1}{\mathcal{N}}\left[\int d^4x\prod_{i,f}\psi(\mathbf{p}_i,x-x_i)\psi^*(\mathbf{p}_f,x-x_f)\right] \\ &\times i\mathcal{M}(\{\mathbf{p}_i,\mathbf{p}_f,r_i,s_f\}, \end{aligned}$$

which yields

$$\mathfrak{A} \simeq \frac{1}{\mathcal{N}}\mathbb{V}(0)i\mathcal{M}(\{\mathbf{p}_i,\mathbf{p}_f,r_i,s_f\}). \quad (175)$$

The approximate equality is valid for WPs that are sufficiently narrow in the momentum space and under the assumption that the variation of matrix element $\mathcal{M}(\{\mathbf{q}_i,\mathbf{k}_f,r_i,s_f\})$ is negligible on a scale of variation of form factor $\phi(\mathbf{q}_i,\mathbf{p}_i)$. The momenta integrals in this approximation turn into functions ψ defined in accordance with (108). Overlap integral

$$\mathbb{V}(0) = \int d^4x\prod\nolimits_{i,f}\psi(\mathbf{p}_i,x-x_i)\psi^*(\mathbf{p}_f,x-x_f)$$

was introduced in (175). A more general integral

$$\mathbb{V}(q) = \int d^4x\prod\nolimits_{i,f}e^{iqx}\psi(\mathbf{p}_i,x-x_i)\psi^*(\mathbf{p}_f,x-x_f),$$

which depends on external momentum q, emerges in the theory of neutrino oscillations with WPs; therefore, we use the same notation at $q=0$. Such an inte-

gral is calculated for the SRGP model in this section. In the next section, the following important relation valid for the SRGP model is proven:

$$|\mathbb{V}(0)|^2 = (2\pi)^4\delta_G(P_i - P_f)\mathrm{V}, \tag{176}$$

where $P_i = \sum_i p_i$, $P_f = \sum_f p_f$, and $\delta_G(K)$ is the Gaussian function with the plane-wave limit corresponding to the four-dimensional Dirac δ function. The explicit form of this function is given in the next section. Here, we use its plane-wave limit. Four-dimensional overlap volume V may be written as

$$\mathrm{V} = \int d^4x \prod_{i,f} |\psi(\mathbf{p}_i, x - x_i)|^2 |\psi(\mathbf{p}_f, x - x_f)|^2.$$

6.2. Number of Interactions for Noncollinear Collisions of Wave Packets

Using (176), we write the amplitude modulus squared in (175):

$$|\mathfrak{R}|^2 = \frac{(2\pi)^4\delta^4(P_i - P_f)|\mathcal{M}|^2}{\prod_i 2\bar{E}_{\mathbf{p}_i}\mathrm{V}(\mathbf{p}_i)\prod_f 2\bar{E}_{\mathbf{p}_f}\mathrm{V}(\mathbf{p}_f)} \times \int d^4x \prod_{i,f} |\psi(\mathbf{p}_i, x - x_i)|^2 |\psi(\mathbf{p}_f, x - x_f)|^2. \tag{177}$$

The microscopic probability of interaction $a + b \to X$, which is given by $|\mathfrak{R}|^2$ in (177), is proportional to the integral over four-dimensional space-time of the product of densities of probabilities of initial $|\psi(\mathbf{p}_i, x - x_i)|^2/\mathrm{V}(\mathbf{p}_i)$ and final $|\psi(\mathbf{p}_f, x - x_f)|^2/\mathrm{V}(\mathbf{p}_f)$ WPs to intersect at point x. Let us multiply (177) by the Lorentz-invariant number density of final states $\left(\prod_f \frac{d\mathbf{p}_f d\mathbf{x}_f}{(2\pi)^3}\right)$ and integrate in spatial coordinates of packets. This corresponds to the setup of many current experiments, where the momenta of particles are measured more accurately than their coordinates. Using the fact that, in accordance with (112), $\int d\mathbf{x}_f |\psi(\mathbf{p}_f, \mathbf{x}_f)|^2 = \mathrm{V}(\mathbf{p}_f)$, we find the number of interactions:

$$dN = \left(\prod_f \frac{d\mathbf{p}_f}{(2\pi)^3}\int d\mathbf{x}_f\right)|\mathfrak{R}|^2 = \frac{(2\pi)^4\delta^4(P_i - P_f)|\mathcal{M}|^2}{2\bar{E}_{\mathbf{p}_a}2\bar{E}_{\mathbf{p}_b}} \times \prod_f \frac{d\mathbf{p}_f}{(2\pi)^3 2\bar{E}_{\mathbf{p}_f}} \int d^4x \frac{|\psi(\mathbf{p}_a, x - x_a)|^2}{\mathrm{V}(\mathbf{p}_a)} \times \frac{|\psi(\mathbf{p}_b, x - x_b)|^2}{\mathrm{V}(\mathbf{p}_b)}. \tag{178}$$

The calculation of the last factor in (178), which is a four-dimensional overlap integral of two scattered WPs a and b, gives

$$\int d^4x \frac{|\psi(\mathbf{p}_a, x - x_a)|^2}{\mathrm{V}(\mathbf{p}_a)} \frac{|\psi(\mathbf{p}_b, x - x_b)|^2}{\mathrm{V}(\mathbf{p}_b)} = \frac{e^{-(\mathbf{b}\times\mathbf{n})^2/2\sigma^2_{x,ab}}}{2\pi\sigma^2_{x,ab}v_{ab}} = \frac{L(|\mathbf{b}\times\mathbf{n}|)}{v_{ab}}, \tag{179}$$

where $\mathbf{v}_a, \mathbf{v}_b$ are the velocities of particles a and b, $v_{ab} = \sqrt{(\mathbf{v}_a - \mathbf{v}_b)^2 - (\mathbf{v}_a \times \mathbf{v}_b)^2}$, $\mathbf{b} = \mathbf{x}_a - \mathbf{x}_b$, $\mathbf{n} = \mathbf{v}_{ab}/|\mathbf{v}_{ab}|$ is a unit vector codirectional with the relative velocity (explicit formulas for relative velocities are presented in Section 6.3), and $\sigma^2_{x,ab} = \sigma^2_{x,a} + \sigma^2_{x,b}$, where $\sigma^2_{x,i} = 1/2\,\sigma^2_i$, $i = a, b$. As a result, (178) may be rewritten in the following form:

$$dN = d\sigma L(|\mathbf{b}\times\mathbf{n}|) = d\sigma L(0)e^{-(\mathbf{b}\times\mathbf{n})^2/2\sigma^2_{x,ab}}. \tag{180}$$

Here, $d\sigma$ is the differential effective scattering cross section in the plane-wave approximation:

$$d\sigma = \frac{(2\pi)^4\delta^4(P_i - P_f)|\mathcal{M}|^2}{4\sqrt{(p_a p_b)^2 - m_a^2 m_b^2}} \prod_b \frac{d\mathbf{p}_f}{(2\pi)^3 2E_f},$$

where identity $\bar{E}^2_{\mathbf{p}_a}\bar{E}^2_{\mathbf{p}_b}v^2_{ab} = (p_a p_b)^2 - m_a^2 m_b^2$ was used. Factor $L(|\mathbf{b}\times\mathbf{n}|)$ in (180) has the physical meaning of luminosity of scattering of two WPs in the definition used in the scattering theory and accelerator physics. $L(|\mathbf{b}\times\mathbf{n}|)$ is defined in accordance with (179) with $L(0) = 1/2\,\pi\sigma^2_{x,ab}$.

The number of interactions of two WPs a and b is given by (180). In the case of noncollinear scattering, the number of such collisions is suppressed by factor $e^{-(\mathbf{b}\times\mathbf{n})^2/2\sigma^2_{x,ab}}$, where $|\mathbf{b}\times\mathbf{n}|$ should be interpreted as the impact parameter of scattered WPs.

The distribution of impact parameter $|\mathbf{b}\times\mathbf{n}|$ in experiments with scattering of particle beams a and b is set by the mode of production of beams. In the case of a Gaussian distribution, the number of pairs of particles a and b with impact parameter $|\mathbf{b}\times\mathbf{n}|$ is

$$n_{ab}(|\mathbf{b}\times\mathbf{n}|) = \frac{n_a n_b}{2\pi\Sigma_{x,ab}} \exp\left(-\frac{|\mathbf{b}\times\mathbf{n}|^2}{2\Sigma^2_{x,ab}}\right), \tag{181}$$

where $\Sigma_{x,ab}$ is the dispersion of impact parameter $|\mathbf{b}_T| = |\mathbf{b}\times\mathbf{n}|$ of particle beams a and b under the assumption of a fixed direction of their relative velocity $\mathbf{n}$; n_a, n_b are the numbers of particles a and b.

Averaging over the impact parameter, we arrive at the following expression for the number of interactions of particles a and b:

$$dN = d\sigma \int d\mathbf{b}_T n_{ab}(|\mathbf{b}_T|)L(|\mathbf{b}_T|) = d\sigma L, \tag{182}$$

where luminosity L is defined by the effective spatial dispersions of WPs of particle beams a and b,

$$L = \frac{1}{2\pi(\sigma_{x,ab}^2 + \Sigma_{x,ab}^2)}. \quad (183)$$

In realistic experimental configurations, $\sigma_{x,ab}^2 \ll \Sigma_{x,ab}^2$. Luminosity L given by (183) is defined in this approximation by the spatial dispersion of particle beams a and b, $L \simeq \frac{1}{2\pi\Sigma_{x,ab}^2}$, in accordance with the plane-wave approximation.

6.3. Relativistic Invariance of the Impact Parameter Squared

The four-dimensional overlap volume

$$\mathrm{V} = \int d^4x \left|\psi(\mathbf{p}_a, x - x_a)\right|^2 \left|\psi(\mathbf{p}_b, x - x_b)\right|^2$$

is Lorentz-invariant due to the relativistic invariance of function $\psi(x)$. The Lorentz-invariant number of events in (180) requires Lorentz invariance of the modulus of vector $\mathbf{b}\times\mathbf{n}$. Let us demonstrate by explicit calculations that, although $\mathbf{b}$, $\mathbf{n}$, and $\mathbf{b}\times\mathbf{n}$ are not invariant, modulus $|\mathbf{b}\times\mathbf{n}|$ is Lorentz-invariant.

Let us denote vector $\mathbf{b} = \mathbf{x}_a - \mathbf{x}_b$ in the rest frames of particles a and b as $\mathbf{b}^{(a)}$ and $\mathbf{b}^{(b)}$. Their explicit form is

$$\mathbf{b}^{(a)} = \mathbf{b} + \frac{\Gamma_a^2}{\Gamma_a + 1}(\mathbf{b}\mathbf{v}_a)\,\mathbf{v}_a$$

$$\text{and} \quad \mathbf{b}^{(b)} = \mathbf{b} + \frac{\Gamma_b^2}{\Gamma_b + 1}(\mathbf{b}\mathbf{v}_b)\,\mathbf{v}_b,$$

where $\Gamma_i = (1 - \mathbf{v}_i^2)^{-1/2}$, $i = (a, b)$.

The relative velocities in the same notation are written as

$$\mathbf{v}_{ab} = \mathbf{v}_b^{(a)} = \frac{\mathbf{p}_b^{(a)}}{E_b^{(a)}}$$

$$= \frac{1}{1 - \mathbf{v}_a\mathbf{v}_b}\left[\frac{1}{\Gamma_a}\mathbf{v}_b - \frac{\Gamma_a(1 - \mathbf{v}_a\mathbf{v}_b) + 1}{\Gamma_a + 1}\mathbf{v}_a\right],$$

$$\mathbf{v}_{ba} = \mathbf{v}_a^{(b)} = \frac{\mathbf{p}_a^{(b)}}{E_a^{(b)}}$$

$$= \frac{1}{1 - \mathbf{v}_a\mathbf{v}_b}\left[\frac{1}{\Gamma_b}\mathbf{v}_a - \frac{\Gamma_b(1 - \mathbf{v}_a\mathbf{v}_a) + 1}{\Gamma_b + 1}\mathbf{v}_b\right].$$

Thus,

$$\mathbf{b}^{(a)} \times \mathbf{v}_{ab} = \frac{1}{1 - \mathbf{v}_a\mathbf{v}_b}\left[\frac{1}{\Gamma_a}(\mathbf{b}\times\mathbf{v}_b) - \frac{\Gamma_a(1 - \mathbf{v}_a\mathbf{v}_b) + 1}{\Gamma_a + 1} \times (\mathbf{b}\times\mathbf{v}_a) + \frac{\Gamma_a}{\Gamma_a + 1}(\mathbf{b}\mathbf{v}_a)(\mathbf{v}_a\times\mathbf{v}_b)\right],$$

$$\mathbf{b}^{(b)} \times \mathbf{v}_{ba} = \frac{1}{1 - \mathbf{v}_a\mathbf{v}_b}\left[\frac{1}{\Gamma_b}(\mathbf{b}\times\mathbf{v}_a) - \frac{\Gamma_b(1 - \mathbf{v}_a\mathbf{v}_b) + 1}{\Gamma_b + 1} \times (\mathbf{b}\times\mathbf{v}_b) + \frac{\Gamma_b}{\Gamma_b + 1}(\mathbf{b}\mathbf{v}_b)(\mathbf{v}_b\times\mathbf{v}_a)\right].$$

Useful formula

$$\mathbf{v}_{ab}\times\mathbf{v}_{ba} = \frac{(\mathbf{v}_a\times\mathbf{v}_b)}{(1 - \mathbf{v}_a\mathbf{v}_b)^2}\left[1 - \frac{1}{\Gamma_a\Gamma_b} - \left(\frac{\Gamma_a}{\Gamma_a + 1} + \frac{\Gamma_b}{\Gamma_b + 1}\right)(\mathbf{v}_a\mathbf{v}_b) + \frac{\Gamma_{ab}(\mathbf{v}_a\mathbf{v}_b)^2}{(\Gamma_a + 1)(\Gamma_b + 1)}\right]$$

demonstrates that $\mathbf{v}_{ab} \neq \mathbf{v}_{ba}$, although $|\mathbf{v}_{ab}| = |\mathbf{v}_{ba}|$. It also shows that the angle between the relative velocities in the rest frame of particles is nonzero. This is a purely relativistic effect. Relative velocities $\mathbf{v}_{ab}$ and $\mathbf{v}_{ba}$ are collinear in the nonrelativistic approximation.

It can be proved that $\left|\mathbf{b}^{(a)}\times\mathbf{n}_{ab}\right|^2$ with $\mathbf{n}_{ab} = \mathbf{v}_{ab}/|\mathbf{v}_{ab}|$ is a relativistic invariant. It is instructive to note that

$$\left|\mathbf{b}^{(a)}\times\mathbf{v}_{ab}\right|^2 = \left|\mathbf{b}^{(a)}\right|^2|\mathbf{v}_{ab}|^2 - (\mathbf{b}^{(a)}\mathbf{v}_{ab})^2.$$

Let us first calculate $\left|\mathbf{b}^{(a)}\right|^2 = (bu_a)^2 - b^2$, where $u_i = \Gamma_i(1, \mathbf{v}_i)$ and $b = (0, \mathbf{b})$ in the laboratory frame with $b^2 = -\mathbf{b}^2$. In the rest frame of particle a, one considers the 4-vector of impact parameter $b = (b_0^{(a)}, \mathbf{b}^{(a)})$ with components

$$b_0^{(a)} = (bu_a), \quad \mathbf{b}^{(a)} = \mathbf{b} - \frac{\Gamma_a(bu_a)\mathbf{v}_a}{\Gamma_a + 1},$$

where $\Gamma_a(\mathbf{b}\mathbf{v}_a) = -(bu_a)$. We then calculate

$$(\mathbf{b}^{(a)}\mathbf{v}_{ab}) = \frac{(bu_a)(u_au_b) - (bu_b)}{(u_au_b)}$$

$$\text{and} \quad |\mathbf{v}_{ab}|^2 = \frac{(u_au_b)^2 - 1}{(u_au_b)^2}.$$

Thus,

$$\left|\mathbf{b}^{(a)}\times\mathbf{n}_{ab}\right|^2 = (bu_a)^2 + \frac{\left[(bu_a)(u_au_b) - (bu_b)\right]^2}{1 - (u_au_b)^2} - b^2$$

$$= \frac{\left[b(u_a - u_b)\right]^2}{1 - (u_au_b)^2} + \frac{(bu_a)(bu_b)}{(u_au_b) + 1} - b^2 = \left|\mathbf{b}^{(b)}\times\mathbf{n}_{ba}\right|^2. \quad (184)$$

Since (184) is written in an invariant form, we may calculate vector product $\left|\mathbf{b}^{(a)}\times\mathbf{n}_{ab}\right|^2$ in the rest frame of any particle (a or b). For example, the following is obtained in the rest frame of particle a:

$$\left|\mathbf{b}^{(a)}\times\mathbf{n}_{ab}\right|^2 = \mathbf{b}^2 - \frac{\Gamma_b^2(\mathbf{b}\mathbf{v}_b)^2}{\Gamma_b^2 - 1},$$

where the right-hand part is the square of the vector transverse to vector $\mathbf{v}_b$:

$$\mathbf{b}_T^2 = \mathbf{b}^2 - \mathbf{b}_L^2 = \mathbf{b}^2 - \left[\frac{(\mathbf{b}\mathbf{v}_b)\mathbf{v}_b}{\mathbf{v}_b^2}\right]^2$$

$$= \mathbf{b}^2 - \frac{\Gamma_b^2(\mathbf{b}\mathbf{v}_b)^2}{\Gamma_b^2 - 1}.$$

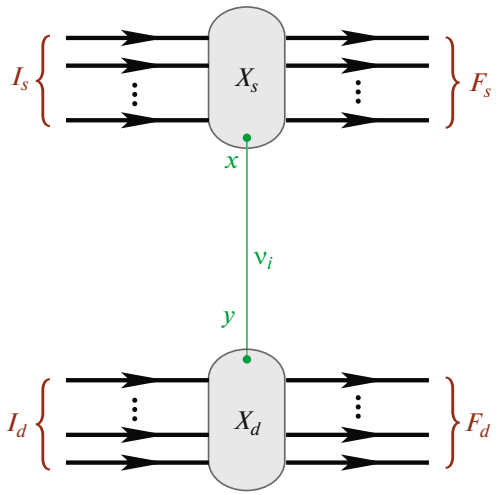

Fig. 6. Macroscopic Feynman diagram of the general form with the exchange of massive neutrinos.

Thus, the relativistic invariance of expression $\left|\mathbf{b}^{(a)} \times \mathbf{n}_{ab}\right| = \left|\mathbf{b}^{(b)} \times \mathbf{n}_{ba}\right|$ was proven.

7. MACROSCOPIC DIAGRAMS

The modification of Feynman rules, which are needed to calculate the scattering amplitudes corresponding to macroscopic Feynman diagrams with their external legs characterized by relativistic WPs rather than by Fock single-particle states, is discussed in this section.

7.1. Macroscopic Diagram of the General Form

We consider single-particle reducible connected diagrams. Their overall structure is presented in Fig. 6. The external legs of such diagrams correspond to asymptotically free initial ("in") and final ("out") WPs $|\mathbf{p}_a, s_a, x_a\rangle$ and $|\mathbf{p}_b, s_b, x_b\rangle$ in the coordinate representation (i.e., wave functions $\psi_a(\mathbf{p}_a, x_a)$ and $\psi_b^*(\mathbf{p}_b, x_b)$ characterized by the most probable momenta $\mathbf{p}_a$, $\mathbf{p}_b$; space-time coordinates x_a, x_b; masses m_a, m_b; and parameters[13] σ_a, σ_b ("dispersions") characterizing the uncertainty in momenta). The following designations are used in what follows: I_s (F_s) is the set of in (out) packets in block X_s ("source"), and I_d (F_d) is the set of in (out) packets in block X_d ("detector"). Blocks X_s and X_d denote the regions of interaction of fields and may contain arbitrary internal lines and loops. The internal line connecting blocks X_s and X_d denotes the causal Green's function of massive neutrino ν_i with mass m_i ($i = 1, 2, 3, \ldots$). It is assumed that vertices x and y are characterized by the SM Lagrangian complemented phenomenologically with the Dirac or Majorana mass term and the corresponding kinetic contribution. Therefore, the initial or the final states (or both of them) should feature a charged lepton or an (anti) neutrino[14]. Blocks X_s and X_d are assumed to be macroscopically separated in space-time (hence the term "macroscopic diagram.")

7.2. Examples of Macrodiagrams

The simplest example of a macrodiagram of the type presented in Fig. 6 is shown in Fig. 7. The sum of such diagrams (over index i) gives the process amplitude:

$$\pi^+ \oplus n \to \mu^+ \oplus \tau^- p, \tag{185}$$

where symbol $\oplus$ denotes that the diagram vertices are macroscopically separated in space-time. Processes (185) violate two lepton numbers, but their sum is conserved. Such simple reactions often produce the greatest contribution to the number of events in experiments on neutrino oscillations with atmospheric and accelerator (anti) neutrinos. In the standard quantum-mechanical approach, process (185) is regarded as a sequence of three independent subprocesses:

(i) pion decay $\pi^+ \to \mu^+\nu_\mu$ in the source (at point x_1);

(ii) neutrino propagation with the "transformation" of ν_μ into ν_τ;

(iii) quasi-elastic interaction $\nu_\tau n \to \tau^+ p$ in the detector (at point x_2).

In the diagrammatic QFT approach, process (185) is regarded as a unified whole, and the intriguing quantum-mechanical phenomenon of flavor transitions ("oscillations") $\nu_\mu \to \nu_\tau$ is reduced to trivial interference of diagrams with virtual neutrino ν_i fields of a certain mass. It is not even necessary to use states or neutrino fields with definite flavors ν_μ and ν_τ.

Let us examine several other examples of potentially interesting macrodiagrams. Figure 8 shows four diagrams of the lowest order in electroweak interaction, which characterize the μ_{e3} decay in the source accompanied by quasi-elastic scattering of a virtual neutrino (antineutrino) off a neutron (proton) with the production of a τ lepton at the detector vertex. Naturally, all these processes are strictly forbidden by the lepton-number conservation law in the SM with massless neutrinos, but they become possible if a Dirac or Majorana mass term is present in the Lagrangian. The diagrams in Figs. 8a and 8b are valid both for Dirac and Majorana (anti) neutrinos, while the diagrams in Figs. 8c and 8d are for Majorana neutrinos, which are the same as antineutrinos, only. In

[13] And, in a more general case, by sets of parameters σ_a, σ_b.

[14] To avoid unnecessary complications, we discount the possibility that the external one-packet states contain gauge or Higgs bosons.

Fig. 7. Example of a macroscopic Feynman diagram describing the $\pi_{\mu 2}$ decay at space-time point x_1 and the subsequent quasi-elastic neutrino production of a τ lepton at point x_2. Points x_1 and x_2 may be separated by a macroscopically large space-time interval.

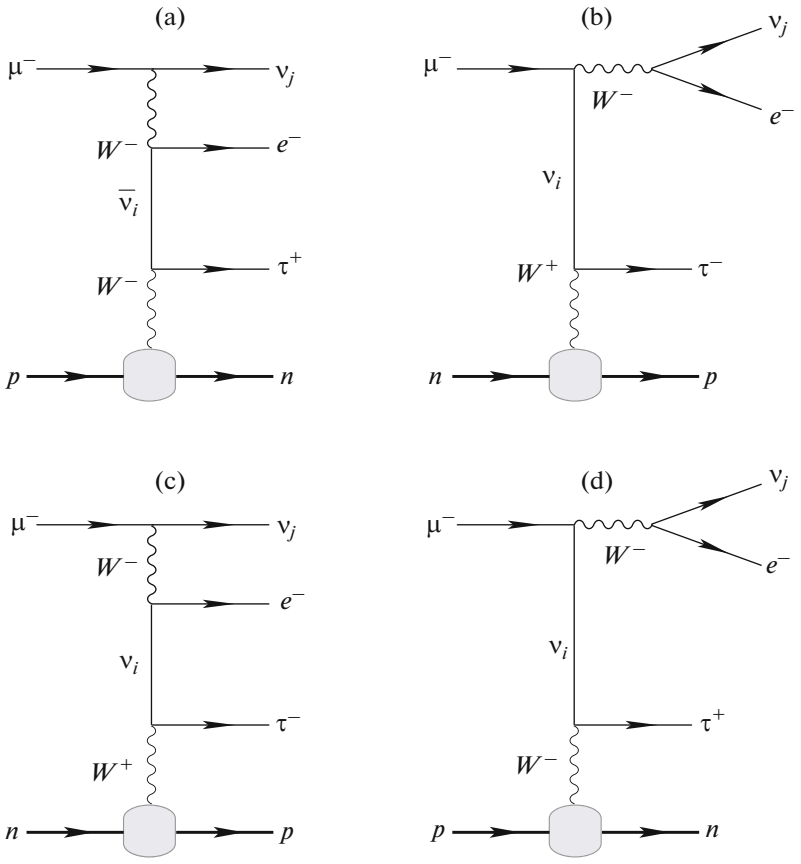

Fig. 8. Diagrams of the lowest order for electroweak interaction that describe the μ_{e3} decay in the source and the quasi-elastic production of a τ lepton in the detector.

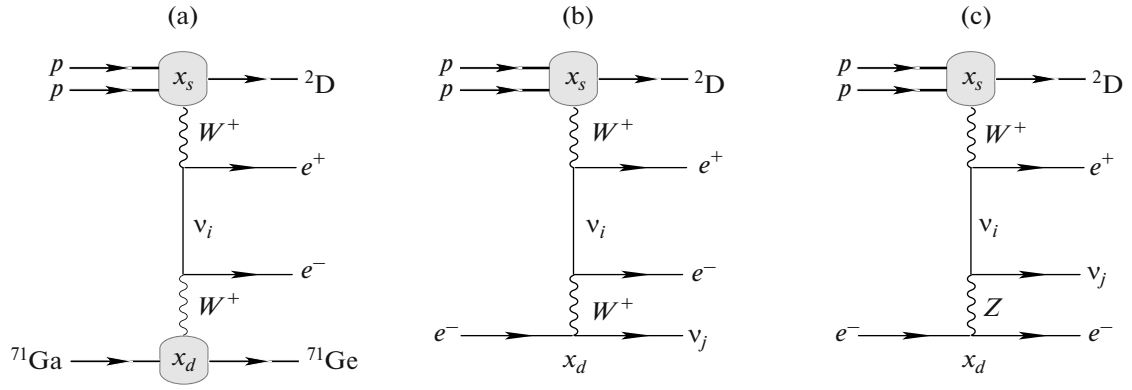

Fig. 9. Diagrams of the lowest order for electroweak interaction that describe the deuteron synthesis in the *pp*-reaction in the source and the neutrinoproduction of an electron off (a) a gallium nucleus and (b, c) a free electron in the detector.

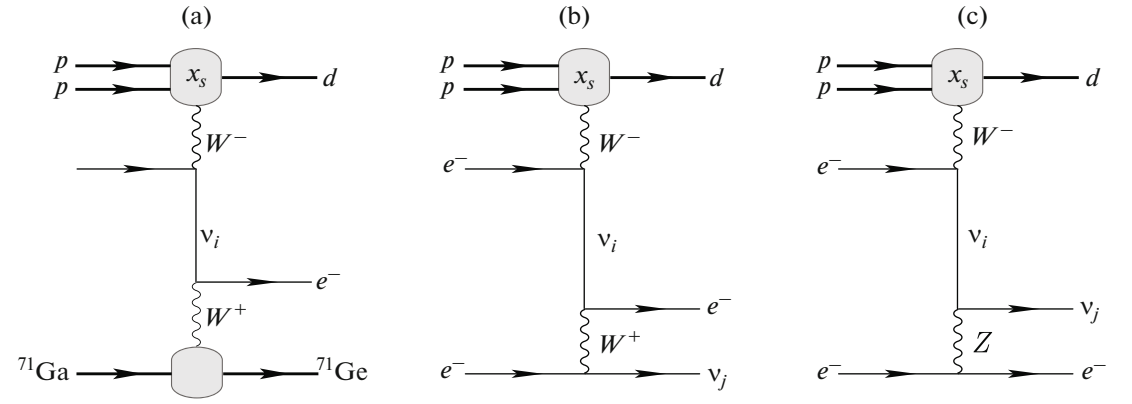

Fig. 10. Diagrams of the lowest order for electroweak interaction that describe the deuteron synthesis in the *pep*-reaction in the source and the neutrinoproduction of an electron off (a) a gallium nucleus and (b, c) a free electron in the detector.

the latter case, the diagrams in Figs. 8a, 8d and 8b, 8c interfere by pairs. Within our formalism, massive neutrinos at the external legs of these diagrams should be characterized by WPs of the same type that is used for all the other massive fields.

The diagrams in Fig. 9 describe the primary reaction of the *pp*-cycle in the Sun

$$^1\mathrm{H} + {}^1\mathrm{H} \to {}^2\mathrm{D} + e^+ + \nu_e \quad (E_\nu < 420\ \mathrm{keV})$$

and the detection of neutrinos in a Ga–Ge detector and a free-electron detector. The diagrams in Figs. 9b and 9c interfere. The diagrams in Fig. 10 describe (in the lowest order in electroweak interaction) the deuterium nuclear synthesis in the so-called *pep*-reaction

$$^1\mathrm{H} + {}^1\mathrm{H} + e^- \to {}^2\mathrm{D} + \nu_i^* \quad (E_\nu = 1.44\ \mathrm{MeV})$$

in the source (the Sun) and the subsequent interaction of virtual neutrino ν_i^* with a gallium target (Fig. 10a) and an electron target (Figs. 10b and 10c). The exceptionally "slow" *pep*-reaction produces approximately 0.25% of deuterium in the Sun and manifests itself in one of the branches of the proton–proton chain of transformation of hydrogen into helium. Although its contribution to the energy balance of the Sun is negligible, it produces a tiny, but measurable contribution to the number of events detected in gallium–germanium experiments (SAGE, GALLEX, GNO). Unfortunately, the detection thresholds for solar neutrinos in modern Cherenkov underground detectors (Super-Kamiokande and SNO) is considerably higher than the expected mean energy of neutrinos (≈ 1.44 MeV) from the *pep*-reaction in the Sun. Therefore, the processes corresponding to the diagrams in Figs. 10b and 10c are still beyond the reach of experimenters. As in the previous example, the diagrams in Figs. 10b and 10c interfere.

The exotic processes demonstrated in Fig. 10 illustrate expediency of examining macrodiagrams with more than two in-packets in each of the macroscopically separated blocks. Such diagrams are also of interest for the study of reactions involving neutrinos in dense hot plasma of the early Universe and in ultra-

dense astrophysical objects such as neutron or quark stars. In the context of neutrino oscillations, the key reason for examining diagrams with an arbitrary number of in- and out-packets at the external legs is somewhat more pragmatic: it will be shown below that the additional symmetry of formulas for amplitudes of the general form allows one to simplify their analysis by unifying the notation.

7.3. Feynman Rules

The formal definition of the initial and final states for the diagram in Fig. 6 may be written as

$$\begin{aligned} |\text{in}\rangle &= |\{\mathbf{p}_a, x_a, s_a\}, a \in I_s \oplus I_d\rangle, \\ |\text{out}\rangle &= |\{\mathbf{p}_b, x_b, s_b\}, b \in F_s \oplus F_d\rangle. \end{aligned} \tag{186}$$

Here, just as in (185), symbol $\oplus$ denotes that the WPs from I_s and I_d (and from F_s and F_d) are macroscopically separated. In addition, it is assumed that all in-packets (a) are in the distant past, while all out-packets (b) are in the distant future relative to the moment (or the time interval) of interaction in blocks X_s and X_d. In order to use the standard diagrammatic technique based on Wick's theorems, we should consider only the configurations of coordinates x_a and x_b with noninteracting packets in each substate I_s, I_d, F_s, and F_d. In other words, the spatial coordinates of the packet centers should be so distant that states (186) could be approximated well by direct products of asymptotically free one-packet states $|\mathbf{p}_a, s_a, x_a\rangle$ and $|\mathbf{p}_b, s_b, x_b\rangle$; i.e.,

$$\begin{aligned} |\text{in}\rangle &= \left(\prod_{a \in I_s \oplus I_d} \int \frac{d\mathbf{k}_a \phi_a(\mathbf{k}_a, \mathbf{p}_a) e^{ik_a x_a}}{(2\pi)^3 2E_{\mathbf{k}_a}} \sqrt{2E_{\mathbf{k}_a}} a^{(a)\dagger}_{\mathbf{k}_a s_a} \right) |0\rangle, \\ |\text{out}\rangle &= \left(\prod_{b \in F_s \oplus F_d} \int \frac{d\mathbf{k}_b \phi_b(\mathbf{k}_b, \mathbf{p}_b) e^{ik_b x_b}}{(2\pi)^3 2E_{\mathbf{k}_b}} \sqrt{2E_{\mathbf{k}_b}} a^{(b)\dagger}_{\mathbf{k}_b s_b} \right) |0\rangle. \end{aligned} \tag{187}$$

The sequence order of creation operators in (187) is not significant even if they correspond to identical fields, because, as it was demonstrated in Section 4.5, quantum correlations between identical WPs with a sufficient separation in space-time may be neglected, and the sign of the scattering amplitude is not important. The above requirements (including the macroscopic separation of interaction regions X_s and X_d) are phenomenologically justified and intuitively clear but are rather vague in the mathematical sense. Mathematically strict conditions will be formulated in Section 7.9 after the derivation of all the needed intermediate formulas.

The norm of in- and out-states may be written as

$$\begin{aligned} \langle \text{in}|\text{in}\rangle &= \prod_{a \in I_s \oplus I_d} 2\bar{E}_a \mathrm{V}_a, \\ \langle \text{out}|\text{out}\rangle &= \prod_{b \in F_s \oplus F_d} 2\bar{E}_b \mathrm{V}_b, \end{aligned} \tag{188}$$

where $\bar{E}_\varkappa \equiv \bar{E}_{\mathbf{p}\varkappa} \approx E_{\mathbf{p}\varkappa}$ and $\mathrm{V}_\varkappa = \mathrm{V}_\varkappa(\mathbf{p}_\varkappa)$ are the mean energy and the effective volume of packet ; here and elsewhere, index $\varkappa$ is used to denote both initial (a) and final (b) packets. The external in- and out-legs of diagrams associated with free fields $\Phi_a(y_a)$ ($a \in I_s \oplus I_d$) and $\Phi_b(y_b)$ ($b \in F_s \oplus F_d$) produce factors

$$\langle 0|\Phi_a(y_a)|\mathbf{p}_a, s_a, x_a\rangle \quad \text{and} \quad \langle \mathbf{p}_b, s_b, x_b|\Phi^\dagger_b(y_b)|0\rangle,$$

in the scattering amplitude. Therefore, in accordance with the adopted approximation of narrow packets in the momentum space, the standard (plane-wave) Feynman factor corresponding to an external leg should be multiplied by

$$\begin{cases} \psi_a(\mathbf{p}_a, y_a - x_a) & \text{for} \quad a \in I_s \oplus I_d, \\ \psi^*_b(\mathbf{p}_b, y_b - x_b) & \text{for} \quad b \in F_s \oplus F_d, \end{cases} \tag{189}$$

where each wave function is given by (108) and is defined by form factor $\phi_\varkappa(\mathbf{k}, \mathbf{p}_\varkappa)$, which depends on mass $m_\varkappa$ and dispersion $\sigma_\varkappa$, and 4-vector $y_\varkappa$ (integration variable) is the coordinate of the internal point (elementary interaction vertex) of intersection of external leg $\varkappa$ with a certain internal line. Therefore, the amplitude corresponding to any macrodiagram should contain factors

$$\int dy_\varkappa \psi_\varkappa(\mathbf{p}_\varkappa, y_\varkappa - x_\varkappa) f_{(\varkappa)}(z_\varkappa - y_\varkappa), \tag{190}$$

where $f_{(\varkappa)}(y_\varkappa - z_\varkappa)$ is the structural factor corresponding to the interaction of an internal line with external (in) field $\Phi_\varkappa(y_\varkappa)$ at point $y_\varkappa$ (for brevity, possible tensor or spinor indices and all arguments of function $f_{(\varkappa)}$ except $z_\varkappa - y_\varkappa$ are omitted). With the definition of function $\psi_\varkappa$ taken into account, integral (190) may be rewritten as

$$\begin{aligned} &\int dy_\varkappa \int \frac{d\mathbf{p}}{(2\pi)^3 2E_{\mathbf{p}}} e^{-ip(y_\varkappa - x_\varkappa)} \phi_\varkappa(\mathbf{p}, \mathbf{p}_\varkappa) \\ &\qquad \times \int \frac{dk}{(2\pi)^4} e^{-ik(z_\varkappa - y_\varkappa)} \tilde{f}_{(\varkappa)}(k) \\ &= \int \frac{d\mathbf{p}}{(2\pi)^3 2E_{\mathbf{p}}} e^{-ip(z_\varkappa - y_\varkappa)} \phi_\varkappa(\mathbf{p}, \mathbf{p}_\varkappa) \tilde{f}_{(\varkappa)}(p), \end{aligned}$$

where $\tilde{f}_{(\varkappa)}(p)$ is the Fourier transform of function $f_{(\varkappa)}(x)$. Owing to the expected δ-like behavior of form factor $\phi_\varkappa(\mathbf{p}, \mathbf{p}_\varkappa)$, argument p of function $\tilde{f}_{(\varkappa)}(p)$ may be replaced by $p_\varkappa = (E_{\mathbf{p}_\varkappa}, \mathbf{p}_\varkappa)$. Integral (190) then assumes the form

$$\begin{aligned} &\int dy_\varkappa \psi_\varkappa(\mathbf{p}_\varkappa, y_\varkappa - x_\varkappa) f_{(\varkappa)}(z_\varkappa - y_\varkappa) \\ &\qquad \approx \psi_\varkappa(\mathbf{p}_\varkappa, z_\varkappa - x_\varkappa) \tilde{f}_{(\varkappa)}(p_\varkappa). \end{aligned} \tag{191}$$

This result holds true for narrow WPs of the general form, but the SRGP approximation will be used in actual calculations. A relation similar to (191) may also

be obtained for out-legs of the diagram. Since the right-hand side of (191) in the plane-wave limit is the standard Feynman factor, it follows from (189) that the Feynman rules for internal lines remain unchanged.

7.4. Overlap Integrals

In what follows, we restrict ourselves to the simple case with interactions in blocks X_s and X_d being characterizable by local lepton or hadronic currents (explicit formulas will be derived in the next section for a special class of diagrams). Since the Fourier representation of the neutrino propagator contains phase factor $\exp[iq(x-y)]$ (where q is the 4-momentum of virtual neutrino ν_i), all functions $\psi_\varkappa$ and $\psi_\varkappa^*$ can be factorized off the "dynamic" diagram part in the form of the following two common factors in the integrand for the scattering amplitude:

$$\begin{aligned}\mathbb{V}_s(q) &= \int dx e^{+iqx}\left[\prod_{a\in I_s}\psi_a(\mathbf{p}_a, x-x_a)\right]\\ &\times\left[\prod_{b\in F_s}\psi_b^*(\mathbf{p}_b, x-x_b)\right],\\ \mathbb{V}_d(q) &= \int dy e^{-iqy}\left[\prod_{a\in I_d}\psi_a(\mathbf{p}_a, y-x_a)\right]\\ &\times\left[\prod_{b\in F_d}\psi_b^*(\mathbf{p}_b, y-x_b)\right].\end{aligned} \tag{192}$$

Lorentz-invariant functions (192) characterize the space-time overlap of in- and out-packets in the source and the detector averaged over the entire space-time[15] and are hereinafter called the overlap integrals. Naturally, $\mathbb{V}_s(q)$ and $\mathbb{V}_d(q)$ are functions of both 4-momentum q and 4-momenta and 4-coordinates of all external packets involved in the reaction; these parameters are omitted for brevity. Let us examine the key properties of overlap integrals needed for subsequent analysis.

7.5. Plane-Wave Limit

It is easy to see that overlap integrals (192) in the plane-wave limit ($\sigma_\varkappa \to 0$, $\forall_\varkappa$) evolve into common singular factors

$$\begin{aligned}\mathbb{V}_s(q) &\to (2\pi)^4\delta(q-q_s),\\ \mathbb{V}_d(q) &\to (2\pi)^4\delta(q+q_d),\end{aligned} \tag{193}$$

where q_s and q_d are the transferred 4-momenta in the source and the detector. They are defined in the following way:

$$q_s = \sum_{a\in I_s} p_a - \sum_{b\in F_s} p_b \quad\text{and}\quad q_d = \sum_{a\in I_d} p_a - \sum_{b\in F_d} p_b. \tag{194}$$

[15] Phase factors e^{+iqx} and e^{-iqy} in (192) may be interpreted as WPs of outgoing and incoming neutrinos.

The δ functions in (193) ensure exact energy-momentum conservation at vertices X_s and X_d (i.e., in subprocesses $I_s \to F_s + \nu_i$ and $\nu_i + I_d \to F_d$) and, as a result, energy-momentum conservation in the $I_s \oplus I_d \to F_s \oplus F_d$ process as a whole:

$$\sum_{a\in I_s\oplus I_d} p_a = \sum_{b\in F_s\oplus F_d} p_b.$$

Note that the information on space-time coordinates of external packets is lost completely in the plane-wave limit.

7.6. Overlap Tensors

The overlap integrals are nonsingular at $\sigma_\varkappa \neq 0$, and they generalize the Dirac delta functions accounting for the energy-momentum conservation. In order to obtain a quantitative description, we pass to the SRGP model and introduce tensors

$$T_\varkappa^{\mu\nu} = \sigma_\varkappa^2\left(u_\varkappa^\mu u_\varkappa^\nu - g^{\mu\nu}\right), \tag{195}$$

where $u_\varkappa = p_\varkappa/m_\varkappa = (1, \mathbf{v}_\varkappa)$ is the 4-velocity of packet $\varkappa$. Overlap integrals (192) then take the form

$$\mathbb{V}_{s,d}(q) = \int dx \exp[i\left(\pm qx - q_{s,d}x\right) - \Upsilon_{s,d}(x)], \tag{196}$$

where

$$\Upsilon_{s,d}(x) = \sum_{\varkappa\in S,D} T_\varkappa^{\mu\nu}\left(x_\varkappa - x\right)_\mu\left(x_\varkappa - x\right)_\nu,$$
$$S = I_s \oplus F_s, \quad D = I_d \oplus F_d.$$

Let us also define tensors

$$\mathfrak{R}_s^{\mu\nu} = \sum_{\varkappa\in S} T_\varkappa^{\mu\nu} \quad\text{and}\quad \mathfrak{R}_d^{\mu\nu} = \sum_{\varkappa\in D} T_\varkappa^{\mu\nu}. \tag{197}$$

Since the Lorentz-invariant quadratic form

$$T_\varkappa^{\mu\nu}x_\mu x_\nu = \sigma_\varkappa^2\left[(u_\varkappa x)^2 - x^2\right] = \sigma_\varkappa^2\mathbf{x}_\star^2$$

(where $\mathbf{x}_\star$ denotes variable $\mathbf{x}$ in the intrinsic frame of packet $\varkappa$) is nonnegative, quadratic forms $\mathfrak{R}_s^{\mu\nu}x_\mu x_\nu$ and $\mathfrak{R}_d^{\mu\nu}x_\mu x_\nu$ are also nonnegative. In addition, they are *positively defined* almost everywhere, because they can vanish only if 3-velocities $\mathbf{v}_\varkappa$ of *all* in- and out-packets are the same (in other words, if there exists a reference frame in which 3-momenta $\mathbf{p}_\varkappa$ of all packets in the source or the detector turn to zero). The later condition implies that the 3-momentum of a virtual neutrino is effectively small in magnitude[16]; specifically, the amplitude contribution for the process with zero momenta of all external particles in the exact energy-momentum conservation limit may be non-

[16] Generally speaking, four-momentum q in (196) is arbitrary and simultaneous vanishing of momenta $\mathbf{p}_\varkappa$ implies only that *the most probable* value of $|\mathbf{q}|$ is small. The order of smallness of $|\mathbf{q}|$ is governed by the smallness of ratios $\sigma_\varkappa/m_\varkappa$. We will discuss this in more detail later.

zero only if $|\mathbf{q}| \equiv 0$. With the exception of this physically irrelevant case, tensors $\Re_s^{\mu\nu}$ and $\Re_d^{\mu\nu}$ are *positively defined*, which is equivalent to the positivity of eigenvalues of matrices $\|\Re_s^{\mu\nu}\|$ and $\|\Re_d^{\mu\nu}\|$. Therefore, there exist positively defined tensors $\tilde{\Re}_s^{\mu\nu}$ and $\tilde{\Re}_d^{\mu\nu}$ such that

$$\tilde{\Re}_s^{\mu\lambda}(R_s)_{\lambda\nu} = \delta_\nu^\mu \quad \text{and} \quad \tilde{\Re}_d^{\mu\lambda}(R_d)_{\lambda\nu} = \delta_\nu^\mu \qquad (198a)$$

or, in the matrix form,

$$\tilde{\Re}_{s,d} = \|\tilde{\Re}_{s,d}^{\mu\nu}\| = g\Re_{s,d}^{-1}g, \quad \Re_{s,d} = \|\Re_{s,d}^{\mu\nu}\|, \qquad (198b)$$

where $g = \|g_{\mu\nu}\| = \mathrm{diag}(1,-1,-1,-1)$. Naturally, $|\Re_{s,d}| > 0$ and $|\tilde{\Re}_{s,d}| = |\Re_{s,d}|^{-1}$. We call $\Re_{s,d}^{\mu\nu}$ and $\tilde{\Re}_{s,d}^{\mu\nu}$ the overlap and inverse overlap tensors, respectively. The explicit form of these tensors (both in the general case and for specific processes in the source and the detector) is rather cumbersome, and the corresponding calculations are tedious. Therefore, these are given in Appendix A. The properties of certain other quantities constructed from the overlap tensors and 4-momenta involved in the calculation of macroscopic diagrams are also examined there.

One may calculate integral (196) in the explicit form using the well-known formula for the 4-dimensional Gaussian quadrature in the Minkowski space (see (B.6), Appendix B):

$$\mathbb{V}_{s,d}(q) = (2\pi)^4\tilde{\delta}_{s,d}(q \mp q_{s,d}) \times \exp[-\mathfrak{S}_{s,d} \pm i(q \mp q_{s,d})X_{s,d}]. \qquad (199)$$

Here,

$$\tilde{\delta}_{s,d}(K) = \frac{1}{(4\pi)^2\sqrt{|\Re_{s,d}|}}\exp\left(-\frac{1}{4}\tilde{\Re}_{s,d}^{\mu\nu}K_\mu K_\nu\right), \qquad (200)$$

$$X_{s,d}^\mu = \tilde{\Re}_{s,d}^{\mu\nu}\sum T_{\varkappa\nu}^\lambda x_{\varkappa\lambda} = \tilde{\Re}_{s,d}^{\mu\nu}\sum \sigma_\varkappa^2[(u_\varkappa x_\varkappa)u_{\varkappa\nu} - x_{\varkappa\nu}], \qquad (201)$$

$$\mathfrak{S}_{s,d} = \sum_{\varkappa,\varkappa'} W_{\varkappa,\varkappa'}^{\mu\nu}x_{\varkappa\mu}x_{\varkappa'\nu}, \quad \varkappa,\varkappa' \in S \quad \text{or} \quad D. \qquad (202)$$

Tensors $W_{\varkappa\varkappa'}^{\mu\nu}$ take the form

$$W_{\varkappa\varkappa'}^{\mu\nu} = \delta_{\varkappa\varkappa'}T_\varkappa^{\mu\nu} - T_{\varkappa\mu'}^\mu\tilde{\Re}_{s,d}^{\mu'\nu'}T_{\varkappa'\nu'}^\nu, \quad W_{\varkappa\varkappa'}^{\mu\nu} = W_{\varkappa'\varkappa}^{\nu\mu}, \qquad (203)$$

where indices s,d are not written explicitly but are implied. Let us clarify the physical meaning of quantities (200)–(202).

7.7. Factors Governing the Energy-Momentum Balance

As one can see from the integral representation of functions (200)

$$\tilde{\delta}_{s,d}(K) = \int\frac{dx}{(2\pi)^4}\exp\left(iKx - \Re_{s,d}^{\mu\nu}x_\mu x_\nu\right),$$

factors $\tilde{\delta}_s(q-q_s)$ and $\tilde{\delta}_d(q+q_d)$ in (199) turn into common δ functions $\delta(q-q_s)$ and $\delta(q+q_d)$ in the plane-wave limit. The probability of the $I_s \oplus I_d \to F_s \oplus F_d$ process at small (but nonzero) σ values will be suppressed strongly at small deviations from the exact 4-momentum conservation (i.e., at a small imbalance between the transfers of 4-momenta q_s and q_d at the macrodiagram vertices and the 4-momentum of a virtual neutrino). The process probabilities averaged in a certain way over the external momenta configurations (including, in general, the momenta of detected secondary particles averaged over finite intervals set by the experimental conditions) are measured in real experiments. Therefore, factors $\tilde{\delta}_s(q-q_s)$ and $\tilde{\delta}_d(q+q_d)$ account for the statistically approximate energy and momentum conservation in subprocesses of neutrino production and absorption. The allowed "imbalance" is defined by the inverse overlap tensors (i.e., the spread of 4-momenta of in- and out-packets). In what follows, only the configurations of external momenta producing a significant contribution to the total process probability averaged over all possible configurations are assumed when we talk about the approximate energy-momentum conservation at the vertices. A specific implementation of such averaging was examined in [58].

7.8. Impact Points, Geometric Suppression Factors, Symmetries, and All That

Let us transform quadratic forms $\mathfrak{S}_s$ and $\mathfrak{S}_d$ using definitions (197), (202), and (203):

$$\mathfrak{S}_{s,d} = \sum_{\varkappa,\varkappa'}T_\varkappa^{\mu\mu'}(\tilde{\Re}_{s,d})_{\mu'\nu'}T_{\varkappa'}^{\nu'\nu}x_{\varkappa\mu}(x_\varkappa - x_{\varkappa'})_\nu$$
$$= \sum_\varkappa T_\varkappa^{\mu\nu}x_{\varkappa\mu}x_{\varkappa\nu} - \sum_{\varkappa,\varkappa'}T_\varkappa^{\mu\mu'}(\tilde{\Re}_{s,d})_{\mu'\nu'}T_{\varkappa'}^{\nu'\nu}x_{\varkappa\mu}x_{\varkappa'\nu}.$$

Inserting a unit matrix into the last terms and taking (201) and (202) into account, we find

$$\mathfrak{S}_{s,d} = \sum_\varkappa T_\varkappa^{\mu\nu}x_{\varkappa\mu}x_{\varkappa\nu} - \left(\sum_\varkappa T_{\varkappa\mu'}^\mu x_{\varkappa\mu}\right) \times \tilde{\Re}_{s,d}^{\mu'\lambda}(\Re_{s,d})_{\lambda\rho}\tilde{\Re}_{s,d}^{\rho\nu'}\left(\sum_{\varkappa'}T_{\varkappa'\nu'}^\nu x_{\varkappa'\nu}\right)$$
$$= \sum_\varkappa T_{\varkappa\mu'}^\mu x_{\varkappa\mu}x_{\varkappa\nu} - (\Re_{s,d})_{\mu\nu}X_{s,d}^\mu X_{s,d}^\nu,$$

whence it follows that

$$\mathfrak{S}_{s,d} = \sum_\varkappa T_{\varkappa\mu\nu}\left(x_\varkappa^\mu x_\varkappa^\nu - X_{s,d}^\mu X_{s,d}^\nu\right). \qquad (204)$$

The obtained expression is the weighted mean (over all external packets at the corresponding vertex) of quadratic deviations of the components of 4-vectors $x_\varkappa$ ($\varkappa \in S, D$) from the corresponding components of the space-time point $X_{s,d}$. Tensor components $T_\varkappa^{\mu\nu}$ act

as "weights." Thus, points X_s and X_d are the centers of space-time regions of packet interactions in the source and the detector. One needs to study the properties of symmetry of $X_{s,d}$ and $\mathfrak{S}_{s,d}$ to clarify the physical and geometrical meaning of this result.

7.8.1. Translation group. It is easy to prove that quadratic forms $\mathfrak{S}_s$ and $\mathfrak{S}_d$ are invariant with respect to translations of all coordinates $x_\varkappa$ by one and the same arbitrary 4-vector y,

$$x_\varkappa \mapsto x'_\varkappa = x_\varkappa + y. \tag{205}$$

Indeed, $X_{s,d} \mapsto X'_{s,d} = X_{s,d} + y$ under this transformation; therefore

$$\mathfrak{S}_{s,d} \mapsto \mathfrak{S}'_{s,d} = \mathfrak{S}_{s,d} + \sum_\varkappa T_{\varkappa\mu\nu} \times \left(y^\mu x_\varkappa^\nu + x_\varkappa^\mu y^\nu - y^\mu X_{s,d}^\nu - X_{s,d}^\mu y^\nu\right) = \mathfrak{S}_{s,d} + 2y_\mu \sum_\varkappa T_{\varkappa\nu}^\mu \left(x_\varkappa^\nu - X_{s,d}^\nu\right).$$

Since, according to (201),

$$\sum_\varkappa T_{\varkappa\nu}^\mu X_{s,d}^\nu = (\mathfrak{R}_{s,d})_\nu^\mu X_{s,d}^\nu = (\mathfrak{R}_{s,d})_\nu^\mu \tilde{\mathfrak{R}}_{s,d}^{\nu\nu'} \sum_\varkappa T_{\varkappa\nu'}^\lambda x_{\varkappa\lambda} = \sum_\varkappa T_\varkappa^{\mu\nu} x_{\varkappa\nu},$$

it follows that, as stated,

$$\mathfrak{S}'_{s,d} = \mathfrak{S}_{s,d}.$$

It should be noted that quadratic forms $\mathfrak{S}_s$ and $\mathfrak{S}_d$ are also invariant with respect to inversion of space-time coordinates, $x_\varkappa \mapsto -x_\varkappa$.

Performing transformation (205) with $y = -X_{s,d}$ in (204), we obtain the following representation for functions $\mathfrak{S}_{s,d}$:

$$\mathfrak{S}_{s,d} = \sum_\varkappa T_\varkappa^{\mu\nu} \left(x_\varkappa - X_{s,d}\right)_\mu \left(x_\varkappa - X_{s,d}\right)_\nu. \tag{206a}$$

It follows immediately from (206a) that quadratic forms $\mathfrak{S}_s$ and $\mathfrak{S}_d$ are nonnegative and, consequently, factors $\exp(-\mathfrak{S}_s)$ and $\exp(-\mathfrak{S}_d)$ in (199) suppress the amplitude for certain configurations of momenta and coordinates of in- and out-packets. Using definition (195), we rewrite (206a) as

$$\mathfrak{S}_{s,d} = \sum_\varkappa \sigma_\varkappa^2 \left\{\left[u\left(x - X_{s,d}\right)\right]^2 - \left(x_\varkappa - X_{s,d}\right)^2\right\} \tag{206b}$$

$$= \sum_\varkappa \sigma_\varkappa^2 \left|\mathbf{x}_\varkappa^{(\varkappa)} - \mathbf{X}_{s,d}^{(\varkappa)}\right|^2. \tag{206c}$$

Here and elsewhere, index "$(\varkappa)$" means that the corresponding vector is written in the intrinsic reference frame of packet $\varkappa$. It follows from (206c) the suppression is weak (i.e., $\mathfrak{S}_{s,d} \ll 1$) for configurations of coordinates and momenta such that $\sigma_\varkappa^2 \left|\mathbf{x}_\varkappa^{(\varkappa)} - \mathbf{X}_{s,d}^{(\varkappa)}\right|^2$ are small at any $\varkappa \in S, D$.

7.8.2. Group of uniform rectilinear motions. It is evident that $\mathfrak{S}_{s,d} = 0$ when all 4-coordinates $x_\varkappa$ are the same (it follows from equality $x_\varkappa = x_{s,d}$, $\forall \varkappa \in S, D$ that $X_{s,d} = x_{s,d}$). Still, is this condition *necessary* for $\mathfrak{S}_{s,d}$ to turn to zero? Fortunately, the answer is negative[17]. To see this, note that 4-vector $X_\varkappa = (u_\varkappa x_\varkappa)u_\varkappa - x_\varkappa$ and its square $X_\varkappa^2 = x_\varkappa^2 - (u_\varkappa x_\varkappa)^2$ are invariant with respect to transformation

$$x_\varkappa^0 \mapsto \tilde{x}_\varkappa^0 = x_\varkappa^0 + \theta_\varkappa, \quad \mathbf{x}_\varkappa \mapsto \tilde{\mathbf{x}}_\varkappa = \mathbf{x}_\varkappa + \mathbf{v}_\varkappa \theta_\varkappa, \tag{207}$$

where $\theta_\varkappa$ is an arbitrary real parameter with a dimension of time. Therefore, 4-vectors $X_{s,d}$ and, as is easily seen from (204), quadratic forms $\mathfrak{S}_{s,d}$ are invariant with respect to $N_{s,d}$-parametric set of transformations (207), where N_s (N_d) is the number of one-packet states contained in the initial and final states in the source (detector). All transformations of the form (207) combine into a group describing uniform rectilinear motions of packets (i.e., shifts along the classical world lines of the packet centers). Therefore, both $X_{s,d}$ and $\mathfrak{S}_{s,d}$ are defined uniquely by specifying velocities $\mathbf{v}_\varkappa$ and arbitrary space-time points $\tilde{x}_\varkappa$ on these world lines. Specifically, if the classical trajectories of all in- and out-packets intersect at the impact point, $\mathfrak{S}_{s,d} = 0$ at any point of each trajectory. Thus, packets may be separated macroscopically in space-time before and after the interaction and be considered asymptotically free, but if velocity vectors $\mathbf{v}_a$ of in-packets and vectors $-\mathbf{v}_b$ contradirectional to the velocities of asymptotically free out-packets are all "pointed" at point X_s (in the source) or X_d (in the detector), $\mathfrak{S}_s$ or $\mathfrak{S}_d$ turn to zero. In view of this, it seems natural to call 4-vectors X_s and X_d impact points of in- and out-packets in the source and the detector, respectively.

If one needs to clarify the pattern of interaction of packets, it is instructive to introduce the notion of a WP world tube, which is defined as the cylindrical space-time volume swept by an oblate ellipsoid (the model of a WP[18]) moving along a classical trajectory. Evidently, the suppression of the overlap integral (and amplitude) produced by factor $\exp(-\mathfrak{S}_s)$ ($\exp(-\mathfrak{S}_d)$) is weak if *all* world tubes of in- and out-packets in the source (detector) intersect with each other (see

[17] "Fortunately", since otherwise there would be no asymptotically free WPs, and it would be impossible to use the perturbation theory.

[18] It bears remembering that the diameter of this ellipsoid perpendicular to the vector of the most probable WP momentum $\mathbf{p}$ (and, consequently, the diameter of the classical world line) is $d_\bigstar \propto 1/\sigma$, while the diameter parallel to $\mathbf{p}$ is suppressed by factor $\Gamma_\mathbf{p}$ emerging as a result of Lorentz contraction.

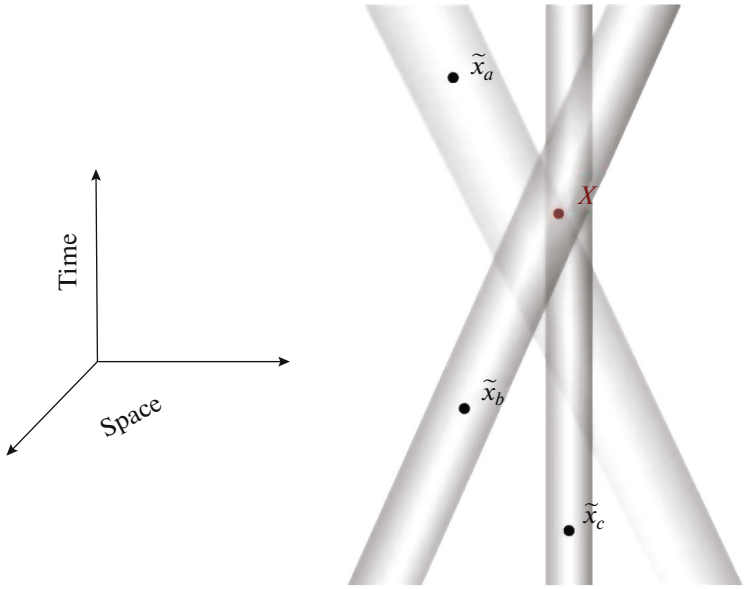

Fig. 11. Schematic representation of classical world tubes of colliding WPs. These tubes are space-time cylindrical volumes swept by classically moving spheroids modeling the WPs. Impact point X is defined unambiguously by packet velocities $\mathbf{v}_\varkappa$ and space-time points $\tilde{x}_\varkappa = \tilde{x}_\varkappa(\theta_\varkappa)$, which were chosen arbitrarily at the symmetry axes of tubes (the centers of packets move, on the average, along them). These axes are by no means required to go through point X, but if the configuration of coordinates and velocities of in- and out-packets is such that the impact point is located within the region of overlap of all world tubes of packets, the suppression of this configuration is weak (and does not take place if the axes intersect exactly at point X). In the opposite case, the suppression is strong.

Fig. 11). WPs behave somewhat like interpenetrating clouds. In order to illustrate this, we present functions $\mathfrak{S}_s$ and $\mathfrak{S}_d$ as ratios of overlap integrals of the special form:

$$\exp\left(-\mathfrak{S}_{s,d}\right) = \frac{\int dx \prod\limits_{\varkappa\in S,D} \left|\psi_\varkappa(\mathbf{p}_\varkappa, x_\varkappa - x)\right|}{\int dx \prod\limits_{\varkappa\in S,D} \left|\psi_\varkappa(\mathbf{p}_\varkappa, x)\right|}. \qquad (208a)$$

In view of the invariance of functions $\left|\psi_\varkappa(\mathbf{p}_\varkappa, x_\varkappa - x)\right|$ with respect to transformations (207), one may replace coordinates $x_\varkappa$ in (208a) by $y_\varkappa$, where

$$y^0_\varkappa = X^0_{s,d}, \quad \mathbf{y}_\varkappa = \mathbf{x}_\varkappa + \left(X^0_{s,d} - x^0_\varkappa\right)\mathbf{v}_\varkappa,$$
$$\varkappa \in S \quad \text{or} \quad D$$

and rewrite (208a) as

$$\exp\left(-\mathfrak{S}_{s,d}\right) = \frac{\int dx \prod\limits_{\varkappa\in S,D} \left|\psi_\varkappa(\mathbf{p}_\varkappa, y_\varkappa - x)\right|}{\int dx \prod\limits_{\varkappa\in S,D} \left|\psi_\varkappa(\mathbf{p}_\varkappa, x)\right|}. \qquad (208b)$$

It then follows from geometric considerations that $\exp(-\mathfrak{S}_{s,d}) < 1$ if any pair of coordinates $\mathbf{y}_\varkappa$ and $\mathbf{y}_{\varkappa'}$ do not coincide at one and the same ("impact") point in time, since the integrand in the numerator of (208b) is no greater than the integrand in the denominator. This is illustrated schematically in Fig. 12, where a pair of overlapping packets 1 and 2 is shown. These packets are presented in Fig. 12 in their center-of-inertia frame ($\mathbf{p}^*_1 + \mathbf{p}^*_2 = 0$), where they take the form of ellipsoids

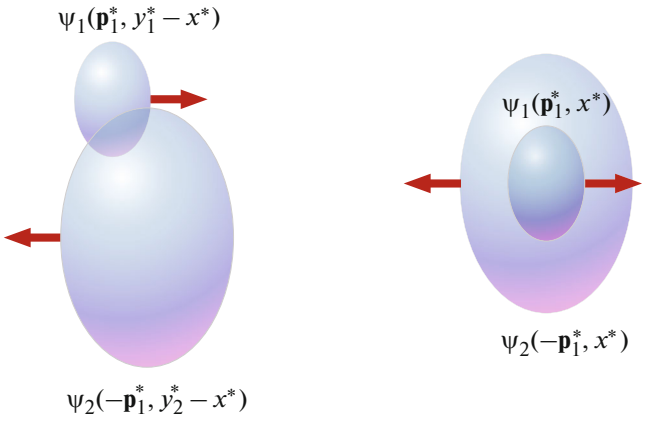

Fig. 12. Schematic illustration of two configurations of a pair of overlapping WPs in their center-of-inertia frame. The left configuration corresponds to factor $\left|\psi_1(\mathbf{p}_1, y_1 - x)\psi_2(\mathbf{p}_2, y_2 - x)\right| = \left|\psi_1(\mathbf{p}^*_1, y^*_1 - x^*)\psi_2(-\mathbf{p}^*_1, y^*_2 - x^*)\right|$ in the integrand in the numerator of (208); the right one, to factor $\left|\psi_1(\mathbf{p}_1, x)\psi_2(\mathbf{p}_2, x)\right| = \left|\psi_1(\mathbf{p}^*_1, x^*)\psi_2(-\mathbf{p}^*_1, x^*)\right|$ in the integrand in the denominator. Arrows denote momenta $\pm\mathbf{p}^*_1$.

with effective volumes $(\pi/2)^{3/2}/(\Gamma_*\sigma_{1,2}^3)$ flattened along vector $\mathbf{p}_1^*$. It can be seen that the following equality holds true for any x^* (and, consequently, for any values of the integration variable in (208b)):

$$\left|\psi_1(\mathbf{p}_1^*, y_1^* - x^*)\psi_2(\mathbf{p}_2^*, y_2^* - x^*)\right| < \left|\psi_1(\mathbf{p}_1^*, x^*)\psi_2(\mathbf{p}_2^*, x^*)\right| \quad \text{at} \quad y_1^* \neq y_2^*.$$

Naturally, the value of (208b) is small if 4-coordinates $y_\varkappa^*$ and $y_{\varkappa'}^*$ of *any* pair of packets $\varkappa$ and $\varkappa'$ differ substantially from each other.

Identity (208b) may be rewritten in the following equivalent form:

$$\exp\left(-2\mathfrak{S}_{s,d}\right) = \frac{\int dx \prod\limits_{\varkappa\in S,D} |\psi_\varkappa(\mathbf{p}_\varkappa, y_\varkappa - x)|^2}{\int dx \prod\limits_{\varkappa\in S,D} |\psi_\varkappa(\mathbf{p}_\varkappa, x)|^2}. \quad (209)$$

Factor $\exp\left[-2\left(\mathfrak{S}_s + \mathfrak{S}_d\right)\right]$ is included in the scattering amplitude squared.

7.8.3. Impact vectors. Let us find the spatial distance between the impact point and classical WP world line $\tilde{\mathbf{x}}_\varkappa(\theta_\varkappa) = \mathbf{x}_\varkappa + \mathbf{v}_\varkappa\theta_\varkappa$. In other words, we aim to determine the classical impact parameter

$$|\mathbf{b}_\varkappa| = \min_{-\infty<\theta_\varkappa<\infty} |\tilde{\mathbf{x}}_\varkappa(\theta_\varkappa) - \mathbf{X}_{s,d}|.$$

It is evident that $|\mathbf{b}_\varkappa| = |\mathbf{x}_\varkappa - \mathbf{X}_{s,d}|$ for a motionless packet $\varkappa$. The impact parameter for a moving packet is defined by the following condition:

$$|\mathbf{v}_\varkappa|\theta_\varkappa = \mathbf{n}_\varkappa(\mathbf{X}_{s,d} - \mathbf{x}_\varkappa), \quad \mathbf{n}_\varkappa = \mathbf{v}_\varkappa/|\mathbf{v}_\varkappa|.$$

Relying on this condition and assuming temporarily that $\mathbf{v}_\varkappa \neq 0$, we construct 4-vector $b_\varkappa$ with components

$$\begin{aligned} b_\varkappa^0 &= \left(x_\varkappa^0 - X_{s,d}^0\right) - |\mathbf{v}_\varkappa|^{-1}\mathbf{n}_\varkappa(\mathbf{x}_\varkappa - \mathbf{X}_{s,d}), \\ \mathbf{b}_\varkappa &= (\mathbf{x}_\varkappa - \mathbf{X}_{s,d}) - [\mathbf{n}_\varkappa(\mathbf{x}_\varkappa - \mathbf{X}_{s,d})]\mathbf{n}_\varkappa. \end{aligned} \quad (210)$$

The last equality implies that

$$\mathbf{n}_\varkappa\mathbf{b}_\varkappa = 0 \quad \text{and} \quad \mathbf{n}_\varkappa \times \mathbf{b}_\varkappa = \mathbf{n}_\varkappa \times (\mathbf{x}_\varkappa - \mathbf{X}_{s,d}), \quad (211)$$

whence it follows that

$$|\mathbf{b}_\varkappa| = |\mathbf{n}_\varkappa \times (\mathbf{x}_\varkappa - \mathbf{X}_{s,d})|.$$

Thus, $|\mathbf{b}_\varkappa| = 0$ if velocity vector $\mathbf{v}_\varkappa$ is collinear to vector $\mathbf{x}_\varkappa - \mathbf{X}_{s,d}$ at any value of $|\mathbf{x}_\varkappa - \mathbf{X}_{s,d}| < \infty$ (i.e., if the classical world line of the center of packet $\varkappa$ goes through the impact point). In addition, $b_\varkappa^0 = |\mathbf{b}_\varkappa| = 0$ if $\mathbf{x}_\varkappa - \mathbf{X}_{s,d} = \mathbf{v}_\varkappa\left(x_\varkappa^0 - X_{s,d}^0\right)$. Since 4-vector $b_\varkappa = (b_\varkappa^0, \mathbf{b}_\varkappa)$ (determined to within its sign) is a straightforward relativistic generalization of a common nonrelativistic impact parameter, it is natural to call it the impact vector. Taking (211) into account, we find

$$(u_\varkappa b_\varkappa)^2 - b_\varkappa^2 = \Gamma_\varkappa^2\left(b_\varkappa^0\right)^2 - b_\varkappa^2 = \left(\Gamma_\varkappa^2 - 1\right)\left(b_\varkappa^0\right)^2 + \mathbf{b}_\varkappa^2. \quad (212)$$

Inserting $b_\varkappa$ instead of $x_\varkappa - X_{s,d}$ into (206b) (the value of $\mathfrak{S}_{s,d}$ remains unchanged) and using (212), we find

$$\begin{aligned} \mathfrak{S}_{s,d} &= \sum_{\varkappa\in S,D} \sigma_\varkappa^2\left[\left(\Gamma_\varkappa^2 - 1\right)\left(b_\varkappa^0\right)^2 + \mathbf{b}_\varkappa^2\right] \\ &= \sum_{\varkappa\in S,D} \sigma_\varkappa^2\left|\mathbf{b}_\varkappa^{(\varkappa)}\right|^2. \end{aligned} \quad (213)$$

The contribution of each packet is written here in its intrinsic frame, where $\left|\mathbf{b}_\varkappa^{(\varkappa)}\right| = \left|\mathbf{x}_\varkappa^{(\varkappa)} - \mathbf{X}_{s,d}^{(\varkappa)}\right|$; therefore, as expected, (213) coincides with (206c). Both equalities in (213) remain true if certain packets are at rest in the laboratory frame, since it follows from (210) that

$$\lim_{\mathbf{v}\to 0}\left[\left(\Gamma_\varkappa^2 - 1\right)\left(b_\varkappa^0\right)^2 + \mathbf{b}_\varkappa^2\right] = |\mathbf{x}_\varkappa - \mathbf{X}_{s,d}|^2. \quad (214)$$

Therefore, provisional constraint $\mathbf{v}_\varkappa \neq 0$, which was used in the derivation of (213), may be removed.

The physical meaning of this result is clear: the interaction of in- and out-packets is not suppressed (i.e., the value of $\mathfrak{S}_{s,d}$ is small) if *all* impact parameters are small compared to the effective sizes of packets ($\sim 1/\sigma_\varkappa$) in their intrinsic reference frames. If all impact parameters $\left|\mathbf{b}_\varkappa^{(\varkappa)}\right|$ are of the same order of magnitude, the greatest contributions to $\mathfrak{S}_{s,d}$ are produced by packets with the largest momentum spread and, consequently, the smallest effective size[19]. If we factor out the effects of the phase space of reaction or decay and the possible influence of the interaction dynamics on the momentum spread of secondary packets, the geometric amplitude suppression becomes stronger as the number of particles (in actual practice, secondary particles) involved in the process increases. The factor of suppression of "incorrect" configurations of world lines of packets is defined in the laboratory frame by both space and time components of impact 4-vectors $b_\varkappa$. The contributions of nonrelativisitc and ultrarelativistic packets to $\mathfrak{S}_{s,d}$ take the form

$$\begin{aligned} &\sigma_\varkappa^2\left\{\left[(\mathbf{x}_\varkappa - \mathbf{X}_{s,d}) - \mathbf{v}_\varkappa\left(x_\varkappa^0 - X_{s,d}^0\right)\right]^2\right. \\ &\left. + \left[\mathbf{v}_\varkappa(\mathbf{x}_\varkappa - \mathbf{X}_{s,d})\right]^2 + \mathbb{O}\left(|\mathbf{v}_\varkappa|^3\right)\right\} \quad (|\mathbf{v}_\varkappa| \ll 1) \end{aligned} \quad (215a)$$

[19] The physical inadequacy of the notions of point-like particles (maximally localized states) and plane waves (states with definite momenta) in the QFT perturbation theory then becomes clear: the former are unable to interact (the amplitude turns to zero if a point-like particle is present in any substate $I_{s,d}$ or $F_{s,d}$), and the latter interact at arbitrarily large distances.

and

$$\sigma_\varkappa^2\{\Gamma_\varkappa^2[(x_\varkappa^0 - X_{s,d}^0) - \mathbf{n}_\varkappa(\mathbf{x}_\varkappa - \mathbf{X}_{s,d})]^2 + [\mathbf{n}_\varkappa \times (\mathbf{x}_\varkappa - \mathbf{X}_{s,d})]^2 - (x_\varkappa^0 - X_{s,d}^0) \times [(x_\varkappa^0 - X_{s,d}^0) - \mathbf{n}_\varkappa(\mathbf{x}_\varkappa - \mathbf{X}_{s,d})] + \mathbb{O}(\Gamma_\varkappa^{-2})\} \quad (\Gamma_\varkappa^2 \gg 1), \tag{215b}$$

respectively. It follows from (215a) that the suppression for nonrelativistic WPs depends only weakly on the velocity vector and time interval $x_\varkappa^0 - X_{s,d}^0$ and is determined by the spatial distance between the packet center and the impact point. In contrast, the suppression for ultrarelativistic packets depends strongly on the velocity direction and magnitude and on the difference between times $x_\varkappa^0$ and $X_{s,d}^0$. The emergence of large factor $\Gamma_\varkappa^2$ in the leading term in (215b) is related to the Lorentz contraction of the effective volume of a packet, which results in significant contraction of the region of its overlap with other packets. The reason for the strong dependence on the direction of the velocity vector is the same: one needs to "aim well" to hit a small target.

It follows from the above analysis that impact points X_s and X_d characterize the space-time positioning of the effective regions of packet interaction in the source and the detector. The interaction of packets grows stronger as the world lines of their geometric centers move closer to these points. The configuration of world lines and the coordinates of impact points are in no way related to the dynamics (i.e., to the interaction Lagrangian), since they are defined uniquely by the coordinates and group velocities of asymptotically free in- and out-packets and their effective sizes. However, if the interaction dynamics is neglected, it will not be possible to calculate the amplitude of process $I_s \oplus I_d \to F_s \oplus F_d$ characterized by the macroscopic diagram in Fig. 6.

7.9. Asymptotic Conditions

We can finally return to the physical requirements formulated at the beginning of Section 7.3 and specify the conditions under which in- and out-packets may be considered free. If the geometric suppression factors are not too small (only these configurations of coordinates and momenta contribute to the measured quantities), the requirement that the effective regions of WP interaction in the source and the detector be macroscopically separated in space-time is equivalent to the required macroscopic separation of impact points X_s and X_d. Let us assume that space and time intervals $X_d^0 - X_s^0$ and $|\mathbf{X}_d - \mathbf{X}_s|$ are large compared to space and time intervals $|x_\varkappa^0 - x_{\varkappa'}^0|$ and $|\mathbf{x}_\varkappa - \mathbf{x}_{\varkappa'}|$ for $\varkappa, \varkappa' \in S$ and $\varkappa, \varkappa' \in D$; i.e., packets from S and D do not overlap. The sought-for conditions for packets from S and D should then be independent. We assume that the effective sizes of packets are large compared to the characteristic radius of interaction at the diagram vertices. Therefore, only the properties of geometric suppression factors $\exp(-\mathfrak{S}_s)$ and $\exp(-\mathfrak{S}_d)$ independent of the interaction dynamics are examined below.

First of all, the requirement that time intervals $X_{s,d}^0 - x_a^0$ $(a \in I_{s,d})$ and $x_b^0 - X_{s,d}^0$ $(b \in F_{s,d})$ be sufficiently long should be set. However, they cannot be arbitrarily large, since packets $\varkappa$ remain stable (i.e., do not spread) within $|X_{s,d}^0 - x_\varkappa^0|$ only under the condition that

$$|X_{s,d}^{0(\varkappa)} - x_\varkappa^{0(\varkappa)}|^2 \ll m_\varkappa^2/\sigma_\varkappa^4, \quad \forall_\varkappa \in S, D. \tag{216}$$

Since the geometric suppression factors do not depend on $X_{s,d}^{0(\varkappa)}$ and $x_\varkappa^{0(\varkappa)}$, one may formulate the requirement that the left-hand side of (216) be large compared to the effective packet size squared:

$$|X_{s,d}^{0(\varkappa)} - x_\varkappa^{0(\varkappa)}|^2 \gg 1/\sigma_\varkappa^2. \tag{217}$$

This requirement does not contradict stability condition (216), since $\sigma_\varkappa^2 \ll m_\varkappa^2$. If, in addition, $\varkappa$ is an unstable particle, it is expected that

$$|X_{s,d}^{0(\varkappa)} - x_\varkappa^{0(\varkappa)}| \sim \tau_\varkappa, \tag{218}$$

where $\tau_\varkappa$ is the lifetime of $\varkappa$. Conditions (217) and (218) do not contradict each other if $\sigma_\varkappa^2 \tau_\varkappa^2 \gg 1$, which is one of the SRGP applicability conditions. The "complete set" of these conditions was obtained in Section 5.8 and has the form

$$1/\tau_\varkappa^2 \ll \sigma_\varkappa^2 \ll m_\varkappa/\tau_\varkappa \ll m_\varkappa^2. \tag{219}$$

Since $m_\varkappa \tau_\varkappa \ggg 1$ for all known long-lived elementary particles and atomic nuclei, the allowed values of σ may vary within a fairly wide interval (see Table 1).

Thus, the asymptotic conditions for time parameters $x_\varkappa^0$, which agree completely with SRGP applicability conditions (219), are given by (217), and the correct time sequence in the laboratory frame is defined by the following inequalities:

$$x_a^0 < X_{s,d}^0 < x_b^0 \quad (a \in I_{s,d}, b \in F_{s,d}). \tag{220}$$

These inequalities are Lorentz-invariant if points $x_{a,b}$ and $X_{s,d}$ are separated by time-like intervals. If intervals $(x - X_{s,d})^2$ are space-like for certain $\varkappa$, inequalities (220) are valid only in the laboratory frame, because a time sequence of two events separated by a space-like interval is not a Lorentz-invariant notion.

This should be taken into account, since a packet (for definiteness, packet a in the source) may be involved in the interaction (i.e., may not produce a significant suppressing contribution to $\mathfrak{S}_s$) even if

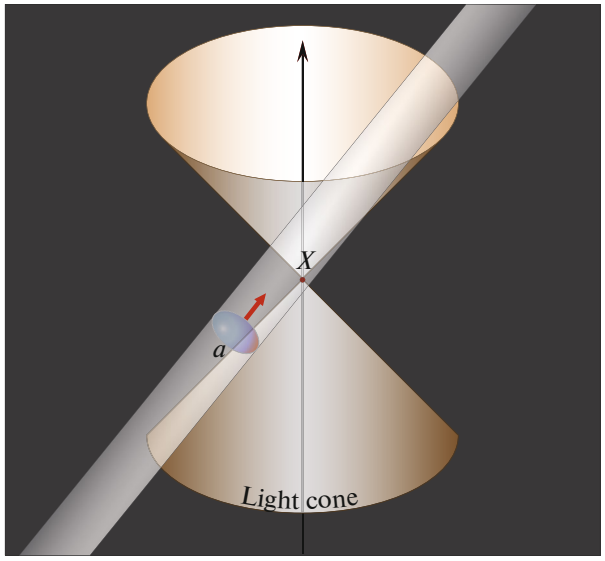

Fig. 13. Schematic illustration of an event in which the initial 4-coordinate of the center of in-packet a is separated by a space-like interval from impact point X, but a part of the effective packet volume is located within the light cone centered at X. The other in- and out-packets, the coordinates and velocities of which define (together with x_a and $\mathbf{v}_a$) the position of the impact point, are not shown.

$(x_a - X_s)^2 < 0$ under the condition that points within a part of its effective volume are separated by time-like intervals from the corresponding impact point: the impact point may then be located within the classical world tube of packet a (see Fig. 13)[20]. The microcausality condition is not violated here, since all signals propagate within the light cone. However, such interactions may potentially produce observable effects imitating causality violations.

The requirement of spatial separation of packets from impact points is, in general, not a necessary one. Certain packets (e.g., a decaying meson or a charged lepton produced in its decay in the source, a target nucleus in the detector, etc.) may indeed be at rest in the laboratory frame before or after the interaction. In this case, they should be spatially close to the corresponding impact points, otherwise, the scattering amplitude is, according to (214), small due to the smallness of factors $\exp(-\mathfrak{S}_s)$ or $\exp(-\mathfrak{S}_d)$. It is clear, however, that all packets in in- and out-states should be spatially separated; i.e., the differences in spatial coordinates of each pair of packets $\varkappa,\varkappa'$ should be large compared to the size of these packets. Representation (208b) and Fig. 12, which illustrates it, suggest that this requirement is formulated in the simplest way in the center-of-inertia frame of the pair. Since the momenta of packets in the center-of-inertia frame are collinear $\left(\mathbf{p}^*_\varkappa = -\mathbf{p}^*_{\varkappa'} = \mathbf{n}_* \left|\mathbf{p}^*_\varkappa\right|\right)$ and the only case of interest is when classical impact parameter $\left|\mathbf{n}_* \times (\mathbf{x}^*_\varkappa - \mathbf{x}^*_{\varkappa'})\right|$ does not exceed significantly the transverse size of each packet, the distance between packets should be large compared to their longitudinal size. Omitting a constant common factor of the order of unity, we write this condition as

$$\left|\mathbf{x}^*_\varkappa - \mathbf{x}^*_{\varkappa'}\right|^2 \geqslant \frac{1}{\left(\sigma_\varkappa \Gamma^*_\varkappa\right)^2} + \frac{1}{\left(\sigma_{\varkappa'} \Gamma^*_{\varkappa'}\right)^2}, \qquad (221)$$

where $\Gamma^*_{\varkappa,\varkappa'} = E^*_{\varkappa,\varkappa'} \big/ m_{\varkappa,\varkappa'}$. If packets $\varkappa$ and $\varkappa'$ are the states of identical particles with equal momenta ($\Gamma^*_\varkappa = \Gamma^*_{\varkappa'} = 1$) and spin projections, condition (217) is the same as the condition of vanishing of quantum correlations at large distances between the packets of identical bosons or fermions. The impact parameters of such packets may be arbitrarily small if one of them is in the in-state, while the other is in the out-state (i.e., the packet pair essentially describes the state of one spectator particle). If both identical packets belong to the in- or out-state of one of the diagram vertices, the corresponding amplitude is suppressed, because the distance between them does not change with time[21]. It follows from (221) that ultrarelativistic (in the center-of-inertia frame) packets forming a pair do not interact with each other even at relatively short distances.

In the general case, conditions (217) and (221) are not necessarily independent (a simple example considered below illustrates this); the only important factor is that they are not mutually exclusive. Inequalities (221) should be matched with the nonspreading conditions, that is, with (216) and similar inequalities for spatial coordinates

$$\left|\mathbf{X}^{(\varkappa)}_{s,d} - \mathbf{x}^{(\varkappa)}_\varkappa\right|^2 \ll m^2_\varkappa \big/ \sigma^4_\varkappa . \qquad (222)$$

If (as assumed) $\left|\mathbf{n}_* \times (\mathbf{x}^*_\varkappa - \mathbf{x}^*_{\varkappa'})\right|^2 \lesssim 1\big/\sigma^2_\varkappa + 1\big/\sigma^2_{\varkappa'}$ for each pair $\varkappa,\varkappa'$ from S or D, impact point $\mathbf{X}^*_{s,d}$ in the center-of-inertia frame of any such pair is located between packets $\varkappa$ and $\varkappa'$ close to their world tubes[22]. Therefore, with (217) factored in, we find

[20] It follows from geometric considerations that $0 < \left|\mathbf{b}^\bigstar_a\right| < d^\bigstar_a \big/ 2$ ($d^\bigstar_a$ is the effective transverse size of a packet) for such events. Therefore, $\sigma^2_a \left|\mathbf{b}^\bigstar_a\right|^2 < 0.605$ and $\exp\left(-\sigma^2_a \left|\mathbf{b}^\bigstar_a\right|^2\right) 0.546$.

[21] This suppression is in no way related to the Pauli Exclusion Principle: if any two packets (not necessarily those characterizing the states of identical fermions) have equal velocities and are sufficiently separated at a certain point in time, their classical world tubes do not intersect. It should also be added that parameters $\sigma_\varkappa$ and $\sigma_{\varkappa'}$ for packets of identical particles should not be regarded as fundamental characteristics of the corresponding quantum field and are not necessarily equal.

[22] More specifically, the distance from $\mathbf{X}^*_{s,d}$ to the classical trajectories of centers of packets $\varkappa$ and $\varkappa'$ in the center-of-inertia frame is much shorter than the distance between these centers.

$$\left|\mathbf{x}^*_\varkappa - \mathbf{x}^*_{\varkappa'}\right| = \left|\left(\mathbf{x}^*_\varkappa - \mathbf{X}^*_{s,d}\right) + \left(\mathbf{X}^*_{s,d} - \mathbf{x}^*_{\varkappa'}\right)\right| \simeq \left|\mathbf{x}^*_\varkappa - \mathbf{X}^*_{s,d}\right| + \left|\mathbf{x}^*_{\varkappa'} - \mathbf{X}^*_{s,d}\right|$$
$$= \Gamma^*_\varkappa \sqrt{\left[\mathbf{x}^{(\varkappa)}_\varkappa - \mathbf{X}^{(\varkappa)}_{s,d} + \mathbf{v}^*_\varkappa\left(x^{0(\varkappa)}_\varkappa - X^{0(\varkappa)}_{s,d}\right)\right]^2 - \left[\mathbf{v}^*_\varkappa \times \left(\mathbf{x}^{(\varkappa)}_\varkappa - \mathbf{X}^{(\varkappa)}_{s,d}\right)\right]^2}$$
$$+ \Gamma^*_{\varkappa'} \sqrt{\left[\mathbf{x}^{(\varkappa')}_{\varkappa'} - \mathbf{X}^{(\varkappa')}_{s,d} + \mathbf{v}^*_{\varkappa'}\left(x^{0(\varkappa')}_{\varkappa'} - X^{0(\varkappa')}_{s,d}\right)\right]^2 - \left[\mathbf{v}^*_{\varkappa'} \times \left(\mathbf{x}^{(\varkappa')}_{\varkappa'} - \mathbf{X}^{(\varkappa')}_{s,d}\right)\right]^2},$$

where $\mathbf{v}^*_\varkappa = \mathbf{p}^*_\varkappa \big/ E^*_\varkappa$ and $\mathbf{v}^*_{\varkappa'} = \mathbf{p}^*_{\varkappa'} \big/ E^*_{\varkappa'}$ are the velocities of packets $\varkappa$ and $\varkappa'$ in the center-of-inertia frame. Since it follows from Lorentz transformations that $\mathbf{v}^*_\varkappa \times \left(\mathbf{x}^*_\varkappa - \mathbf{X}^*_{s,d}\right) = \mathbf{v}^*_\varkappa \times \left(\mathbf{x}^{(\varkappa)}_\varkappa - \mathbf{X}^{(\varkappa)}_{s,d}\right)$ (the relation for $\varkappa'$ is similar), the following approximate inequality holds true:

$$\left|\mathbf{x}^*_\varkappa - \mathbf{x}^*_{\varkappa'}\right| \lesssim \Gamma^*_\varkappa \left(\left|\mathbf{x}^{(\varkappa)}_\varkappa - \mathbf{X}^{(\varkappa)}_{s,d}\right| + \left|\mathbf{v}^*_\varkappa\right|\left|x^{0(\varkappa)}_\varkappa - X^{0(\varkappa)}_{s,d}\right|\right)$$
$$+ \Gamma^*_{\varkappa'} \left(\left|\mathbf{x}^{(\varkappa')}_{\varkappa'} - \mathbf{X}^{(\varkappa')}_{s,d}\right| + \left|\mathbf{v}^*_{\varkappa'}\right|\left|x^{0(\varkappa')}_{\varkappa'} - X^{0(\varkappa')}_{s,d}\right|\right),$$

where the mutual orientations of spatial vectors and velocities in different reference frames were considered. Thus, taking conditions (216) and (222) into account, one may state that

$$\left|\mathbf{x}^*_\varkappa - \mathbf{x}^*_{\varkappa'}\right|^2 \ll 4\left(E^*_\varkappa \big/ \sigma^2_\varkappa + E^*_\varkappa \big/ \sigma^2_{\varkappa'}\right)^2 \qquad (223)$$

at any $\mathbf{v}^*_{\varkappa,\varkappa'}$.

Comparing (223) with (221), we find that SRGP applicability conditions (216) and (222) do not contradict the requirement of spatial separation of packets; i.e., no additional constraints are imposed on parameters $\sigma_{\varkappa,\varkappa'}$.

Let us illustrate condition (221) by a simple, but important (for experiments on neutrino oscillations) example in which states I_s and F_s contain just a single packet. For definiteness, we consider two-particle decay $\pi \to \mu\nu$ in the source (see Fig. 7). The two-packet integral corresponding to this process in the center-of-inertia frame of a pion and a muon ($\mathbf{p}^*_\pi = -\mathbf{p}^*_\mu \equiv \mathbf{p}_*$) is[23]

$$\mathrm{V}_{\pi\mu} = \int dx \left|\psi_\pi(\mathbf{p}_\pi, x_\pi - x)\right|\left|\psi_\mu(\mathbf{p}_\mu, x_\mu - x)\right|.$$

Changing the integration variable ($x \mapsto x + (x^*_\pi + x^*_\mu)\big/2$), we obtain the following integral:

$$\mathrm{V}_{\pi\mu} = \int dx \times \left|\psi_\pi\left(\mathbf{p}_*, x + \frac{x^*_\mu - x^*_\pi}{2}\right)\psi_\mu\left(-\mathbf{p}_*, x + \frac{x^*_\pi - x^*_\mu}{2}\right)\right|.$$

[23] Through to the end of the present section, π and μ denote particle types rather than Lorentz indices.

Its calculation in the SRGP model comes down to the consecutive computation of four standard Gaussian quadratures, which yields

$$\mathrm{V}_{\pi\mu} = \frac{\pi^2 m_\pi m_\mu}{\sigma_\pi\sigma_\mu\left(\sigma^2_\pi + \sigma^2_\mu\right)(E^*_\pi + E^*_\mu)|\mathbf{p}_*|} \times \exp\left(-\frac{\sigma^2_\pi\sigma^2_\mu}{\sigma^2_\pi + \sigma^2_\mu}\left|\mathbf{b}^*_{\pi\mu}\right|^2\right), \qquad (224)$$

where $E^*_\pi = \sqrt{\mathbf{p}^2_* + m^2_\pi}$ and $E^*_\mu = \sqrt{\mathbf{p}^2_* + m^2_\mu}$ are the energies of a pion and a muon, $\mathbf{n}_* = \mathbf{p}_*\big/|\mathbf{p}_*|$ is a unit vector, and

$$\left|\mathbf{b}^*_{\pi\mu}\right| = \left|\mathbf{n}_* \times (\mathbf{x}^*_\mu - \mathbf{x}^*_\pi)\right|$$

is the classical impact parameter in the center-of-inertia frame of a pion and a muon. Inserting (224) into (208b), we find[24]

$$\mathfrak{S}_s = \left(\frac{1}{\sigma^2_\pi} + \frac{1}{\sigma^2_\mu}\right)^{-1}\left|\mathbf{b}^*_{\pi\mu}\right|^2. \qquad (225)$$

If vectors $\mathbf{n}_*$ and $\mathbf{x}^*_\mu - \mathbf{x}^*_\pi$ are collinear, it follows from (225) that $\mathfrak{S}_s = 0$ at any distance between the centers of wave packets of a pion and a muon. If this distance is sufficiently large (e.g., $\left|\mathbf{x}^*_\mu - \mathbf{x}^*_\pi\right|^2 \gg 1\big/\sigma^2_\pi + 1\big/\sigma^2_\mu$, so that condition (221) is fulfilled), function $\mathfrak{S}_s$ is small in magnitude only at small angles α_* between vectors $\mathbf{n}_*$ and $\mathbf{x}^*_\mu - \mathbf{x}^*_\pi$, viz., $\alpha^2_* \ll \rho^{-2}_*$, where

$$\rho_* = \left(\frac{1}{\sigma^2_\pi} + \frac{1}{\sigma^2_\mu}\right)^{-1/2}\left|\mathbf{x}^*_\mu - \mathbf{x}^*_\pi\right|;$$

as α_* increases, function $\mathfrak{S}_s$ grows rapidly, while factor $\exp(-\mathfrak{S}_s)$ decreases, ruling out the possibility of $\pi_{\mu 2}$ decay for $\alpha^2_* \gg \rho^{-2}_*$. The dependence of $\exp(-\mathfrak{S}_s)$

[24] Comparing (225) with (213), we also find the relation between impact parameters

$$\left|\mathbf{b}^*_{\pi\mu}\right|^2 = \left(1 + \frac{\sigma^2_\pi}{\sigma^2_\mu}\right)\left|\mathbf{b}^{(\pi)}_\pi\right|^2 + \left(1 + \frac{\sigma^2_\mu}{\sigma^2_\pi}\right)\left|\mathbf{b}^{(\mu)}_\mu\right|^2,$$

which implies, among other things, that $\left|\mathbf{b}^{(\pi)}_\pi\right| = \left|\mathbf{b}^{(\mu)}_\mu\right| = 0$ at $\left|\mathbf{b}^*_{\pi\mu}\right| = 0$.

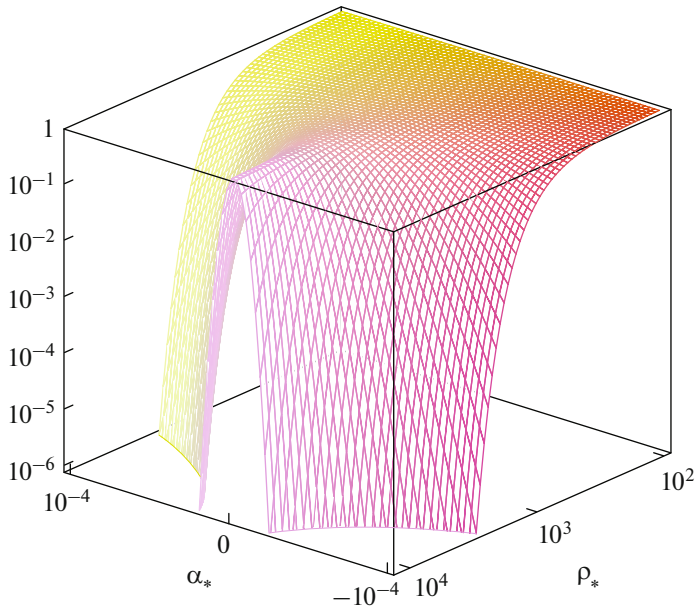

Fig. 14. Geometric suppression factor $\exp(-\mathfrak{S}_s)$ for the two-particle decay as a function of ρ_* and α_*.

on ρ_* and α_* is shown in Fig. 14 for intervals $10^2 \lesssim \rho_* \lesssim 10^4$ and $|\alpha_*| 10^{-4}$. In experiments, a muon produced in the $\pi_{\mu 2}$ decay is always seen emitted from the same point (more specifically, from the spatial region limited by the instrumental resolution) in which a pion vanished. In the center-of-inertia frame of a pion and a muon, this implies that impact parameter $\left|\mathbf{b}^*_{\pi\mu}\right| \approx \alpha_*\rho_*$ is zero or very small, thus providing an explanation for the obvious experimental fact that remains unexplained in the theory with plane waves[25].

It is evident that conditions similar to (217) and (221) are impossible to formulate for single-particle Fock states of the standard QFT perturbation theory, which utilizes a rather meaningless condition of asymptotic freedom at infinity. This condition is inapplicable to unstable particles, which serve as the primary source of (anti) neutrinos in many experiments on neutrino oscillations.

The size of the interaction region (r_I) at vertices was neglected in the above analysis. This is justifiable if the effective size of wave packets is much larger than r_I. This requirement is satisfied when weak and strong interactions are considered. If electromagnetic interactions are considered, this analysis (just as the standard QFT approach) is, apparently, nonexhaustive, and the formulated conditions may not be sufficient.

[25] We leave open the question of the possibility of experimental measurement of impact parameter $\left|\mathbf{b}^*_{\pi\mu}\right|$, which could help verify the above theoretical constructs.

7.10. Phase Factors

Overlap integrals (199) are not translationally invariant due to the presence of phase factors $\exp\left[\pm i\left(q \mp q_{s,d}\right) X_{s,d}\right]$. Note, however, that the q-dependent factor in product $\mathbb{V}_s(q)\mathbb{V}_d(q)$ is proportional to translationally invariant phase factor

$$\exp\left[iq\left(X_s - X_d\right)\right]. \tag{226}$$

As a result (see the next section), the square of the amplitude modulus is translationally invariant. It was demonstrated in [58] that factor (226) governs the oscillation behavior of the amplitude squared (as a function of $X_s - X_d$) under the condition that impact points X_s and X_d are macroscopically separated.

7.11. Overlap Volumes

A representation of quantities $\left|\mathbb{V}_s(q)\right|^2$ and $\left|\mathbb{V}_d(q)\right|^2$ differing from the one obtained by applying formula (199) directly is better suited for the analysis of such measurable characteristics as the count rate of neutrino events. It is more convenient to go back to definition (196) and write $\left|\mathbb{V}_{s,d}(q)\right|^2$ as

$$\left|\mathbb{V}_{s,d}(q)\right|^2 = \int dx \int dy$$
$$\times \exp\left[i\left(q_{s,d} \pm q\right)(x-y) - \Upsilon_{s,d}(x) - \Upsilon_{s,d}(y)\right].$$

Performing a change of integration variables $x = x' + y'/2$ and $y = x' - y'/2$ (with a unit Jacobian), one may rewrite the last integral as

$$\left|\mathbb{V}_{s,d}(q)\right|^2 = \int dy' \exp\left[i\left(q_{s,d} \pm q\right)y' - \frac{1}{2}\Re^{\mu\nu}_{s,d} y'_\mu y'_\nu\right] \tag{227}$$
$$\times \int dx' \exp\left[-2\Upsilon_{s,d}(x')\right].$$

Introducing notations

$$\delta_{s,d}(K) = \int \frac{dx}{(2\pi)^4} \exp\left(iKx - \frac{1}{2}\Re^{\mu\nu}_{s,d} x_\mu x_\nu\right) = \frac{\exp\left(-\frac{1}{2}\tilde{\Re}^{\mu\nu}_{s,d} K_\mu K_\nu\right)}{(2\pi)^2\sqrt{|\Re_{s,d}|}}, \quad (228)$$

$$\mathrm{V}_{s,d} = \int dx \prod_{\varkappa\in S,D} |\psi_\varkappa(\mathbf{p}_\varkappa, x_\varkappa - x)|^2 = \frac{\pi^2 \exp(-2\mathfrak{S}_{s,d})}{4\sqrt{|\Re_{s,d}|}}, \quad (229)$$

we present (227) in the following compact form:

$$|\mathbb{V}_{s,d}(q)|^2 = (2\pi)^4 \delta_{s,d}(q \mp q_{s,d})\,\mathrm{V}_{s,d}. \quad (230)$$

Functions $\delta_s(K)$ and $\delta_d(K)$ obviously do not match functions $\tilde{\delta}_s(K)$ and $\tilde{\delta}_d(K)$ used earlier, but have the same plane-wave limit (i.e., $\delta_{s,d}(K) = \tilde{\delta}_{s,d}(K) = \delta(K)$ in this limit) and similar properties. The physical meaning and the symmetry properties of functions (229) follow clearly from the above analysis, and their integral representation suggests that quantities V_s and V_d may be interpreted as 4-dimensional overlap volumes of in- and out-packets in the source and the detector. It follows from the explicit form of these functions that they assume their maximum values, $\mathrm{V}^0_{s,d} = \pi^2/(4\sqrt{|\Re_{s,d}|})$, when the classical world lines of packets intersect at impact points.

8. AMPLITUDE OF THE PROCESS WITH THE PRODUCTION OF CHARGED LEPTONS IN THE SOURCE AND THE DETECTOR AND A VIRTUAL NEUTRINO

Let us examine the class of processes[26]

$$I_s \oplus I_d \to F_s' + \ell^+_\alpha \oplus F_d' + \ell^-_\beta, \quad (231)$$

which are sustained by the weak charged current, as a practically important application of the formalism. Here, I_s, I_d, F_s', and F_d' denote the sets of asymptotically free WPs characterizing hadronic states, and ℓ^+_α and ℓ^-_β are packets of charged leptons ($\alpha,\beta = e,\mu,\tau$). If $\alpha \neq \beta$, lepton numbers L_α and L_β are violated in process (231). This is made possible by the exchange of massive (Dirac or Majorana) neutrinos. In the leading nonvanishing order in electroweak interaction, process (231) is characterized by the sum of diagrams shown in Fig. 15. Let X_s and X_d be impact points

[26] Note that the examples presented in Figs. 8 and 10 (Section 7.2) do not belong to this class, although the technique of calculation of the corresponding amplitudes does not differ much from the one developed below.

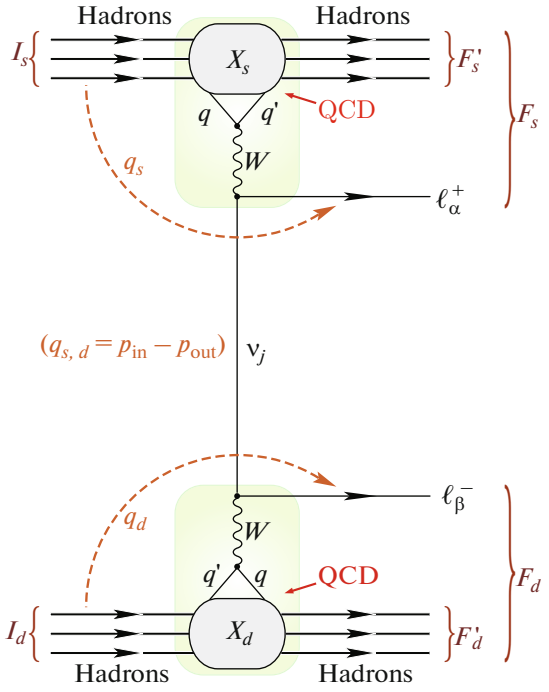

Fig. 15. Macroscopic diagram describing process (231).

defined by formula (201) (where $F_s = F_s' + \ell^+_\alpha$ and $F_d = F_d' + \ell^-_\beta$). It is assumed that they (and, consequently, the effective interaction regions in the source and the detector, which are denoted by dashed curves in Fig. 15) are macroscopically separated in space-time and that all asymptotic conditions discussed in Section 7.9 are fulfilled. The initial and final states may then be regarded as direct products of free one-packet states, and normalization (188) may be used.

In the standard model minimally extended by the inclusion of a neutrino mass matrix, quark-lepton blocks of the diagram in the lowest nonvanishing order are described by Lagrangian

$$\mathcal{L}_W(x) = -\frac{g}{2\sqrt{2}}\left[j_\ell(x)W(x) + j_q(x)W(x) + \mathrm{H.c.}\right],$$

where g is the $SU(2)$ coupling constant; j_ℓ and j_q are the lepton and quark charged currents,

$$j^\mu_\ell(x) = \sum_{\alpha i} V^*_{\alpha i}\bar{\nu}_i(x)O^\mu\ell_\alpha(x),$$

$$j^\mu_q(x) = \sum_{qq'} V'^*_{qq'}\bar{q}(x)O^\mu q'(x);$$

$V_{\alpha i}$ ($\alpha = e,\mu,\tau$, $i = 1,2,3$) and $V_{qq'}$ ($q = u,c,t$, $q' = d,s,b$) are the elements of the neutrino and quark mixing matrices ($\mathbf{V} = \mathbf{V}_{\mathrm{PMNS}}$ and $\mathbf{V}' = \mathbf{V}_{\mathrm{CKM}}$, respectively); $O^\mu = \gamma^\mu(1-\gamma_5)$; $\ell_{\alpha,\beta}(x)$ are the charged lepton fields; and standard notations are used for the other fields and Dirac γ-matrices. Hadronic blocks (colored

regions in the diagram in Fig. 15), which are impossible to calculate within the perturbation theory, are characterized by phenomenological hadronic currents. The normalized dimensionless amplitude of process (231)

$$\langle \text{out}|\mathbb{S}|\text{in}\rangle(\langle \text{in}|\text{in}\rangle\langle \text{out}|\text{out}\rangle)^{-1/2} \stackrel{\text{def}}{=} \mathfrak{A}_{\beta\alpha}$$

is given by the fourth order of the perturbation theory in constant g:

$$\begin{aligned}\mathfrak{A}_{\beta\alpha} = \frac{1}{\mathcal{N}}\left(\frac{-ig}{2\sqrt{2}}\right)^4 \langle F_s \oplus F_d | T\int dxdx'dydy' : \\ \times j_\ell(x)W(x) :: j_q(x')W^\dagger(x') : \\ \times : j_\ell^\dagger(y)W^\dagger(y) :: j_q^\dagger(y')W(y') : \mathbb{S}_h | I_s \oplus I_d\rangle.\end{aligned}$$

Here,

$$\mathbb{S}_h = T\exp\left[i\int dz\mathcal{L}_{\text{h}}(z)\right],$$

$\mathcal{L}_{\text{h}}(z)$ is the Lagrangian of strong and electromagnetic SM interactions governing the nonperturbative processes of fragmentation and hadronization, and T and $:\ldots:$ are the standard symbols of chronological and normal ordering of local operators. Normalization factor $\mathcal{N}$ in the SRGP approximation is given by

$$\mathcal{N}^2 = \langle \text{in}|\text{in}\rangle\langle \text{out}|\text{out}\rangle = \prod_{\varkappa\in I_s\oplus I_d\oplus F_s\oplus F_d} 2\bar{E}_\varkappa \text{V}_\varkappa. \quad (232)$$

Let us consider hadronic matrix element

$$\begin{aligned}\left\langle F_s' \oplus F_d' \middle| T\left[: j_q^\mu(x) :: j_q^{\dagger\nu}(y) : \mathbb{S}_h\right] \middle| I_s \oplus I_d\right\rangle \\ = \int\left[\prod_a \frac{d\mathbf{k}_a\phi_a(\mathbf{k}_a,\mathbf{p}_a)e^{ik_ax_a}}{(2\pi)^3 2E_{\mathbf{k}_a}}\right] \\ \times \int\left[\prod_b \frac{d\mathbf{k}_b\phi_b^*(\mathbf{k}_b,\mathbf{p}_b)e^{-ik_bx_b}}{(2\pi)^3 2E_{\mathbf{k}_b}}\right] \\ \times \left\langle \{k_b\}\middle| T\left[: j_q^\mu(x) :: j_q^{\dagger\nu}(y) : S_h\right] \middle| \{k_a\}\right\rangle.\end{aligned} \quad (233)$$

Here, the WP definition

$$|\mathbf{p}_\varkappa, s_\varkappa, x_\varkappa\rangle_\varkappa = \int \frac{d\mathbf{k}\phi_\varkappa(\mathbf{k},\mathbf{p})e^{i(k-p_\varkappa)x_\varkappa}}{(2\pi)^3 2E_{\mathbf{k}}} |\mathbf{k}, s_\varkappa\rangle_\varkappa \quad (234)$$

was used, and a contracted notation for many-particle Fock states was introduced:

$$\begin{aligned}|\ldots,\mathbf{k}_a,s_a,\ldots;a\in I_s\oplus I_d\rangle = |\{k_a\}\rangle, \\ \left|\ldots,\mathbf{k}_b,s_b,\ldots;b\in F_s'\oplus F_d'\right\rangle = |\{k_b\}\rangle.\end{aligned}$$

We may write the following for stable relatively strong and electromagnetic interactions of the initial and final hadrons separated macroscopically in space by the source–detector distance:

$$\begin{aligned}\left\langle F_s' \oplus F_d' \middle| T\left[: j_q^\mu(x) :: j_q^{\dagger\nu}(y) : \mathbb{S}_h\right] \middle| I_s \oplus I_d\right\rangle \\ = \Pi'(x,y;\{\mathbf{p}_\varkappa, x_\varkappa\}) \\ \times \mathcal{J}_s^\mu(X_s;\{p_a,p_b\})\mathcal{J}_d^{\nu*}(X_d;\{p_a,p_b\}),\end{aligned} \quad (235)$$

where

$$\begin{aligned}\Pi'(x,y;\{\mathbf{p},x\}) = \left[\prod_{a\in I_s} e^{-ip_ax_a}\psi_a(\mathbf{p}_a, x_a - x)\right] \\ \times\left[\prod_{b\in F_s} e^{ip_bx_b}\psi_b^*(\mathbf{p}_b, x_b - x)\right] \\ \times\left[\prod_{a\in I_d} e^{-ip_ax_a}\psi_a(\mathbf{p}_a, x_a - y)\right] \\ \times\left[\prod_{b\in F_d} e^{ip_bx_b}\psi_b^*(\mathbf{p}_b, x_b - y)\right],\end{aligned}$$

and $\mathcal{J}_s$ and $\mathcal{J}_d$ are the corresponding c-number hadronic currents in the source and the detector. The proof of "factorization formula" (235) is given in Appendix C. The explicit form of hadronic currents is not needed in this study.

Let us introduce the causal Green's functions for a neutrino and a W boson:

$$\begin{aligned}G^j(x-y) = \left\langle T\left[\nu_j(x)\bar{\nu}_j(y)\right]\right\rangle_0 \\ = \int\frac{dq}{(2\pi)^4}\Delta^j(q)e^{-iq(x-y)}, \\ G_{\mu\nu}^W(x-y) = \left\langle T\left[W_\mu(x)W_\nu^\dagger(y)\right]\right\rangle_0 \\ = \int\frac{dk}{(2\pi)^4}\Delta_{\mu\nu}(k)e^{-ik(x-y)}.\end{aligned} \quad (236)$$

Here,

$$\begin{aligned}\Delta^j(q) = \frac{i}{\hat{q} - m_j + i0} = \frac{i(\hat{q}+m_j)}{q^2 - m_j^2 + i0}, \\ (\hat{q} = q^\mu\gamma_\mu)\end{aligned} \quad (237)$$

and

$$\Delta_{\mu\nu}(k) = -i\frac{g_{\mu\nu} - k_\mu k_\nu/m_W^2}{k^2 - m_W^2 + i0} \quad (238)$$

are the bare propagators of neutrino j (with mass m_j) and a W boson (with mass m_W), respectively. The latter propagator is written in the unitary calibration. Performing standard transformations, we arrive at the following expression for amplitude:

$$\mathfrak{A}_{\beta\alpha} = \frac{g^4}{64\mathcal{N}}\sum_j V_{\alpha j}^* V_{\beta j}\int dxdx'dydy'\mathfrak{A}^j(x,x',y,y'), \quad (239)$$

where

$$\mathfrak{V}^j(x,x',y,y') = \mathcal{J}_d^{\nu *} G^W_{\nu\nu'}(y-y')\bar{u}(\mathbf{p}_\beta) \times O^{\nu'} G^j(y'-x') O^{\mu'} G^W_{\mu'\mu}(x'-x) v(\mathbf{p}_\alpha)\mathcal{J}_s^\mu \times \psi^*_\alpha(\mathbf{p}_\alpha, x'-x_\alpha)\psi^*_\beta(\mathbf{p}_\beta, y'-x_\beta)\Pi'(x,y;\{\mathbf{p},x\});$$

spin indices and arguments of functions $\mathcal{J}_s$ and $\mathcal{J}_d$ are omitted for brevity. The integration of function $\mathfrak{V}^j(x,x',y,y')$ over y' yields

$$I^j_{\nu\nu'} = \int dy' \psi^*_\beta(\mathbf{p}_\beta, y'-x_\beta) G^W_{\nu\nu'}(y-y') G^j(y'-x') = \int \frac{d\mathbf{p} e^{-ipx_\beta}\phi^*_\beta(\mathbf{p},\mathbf{p}_\beta)}{(2\pi)^3 2E_\mathbf{p}} \int \frac{dk e^{-iky}\Delta_{\nu\nu'}(k)}{(2\pi)^4} \int \frac{dq e^{iqx'}\Delta^j(q)}{(2\pi)^4} \times \int dy' e^{i(k-q+p)y'} = \int \frac{d\mathbf{p}}{(2\pi)^3 2E_\mathbf{p}} \phi^*_\beta(\mathbf{p},\mathbf{p}_\beta) e^{-ip(x_\beta - y)} \times \int \frac{dq}{(2\pi)^4}\Delta_{\nu\nu'}(q-p)\Delta^j(q) e^{iq(x'-y)}.$$

Using the definitions in (236) and our standard approximation, we can rewrite this integral as follows:

$$I^j_{\nu\nu'} = \psi^*_\beta(\mathbf{p}_\beta, y - x_\beta) \times \int \frac{dq}{(2\pi)^4}\Delta_{\nu\nu'}(q-p_\beta)\Delta^j(q) e^{iq(x'-y)}.$$

The integration over x' is performed in much the same way and yields factor

$$\psi^*_\beta(\mathbf{p}_\beta, y-x_\beta)\psi^*_\alpha(\mathbf{p}_\alpha, x-x_\alpha) \times \int \frac{dq}{(2\pi)^4}\Delta_{\nu\nu'}(q-p_\beta)\Delta^j(q)\Delta_{\mu'\mu}(q+p_\alpha) e^{iq(x-y)}$$

in the integrand in (239). Collecting all factors, using the definition of overlap integrals (192), and introducing tensor function

$$\mathbb{G}^j_{\nu\nu'\mu'\mu}(\{\mathbf{p},x\}) = \int \frac{dq}{(2\pi)^4}\mathbb{V}_d(q)\mathbb{V}_s(q)\Delta_{\nu\nu'} \times (q-p_\beta)\Delta^j(q)\Delta_{\mu'\mu}(q+p_\alpha), \quad (240)$$

we arrive at the following expression for amplitude:

$$\mathfrak{V}_{\beta\alpha} = \frac{g^4}{64\mathcal{N}} \sum_j V_{\beta j}\mathcal{J}_d^{\nu *}\bar{u}(\mathbf{p}_\beta) O^{\nu'} \times \mathbb{G}^j_{\nu\nu'\mu'\mu}(\{\mathbf{p},x\}) O^{\mu'} v(\mathbf{p}_\alpha)\mathcal{J}_s^\mu V^*_{\alpha j}. \quad (241)$$

8.1. Amplitude Asymptotics at Large L

The asymptotic behavior of function (240) at a large spatial distance between impact points $\mathbf{X}_s$ and $\mathbf{X}_d$ is relevant to our purpose. One may use the Grimus–Stockinger (GS) theorem [33] to study this behavior. The theorem states the following[27]:

Let $\Phi(\mathbf{q}) \in C^3(\mathbb{R}^3)$ be a function that decreases together with its first and second derivatives no slower than $|\mathbf{q}|^{-2}$ at $|\mathbf{q}| \to \infty$, $\kappa^2 \in \mathbb{R}$, $\mathbf{l} = \mathbf{L}/L$, $L = |\mathbf{L}|$, and

$$J(\mathbf{L},\kappa) = \int \frac{d\mathbf{q}}{(2\pi)^3}\frac{\Phi(\mathbf{q})e^{-i\mathbf{qL}}}{\mathbf{q}^2 - \kappa^2 - i\epsilon}. \quad (243)$$

Then, in the asymptotic $L \to \infty$ limit for $\kappa > 0$,

$$J(\mathbf{L},\kappa) = \frac{e^{i\kappa L}(-\kappa\mathbf{l})}{4\pi L}\left[1 + \mathbb{O}\left(\frac{1}{L^{1/2}}\right)\right], \quad (244)$$

whereas integral (243) decreases as L^{-2} at $\kappa^2 < 0$. Considering the definition in (240) and the explicit form of integrals in (199) and the neutrino propagator in (237), we find that, in the present case,

$$\mathbf{L} = \mathbf{X}_d - \mathbf{X}_s, \quad T = X^0_d - X^0_s, \quad \kappa^2 = q_0^2 - m_j^2.$$

The function corresponding to $\Phi(\mathbf{q})$ in the GS theorem to within an insignificant (independent of q) factor is written as follows:[28]

$$\tilde{\delta}_s(q-q_s)\tilde{\delta}_d(q+q_d)\Delta_{\nu\nu'}(q-p_\beta) \times (\hat{q}+m_j)\Delta_{\mu'\mu}(q+p_\alpha). \quad (245)$$

The first requirement of the theorem may be violated formally by the poles of bare boson propagators (238). In order to eliminate this possibility, we use the renormalized (full) propagator, which has no singularity in the resonance region, instead of (238). This propagator is obtained by performing the standard $m_W^2 \mapsto m_W^2 - im_W\Gamma_W$ substitution, where Γ_W is the total width of a W boson, in the denominator of (238)[29].

Since functions $\tilde{\delta}_s(q-q_s)$ and $\tilde{\delta}_d(q+q_d)$ decrease faster than any power of $|\mathbf{q}|^{-1}$ as $|\mathbf{q}| \to \infty$, we conclude that function (245) satisfies the GS theorem condi-

[27] It was proven in [123] that the asymptotics of integral (243) under somewhat more stringent conditions imposed on function $\Phi(\mathbf{q})$ takes the form

$$J(\mathbf{L},\kappa) = \frac{e^{i\kappa L}}{4\pi L} \times \left\{1 - \frac{i}{L}\left[(\mathbf{l}\nabla_\mathbf{q}) + \frac{\kappa}{2}(\mathbf{l}\times\nabla_\mathbf{q})^2\right] + \mathbb{O}\left(\frac{1}{L^2}\right)\right\}\Phi(\mathbf{q})\Big|_{\mathbf{q}=-\kappa\mathbf{l}}. \quad (242)$$

If $\Phi(\mathbf{q}) \in S(\mathbb{R}^3)$ (which is true in almost all practically relevant cases), integral (243) is an asymptotic series in inverse powers of L, and $|J(\mathbf{L},\kappa)|^2$ is an asymptotic series in inverse powers of L^2. The properties of these series were studied in detail in [123–125], and several physical applications of these results were discussed in [126–129].

[28] Note that the term $\propto m_j$ in (245) does not contribute to amplitude (241) due to matrix factors $O^{\mu'}$ and $O^{\nu'}$.

[29] A more accurate modification was discussed, e.g., in [130, 131] (see also the references therein).

tions. Therefore, function (240) behaves in the leading order in $1/L$ as

$$\mathbb{G}^{j}_{\nu\nu'\mu'\mu}(\{\mathbf{p}_\varkappa, x_\varkappa\}) = \frac{e^{-\mathfrak{S}-i\Theta}}{8\pi^2 L}\int\limits_{-\infty}^{\infty} dq_0 e^{-i(q_0T-|\mathbf{q}_j|L)}\tilde{\delta}_s \times (q_j - q_s)\tilde{\delta}_d(q_j + q_d) \times \Delta_{\nu\nu'}(q_j - p_\beta)(\hat{q}_j + m_j)\Delta_{\mu'\mu}(q_j + p_\alpha), \quad (246)$$

where

$$q_j = (q_0, \mathbf{q}_j), \quad \mathbf{q}_j = \sqrt{q_0^2 - m_j^2}\mathbf{l}, \quad \mathbf{l} = \mathbf{L}/L,$$
$$\mathfrak{S} = \mathfrak{S}_s + \mathfrak{S}_d \quad \text{and} \quad \Theta = X_s q_s + X_d q_d.$$

Since factors $\tilde{\delta}_s(q_j - q_s)$ and $\tilde{\delta}_d(q_j + q_d)$ under the integral sign at the right-hand side of (246) have, as functions of q_0, sharp and close maxima, the integral is saturated by a small neighborhood of these maxima and can be evaluated by the regular saddle-point method. All calculations below are performed within the SRGP model.

The corrections to the GS theorem were discussed in [123].

8.2. Integration over q_0

According to (200),

$$\tilde{\delta}_s(q_j - q_s)\tilde{\delta}_d(q_j + q_d) = \frac{1}{(4\pi)^4\sqrt{|\Re_s||\Re_d|}}\exp\left[-\frac{1}{4}F_j(q_0)\right],$$
$$F_j(q_0) = \tilde{\Re}^{\mu\nu}_s(q_j - q_s)_\mu(q_j - q_s)_\nu + \tilde{\Re}^{\mu\nu}_d(q_j + q_d)_\mu(q_j + q_d)_\nu.$$

Introducing notations

$$F_0 = \tilde{\Re}^{\mu\nu}_s q_{s\mu} q_{s\nu} + \tilde{\Re}^{\mu\nu}_d q_{d\mu} q_{d\nu},$$
$$Y^\mu = \tilde{\Re}^{\mu\nu}_s q_{s\nu} - \tilde{\Re}^{\mu\nu}_d q_{d\nu}, \quad R^{\mu\nu} = \tilde{\Re}^{\mu\nu}_s + \tilde{\Re}^{\mu\nu}_d, \quad (247)$$

we rewrite the expression for $F_j(q_0)$ in the following form:

$$F_j(q_0) = F_0 - 2Y_\mu q_j^\mu + R_{\mu\nu}q_j^\mu q_j^\nu. \quad (248)$$

The extremum of this function is defined by

$$\frac{dF_j(q_0)}{dq_0} = \frac{2}{|\mathbf{q}_j|} \times \left[Rq_0|\mathbf{q}_j| - (\mathbf{Rl})(q_0 - |\mathbf{q}_j|)^2 - Y_0|\mathbf{q}_j| + (\mathbf{Yl})q_0\right] = 0, \quad (249)$$

where

$$R = R^{\mu\nu}l_\mu l_\nu = R_{00} - 2(\mathbf{Rl}) + \mathcal{R},$$
$$\mathcal{R} = R_{kn}l_k l_n,$$
$$\mathbf{R} = (R_{01}, R_{02}, R_{03}), \quad \mathbf{Y} = (Y_1, Y_2, Y_3) \quad \text{and} \quad l = (1, \mathbf{l}). \quad (250)$$

Here and elsewhere, summation over repeated Latin indices $(k, n = 1, 2, 3)$ is assumed. The root of (249), $q_0 = E_j$, is the saddle point if the second derivative

$$\frac{d^2F_j(q_0)}{dq_0^2} = 2R + \frac{2(q_0 - |\mathbf{q}_j|)}{|\mathbf{q}_j|^3} \times \left[(\mathbf{Rl})(q_0 + 2|\mathbf{q}_j|)(q_0 - |\mathbf{q}_j|) - (\mathbf{Yl})(q_0 + |\mathbf{q}_j|)\right] \quad (251a)$$

$$= 2R + \frac{2}{v_j^3}\left[(\mathbf{Rl})(1 + 2v_j)(1 - v_j^2) - \frac{(\mathbf{Yl})}{m_j\Gamma_j^3}\right] \quad (251b)$$

(where $v_j = |\mathbf{q}_j|/q_0$ and $\Gamma_j = q_0/m_j$) is positive at this point. Two intriguing special cases with relatively simple approximate solutions of (249) corresponding to them are considered below. The general solution is examined in Appendix D.

8.2.1. Ultrarelativistic case. Let us examine the configurations of momenta of external packets satisfying conditions

$$q_s^0 \sim -q_d^0 \sim |\mathbf{q}_s| \sim |\mathbf{q}_d|. \quad (252)$$

These relations hold true in all current neutrino experiments. Therefore, this special case is of principal interest.

In the plane-wave limit ($\sigma_\varkappa = 0, \forall_\varkappa$) and under the assumption that $m_j = 0$ (in what follows, this special case is referred to as the PW_0 limit), equalities

$$q_s^0 = -q_d^0, \quad \mathbf{q}_s = -\mathbf{q}_d = q_s^0\mathbf{l}$$

need to be satisfied to achieve exact energy-momentum conservation at each vertex of the diagram.

According to (247) and (250), the root of (249) is

$$q_0 = \lim_{\sigma_\varkappa = 0, \forall_\varkappa}\frac{Y_0 - (\mathbf{Yl})}{R} = q_s^0, \quad (253)$$

which is the energy of a real massless neutrino ($q_j = E_0 l$, $q_j^2 = 0$).

In the general case with $\sigma_\varkappa \neq 0$, if conditions (252) are satisfied and a natural additional assumption that neutrino masses m_j are small compared to the minimum absolute values of energy transfers q_s^0 and q_d^0 at the diagram vertices[30] is fulfilled, the solution of (249) can be presented in the form of a series in powers of small dimensionless parameter

$$r_j = \frac{m_j^2}{2E_\nu^2}. \quad (254)$$

[30] It is assumed that the minimum is taken over the entire set (defined by the specific experimental conditions) of the most probable momenta $\mathbf{p}_\varkappa$ of external packets in the source and the detector.

The definition in (254) features "representative" virtual neutrino energy[31]

$$E_\nu = \frac{(Yl)}{R}, \tag{255}$$

which becomes the energy transfer q_s^0 in the PW_0 limit and is close to it in magnitude at sufficiently small $\sigma_\varkappa$ (this statement is clarified below). According to (255), E_ν is a rotationally invariant function of momenta, masses, and dispersions of momenta of all external packets. Owing to the approximate energy-momentum conservation, this quantity is nonnegative and is transformed as the zeroth 4-momentum component.

Thus, let us write q_0 and $|\mathbf{q}_j| = \sqrt{q_0 - m_j^2}$ as power series

$$\begin{aligned} q_0 \equiv E_j &= E_\nu\left(1 - \sum_{n=1}^{\infty} C_n^E r_j^n\right), \\ |\mathbf{q}_j| \equiv P_j &= E_\nu\left(1 - \sum_{n=1}^{\infty} C_n^P r_j^n\right). \end{aligned} \tag{256}$$

It is convenient to rewrite (249) in the following form:

$$\begin{aligned} &q_0|\mathbf{q}_j| - \mathfrak{m}(q_0 - |\mathbf{q}_j|)^2 \\ &- E_\nu[(\mathfrak{n}+1)|\mathbf{q}_j| - \mathfrak{n}q_0] = 0, \end{aligned} \tag{257}$$

which features dimensionless rotationally invariant functions

$$\mathfrak{n} = \frac{(\mathbf{Yl})}{(Yl)} \quad \text{and} \quad \mathfrak{m} = \frac{(\mathbf{Rl})}{R}.$$

It can be seen from (257) that coefficients C_n^E and C_n^P are expressed in terms of these two functions only at all $n \geq 1$. It is easy to determine the coefficients using the standard recurrent procedure: one needs to insert series (256) into (257), expand the obtained expression into a series in r_j, and set the factors at powers of r_j to zero. The first three pairs are as follows:

$$\begin{aligned} &C_1^E = \mathfrak{n}, \quad C_2^E = \mathfrak{n}\left(2\mathfrak{n} + \frac{3}{2}\right) - \mathfrak{m}, \\ &C_3^E = \mathfrak{n}\left(7\mathfrak{n}^2 + 9\mathfrak{n} + \frac{5}{2}\right) - (5\mathfrak{n}+2)\mathfrak{m}; \end{aligned} \tag{258}$$

$$\begin{aligned} &C_1^P = \mathfrak{n}+1, \quad C_2^P = (\mathfrak{n}+1)\left(2\mathfrak{n} + \frac{1}{2}\right) - \mathfrak{m}, \\ &C_3^P = (\mathfrak{n}+1)\left(7\mathfrak{n}^2 + 5\mathfrak{n} + \frac{1}{2}\right) - (5\mathfrak{n}+3)\mathfrak{m}. \end{aligned} \tag{259}$$

It is evident that the coefficients satisfy the symmetry relation

$$C_n^P = (-1)^n C_n^E\big|_{\mathfrak{n}\mapsto -(\mathfrak{n}+1)}.$$

[31] Here, ν is not a Lorentzian index.

It follows from (257) that this holds true for all n. Quantities E_j and $\mathbf{p}_j = P_j\mathbf{l}$ are naturally interpreted as the effective (or the most probable) energy and 3-momentum of virtual massive neutrino ν_j, respectively. They also provide an opportunity to define effective neutrino velocity $\mathbf{v}_j = v_j\mathbf{l} = \mathbf{p}_j/E_j$, which is given by

$$\begin{aligned} v_j &= 1 - r_j - \left(2\mathfrak{n} + \frac{1}{2}\right)r_j^2 \\ &- \left(7\mathfrak{n}^2 + 5\mathfrak{n} + \frac{1}{2} - 2\mathfrak{m}\right)r_j^3 + \mathbb{O}\left(r_j^4\right). \end{aligned} \tag{260}$$

As expected, $0 < 1 - v_j \ll 1$; i.e., neutrinos are ultrarelativistic. Since, in addition[32],

$$R = R^{\mu\nu}l_\mu l_\nu = \mathfrak{F}E_\nu^{-2}, \tag{261}$$

where

$$\mathfrak{F} \equiv \left[R^{\mu\nu}q_\mu q_\nu\right]_{q=E_\nu l} > 0, \tag{262}$$

the second derivative in (251) at $q_0 = E_j$ and $r_j \ll 1$ is positive,

$$\begin{aligned} &\left.\frac{d^2F_j(q_0)}{dq_0^2}\right|_{q_0=E_j} \\ &= 2R\{1 - 2\mathfrak{n}r_j - 3[2\mathfrak{n}(\mathfrak{n}+1) - \mathfrak{m}]r_j^2 \\ &- [3\mathfrak{n}(\mathfrak{n}+1)(8\mathfrak{n}+5) - 2(9\mathfrak{n}+5)\mathfrak{m}]r_j^3 + \mathbb{O}\left(r_j^4\right)\}, \end{aligned} \tag{263}$$

and, consequently, function $F_j(q_0)$ has an absolute minimum at this point. We note once again that quantities E_j, $\mathbf{p}_j$, and $\mathbf{v}_j$ are defined uniquely not only by the most probable momenta $\mathbf{p}_\varkappa$ of external packets in the source and the detector, but also by their masses and dispersions of momenta.

A special configuration of external momenta. In order to illustrate the obtained results, we consider the following special configuration of external momenta:

$$q_s^0 = -q_d^0 \equiv \mathscr{E} > 0, \quad \mathbf{q}_s = -\mathbf{q}_d \equiv \mathscr{P}\mathbf{l}, \quad \mathscr{P} > 0, \tag{264}$$

which corresponds to the exact conservation of energy and momentum "flowing" from S to D. Quantity $\mathscr{Q}^2 = \mathscr{E}^2 - \mathscr{P}^2$ is called the virtuality of a neutrino. The ultrarelativistic case is defined by conditions $|\mathscr{Q}^2| \ll \mathscr{E}^2$ and $m_j^2 \ll \mathscr{E}^2$, but the virtuality is not bound to match m_j^2

[32] It bears reminding that quadratic forms $\tilde{\mathfrak{K}}_s^{\mu\nu}q_\mu q_\nu$ and $\tilde{\mathfrak{K}}_d^{\mu\nu}q_\mu q_\nu$ are positive for arbitrary 4-vector $q \neq 0$.

even in the order of magnitude. It is easy to demonstrate that the following is true for configuration (264):

$$E_\nu = \mathscr{E}\left[1 + \mathfrak{n}_0\left(1 - \frac{\mathscr{P}}{\mathscr{E}}\right)\right],$$

$$\mathfrak{n} = \mathfrak{n}_0 - \left(1 - \frac{P}{\mathscr{E}}\right)\left(\mathfrak{n}_0^2 - \frac{\mathscr{B}}{R}\right)\left[1 + \mathfrak{n}_0\left(1 - \frac{\mathscr{P}}{\mathscr{E}}\right)\right]^{-1},$$

where

$$\mathfrak{n}_0 = \frac{(\mathbf{Rl}) - \mathscr{B}}{R} = \mathfrak{m} - \frac{\mathscr{B}}{R}. \tag{265}$$

Expanding E_ν and $\mathfrak{n}$ with respect to small parameter $\mathscr{Q}^2/\mathscr{E}^2$, we obtain

$$E_\nu = \mathscr{E}\left[1 + \mathfrak{n}_0\frac{\mathscr{Q}^2}{2\mathscr{E}^2}\left(1 + \frac{\mathscr{Q}^2}{2\mathscr{E}^2} + \frac{\mathscr{Q}^4}{8\mathscr{E}^4} + \ldots\right)\right],$$

$$\mathfrak{n} = \mathfrak{n}_0 + (\mathfrak{m} - \mathfrak{n}_0 - \mathfrak{n}_0^2)\frac{\mathscr{Q}^2}{2\mathscr{E}^2}$$

$$\times\left[1 - (2\mathfrak{n}_0 - 1)\frac{\mathscr{Q}^2}{4\mathscr{E}^2} + \left(2\mathfrak{n}_0^2 - 2\mathfrak{n}_0 + 1\right)\frac{\mathscr{Q}^4}{8\mathscr{E}^4} + \ldots\right],$$

where, as usual, dots denote higher-order corrections. Thus, $E_\nu \to \mathscr{E}$ and $\mathfrak{n} \to \mathfrak{n}_0$ at $\mathscr{Q}^2 \to 0$. Reexpanding the above expressions for E_j and P_j with respect to two small (independent) parameters $\mathscr{Q}^2/\mathscr{E}^2$ and $m_j^2/\mathscr{E}^2$, we find

$$E_j = \mathscr{E} + \frac{\mathscr{Q}^2 - m_j^2}{2\mathscr{E}}$$

$$\times\left[\mathfrak{n}_0\left(1 + \frac{\mathscr{Q}^2}{4\mathscr{E}^2}\right) + \left(4\mathfrak{n}_0^2 + 3\mathfrak{n}_0 - 2\mathfrak{m}\right)\frac{m_j^2}{4\mathscr{E}^2} + \ldots\right],$$

$$P_j = \mathscr{P} + \frac{\mathscr{Q}^2 - m_j^2}{2\mathscr{E}}$$

$$\times\left[(\mathfrak{n}_0 + 1)\left(1 + \frac{\mathscr{Q}^2}{4\mathscr{E}^2}\right)\right.$$

$$\left. + \left(4\mathfrak{n}_0^2 + 5\mathfrak{n}_0 - 2\mathfrak{m} + 1\right)\frac{m_j^2}{4\mathscr{E}^2} + \ldots\right].$$

It can be seen that the effective energy (momentum) of a neutrino may be both smaller and larger than transferred energy $\mathscr{E}$ (transferred momentum $\mathscr{P}$); naturally, $E_j = \mathscr{E}$ and $P_j = \mathscr{P}$ at $\mathscr{Q}^2 = m_j^2$ (and in this case only). In other words, even if the transferred 4-momenta at the diagram vertices are perfectly balanced, the effective 4-momentum of a virtual neutrino $(E_j, P_j\mathbf{l})$ is, generally speaking, not the same as $(\mathscr{E}, \mathscr{P}\mathbf{l})$. Since the expansion for the effective neutrino velocity takes the form

$$v_j = 1 - \frac{m_j^2}{2\mathscr{E}^2}\left[1 - \mathfrak{n}_0\frac{\mathscr{Q}^2}{\mathscr{E}^2} + (4\mathfrak{n}_0 + 1)\frac{m_j^2}{4\mathscr{E}^2} + \ldots\right],$$

the leading correction to the ultrarelativistic limit $v_j = 1$ is independent of the neutrino virtuality.

8.2.2. Nonrelativistic case. Let us now examine the contrary case corresponding to the following configuration of external momenta:

$$q_s^0 \sim -q_d^0 \sim m_j \gg |\mathbf{q}_s| \sim |\mathbf{q}_d|. \tag{266}$$

This case is of potential interest for future experiments on (hypothetical) heavy neutrinos and for cosmological applications. It is convenient to rewrite (249) in terms of velocity $v_j = |\mathbf{q}_j|/q_0$ of a virtual neutrino:

$$\frac{m_j}{\sqrt{1 - v_j^2}}\left[R - (\mathbf{Rl})\frac{(1 - v_j)^2}{v_j}\right] = Y_0 - \frac{(\mathbf{Yl})}{v_j}. \tag{267}$$

Let us introduce dimensionless 4-vector $\varrho_j = (\varrho_j^0, \boldsymbol{\varrho}_j)$ with components

$$\varrho_j^\mu = \frac{1}{\mathscr{B}}\left(R_0^\mu - \frac{1}{m_j}Y^\mu\right). \tag{268}$$

It is evident that these components are small in magnitude if conditions (266) are satisfied. Inserting the expression for 4-vector Y, which is written component-wise as

$$Y^\mu = \tilde{\mathfrak{R}}_s^{\mu 0}q_s^0 - \tilde{\mathfrak{R}}_d^{\mu 0}q_d^0 + \tilde{\mathfrak{R}}_s^{\mu k}q_s^k - \tilde{\mathfrak{R}}_d^{\mu k}q_d^k,$$

into definition (268), we indeed find

$$\varrho_j^\mu = \frac{1}{m_j\mathscr{R}}\left[\tilde{\mathfrak{R}}_s^{\mu 0}(m_j - q_s^0)\right.$$

$$\left. + \tilde{\mathfrak{R}}_d^{\mu 0}(m_j + q_d^0) - \tilde{\mathfrak{R}}_s^{\mu k}q_s^k + \tilde{\mathfrak{R}}_d^{\mu k}q_d^k\right]. \tag{269}$$

Since all the terms in (269) contain small factors $(1 - q_s^0/m_j$, q_s^k/m_j, etc.), one may conclude that $|\varrho_{j\mu}| \ll 1$. Taking this into account, we seek the solution of Eq. (267) in the form of a double power series

$$v_j = \bar{v}_j\left[1 + \sum_{n=1}^{\infty}\sum_{m=0}^{\infty}C_{nm}^{(v)}(\boldsymbol{\varrho}_j\mathbf{l})^n\varrho_{j0}^m\right], \tag{270}$$

where

$$\bar{v}_j = \frac{(\boldsymbol{\varrho}_j\mathbf{l})}{1 + \varrho_{j0}}.$$

The first six dimensionless coefficient functions $C_{nm}^{(v)}$ are as follows:

$$C_{10}^{(v)} = -\frac{1}{2}C_{11}^{(v)} = 3C_{12}^{(v)} = \frac{3(\mathbf{Rl})}{2\mathscr{R}},$$

$$C_{20}^{(v)} = \frac{9(\mathbf{Rl})^2}{2\mathscr{R}^2} - \frac{R_{00}}{2\mathscr{R}} + \frac{1}{2},$$

$$C_{21}^{(v)} = -\frac{18(\mathbf{Rl})^2}{\mathscr{R}^2} + \frac{3R_{00}}{2\mathscr{R}} + \frac{3}{2}, \tag{271}$$

$$C_{30}^{(v)} = \frac{3(\mathbf{Rl})}{8\mathscr{R}}\left[\frac{45(\mathbf{Rl})^2}{\mathscr{R}^2} - \frac{10R_{00}}{\mathscr{R}} - \frac{23}{3}\right].$$

The following is obtained from (270) and (271):

$$E_j = m_j + \frac{m_j v_j^2}{2}\left(1 + \frac{3}{4}\delta_j + ...\right), \quad P_j = m_j v_j\left(1 + \frac{1}{2}\delta_j + ...\right). \tag{272}$$

Here, function

$$\delta_j = (\boldsymbol{\varrho}_j\mathbf{l})^2\left[1 + \frac{3(\mathbf{Rl})}{\mathcal{B}}(\boldsymbol{\varrho}_j\mathbf{l}) - \varrho_{j0}\right]$$

defines the leading relativistic corrections, and dots denote higher-order corrections in $(\boldsymbol{\varrho}_j\mathbf{l})$ and ϱ_{j0}. It can be seen that the nonrelativisitc relation between the effective velocity, energy, and momentum remains valid up to the second order in $(\boldsymbol{\varrho}_j\mathbf{l})$ and that the relativistic corrections to E_j and P_j are positive.

It can be shown that function $\mathcal{R}$ is positive. If this is taken into account, one needs just to insert (270) and (271) into (251b) to find that the second derivative in (251b) is positive at the stationary point:

$$\left.\frac{d^2F_j(q_0)}{dq_0^2}\right|_{q_0=E_j} = 2R + \frac{2\mathcal{B}}{\bar{v}_j^2} \times\left[1 - \frac{6(\mathbf{Rl})}{\mathcal{B}}(\boldsymbol{\varrho}_j\mathbf{l}) + \varrho_{j0} + ...\right] > 0. \tag{273}$$

The singularity at $\bar{v}_j = 0$ is hardly a surprise, since it only reinforces the intuitive expectation that the amplitude of a process with a neutrino "at rest" in the intermediate state should be equal to zero. However, this case requires a more detailed examination of the conditions of applicability of the saddle-point method and the GS theorem. These issues will be discussed in a separate paper.

Let us turn to the special case of the accurate balance of the energy and momentum transfer at the macrodiagram vertices. We use designations (264) and, in accordance with (266), assume that

$$0 \le \mathcal{E}/m_j - 1 \ll 1 \quad \text{and} \quad 0 \le \mathcal{P}/m_j \ll 1.$$

Thus,

$$\varrho_j^\mu = \frac{1}{\mathcal{R}}\left[R_k^\mu l_k\frac{\mathcal{P}}{m_j} - R_0^\mu\left(\frac{\mathcal{E}}{m_j} - 1\right)\right]$$

and, consequently,

$$\varrho_{j0} = \frac{(\mathbf{Rl})}{\mathcal{R}}\frac{\mathcal{P}}{m_j} - \frac{R_{00}}{\mathcal{R}}\left(\frac{\mathcal{E}}{m_j} - 1\right), \quad (\boldsymbol{\varrho}_j\mathbf{l}) = \frac{\mathcal{P}}{m_j} - \frac{(\mathbf{Rl})}{\mathcal{R}}\left(\frac{\mathcal{E}}{m_j} - 1\right).$$

Inserting these relations into (270), taking (271) into account, and reexpanding the obtained expression in powers of two small independent parameters $\mathcal{P}/m_j$ and $\mathcal{E}/m_j - 1$, we arrive at the following expression for the effective velocity of a virtual neutrino:

$$v_j = \bar{v}_j\left\{1 + \frac{(\mathbf{Rl})}{2\mathcal{R}}\frac{\mathcal{P}}{m_j} + \left[\frac{R_{00}}{\mathcal{R}} - \frac{3(\mathbf{Rl})^2}{2\mathcal{R}^2}\right] \times\left(\frac{\mathcal{E}}{m_j} - 1\right) + ...\right\}, \quad \bar{v}_j = (\boldsymbol{\varrho}_j\mathbf{l}). \tag{274}$$

The effective energy and momentum of a virtual neutrino in the leading order in $\mathcal{P}/m_j$ and $\mathcal{E}/m_j - 1$ are determined from (274):

$$E_j \approx m_j + m_j\bar{v}_j^2/2, \quad P_j \approx m_j\bar{v}_j.$$

These simple formulas agree completely with intuitive expectations only at $|\mathcal{E}/m_j - 1| \lesssim \mathcal{P}^2/m_j^2$. It is only in this special case that the following relations hold true:

$$\bar{v}_j \approx \mathcal{P}/m_j, \quad E_j \approx m_j + \mathcal{P}^2/(2m_j) \quad \text{and} \quad P_j \approx \mathcal{P}.$$

8.3. Resulting Formula for the Amplitude

It was proven above that function $F_j(q_0)$ has an absolute minimum at $q_0 = E_j$ both in ultrarelativistic and nonrelativistic cases; in the neighborhood of this minimum, it may be approximated by a parabola:

$$F_j(q_0) \simeq F_j(E_j) + \frac{(q_0 - E_j)^2}{4\mathfrak{D}_j^2}. \tag{275}$$

Positively defined function

$$\frac{1}{\mathfrak{D}_j} = \sqrt{\left[2d^2F_j(q_0)/dq_0^2\right]_{q_0=E_j}}, \tag{276}$$

was introduced here. It will be demonstrated below that this function may be interpreted as the effective energy uncertainty of a virtual neutrino. In the ultrarelativistic case, which will be the only one considered below,

$$\mathfrak{D}_j = \frac{1 + \mathfrak{n}r_j + \mathbb{O}(r_j^2)}{2\sqrt{R}} \simeq \frac{\mathfrak{D}}{v_j} \simeq \mathfrak{D}, \quad \mathfrak{D} = \frac{1}{2\sqrt{R}} = \frac{E_\nu}{2\sqrt{\mathfrak{F}}}. \tag{277}$$

Within our approximations, function $\mathfrak{D}_j$ may be considered essentially independent of j (i.e., universal for all neutrinos ν_j), since $r_j \ll 1$ and function $\mathfrak{D}$ is itself small compared to the neutrino energies available in current experiments. Let us also take into account the fact that all factors of the integrand at the right-hand side of (246), with the exception of exponent

$$\exp\left[-\frac{1}{4}F_j(q_0) - i\left(q_0T - \sqrt{q_0^2 - m_j^2}L\right)\right],$$

are weakly varying functions of integration variable q_0 in the neighborhood of stationary point E_j and may, therefore, be taken out of the integral at point $q_0 = E_j$. Using (275) and expansion

$$\sqrt{q_0^2 - m_j^2} = P_j + \frac{1}{v_j}(q_0 - E_j) - \frac{m_j^2}{2P_j^3}(q_0 - E_j)^2 + \ldots,$$

we arrive at the following simple integral:

$$I_j = \int_{-\infty}^{\infty} dq_0 \exp\left[-i\left(E_jT - P_jL\right) + i\left(\frac{L}{v_j} - T\right) \times (q_0 - E_j) - \frac{1}{4}F_j(E_j) - \left(\frac{1}{4\mathfrak{D}_j^2} + \frac{im_j^2L}{2P_j^3}\right)(q_0 - E_j)^2\right].$$

Introducing complex-valued phase function

$$\Omega_j(T, L) = i\left(E_jT - P_jL\right) + \tilde{\mathfrak{D}}_j^2\left(\frac{L}{v_j} - T\right)^2, \quad (278)$$

which features

$$\tilde{\mathfrak{D}}_j^2 = \frac{\mathfrak{D}_j^2}{1 + i\mathfrak{r}_j} \simeq \frac{\mathfrak{D}^2}{1 + i\mathfrak{r}_j}, \quad \mathfrak{r}_j = \frac{2m_j^2\mathfrak{D}_j^2L}{P_j^3} \simeq \frac{2m_j^2\mathfrak{D}^2L}{E_\nu^3} = \frac{L}{\tau_{Lj}}, \quad (279)$$

where parameter $\tau_{j,L}$ is exactly the same as in the quantum-mechanical case in (53), we obtain

$$I_j = 2\sqrt{\pi}\tilde{\mathfrak{D}}_j \exp\left[-\frac{1}{4}F_j(E_j) - \Omega_j(T, L)\right].$$

Complex dispersion $\tilde{\mathfrak{D}}_j$ depends on the effective neutrino energy and spatial distance L between the impact points in the source and the detector; its modulus and argument are given by

$$\left|\tilde{\mathfrak{D}}_j\right| \simeq \mathfrak{D}\left(1 + r_j^2\right)^{-1/4}, \quad \arg(\tilde{\mathfrak{D}}_j) \simeq \frac{1}{2}\arctan\left(\mathfrak{r}_j\right).$$

Collecting all factors, we obtain the following resulting expression for the function in (246):

$$\mathbb{G}^j_{\nu\nu'\mu'\mu}\left(\{\mathbf{p}_\varkappa, x_\varkappa\}\right) = \Delta_{\nu\nu'}(p_j - p_\beta)\hat{p}_j\Delta_{\mu'\mu} \times (p_j + p_\alpha)\left|\mathbb{V}_d(p_j)\mathbb{V}_s(p_j)\right|\frac{\tilde{\mathfrak{D}}_j e^{-\Omega_j - i\Theta}}{i4\pi^{3/2}L}. \quad (280)$$

Here, 4-vector $p_j = (E_j, P_j\mathbf{l})$ was introduced, and the contribution proportional to m_j (see footnote (28)) was omitted. Phase factor $-ie^{-i\Theta}$ in (280) is insignificant, since it vanishes in the amplitude modulus squared.

Owing to the presence of smeared δ functions $\tilde{\delta}_s(p_j - q_s)$ and $\tilde{\delta}_d(p_j + q_d)$, which are involved in the expressions for overlap integrals $\mathbb{V}_s(p_j)$ and $\mathbb{V}_d(p_j)$ and establish the approximate energy-momentum conservation ($p_j \approx q_s \approx -q_d$), and to the assumed smallness of neutrino masses compared to representative energy E_ν, we may set $m_j = 0$ in the entire preexponential factor at the right-hand side of (280). Let us now use identity

$$P_-\hat{p}_\nu P_+ = P_-u_-(\mathbf{p}_\nu)\bar{u}_-(\mathbf{p}_\nu)P_+$$

(where $P_\pm = \frac{1}{2}(1 \pm \gamma_5)$, $\mathbf{p}_\nu = E_\nu\mathbf{l}$, and $u_-(\mathbf{p}_\nu)$ is the common Dirac bispinor for free left-handed massless neutrino ν) to define matrix elements

$$M_s = \frac{g^2}{8}\bar{u}_-(\mathbf{p}_\nu)\mathcal{J}_s^\mu\Delta_{\mu\mu'}(p_\nu + p_\alpha)O^{\mu'}u(\mathbf{p}_\alpha), \quad M_d^* = \frac{g^2}{8}\bar{v}(\mathbf{p}_\beta)O^{\mu'}\Delta_{\mu'\mu}(p_\nu - p_\beta)\mathcal{J}_d^{*\mu}u_-(\mathbf{p}_\nu), \quad (281)$$

which characterize the production and absorption of a real massless neutrino in reactions $I_s \to F_s'\ell_\alpha^+\nu$ and $\nu I_d \to F_d'\ell_\beta^-$, respectively[33]. Taking the above results into account, we then obtain the final expression for the amplitude in (241):

$$\mathfrak{A}_{\beta\alpha} = \sum_j \mathfrak{A}^j_{\beta\alpha}, \quad \mathfrak{A}^j_{\beta\alpha} = \frac{\left|\mathbb{V}_s(p_j)\mathbb{V}_d(p_j)\right| M_sM_d^*}{i4\pi^{3/2}\mathcal{N}L}V^*_{\alpha j}\tilde{\mathfrak{D}}_jV_{\beta j}e^{-\Omega_j - i\Theta}. \quad (282)$$

It is instructive to isolate the j-independent common factor establishing the approximate energy-momentum conservation at vertices. To this end, we use (200) and definitions (247) to obtain

$$\tilde{\delta}_s(p_j - q_s)\tilde{\delta}_d(p_j + q_d) = \tilde{\delta}_s(p_\nu - q_s)\tilde{\delta}_d(p_\nu + q_d)e^{-\Theta_j},$$

[33] Under additional conditions $\left|(p_\nu + p_\alpha)^2\right| \ll m_W^2$ and $\left|(p_\nu - p_\beta)^2\right| \ll m_W^2$, the W-boson propagator may be written approximately as $-ig_{\mu\nu}/m_W^2$, which corresponds to the four-fermion theory of weak interaction. Using well-known SM identity $g^2/8 = G_Fm_W^2/\sqrt{2}$, one may then rewrite matrix elements (281) in the following form:

$$M_s \approx -i\frac{G_F}{\sqrt{2}}\bar{u}_-(\mathbf{p}_\nu)\mathcal{J}_s^\mu O_{\mu\nu}(\mathbf{p}_\alpha), \quad M_d^* \approx -i\frac{G_F}{\sqrt{2}}\bar{u}(\mathbf{p}_\beta)\mathcal{J}_d^{*\mu}O_\mu u_-(\mathbf{p}_\nu).$$

However, this slightly restrictive simplification (inapplicable at ultrahigh energies) is not required and will not be used in subsequent analysis.

where

$$\Theta_j = \frac{1}{4}\Big[2\big(Y_\mu - R_{\mu\mu'}p_\nu^{\mu'}\big) + R_{\mu\mu'}(p_\nu - p_j)^{\mu'}\Big] \times (p_\nu - p_j)^\mu = \frac{1}{2}\{E_\nu[(\mathbf{Rl}) - R_{00}] + Y_0\}(E_\nu - E_j) + \frac{1}{2}\{E_\nu[(\mathbf{Rl}) - R] - (\mathbf{Yl})\}(E_\nu - P_j) + \frac{1}{4}\Big[R_{00}(E_\nu - E_j)^2 - 2(\mathbf{Rl})(E_\nu - E_j) \times (E_\nu - P_j) + R(E_\nu - P_j)^2\Big].$$

Amplitude (282) may then be presented in the following form:

$$\mathfrak{A}_{\beta\alpha} = \frac{|\mathbb{V}_s(p_\nu)\mathbb{V}_d(p_\nu)|\,M_s M_d^*}{i4\pi^{3/2}\mathcal{N}L} \times \sum_j V_{\alpha j}^*\tilde{\mathfrak{D}}_j V_{\beta j} e^{-\Omega_j - \Theta_j - i\Theta}. \quad (283)$$

Using (256), one can present function Θ_j as an expansion in r_j:

$$\Theta_j = m_j^2 R\Big[(\mathfrak{n}_0 - \mathfrak{n}) + \frac{1}{2}(\mathfrak{m} - \mathfrak{n} - \mathfrak{n}^2)r_j + \Big(\mathfrak{n} + \frac{1}{2}\Big)(\mathfrak{m} - \mathfrak{n} - \mathfrak{n}^2)r_j^2 + \mathbb{O}(r_j^3)\Big].$$

We should recall that function $\mathfrak{n}_0$ is defined in accordance with (265) and matches $\mathfrak{n}$ in the case of the exact energy-momentum conservation at vertices (see Section 8.2.1). If

$$|\mathfrak{n}|r_j \ll 1 \quad \text{and} \quad |\mathfrak{m}|r_j \ll |\mathfrak{n}|, \quad \forall j, \quad (284)$$

the following approximate relation is valid:

$$\Theta_j \approx m_j^2 R\Big[(\mathfrak{n}_0 - \mathfrak{n}) + \frac{1}{2}(\mathfrak{m} - \mathfrak{n} - \mathfrak{n}^2)r_j\Big],$$

and sign-indefinite difference $\mathfrak{n}_0 - \mathfrak{n}$ may be neglected in the neighborhood of the maximum of product $\tilde{\delta}_s(p_\nu - q_s)\tilde{\delta}_d(p_\nu + q_d)$ (i.e., at $q_s \approx -q_d \approx p_\nu$). Then,

$$\Theta_j \approx \frac{m_j^4 R(\mathfrak{m} - \mathfrak{n}_0 - \mathfrak{n}_0^2)}{4E_\nu^2} = \frac{m_j^4[R_{00}\mathcal{R} - (\mathbf{Rl})^2]}{4RE_\nu^2}. \quad (285)$$

It can be proven that this quantity is positive.

It can be seen from the derivation of formula (283) and its structure that it holds true both for the considered class of processes and, if matrix elements (281) are redefined accordingly, for all other processes sustained by the exchange of virtual neutrinos between macrodiagram vertices. It is easy to generalize formula (282) to the case of reactions with the exchange of antineutrinos: one needs just to perform the $\mathbf{V} \mapsto \mathbf{V}^\dagger$ substitution (i.e., $V_{\alpha j}^* \mapsto V_{\alpha j}$, $V_{\beta j} \mapsto V_{\beta j}^*$) and modify matrix elements (281) accordingly.

8.4. Effective Wave Packet of an Ultrarelativistic Neutrino

Let us return to expression (282). Phase function (278) involved in it may be rewritten in the following approximately[34] Lorentz-invariant form:

$$\Omega_j(T, L) = i(p_j X) + \frac{2\tilde{\mathfrak{D}}_j^2}{E_\nu^2}\Big[(p_j X)^2 - m_j^2 X^2\Big], \quad (286)$$

where $X = X_d - X_s$. Obviously, $(p_j X)^2 - m_j^2 X^2 = 0$ at $\mathbf{L} = \mathbf{v}_j T$. However, it is clear that quantities $(p_j X)^2 - m_j^2 X^2$ cannot simultaneously vanish at all j values if the neutrino mass spectrum is nondegenerate. Therefore, relation $L/T = |\mathbf{X}|/X_0$, which is set by the space-time configurations and velocities of external wave packets and is in no way associated with the effective velocities of virtual neutrinos, should not be interpreted as a certain mean neutrino velocity. Thus, with the j and T values fixed, vector $\delta\mathbf{x} = \mathbf{L} - \mathbf{v}_j T$ is, in general, nonzero, but is collinear to velocity vector $\mathbf{v}_j = v_j\mathbf{l}$. It is easy to show that if the direction of vector $\delta\mathbf{x}$ is arbitrary, the following identity holds true:

$$(p_j X)^2 - m_j^2 X^2 = E_j^2(\delta\mathbf{x}\cdot\mathbf{l})^2 + (\delta\mathbf{x}\times\mathbf{l})^2 = E_j^2\delta\mathbf{x}_\parallel^2 + m_j^2\delta\mathbf{x}_\perp^2, \quad (287)$$

where $\delta\mathbf{x}_\parallel$ and $\delta\mathbf{x}_\perp$ are the components of $\delta\mathbf{x}$ that are parallel and perpendicular to vector $\mathbf{l}$. It then follows from (287) that the value of $\exp(-|\Omega_j|)$ at

$$2\big|\tilde{\mathfrak{D}}_j\big|^2\big(\delta\mathbf{x}_\parallel^2 + \Gamma_j^{-2}\delta\mathbf{x}_\perp^2\big) < 1, \quad (288)$$

(where, naturally, $\Gamma_j = E_j/m_j \simeq E_\nu/m_j$) decreases by a factor of no more than e with respect to its maximum value at $\delta\mathbf{x} = 0$. The region defined by condition (288) is the interior of an oblate spheroid with radius $1/\big(\sqrt{2}\big|\tilde{\mathfrak{D}}_j\big|\big)$ that is flattened by a factor of Γ_j along the $\mathbf{l}$ direction.

Let us now examine the transformation under which the positions of centers of all external packets in the source, the value of T, and unit vector $\mathbf{l}$ remain unchanged, while all packets $\varkappa \in F_d$ are shifted by $\delta\mathbf{x}$; for simplicity, we set $\delta\mathbf{x} = \delta\mathbf{x}_\perp$. This transformation shifts impact point $\mathbf{X}_d$ and vector $\mathbf{L}$ by the same amount:

$$\mathbf{X}_d \mapsto \mathbf{X}_d' = \mathbf{X}_d + \delta\mathbf{x}, \quad \mathbf{L} \mapsto \mathbf{L}' = \mathbf{L} + \delta\mathbf{x}.$$

Since suppression factor $\exp(-\mathfrak{S}_d)$ in (282) is invariant with respect to spatial translations $\mathbf{x}_\varkappa \mapsto \mathbf{x}_\varkappa + \delta\mathbf{x}$ and all external momenta remain unchanged, quantity $\mathfrak{A}'^j_{\beta\alpha} = \mathfrak{A}^j_{\beta\alpha}\big|_{\mathbf{X}_d \mapsto \mathbf{X}_d'}$ may be inter-

[34] Function $\tilde{\mathfrak{D}}_j^2/E_\nu^2$ is invariant to within corrections $\mathbb{O}(\mathfrak{r}_j)$.

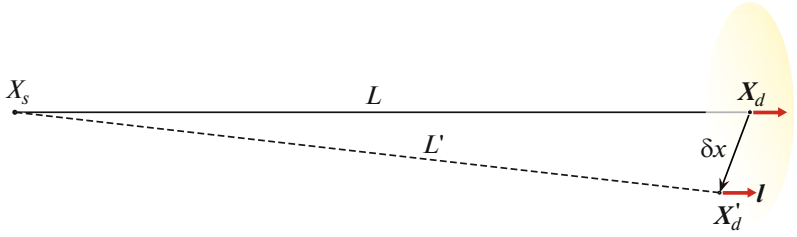

Fig. 16.

preted as the amplitude of the probability of interaction of neutrino j with 4-momentum $p_j = (E_j, P_j\mathbf{l})$ at point $\mathbf{X}'_d$ (see Fig. 16). This interpretation may seem artificial, but we will provide certain arguments in favor of it below (in the analysis of the expression for the count rate of neutrino events). If distance L is sufficiently large (i.e., $4\left|\tilde{\mathfrak{D}}_j\right|^2 L^2 \gg 1$), its relative variation induced by shifts $\delta\mathbf{x}$ satisfying conditions (288) is insignificant,

$$L'/L - 1 \approx \delta\mathbf{x}^2/(2L^2) \ll 1,$$

and the $\mathfrak{V}^j_{\beta\alpha}$ amplitude suppression is determined exclusively by factor $\exp(-|\Omega_j|)$, which is close to unity at $2\left|\tilde{\mathfrak{D}}_j\right|^2 \delta\mathbf{x}_\perp^2 \ll \Gamma_j^2$. The absolute values of transverse shift $\delta\mathbf{x}_\perp$ and length difference $L' - L \approx \delta\mathbf{x}^2/(2L)$ may be so large that the L'/T ratio exceeds unity. If this ratio is interpreted erroneously as the velocity of a point-like neutrino, one may conclude incorrectly that special relativity is violated. It is instructive to clarify this purely quantum effect within a more intuitive approach by introducing an effective neutrino WP. To this end, we isolate the following factor from amplitude (282):

$$\bar{u}_-(\mathbf{p}_\nu)\frac{1}{L}e^{-\Omega_j(T,L)}u_-(\mathbf{p}_\nu) \approx \bar{u}_-(\mathbf{p}_j)\frac{1}{L}e^{-\Omega_j(T,L)}u_-(\mathbf{p}_j) \quad (289)$$

(note that spinors $u_-(\mathbf{p}_\nu)$ and $\bar{u}_-(\mathbf{p}_\nu)$ are contained in matrix elements (281)). Neglecting the imaginary part of function $\tilde{\mathfrak{D}}_j^2$, we rewrite expression (289) in the form of a product:

$$\frac{1}{|\mathbf{X}_d - \mathbf{X}_s|}\bar{\Psi}^j_{X_s}(\mathbf{p}_j, X_d - X_s)\Psi^j_{X_d}(\mathbf{p}_j, X_s - X_d), \quad (290)$$

where

$$\Psi^j_y(\mathbf{p}_j, x) = \exp\left\{-i(p_j y) - \frac{\tilde{\mathfrak{D}}_j^2}{E_\nu^2}\left[(p_j x)^2 - m_j^2 x^2\right]\right\}u_-(\mathbf{p}_j),$$

and

$$\bar{\Psi}^j_y(\mathbf{p}_j, x) = \left[\Psi^j_y(\mathbf{p}_j, x)\right]^\dagger\gamma_0 = \bar{u}_-(\mathbf{p}_j)\exp\left\{i(p_j y) - \frac{\tilde{\mathfrak{D}}_j^2}{E_\nu^2}\left[(p_j x)^2 - m_j^2 x^2\right]\right\}.$$

Comparing spinor function $\Psi_y(\mathbf{p}_j, x)$ with the wave function of a fermion packet of the general form in the SRGP approximation

$$\Psi_y(\mathbf{p}, s, x) = e^{-ipx}u_s(\mathbf{p})\psi(\mathbf{p}, x - y) = u_s(\mathbf{p})\exp\left\{-i(py) - \frac{\sigma^2}{m^2}\left[(px)^2 - m^2x^2\right]\right\},$$

we see that spinor function $\Psi^j_{X_d}(\mathbf{p}_j, X_s - X_d)$ may be interpreted as the wave function in the x-representation characterizing an incoming WP of a real massive neutrino ν_j with $\sigma_j = \mathfrak{D}_j/\Gamma_j$ acting as parameter σ. The second spinor cofactor in (290), $\bar{\Psi}^j_{X_s}(\mathbf{p}_j, X_d - X_s)/|\mathbf{X}_d - \mathbf{X}_s|$, is naturally interpreted as a spherical neutrino wave outgoing from the source at distance $|\mathbf{X}_d - \mathbf{X}_s|$ from production point $\mathbf{X}_s$.

It is instructive to present the result obtained in a simpler quantum-mechanical formulation by performing calculations similar to the transition amplitude calculation in the QM approach (see (61)). Let us determine the amplitude of transition from the ν_j WP state in the source defined by the most probable momentum $\mathbf{p}_j$, momentum dispersion σ_{sj}, and 4-coordinate X_s to the ν_j WP state in the detector with the same momentum, dispersion σ_{dj}, and 4-coordinate X_d (the WP spread in the configuration space is neglected; i.e., the SRGP approximation is applied):

$$\frac{1}{\mathcal{N}_{sd}}\langle\mathbf{p}_j, X_d; \sigma_{dj}|\mathbf{p}_j, X_s; \sigma_{sj}\rangle = \left(\frac{2\sigma_{sj}\sigma_{dj}}{\sigma_{sj}^2 + \sigma_{dj}^2}\right)^{3/2}\psi(\mathbf{p}_j, X_d - X_s, \sigma_j). \quad (291)$$

Here,

$$\frac{1}{\sigma_j^2} = \frac{1}{\sigma_{sj}^2} + \frac{1}{\sigma_{dj}^2}, \quad (292)$$

and

$$\mathcal{N}_{sd} = \sqrt{\langle \mathbf{p}_j, X_d; \sigma_{dj} | \mathbf{p}_j, X_d; \sigma_{dj} \rangle \langle \mathbf{p}_j, X_s; \sigma_{sj} | \mathbf{p}_j, X_s; \sigma_{sj} \rangle}.$$

We obtained an expression proportional to function $\psi(\mathbf{p}, x)$ in the SRGP approximation, which should be compared to $e^{-\Omega_j(T,L)}$. The result is $\sigma_j = \mathfrak{D}_j / \Gamma_j$. Thus, $\mathfrak{D}_j$ is the effective neutrino energy uncertainty with interactions in the source and the detector factored in. It should be compared to σ_p defined in accordance with (63). Since σ_{sj} and σ_{dj} are the neutrino WP dispersions in the source and the detector, respectively, it is easy to determined their explicit form by rewriting the first formula in (250) as $R = \sigma_{xs}^2 + \sigma_{xd}^2$, where $\sigma_{xs}^2 = \tilde{\Re}_s^{\mu\nu} l_\mu l_\nu$, $\sigma_{xd}^2 = \tilde{\Re}_d^{\mu\nu} l_\mu l_\nu$. It is clear that quantities σ_{xs} and σ_{xd} have the physical meaning of spatial dispersions of a neutrino WP in the source and the detector, which are related to the momenta dispersions by the following standard (for a Gaussian packet) expressions:

$$\begin{aligned} \sigma_{sj}^{-2} &= 4\sigma_{xs}^2 = 4\tilde{\Re}_s^{\mu\nu} l_\mu l_\nu, \\ \sigma_{dj}^{-2} &= 4\sigma_{xd}^2 = 4\tilde{\Re}_d^{\mu\nu} l_\mu l_\nu. \end{aligned} \tag{293}$$

Inserting σ_{sj} and σ_{dj} from (293) into (292) to calculate the amplitude in (291), we indeed obtain, to within a dimensionless factor of the order of unity, $e^{-\Omega_j(T,L)}$ with function $\mathfrak{D}_j$ defined in accordance with (276).

Since $\tilde{\mathfrak{D}}_j$ is a complex-valued function, factorization (290) is not possible in the general case, but the corresponding correction, which is clearly of interest for neutrino astrophysics, can be interpreted as the result of a peculiar interference of spreading in- and out-neutrino packets. This correction becomes significant at very large distances L and induces overall suppression of amplitude (241) and modification of oscillation factors $\propto \exp[i\mathrm{Im}\Omega_j(T,L)]$. To study these effects in detail, one needs to analyze observables (such as the count rate for a given type of event) that are obtained after appropriate averaging of the amplitude modulus squared over all unmeasured variables on which amplitude (241) is dependent. This averaging depends on the statistical distributions (or, in a more general case, on the kinetics) of ensembles of in-packets and on the detection procedure [57, 58]. Here, we limit ourselves to the case when the imaginary part of $\tilde{\mathfrak{D}}_j$ is negligible. Let us determine the applicability conditions of this approximation. Using (277) and (279), we write

$$\mathfrak{r}_j \simeq \frac{10^5}{\mathfrak{F}} \left(\frac{m_j}{1\ \mathrm{eV}} \right)^2 \left(\frac{1\ \mathrm{GeV}}{E_\nu} \right) \left(\frac{L}{10^4\ \mathrm{km}} \right). \tag{294}$$

It can be seen that $\mathfrak{r}_j \ll 1$ for all current experiments with reactor ($E_\nu \gtrsim 1$ MeV, $L \lesssim 10^3$ km), accelerator ($E_\nu \gtrsim 100$ MeV, $L \lesssim 10^3$ km), and atmospheric ($E_\nu \gtrsim 100$ MeV, $L \lesssim 1.3 \times 10^4$ km) (anti) neutrinos if $m_j \lesssim 1$ eV and $F \gg 10^7$. Using typical examples, we will demonstrate in Appendix A.3.2 that the $F \gg 10^7$ condition is definitely fulfilled in the domain of applicability of the SRGP model.[35] In addition, $\tilde{\mathfrak{D}}_j^2 \simeq \mathfrak{D}_j^2 \simeq \mathfrak{D}^2$; therefore,

$$\frac{\sigma_j^2}{m_j^2} \simeq \frac{\mathfrak{D}^2}{E_\nu^2} = \frac{1}{2E_\nu^2 R} \simeq \frac{1}{2\mathfrak{F}}. \tag{295}$$

With the adopted conditions of narrowness of external packets in the momentum space, $\sigma_\varkappa^2 \ll m_\varkappa^2$, factored in, it follows automatically that $\sigma_j^2 / m_j^2 \ll 10^{-7}$ and $\sigma_j^2 L^2 \ll m_j^2 / \sigma_j^2$ (packet stability condition).

It was demonstrated in Section 5.7 that the uncertainties of the energy and the momentum components of an ultrarelativistic WP in the SRGP approximation are

$$\begin{aligned} \delta E_\mathbf{p} \approx |\delta \mathbf{p}| \approx |\delta \mathbf{p}_\parallel| \approx \sqrt{2\ln 2}\, \Gamma_\mathbf{p} \sigma, \\ |\delta \mathbf{p}_\perp| \approx 2\sqrt{\ln 2}\, \sigma \end{aligned}$$

($\delta \mathbf{p}_\parallel \times \mathbf{p} = 0$, $\delta \mathbf{p}_\perp \cdot \mathbf{p} = 0$); thus, the corresponding uncertainties for an ultrarelativistic neutrino packet are

$$\begin{aligned} \delta E_j \approx |\delta \mathbf{p}_j| \approx |\delta \mathbf{p}_{j\parallel}| \approx 2\sqrt{\ln 2}\, \mathfrak{D}, \\ |\delta \mathbf{p}_{j\perp}| \approx 2\sqrt{2\ln 2}\, \mathfrak{D} / \Gamma_j \ll |\delta \mathbf{p}_{j\parallel}|, \end{aligned}$$

i.e., function $\mathfrak{D}$, which depends on the masses, momenta, and momentum spreads of external in and out packets, characterizes the neutrino energy uncertainty, and $1/\mathfrak{D}$ defines (to within a numerical factor of the order of unity) the effective size of a neutrino wave packet transverse to momentum $\mathbf{p}_j$. A huge and very thin disk with ratio $\Gamma_j \gg 1$ of the transverse size to the longitudinal one may serve as an illustration of an ultrarelativistic neutrino WP. The relative neutrino energy and momentum uncertainty

$$\delta E_j / E_j \simeq \delta P_j / P_j \sim \mathfrak{D} / E_\nu \sim 1 / \sqrt{\mathfrak{F}}$$

is always very small and independent of the neutrino energy and mass. This is how one should interpret the standard quantum-mechanical assumption that the states of neutrinos with definite masses $|\nu_i\rangle$ (and, consequently, the states with definite flavors $|\nu_\alpha\rangle$) have definite 4-momenta.

[35] In particular, taking into account modern cosmological constraints on the sum of neutrino masses (see, e.g., [132]).

Just as any other SRGP, a neutrino WP moves, in the average, along classical trajectory $\bar{\mathbf{L}}_j = \mathbf{v}_j T$. Quantum deviations $\delta\mathbf{L}_j$ from this trajectory are suppressed (in amplitude) by factor

$$\exp\left\{-2\mathfrak{D}^2\left[(\delta\mathbf{L}_j)^2/\Gamma_j^2 + (\mathbf{L}\delta\mathbf{L}_j)^2/L^2\right]\right\}.$$

Owing to the smallness of ratio $\mathfrak{D}^2/\Gamma_j^2 \sim m_j^2/\mathfrak{F}$, transverse deviations may be macroscopically large (or infinite, if neutrinos are massless). This conclusion agrees with the result formulated at the beginning of this section without invoking the notion of a neutrino WP.

Thus, we verified that the effective WP of an ultrarelativistic neutrino reproduces all the properties of an SRGP of the general form, with the only caveat that parameter σ_j actually depends on the momenta (as well as masses and momentum dispersions) of all external packets. It should be noted here that this dependence is not a specific feature of neutrinos or the covariant formalism, since, as was discussed in Section 4.3, a WP characterizing the state of any massive particle should depend on the momenta of particles involved both in its production and its absorption, and the $\sigma_\varkappa = \text{const}$ assumption used here is just a simplifying approximation.

9. MICROSCOPIC PROBABILITY OF MACROSCOPICALLY SEPARATED EVENTS

Using (282) and the formulas for four-dimensional overlap volumes $\mathrm{V}_{s,d}$ derived in Section 7.11, we obtain the following expression for the microscopic probability of process (231):

$$\begin{aligned}\left|\mathfrak{A}_{\beta\alpha}\right|^2 &= \frac{(2\pi)^4\delta_s(p_\nu - q_s)\mathrm{V}_s\left|M_s\right|^2}{\prod\limits_{\varkappa\in S}2E_\varkappa\mathrm{V}_\varkappa}\\ &\times\frac{(2\pi)^4\delta_d(p_\nu + q_d)\mathrm{V}_d\left|M_d\right|^2}{\prod\limits_{\varkappa\in D}2E_\varkappa\mathrm{V}_\varkappa}\\ &\times\frac{1}{2(2\pi)^3L^2}\left|\sum_j\tilde{\mathfrak{D}}_j V_{\alpha j}^* V_{\beta j}e^{-\Omega_j-\Theta_j}\right|^2.\end{aligned}\qquad(296)$$

This expression depends on coordinates $x_\varkappa$ and mean momenta $\mathbf{p}_\varkappa$ of all WPs involved in the reaction and on parameters $\sigma_\varkappa$. Probability (296) is vanishingly small if the product of overlap volumes

$$\begin{aligned}\mathrm{V}_s\mathrm{V}_d &= \left(\frac{\pi}{2}\right)^4\left((|\Re_s||\Re_d|)\right)^{-1/2}\\ &\times\exp[-2(\mathfrak{S}_s+\mathfrak{S}_d)],\end{aligned}$$

is small (i.e., if in- and out-packets in the source and the detector do not overlap in space-time regions surrounding impact points X_s and X_d).

Note that 4-vector p_ν is also a function of $p_\varkappa$ and $\sigma_\varkappa$, and $p_\nu = q_s = -q_d$ in the $\sigma_\varkappa = 0$, $\forall\varkappa$ limit. Therefore, at sufficiently small $\sigma_\varkappa$,

$$\begin{aligned}\delta_s(p_\nu - q_s)\delta_d(p_\nu + q_d) &\approx \delta_s(0)\delta_d(0)\\ &= (2\pi)^{-4}\left(|\Re_s||\Re_d|\right)^{-1/2}.\end{aligned}$$

What determines the approximate equality of q_s and q_d? To answer this question, we transform expression (296) in a way proposed by Cardall [42]. Using the explicit form of functions $\delta_{s,d}$ and $\mathfrak{D}$, one readily derives an approximate relation[36]

$$\begin{aligned}&\sqrt{2\pi}\mathfrak{D}\delta_s(p_\nu - q_s)\delta_d(p_\nu + q_d)F(p_\nu)\\ &= \int dE_\nu'\left(p_\nu' - q_s\right)\delta_d\left(p_\nu' + q_d\right)F(p_\nu'),\end{aligned}$$

where $F(p_\nu)$ is an arbitrary slowly varying function of p_ν, and $p_\nu' = (E_\nu', \mathbf{p}_\nu') = E_\nu' l$. This relation yields

$$\begin{aligned}\left|\mathfrak{A}_{\beta\alpha}\right|^2 &= \int dE_\nu\frac{(2\pi)^4\delta_s(p_\nu - q_s)\mathrm{V}_s\left|M_s\right|^2}{\prod\limits_{\varkappa\in S}2E_\varkappa\mathrm{V}_\varkappa}\\ &\times\frac{(2\pi)^4\delta_d(p_\nu + q_d)\mathrm{V}_d\left|M_d\right|^2}{\prod\limits_{\varkappa\in D}2E_\varkappa\mathrm{V}_\varkappa}\\ &\times\frac{\mathfrak{D}}{2\sqrt{2\pi}(2\pi)^3L^2}\left|\sum_j V_{\alpha j}^* V_{\beta j}e^{-\Omega_j-\Theta_j}\frac{1}{1+i\mathfrak{r}_j}\right|^2,\end{aligned}\qquad(297)$$

where the prime on "silent" integration variable E_ν is omitted, but it (just as vector $\mathbf{p}_\nu = E_\nu\mathbf{l}$) is no longer related in any way to the parameters of external packets. Formulas (296) and (297) are equivalent within the adopted approximations, but it follows from (297) that the energy-momentum conservation law is governed by subintegral factors $\delta_s(p_\nu - q_s)$ and $\delta_d(p_\nu + q_d)$, which may be replaced by common δ functions at sufficiently small $\sigma_\varkappa$. The obtained result will serve as a basis for calculation of the quantities measured in current experiments on neutrino oscillations.

10. PROBABILITY AND COUNT RATE

Expression (297) is the most general result of this study. At the same time, it is too abstract for direct processing and analysis of the data provided by current neutrino experiments. In the majority of such experiments, information on the particle coordinates in the source (and, more often than not, in the detector) is unavailable or is not used in data processing. In addition, it is often the case that only the momenta of secondary particles in the detector are measured. To obtain an actually observable quantity, one needs to average (sum) probability (297) over all variables of in-

[36] The accuracy of this relation is the same as that of formula (282) for the amplitude: it is the accuracy of the saddle-point method used in the derivation.

(out-) particle states that are unmeasured or unused in the analysis. We call this procedure the macroscopic averaging. In each particular experiment, one needs to factor in the actual physical conditions (by constructing an adequate mathematical model of the experiment) to perform macroscopic averaging. The subsequent analysis becomes model-dependent in this respect.

10.1. Macroscopic Averaging

In what follows, we use a simple but fairly realistic model. It is assumed in this model that the distributions of WPs of in-particles over mean momenta, spin projections, and coordinates in the source and the detector (regarded as physical macroscopic objects) may be characterized by classical single-particle distribution functions $f_a(\mathbf{p}_a, s_a, x_a)$ normalized at each point in time in accordance with the following condition:

$$\sum_{s_a}\int\frac{d\mathbf{x}_a d\mathbf{p}_a}{(2\pi)^3}f_a(\mathbf{p}_a, s_a, x_a) = N_a(x_a^0) \quad (a\in I_{s,d}),$$

where $N_a(x_a^0)$ is the total number of particles a at time x_a^0. We may now clarify (or, more exactly, redefine) the terms "source" and "detector" that were used in calculations of the amplitude to denote the blocks of macroscopic Feynman diagrams. In what follows, the terms source and detector are used to denote the corresponding experimental devices and (in an abstract, but mathematically more rigorous sense) supports $\mathcal{S}$ and $\mathcal{D}$ of products of the distribution functions of over space-time variables (i.e., $\mathcal{S} = \mathrm{supp}_{\{x_a\}}\prod_a f_a$, $a\in I_s$; the definition of $\mathcal{D}$ is similar), which are assumed to be bounded and nonoverlapping. It is assumed that the characteristic spatial sizes of $\mathcal{S}$ and $\mathcal{D}$ are small compared to the distance between them but are very large compared to the effective sizes of all wave packets moving within them. For definiteness, we assume that only the mean momenta of secondary particles in $\mathcal{D}$ are measured in our experiment and that the background of secondary particles from $\mathcal{S}$ in $\mathcal{D}$ is negligible (due to the fact that $\mathcal{S}$ is located far from $\mathcal{D}$). Under these assumptions, the macroscopically averaged probability of process (231) may be written as follows:

$$\begin{aligned}\left\langle\left\langle\left|\mathfrak{N}_{\beta\alpha}\right|^2\right\rangle\right\rangle &= \sum_{\text{spins}}\int\prod_{a\in I_s}\frac{d\mathbf{x}_a d\mathbf{p}_a f_a(\mathbf{p}_a, s_a, x_a)}{(2\pi)^3 2E_a V_a}\\ &\times\int\prod_{b\in F_s}\frac{d\mathbf{x}_b d\mathbf{p}_b}{(2\pi)^3 2E_b V_b}V_s\int\prod_{a\in I_d}\frac{d\mathbf{x}_a d\mathbf{p}_a f_a(\mathbf{p}_a, s_a, x_a)}{(2\pi)^3 2E_a V_a}\\ &\times\int\prod_{b\in F_d}\frac{d\mathbf{x}_b[d\mathbf{p}_b]}{(2\pi)^3 2E_b V_b}V_d\int dE_\nu(2\pi)^4\delta_s(p_\nu - q_s)\\ &\times|M_s|^2(2\pi)^4\delta_d(p_\nu + q_d)|M_d|^2\\ &\times\frac{\mathcal{D}}{2\sqrt{\pi}(2\pi)^3 L^2}\left|\sum_j V_{\alpha j}^* V_{\beta j}e^{-\Omega_j - \Theta_j}\right|^2.\end{aligned} \tag{298}$$

Here and elsewhere, symbol $\sum_{\text{spins}}$ denotes averaging over spins of all in-particles and summing over spins of all out-particles in $\mathcal{S}$ and $\mathcal{D}$, and symbol $[d\mathbf{p}_b]$ indicates that integration over $\mathbf{p}_b$ is not performed; i.e., $\int[d\mathbf{p}_b] = d\mathbf{p}_b$. It is thus implied in (298) that one can measure the momenta of all secondary particles in the detector[37]. It is evident that (298) is the total number, $dN_{\alpha\beta}$, of events that are detected in $\mathcal{D}$ and involve particles $b\in F_d$ with their momenta falling within the interval from $\mathbf{p}_b$ to $\mathbf{p}_b + d\mathbf{p}_b$ (i.e., $\left\langle\left\langle\left|\mathfrak{N}_{\beta\alpha}\right|^2\right\rangle\right\rangle = dN_{\alpha\beta}$[38]). For simplicity, we neglect effects of the order of L/τ_{Lj} (see (279)) that are related to the spreading of an effective neutrino WP at very large distances. These effects are of potential interest for experiments with astrophysical neutrinos, but are usually insignificant in terrestrial oscillation experiments (including the experiments with solar neutrinos). Certain results corresponding to very long baselines are presented in Appendix E.

The integration over packet coordinates in (298) can be performed explicitly if one uses integral representation (229) for overlap volumes $V_{s,d}$ and takes into account the fact that factor $e^{-\Omega_j - \Omega_i^*}/L^2$ and distribution functions f_a in $\mathcal{S}$ and $\mathcal{D}$ vary considerably in time and space only on macroscopic scales, while the subintegral factors in V_s and V_d differ significantly from zero only in a small neighborhood of the corresponding integration variable.

Let us formulate this more rigorously. In effect, we demonstrate that a configuration of spatially separated points x such that

$$\mathcal{P}_{s,d} \equiv \prod_{\varkappa\in S,D}\left|\psi_\varkappa(\mathbf{p}_\varkappa, x_\varkappa - x)\right|^2 = 1,$$

(i.e., $\mathcal{P}_s$ and $\mathcal{P}_d$ reach their maxima) may be found for any configuration of external momenta and arbitrary x. For definiteness, $\varkappa\in S$. In view of the invariance of functions $|\psi_\varkappa(\mathbf{p}_\varkappa, x_\varkappa - x)|$ with respect to shifts along the world lines of packet centers, one may replace coordinates $x_\varkappa$ by $y_\varkappa$, where

$$y_\varkappa^0 = X_s^0, \quad \mathbf{y}_\varkappa = \mathbf{x}_\varkappa + (X_s^0 - x_\varkappa^0)\mathbf{v}_\varkappa.$$

[37] Naturally, this assumption is optional; the "placement of square brackets" in (298) is dictated by the conditions of a specific experiment. For example, in the hypothetical experiment with "labeled" neutrinos, the momenta of all secondary particles both in the source and in the detector should be measurable.

[38] For simplicity, we consider an "ideal" experiment with a detection efficiency of 1, although real efficiency and acceptance values, trigger conditions, and event selection criteria are easy to introduce into the formalism.

It is evident that $\mathcal{P}_s = \prod_\varkappa |\psi_\varkappa(\mathbf{p}_\varkappa, y_\varkappa - x)|^2 = 1$ at $y_\varkappa = x$; i.e., at one and the same point in time, but with mismatched spatial coordinates $\mathbf{x} = \mathbf{x} + (x_\varkappa^0 - x^0)\mathbf{v}_\varkappa$, which are sufficiently separated by construction, since variables $x_\varkappa^0$ are external and we have set the needed conditions for them. Naturally, $X_s = x$ (since X_s remains unchanged if $x_\varkappa$ is replaced by $y_\varkappa$). It is implied here that a maximum of one packet may have zero velocity. However, it is clear that the contributions from configurations with two (or more) packets with zero velocities are insignificant. Neglecting them and edge effects, we rewrite (298) in the following form:

$$dN_{\alpha\beta} = \sum_{\text{spins}} \int dx \int dy \int d\mathfrak{P}_s \int d\mathfrak{P}_d \times \int dE_\nu \frac{\mathfrak{D}\left|\sum_j V_{\alpha j}^* V_{\beta j} e^{-\Omega_j - \Theta_j}\right|^2}{16\pi^{7/2}|\mathbf{y} - \mathbf{x}|^2}, \tag{299}$$

where differential forms $d\mathfrak{P}_{s,d}$ are defined as

$$d\mathfrak{P}_s = \prod_{a\in I_s} \frac{d\mathbf{p}_a f_a(\mathbf{p}_a, s_a, x)}{(2\pi)^3 2E_a} \times \prod_{b\in F_s} \frac{d\mathbf{p}_b}{(2\pi)^3 2E_b} (2\pi)^4 \delta_s(p_\nu - q_s)|M_s|^2, \tag{300a}$$

$$d\mathfrak{P}_d = \prod_{a\in I_d} \frac{d\mathbf{p}_a f_a(\mathbf{p}_a, s_a, y)}{(2\pi)^3 2E_a} \times \prod_{b\in F_d} \frac{[d\mathbf{p}_b]}{(2\pi)^3 2E_b} (2\pi)^4 \delta_d(p_\nu + q_d)|M_d|^2. \tag{300b}$$

Definition (278) and its Lorentz-invariant form (286), where

$$T = X_0 = y_0 - x_0, \quad \mathbf{X} = \mathbf{y} - \mathbf{x},$$
$$L = |\mathbf{X}|, \quad X = (X_0, \mathbf{X}),$$

and all the other designations remain unchanged, are still valid for complex phase Ω_j in (299). It should be stressed that the derivation of (299) relies on the properties of the adopted mathematical model, which does not necessarily characterize faithfully the real experiments on neutrino oscillations. The experimental constraints on neutrino masses, which make it natural to assume that $\mathrm{Im}(\Omega_j + \Omega_i^*)$ varies significantly only on macroscopically large spatial scales L_{ij} and $\mathrm{Re}(\Omega_j + \Omega_i^*)$ varies on scales much larger than L_{ij}, were also used implicitly. It bears recalling, however, that this interpretation is based on the quantum-mechanical analysis of experimental data. Therefore, simple approximate formula (299) is actually not equivalent to more general expression (298) and certainly not to (297).

The integration in x^0 and y^0 in the source and the detector in (299) is formally performed over time intervals in which functions f_a are defined. Thus, (299) is applicable to a wide range of experiments with both stationary and nonstationary sources and detectors. To simplify the analysis further, we integrate with respect to these variables in (299). This is done for a simple model, which is easy to generalize to a more realistic case. More precisely, we assume that distribution functions f_a in $\mathcal{S}$ and $\mathcal{D}$ depend only weakly on time in the course of the experiment and may be approximated with a sufficient accuracy by "rectangular" dependences

$$\begin{aligned} f_a(\mathbf{p}_a, s_a; x) &= \theta(x^0 - x_1^0)\theta(x_2^0 - x^0) \\ &\times \bar{f}_a(\mathbf{p}_a, s_a; \mathbf{x}) \quad \text{for} \quad a \in I_s, \\ f_a(\mathbf{p}_a, s_a; y) &= \theta(y^0 - y_1^0)\theta(y_2^0 - y^0) \\ &\times \bar{f}_a(\mathbf{p}_a, s_a; \mathbf{y}) \quad \text{for} \quad a \in I_d, \end{aligned} \tag{301}$$

where functions $\bar{f}_a$ are time-independent. Step functions for particle distributions in the detector should be understood as hardware or software trigger conditions. The steady periods $\tau_s = x_2^0 - x_1^0$ and $\tau_d = y_2^0 - y_1^0$ may be very long (in experiments with solar or atmospheric neutrinos, where $\tau_s \ggg \tau_d$) or very short (in experiments with pulsed accelerator beams, where the $\tau_s \lesssim \tau_d$ condition is usually satisfied). In either case, it is assumed in model (301) that the "on" and "off" time intervals of the source (detector) are negligible compared to τ_s (τ_d). If model (301) is used, $e^{-\Omega_j - \Theta_i^*}$ is the only factor in the integrand in (299) depending on x^0 and y^0. Thus, the problem is reduced to calculating a relatively simple integral

$$\begin{aligned} \mathfrak{I} &= \int_{y_1^0}^{y_2^0} dy^0 \int_{x_1^0}^{x_2^0} dx^0 \\ &\times \exp\left[-\Omega_j(y^0 - x^0, L) - \Omega_i^*(y^0 - x^0, L)\right] \\ &\equiv \frac{\sqrt{\pi}}{2\mathfrak{D}} \tau_d \exp\left(i\varphi_{ij} - \mathscr{A}_{ij}^2\right) S_{ij}. \end{aligned} \tag{302}$$

The following designations were used in (302):

$$S_{ij} = \frac{\exp(-\mathscr{B}_{ij}^2)}{4\tau_d \mathfrak{D}} \sum_{l,l'=1}^{2} (-1)^{l+l'+1} \times \mathrm{Ierf}\left[2\mathfrak{D}\left(x_l^0 - y_{l'}^0 + \frac{L}{v_{ij}}\right) - i\mathscr{B}_{ij}\right], \tag{303}$$

$$\varphi_{ij} = \frac{2\pi L}{L_{ij}}, \quad \mathscr{A}_{ij} = (v_j - v_i)\mathfrak{D}L = \frac{2\pi\mathfrak{D}L}{E_\nu L_{ij}}, \quad \mathscr{B}_{ij} = \frac{\Delta E_{ij}}{4\mathfrak{D}} = \frac{\pi\mathfrak{n}}{2\mathfrak{D}L_{ij}}, \tag{304}$$

$$L_{ij} = \frac{4\pi E_\nu}{\Delta m_{ij}^2}, \quad \Delta m_{ij}^2 = m_i^2 - m_j^2,$$
$$\Delta E_{ij} = E_i - E_j, \quad \frac{2}{v_{ij}} = \frac{1}{v_i} + \frac{1}{v_j}, \tag{305}$$

$$\mathrm{Ierf}(z) = \int_0^z dz' \,\mathrm{erf}(z') + \frac{1}{\sqrt{\pi}} = z\,\mathrm{erf}(z) + \frac{1}{\sqrt{\pi}} e^{-z^2}, \tag{306}$$

where $\mathrm{erf}(z)$ is the error function integral. To obtain a more realistic description of experiments with a pulsed particle beam in the source (e.g., mesons in the decay channel), one may generalize model (301) by introducing, e.g., a series of rectangular (or more complex) pulses with pauses between the pulses, in which $f_a = 0$. Here, we focus on the simplest case (301), which reproduces the most significant effects. Taking (302) into account, we obtain the following instead of (299):

$$dN_{\alpha\beta} = \tau_d \sum_{\text{spins}} \int d\mathbf{x} \int d\mathbf{y} \int d\mathfrak{P}_s \int d\mathfrak{P}_d \times \int dE_\nu \frac{\mathcal{P}_{\alpha\beta}(E_\nu, |\mathbf{y}-\mathbf{x}|)}{4(2\pi)^3 |\mathbf{y}-\mathbf{x}|^2}, \tag{307a}$$

$$= \frac{\tau_d}{V_{\mathcal{D}} V_{\mathcal{S}}} \int d\mathbf{x} \int d\mathbf{y} \int d\Phi_\nu \int d\sigma_{\nu\mathcal{D}} \mathcal{P}_{\alpha\beta}(E_\nu, |\mathbf{y}-\mathbf{x}|). \tag{307b}$$

We should recall that the effect of spreading of a neutrino WP is neglected in base formula (297), which was used to derive expression (307a). As was demonstrated, this approximation is valid at distances L satisfying condition (294). It can be seen from (294) that formula (297) is applicable to all current experiments with reactor ($E_\nu \gtrsim 1$ MeV, $L \lesssim 10^3$ km), accelerator ($E_\nu \gtrsim 100$ MeV, $L \lesssim 10^3$ km), and atmospheric ($E_\nu \gtrsim 100$ MeV, $L \lesssim 1.3\times 10^4$ km) (anti)neutrino if $m_j \lesssim 1$ eV and $\mathfrak{F} \gg 10^7$; the last two conditions are definitely satisfied. A more general case with significant spreading of a neutrino packet is considered in Appendix E. This regime is of potential interest for experiments with astrophysical neutrinos, but here we limit ourselves to the conditions of "terrestrial" experiments.

Differential forms $d\mathfrak{P}_{s,d}$ in (307a) are defined in accordance with (300), where functions f_a should be replaced by $\bar{f}_a$, and expression (307b) is written using identity

$$\sum_{\text{spins}} \frac{d\mathfrak{P}_s d\mathfrak{P}_d dE_\nu}{4(2\pi)^3 |\mathbf{y}-\mathbf{x}|^2} = \sum_{\text{spins}\in S} \frac{d\mathfrak{P}_s d\mathbf{p}_\nu}{(2\pi)^3 2E_\nu |\mathbf{y}-\mathbf{x}|^2 d\Omega_\nu} \times \sum_{\text{spins}\in D} \frac{d\mathfrak{P}_d}{2E_\nu} \equiv \frac{d\Phi_\nu d\sigma_{\nu\mathcal{D}}}{V_{\mathcal{D}} V_{\mathcal{S}}},$$

where $V_{\mathcal{S}}$ and $V_{\mathcal{D}}$ are the spatial source and detector volumes, taken into account. Differential form $d\Phi_\nu$ is defined in such a way that integral

$$\frac{d\mathbf{x}}{V_S} \int \frac{d\Phi_\nu}{dE_\nu} = d\mathbf{x} \sum_{\text{spins}\in S} \int \frac{d\mathfrak{P}_s E_\nu}{2(2\pi)^3 |\mathbf{y}-\mathbf{x}|^2} \tag{308}$$

is simply the flux density of neutrinos, which are produced in S in reactions $I_s \to F_s' \ell_\alpha^+ \nu$, in $\mathcal{D}$[39]. Quantity $d\sigma_{\nu\mathcal{D}}$ is defined so that

$$\frac{1}{V_{\mathcal{D}}} \int d\mathbf{y} d\sigma_{\nu\mathcal{D}} = \sum_{\text{spins}\in D} \int \frac{d\mathbf{y} d\mathfrak{P}_d}{2E_\nu} \tag{309}$$

is the differential transverse cross section of neutrino scattering off detector $\mathcal{D}$ as a whole. In the special (and practically important) case of neutrino scattering in reaction $\nu a \to F_d' \ell_\beta^-$ with a sufficiently narrow momentum distribution of target particles a, differential form $d\sigma_{\nu\mathcal{D}}$ becomes the elementary differential transverse cross section of this reaction multiplied by the number of particles of type a in the detector.

Let us finally turn to subintegral factor

$$\mathcal{P}_{\alpha\beta}(E_\nu, L) = \sum_{ij} V_{\alpha i} V_{\beta j} V_{\alpha j}^* V_{\beta i}^* S_{ij} \exp\left(i\varphi_{ij} - \mathcal{A}_{ij}^2 - \Theta_{ij}\right), \tag{310}$$

where

$$\Theta_{ij} = \Theta_i + \Theta_j, \tag{311}$$

$$\Theta_j = \frac{m_j^2}{2\mathfrak{D}^2}\left[(\mathfrak{n}_0 - \mathfrak{n}) + \frac{1}{2}(\mathfrak{m} - \mathfrak{n} - \mathfrak{n}^2) r_j + \left(\mathfrak{n} + \frac{1}{2}\right)(\mathfrak{m} - \mathfrak{n} - \mathfrak{n}^2) r_j^2 + \mathbb{O}(r_j^3)\right]. \tag{312}$$

Let us recall that function $\mathfrak{n}_0$ is the same as $\mathfrak{n}$ in the case of the exact energy-momentum conservation at the diagram vertices in Fig. 15. Therefore, sign-variable difference $\mathfrak{n}_0 - \mathfrak{n}$ in (312) may be neglected in the neighborhood of the maximum of product $\tilde{\delta}_s(p_\nu - q_s)\tilde{\delta}_d(p_\nu + q_d)$ (i.e., at $q_s \approx -q_d \approx p_\nu$), which produces the greatest contribution to the count rate. In view of the properties of function $\mathfrak{n}$, contributions of the order of $\mathbb{O}(r_j^2)$ or higher can also be neglected in (312). As was demonstrated, $\Theta_j > 0$ in this approximation. At $S_{ij} = 1$, $\Theta_{ij} = 0$, and $\mathcal{A}_{ij} = 0$, factor (310) matches the well-known quantum-mechanical

[39] In more correct terms, integral (308) is the number of neutrinos produced in unit time within volume $d\mathbf{x}$, which is centered at point $\mathbf{x} \in \mathcal{S}$, propagating within solid angle $d\Omega_\nu$ in direction $\mathbf{l} = (\mathbf{y}-\mathbf{x})/|\mathbf{y}-\mathbf{x}|$ and crossing a unit area that is centered at point $\mathbf{y} \in \mathcal{D}$ and perpendicular to $\mathbf{l}$.

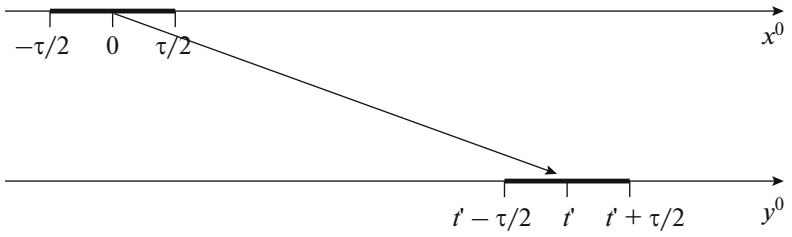

Fig. 17. Simplified (symmetrized) layout of a nonsynchronized measurement. The time "windows" of neutrino emission and absorption are highlighted. It is assumed that $t' = L + t$ and $|t| \gg \tau$.

expression for the probability of neutrino flavor transitions:

$$\mathcal{P}^{(\mathrm{QM})}_{\alpha\beta}(E_\nu, L) = \sum_{ij} V_{\alpha i} V_{\beta j} V^*_{\alpha j} V^*_{\beta i} \exp(i\varphi_{ij}). \qquad (313)$$

It is thus natural to regard (310) as a generalization of the quantum-mechanical result.

It will be demonstrated in Section 11.3 that $|S_{ij}| < 1$. Therefore, all quantum-field corrections (with the approximations used) reduce the value of (310) compared to its quantum-mechanical version (313). In addition to this quantitative difference, one should bear in mind that the probabilistic interpretation of $\mathcal{P}_{\alpha\beta}$ becomes technically impossible, since functions $\mathfrak{D}$, $\mathfrak{n}$, and $\mathfrak{m}$ involved in it (the last two functions are contained in factors S_{ij} and phases Θ_{ij}) depend on the momenta of external packets $\varkappa$ and the neutrino energy; notably, momenta $\mathbf{p}_\varkappa$ with $\varkappa \in I_s \oplus I_d \oplus F_s$ and E_ν are integration variables. The phase space of processes (231) and the behavior of functions $\mathfrak{D}$, $\mathfrak{n}$, and $\mathfrak{m}$ within these volumes do indeed differ for different pairs of leptons $(\ell_\alpha, \ell_\beta)$. This is attributable both to the reaction kinematics in $\mathcal{S}$ and $\mathcal{D}$ (in particular, the reaction thresholds) and to the uncertainties of momenta of lepton packets σ_e, σ_μ, and σ_τ, which may differ even by orders of magnitude. Thus, quantity $\mathcal{P}_{\alpha\beta}$ does not satisfy the expected "standard" relations like Eq. (19), which are simply the corollary of the unitary property of mixing matrix $\mathbf{V} = \|V_{\alpha i}\|$ in the quantum-mechanical theory of neutrino oscillations.

In real experiments, this scenario is complicated further by the fact that the count rate of neutrino events (in the special case considered here, events with the production of a ℓ_β lepton) is not determined by reactions of just a single type; instead, it is affected by a large number of processes of different types such as (in experiments with atmospheric and accelerator neutrinos) decays of mesons ($\pi_{\mu 2}$, $K_{\mu 2}$, $K_{\mu 3}$, K_{e3}, etc.) and muons in the source (atmosphere or decay channel of the accelerator) and various neutrino interactions in the detector ranging from (quasi) elastic to deep-inelastic ones. The phase space and functions $\mathfrak{D}$ and $\mathfrak{n}$ for different combination of such subprocesses in $\mathcal{S}$ and $\mathcal{D}$ differ considerably. It helps comprehend this better if one imagines functions $\mathfrak{D}$, $\mathfrak{n}$, and $\mathfrak{m}$ and all quantities depending on these functions as having indices α and β attached to them.

Another technical and rather nontrivial obstruction to interpreting formula (310) and analyzing experimental data stems from the dependence of factors S_{ij}, which are called the decoherence factors below, on instrumental parameters $x^0_{1,2}$ and $y^0_{1,2}$. Formula (303) was derived with no assumptions regarding the synchronization of time intervals (x^0_1, x^0_2) and (y^0_1, y^0_2). It is then hardly surprising that the decoherence factors may be arbitrarily small in magnitude if these intervals are not matched to allow for the obvious fact that the characteristic time of arrival of ultrarelativistic neutrinos from $\mathcal{S}$ to $\mathcal{D}$ is approximately equal to mean distance $\bar{L}$ between $\mathcal{S}$ and $\mathcal{D}$. The example of a nonsynchronized measurement is presented in Fig. 17, where $t' = L + t$ and $|t| \gg \tau$ is assumed (for simplicity, it is also assumed that $\tau_s = \tau_d$). The QFT causality principle and common sense suggest that factor S_{ij} should tend to zero under such conditions. The general formula for S_{ij} substantiates these expectations and allows one to determine the law of suppression of the count rate. We will not dwell on this issue, since synchronized measurements are our main concern.

Prior to discussing the role of decoherence factors, we introduce another (final) simplifying modification to the formula for the number of events. This simplification is again based on the assumption that the characteristic sizes of $\mathcal{S}$ and $\mathcal{D}$ (at the very least, their characteristic linear sizes along the neutrino beam) are sufficiently small compared to $\bar{L}$. Note that this condition is not satisfied for several short-baseline accelerator and reactor experiments; the analysis for such experiments is much more complicated[40]. If the simplification is applicable, one may substitute $|\mathbf{y} - \mathbf{x}|$ by

[40] Naturally, this complication should not be regarded as a drawback of our formalism, since quantum-mechanical formulas are simply inapplicable in this case.

$\bar{L}$ and differential forms $d\Phi_\nu$ and $d\sigma_{\nu\mathcal{D}}$ by their averaged (over $\mathcal{S}$ and $\mathcal{D}$, respectively) values $d\bar{\Phi}_\nu$ and $d\bar{\sigma}_{\nu\mathcal{D}}$ in (307b). The result is

$$dN_{\alpha\beta} = \tau_d \int d\bar{\Phi}_\nu \int d\bar{\sigma}_{\nu\mathcal{D}} \mathcal{P}_{\alpha\beta}(E_\nu, \bar{L}). \quad (314)$$

Evidently, the domain of applicability of approximation (314) is much narrower than that of (307). This is attributable to the additional constraints on distribution functions $\bar{f}_a$ and on the absolute sizes and geometry of $\mathcal{S}$ and $\mathcal{D}$, which were used implicitly in the transition from (307) to (314). The following is obtained in the "nonspreading" regime of a neutrino WP:

$$\mathcal{P}_{\alpha\beta}(E_\nu, L) = \sum_{ij} V_{\alpha i} V_{\beta j} V^*_{\alpha j} V^*_{\beta i} S_{ij} \exp\left(i\varphi_{ij} - \mathcal{A}^2_{ij}\right). \quad (315)$$

Let us discuss the function involved in (315). Function $\mathcal{A}_{ij}$ governs the suppression of interference at distances exceeding the coherence length in the regime with a negligible contribution of the effect of spatial dispersion of a WP:

$$\mathcal{A}_{ij} = \frac{(v_j - v_i)\mathfrak{D} L}{\sqrt{2}} = \frac{\sqrt{2}\pi \mathfrak{D} L}{E_\nu L_{ij}} = \frac{L}{L^{\mathrm{coh}}_{ij}}, \quad (316)$$

where

$$L^{\mathrm{coh}}_{ij} = \frac{E_\nu L^{\mathrm{osc}}_{ij}}{\sqrt{2}\pi \mathfrak{D}} \quad (317)$$

is the quantum-field generalization of the quantum-mechanical coherence length in (73b). This quantity matches (73b) if one performs the $\sigma_p \to \mathfrak{D}$ substitution. Dimensionless factor S_{ij}, which is new compared to the quantum-mechanical approach, covers the finite intervals of integration over the operating times of the source and the detector and the probable lack of synchronization between the times of emission and detection of neutrinos. Let us examine this factor, which will be called the decoherence function, in more detail.

11. DECOHERENCE FUNCTION

The decoherence factors and the method for their measurement in neutrino experiments are discussed in this section. Some complementary results are presented in Appendix F. The above analysis of interactions in the source and the detector was rather generic. In particular, it was not assumed that the time intervals of emission and detection of neutrinos are synchronized in some way. It is easy to demonstrate that factors S_{ij} may be arbitrarily small if the effective times of emission and detection of neutrinos X^0_s and X^0_d are not synchronized (an exact condition will be formulated below). This important factor alone explains why the "oscillation probability" is written in quotes. Evidently, quantities $\mathcal{P}_{\alpha\beta}$ are not the probabilities of flavor transitions, since they do not satisfy unitarity relations (19). The reason for this is that factors S_{ij} and $\mathcal{A}_{ij}$ depend on the momenta, masses, and dispersions of external WPs; i.e., they depend (formally) on indices α and β. The unitarity relations are satisfied approximately only if these dependences are rather weak or if the decoherence factors themselves are insignificant ($S_{ij} \approx \delta_{ij}$, $\mathcal{A}_{ij} \ll 1$). This effect is a direct and rather nontrivial corollary of the quantum-field approach. It will be demonstrated below that diagonal functions S_{ii} are independent of neutrino masses and, consequently, of index i. Universal function $S_0 = S_{ii}$ describes the suppression of the event number in the case of nonsynchronized processes of emission and detection of neutrinos and when the detector exposure time is either much longer than the source operation time or much shorter than the space-time "width" of the effective neutrino WP. Since these effects are not related to the interference of neutrino states, it seems reasonable to redefine the oscillation probability of neutrinos by isolating factor S_0:

$$\mathcal{P}_{\alpha\beta}(E_\nu, L) = S_0 P_{\alpha\beta}(E_\nu, L),$$

where

$$P_{\alpha\beta}(E_\nu, L) = \frac{1}{S_0} \sum_{ij} V_{\alpha i} V_{\beta j} V^*_{\alpha j} V^*_{\beta i} S_{ij} \exp\left(i\varphi_{ij} - \mathcal{A}^2_{ij}\right). \quad (318)$$

However, this redefinition is immaterial and a matter of taste, since relations (19) are also not fulfilled for quantities $P_{\alpha\beta}(E_\nu, L)$ in the general case.

In the next subsection, we assume that the times of emission and detection of neutrinos are synchronized and examine novel effects related to the finiteness of intervals of neutrino emission and detection.

11.1. Synchronized Measurements

Note that general suppression factor

$$\exp\left\{-2\left[\frac{\mathfrak{D}^2_j}{v^2_i}(L - v_i T)^2 + \frac{\mathfrak{D}^2_j}{v^2_j}(L - v_j T)^2\right]\right\}$$

in the integrand in (302) is minimized at $T = L/v_{ij}$. Therefore, time L/v_{ij} may be interpreted as the effective (or the most probable) delay time between the production and absorption of virtual neutrinos ν_i and ν_j. Since

$$v_{ij} \approx \frac{v_i + v_j}{2} \approx 1 - \frac{m^2_i + m^2_j}{4E^2_\nu},$$

this delay time is almost equal to L. The count rate is thus expected to be maximized if the "on" periods of the source and the detector are shifted so that time windows $[x^0_1, x^0_2]$ and $[y^0_1 - L, y^0_2 - L]$ overlap. The

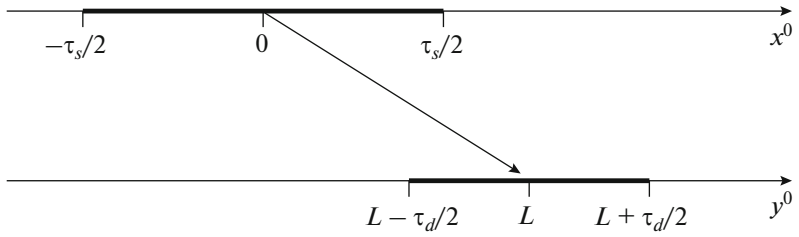

Fig. 18. Simplified (symmetrized) layout of a synchronized measurement. The time "windows" of neutrino emission and absorption are highlighted.

dependence of the count rate on time intervals $x_l^0 - y_{l'}^0$ involved in function Ierf(...) in (303) may be studied for such synchronized measurements. In order to reduce the number of independent variables in the decoherence factors, we set (without any significant loss of generality) a certain "timing" symmetry:

$$x_1^0 = -\frac{\tau_s}{2},\quad x_2^0 = \frac{\tau_s}{2},\quad y_1^0 = L - \frac{\tau_d}{2},\quad y_2^0 = L + \frac{\tau_d}{2},$$

where, naturally, $\tau_{s,d} > 0$. This timing diagram is shown schematically in Fig. 18.

Since $\mathrm{Ierf}(z)$ is an even function, decoherence factors (303) may be written as

$$\begin{aligned} S_{ij} = \frac{\exp\left(-\mathcal{B}_{ij}^2\right)}{4\tau_d\mathfrak{D}}\{&\mathrm{Ierf}\left[\mathfrak{D}\left(\tau_s + \tau_d + \varrho_{ij}L\right) - i\mathcal{B}_{ij}\right] \\ &+ \mathrm{Ierf}\left[\mathfrak{D}\left(\tau_s + \tau_d - \varrho_{ij}L\right) + i\mathcal{B}_{ij}\right] \\ &- \mathrm{Ierf}\left[\mathfrak{D}\left(\tau_s - \tau_d + \varrho_{ij}L\right) - i\mathcal{B}_{ij}\right] \\ &- \mathrm{Ierf}\left[\mathfrak{D}\left(\tau_s - \tau_d - \varrho_{ij}L\right) + i\mathcal{B}_{ij}\right]\}, \end{aligned} \tag{319}$$

where

$$\varrho_{ij} = 2(r_i + r_j) = \frac{m_i^2 + m_j^2}{E_\nu^2}.$$

In the majority of current neutrino experiments (astrophysical ones included), terms $\varrho_{ij}L$ in the arguments of functions Ierf[...] involved in (319) can be neglected. Indeed, using the current (model-dependent[41]) cosmological constraint [132] $\sum_i m_i \lesssim 0.12$ eV, we obtain the following estimate:

$$\varrho_{ij}L \lesssim 5\times10^{-22}\left(\frac{1\ \mathrm{GeV}}{E_\nu}\right)^2\left(\frac{L}{10^4\ \mathrm{km}}\right)\mathrm{s}.$$

On terrestrial scales, this value is exceptionally small compared to the duration of even the shortest neutrino pulses in accelerator experiments. In addition, $\varrho_{ij}L$ terms for sufficiently high neutrino energies remain negligible even at distances exceeding the size of the Galaxy. For example, the value of $\varrho_{ij}L$ for the (anti)neutrino signal from the SN1987A supernova explosion in the Large Magellanic Cloud ($\langle E_\nu\rangle \simeq 20$ MeV, $L \simeq 51.4$ kpc) is no larger than $\sim 2\times10^{-4}$ s. This estimate should be compared to the typical duration of a neutrino burst in a supernova explosion, which is ≈10 s. Let us bring forward one more argument as to why the $\varrho_{ij}L$ terms should be neglected. The formal sufficient condition for this is written as

$$|\tau_s - \tau_d| \gg \varrho_{ij}L.$$

This inequality should be fulfilled within our idealized model if for no other reason than because time intervals τ_s and τ_d cannot be set with a resolution better than the "on/off" times of the source and the detector, which are neglected. Thus, with these reservations[42], decoherence factors (319) are expressed in terms of universal (independent of indices i, j) real-valued function $S(t,t',b)$ of three dimensionless real variables:

$$\begin{aligned} S_{ij} &= S(\mathfrak{D}\tau_s, \mathfrak{D}\tau_d, \mathcal{B}_{ij}), \\ S(t,t',b) &= \frac{e^{-b^2}}{2t'} \\ &\times \mathrm{Re}\left[\mathrm{Ierf}\left(t + t' + ib\right) - \mathrm{Ierf}\left(t - t' + ib\right)\right]. \end{aligned} \tag{320}$$

Let us examine the properties of function $S(t,t',b)$ relevant to its experimental measurement.

11.2. Diagonal Decoherence Function

The mean event count rate of the detector, $dN_{\alpha\beta}/\tau_d$, is proportional to function $S_0(\mathfrak{D}\tau_s, \mathfrak{D}\tau_d)$ of two dimensionless variables, which is defined as

$$\begin{aligned} S_0(t,t') &= S(t,t',0) \\ &= \frac{1}{2t'}\left[\mathrm{Ierf}\left(t + t'\right) - \mathrm{Ierf}\left(t - t'\right)\right]. \end{aligned} \tag{321}$$

[41] The available estimates of the upper bound of $\sum_i m_i$, which were obtained by analyzing cosmological data within the $\Lambda\mathrm{CDM} + \sum m_\nu$ model and its extensions, span (roughly) the interval from 0.07 to 0.30 eV.

[42] Note that all these reservations bear no relation to the applicability domain of our formalism; they just outline the region of applicability of the simplified model used for qualitative analysis of the simplest corollaries of the theory. Models that are more realistic simply require calculations that are more tedious.

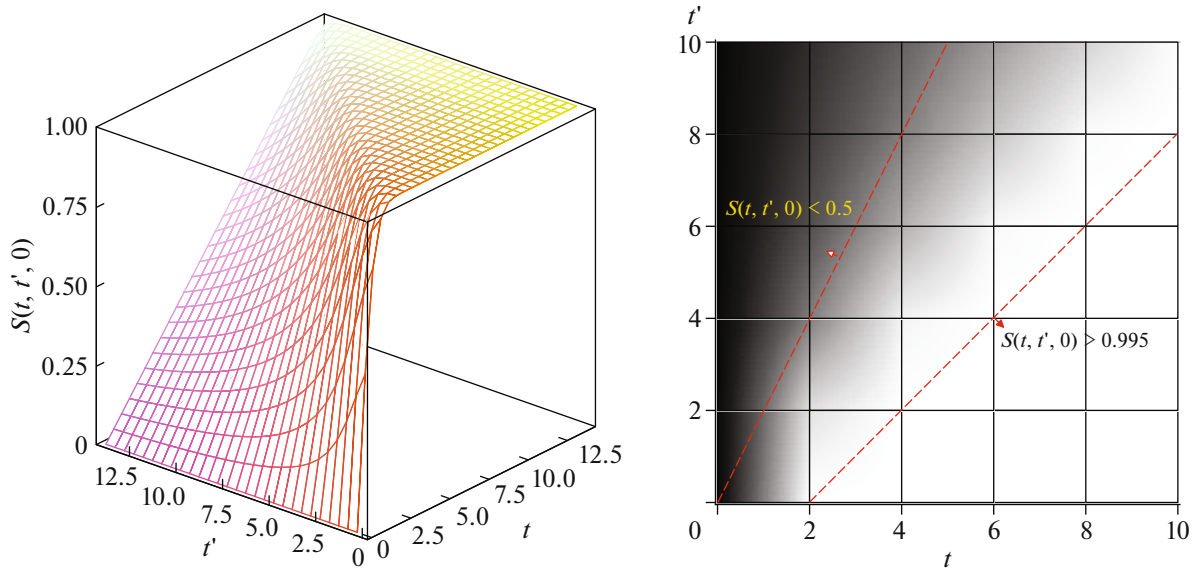

Fig. 19. Decoherence function $S_0(t,t') = S(t,t',0)$ (left) and its distribution density in plane (t,t') (right). Dark and light regions in the right panel correspond to smaller and larger values of $S_0(t,t')$, respectively.

It is easy to demonstrate that this function, which corresponds to noninterference (independent of the neutrino mass) decoherence factors S_{ii}, varies in the interval from 0 to 1. Since

$$2t'\frac{\partial S_0(t,t')}{\partial t} = \mathrm{erf}\,(t+t') - \mathrm{erf}\,(t-t') > 0 \quad (t,t' > 0),$$

$S_0(t,t')$ is a steadily increasing function of t. It follows from (388a) (see Appendix G) that $S_0(t,t') \to 0$ at $t \to 0$ for any $t' > 0$; thus, $S_0(t,t') > 0$ at $t,t' > 0$. It can be seen from asymptotic formula (389) that $S_0(t,t') \to 1$ at $t \to \infty$ and $0 < t' < \infty$. This proves that

$$0 < S_0(t,t') < 1,$$

for all positive values of t and t'.

Formulas (388) and (389) define the asymptotic behavior of $S_0(t,t')$ in different regimes. In particular, at small t and t',

$$S_0(t,t') \approx \frac{2}{\sqrt{\pi}} \times t\left[1 - \frac{1}{3}\left(t^2 + t'^2\right) + \frac{1}{30}\left(t^2 + 3t'^2\right)\left(t'^2 + 3t^2\right)\right].$$

If t is large but finite (i.e., $t - t' \gg 1$), we obtain

$$S_0(t,t') \approx 1 - \frac{1}{4\sqrt{\pi}t'}\left[\frac{e^{-(t-t')^2}}{(t-t')^2} - \frac{e^{-(t+t')^2}}{(t+t')^2}\right] \approx 1$$

and in particular

$$S_0(t,t') \approx 1 - e^{-t^2}\big/(\sqrt{\pi}t) \to 1,$$

if $t' \ll 1$. In the contrary limiting case, $t' - t \gg 1$, we have

$$S_0(t,t') \approx \frac{t}{t'}\left\{1 - \frac{1}{4\sqrt{\pi}t}\left[\frac{e^{-(t'-t)^2}}{(t'-t)^2} - \frac{e^{-(t'+t)^2}}{(t'+t)^2}\right]\right\} \ll 1.$$

Figure 19 presents the behavior of function $S_0(t,t')$ and its distribution density in the (t,t') plane. The validity of the following important inequalities is easy to prove:

$$S_0(t,t') < t/t' \quad \text{for} \quad t' \geq t$$
$$\text{and} \quad S_0(t+\delta t,t) > \mathrm{erf}(\delta t) \quad \text{for} \quad \delta t > 0. \qquad (322)$$

They help isolate the regions of weak and strong suppression of the total number of events due to the decoherence effects[43]. The right panel of Fig. 19, which presents the two-dimensional $S_0(t,t')$ distribution density (the darker the shade, the smaller the value of function $S_0(t,t')$), illustrates these inequalities. The regions of transition between the abovementioned asymptotic regimes are seen clearly.

It follows from Fig. 19 that mean event count rate $dN_{\alpha\beta}/\tau_d$ of the detector decreases as the $\tau_d/\tau_s > 1$ ratio increases (note that this is not true for the total number of events). The reason for this is clear: the

[43] For example, the suppression does not exceed 10^{-4} ($S_0(t,t') > 0.999$) if $t > t' + 2.3273$ (i.e., $\tau_s > \tau_d + 2.3273/\mathfrak{D}$).

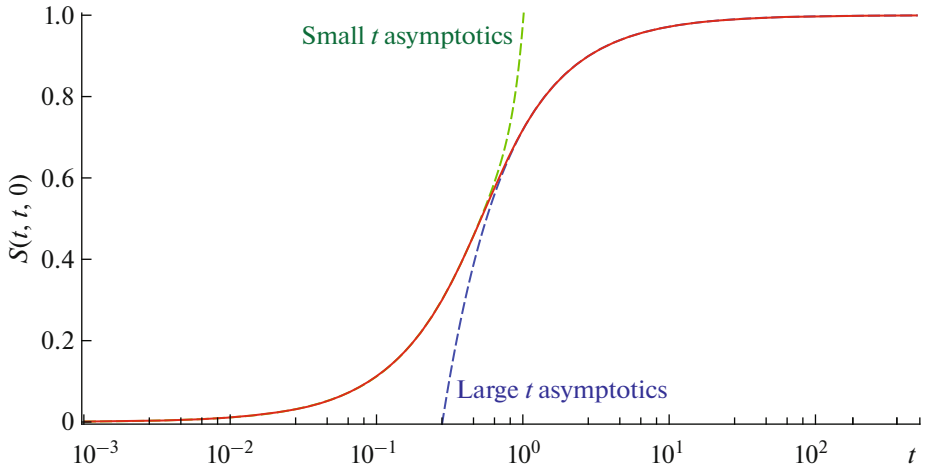

Fig. 20. Function $S_0(t,t)$ (solid curve) and its asymptotics at large and small values of t (dashed curves) plotted in accordance with (323).

number of detected neutrinos cannot exceed the number of particles emitted by the source. The second inequality in (322) has a less evident corollary: $dN_{\alpha\beta}/\tau_d$ is not suppressed at sufficiently large τ_s/τ_d ratios[44]. Two dashed lines in the right panel of Fig. 19 separate the regions in which $S_0 < 0.5$ ($\tau_s < 2\tau_d$) and $S_0 > 0.995$ ($\tau_s > \tau_d + 2/\mathfrak{D}$). Thus, the condition necessary (although still not sufficient) to set $S_0(t,t') = 1$ is that detector exposure time τ_d is either short compared to τ_s or (at $\tau_d \approx \tau_s$) much longer than effective time scale $\tau_v = 1/\min(\mathfrak{D})$ determined in those regions of the phase space of reactions in $\mathcal{S}$ and $\mathcal{D}$ that produce a significant contribution to the count rate. In the intermediate region, the decoherence factor induces moderate suppression of noninterference terms in the integrand for the count rate.

The following is obtained at $t' = t$, which is a special case of particular interest for experiments with accelerator neutrinos:

$$S_0(t,t) = \mathrm{erf}(2t) - \frac{1-e^{-4t^2}}{2\sqrt{\pi}t} \approx \begin{cases} \dfrac{2t}{\sqrt{\pi}}\left(1 - \dfrac{2t^2}{3} + \dfrac{8t^4}{15}\right) & \text{for} \quad t \ll 1, \\ 1 - \dfrac{1}{2\sqrt{\pi}t} & \text{for} \quad t \gg 1. \end{cases} \qquad (323)$$

Figure 20 shows function $S_0(t,t)$. Asymptotics (323) at small and large values of t are also shown for comparison. It can be seen that these asymptotics are well defined everywhere except a relatively narrow region of $0.5 \lesssim t \lesssim 0.8$. It is also evident that $S_0(t,t)$ approaches unity only at $t \gg 1$ (in practice, at $t \gtrsim 100$).

11.3. Nondiagonal Decoherence Function

The behavior of function $S(t,t',b)$ at $b \neq 0$ is much more complex than that at $b = 0$. It is hard and pointless to perform a full analytical examination of this function of three independent variables, since it is impossible to avoid Monte Caro modeling in processing the data from a real experiment with its specific features. We have performed a thorough numerical analysis and analytical examination of the most important special cases and found that $S(t,t',b) < S_0(t,t')$ at $b \neq 0$. Let us consider several typical examples clarifying this result.

Figures 21 and 22 present the profiles of function $S(t,t',b)$ calculated for 18 values of parameter b. Numerical calculations were carried out with the use of formulas from Appendix G. It can be seen that the behavior of $S(t,t',b)$ as a function of t and t' becomes more and more involved as b increases. For example, at $b > 3$–4, function $S(t,t',b)$ oscillates rapidly near zero even under relatively small variations of variables t and t'. This results in strong suppression of nondiagonal (with $i \neq j$) contributions to $\mathcal{P}_{\alpha\beta}(E_\nu, \bar{L})$.

Figure 23 presents $S(t,t,b)$ as a function of b at fixed values of t. At small t, this dependence has a quasi-periodic nature, which is manifested against the background of rapid decay of $S(t,t,b)$ with increasing b. Function $S(t,t',b)$ depends strongly on the ratio of parameters t and t'. At very large values of $t = t'$, $S(t,t',b)$ ceases to depend on t and approaches very

[44] This condition is definitely satisfied in experiments with solar, atmospheric, and geophysical (anti) neutrinos, but may be violated in accelerator experiments.

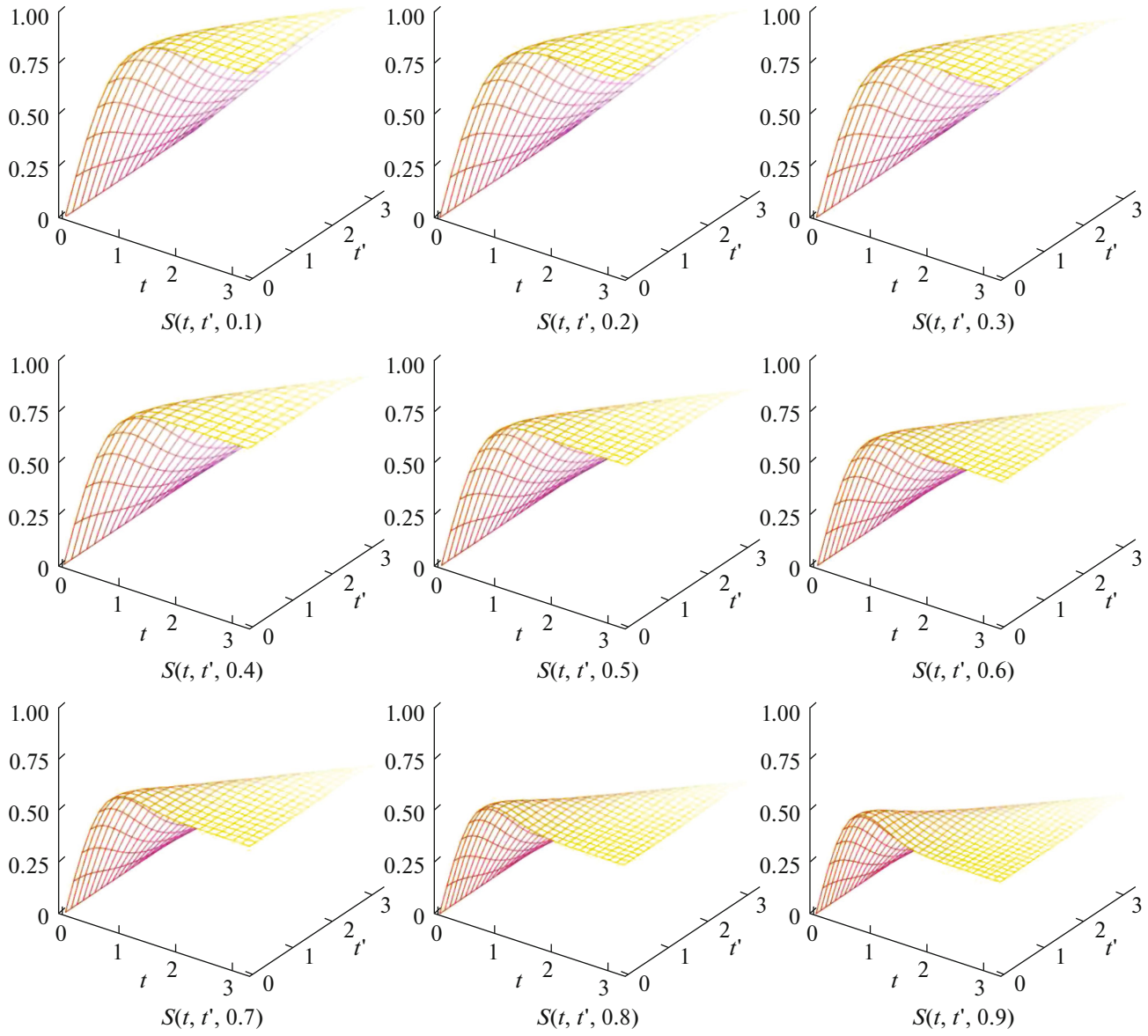

Fig. 21. Profiles of decoherence function $S(t,t',b)$ calculated for nine different values of parameter b varying from 0.1 to 0.9.

slowly its asymptotic form $\exp(-b^2)$. Probability (310) in this asymptotic regime takes the following form known from literature (see, e.g., [45, 46, 66] and references therein):

$$\mathcal{P}_{\alpha\beta}(E_\nu, L) = \sum_{ij} V_{\alpha i} V_{\beta j} V_{\alpha j}^* V_{\beta i}^* \times \exp\left(i\varphi_{ij} - \mathcal{A}_{ij}^2 - \mathcal{B}_{ij}^2 - \Theta_{ij}\right), \quad (324)$$

the only difference being that functions $\mathfrak{D}$, $\mathfrak{n}$, and $\mathfrak{m}$ involved in $\mathcal{A}_{ij}$, $\mathcal{B}_{ij}$, and Θ_{ij} depend on the momenta of external packets and the neutrino energy. This dependence alters qualitatively the behavior of oscillation suppression factors if at least some of the external WPs have relativistic mean momenta. Since $\Theta_{ij} \geq 0$, $\mathcal{P}_{\alpha\beta}(E_\nu, L) \leq \mathcal{P}_{\alpha\beta}^{(\mathrm{QM})}(E_\nu, L)$. Let us clarify the physical meaning of the other suppression factors.

Factor $\exp\left(-\mathcal{A}_{ij}^2\right)$ in (324) suppresses the interference of contributions with $i \neq j$ at distances exceeding the coherence length

$$L_{ij}^{\mathrm{coh}} = \frac{1}{\Delta v_{ij}\mathfrak{D}} \gg |L_{ij}|, \quad (\Delta v_{ij} = |v_j - v_i|)$$

at which neutrino WPs ψ_i^* and ψ_j^* are already separated sufficiently in space (due to the difference between their phase velocities) and cease to interfere.

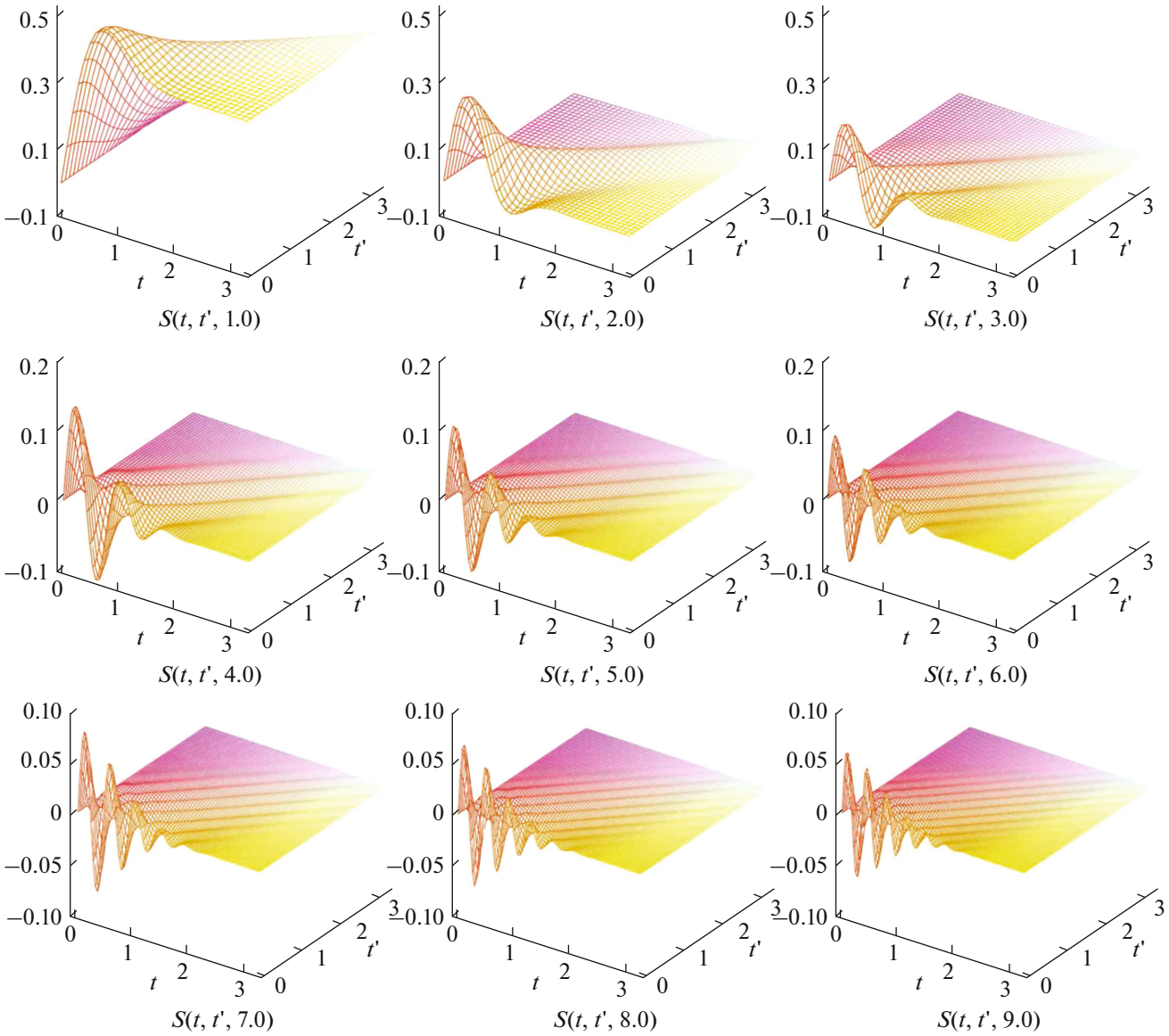

Fig. 22. Profiles of decoherence function $S(t,t',b)$ calculated for nine different values of parameter b varying from 1.0 to 9.0.

Naturally, $L_{ij}^{\mathrm{coh}} \to \infty$ in the plane-wave limit. Factor $\exp\left(-\mathfrak{B}_{ij}^2\right)$ suppresses interference contributions in the contrary case, when external WPs in $\mathcal{S}$ or $\mathcal{D}$ (or in $\mathcal{S}$ and $\mathcal{D}$) are strongly delocalized (or, in the plane-wave limit, smeared over the entire space). The total size of the neutrino production and absorption regions in $\mathcal{S}$ and $\mathcal{D}$ is of the order of $1/\mathfrak{D}$. Interference contributions vanish if this size is large compared to the interference length

$$L_{ij}^{\mathrm{int}} = \frac{1}{4\Delta E_{ij}} = \frac{2L_{ij}}{\pi\mathfrak{n}}.$$

In other words, the quantum-field theory predicts that neutrino oscillations should vanish in the plane-wave limit. The probability of flavor transitions is then independent of L and becomes equal to

$$\sum_i |V_{\alpha i}|^2 |V_{\beta i}|^2.$$

Thus, nontrivial (L-dependent) interference of amplitudes with intermediate neutrinos of different masses is possible only at $\mathfrak{D} \neq 0$. It follows from the detailed analysis of processes $1 \to 2$, $1 \to 3$, and $2 \to 2$ (see Appendix A) that function $\mathfrak{D}$ is nonzero if at least two (in- or out-) WPs $\varkappa$ with $\sigma_\varkappa \neq 0$ interact at both vertices of the diagram in Fig. 15 characterizing process (231). The same conditions necessarily imply that nondiagonal contributions vanish at sufficiently large distances between $\mathcal{S}$ and $\mathcal{D}$ ($L \gg \max L_{ij}^{\mathrm{coh}}$).

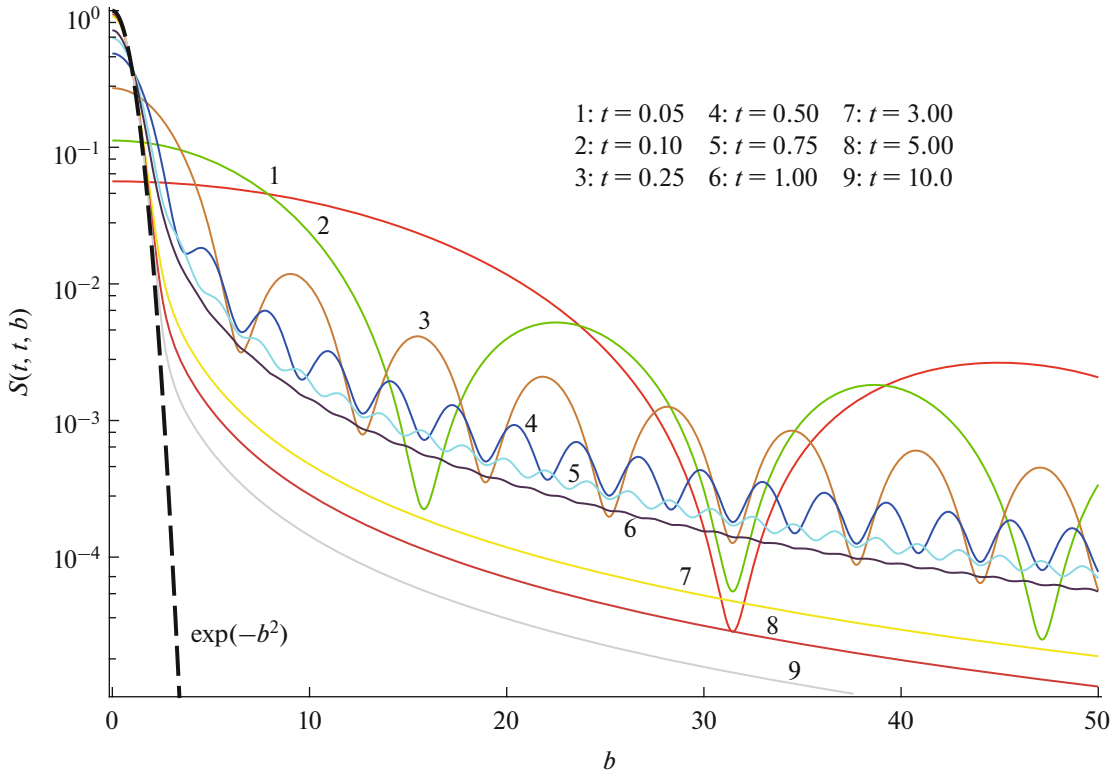

Fig. 23. Dependences of function $S(t,t,b)$ on b at various fixed values of t (see legend). The asymptotics of function $S(t,t,b)$ at $t \to \infty$ is shown by the dashed curve for comparison.

Thus, the domain of applicability of the standard quantum-mechanical formula for the probability of neutrino flavor transitions (adopted by default in all data processing programs of current oscillation experiments) is constrained by rather stringent conditions:

$$\left\langle \left(\frac{2\pi \mathfrak{D} L}{E_\nu L_{ij}} \right)^2 \right\rangle \ll 1, \quad \left\langle \left(\frac{\pi \mathfrak{n}}{2\mathfrak{D} L_{ij}} \right)^2 \right\rangle \ll 1, \quad \left\langle |\Theta_{ij}| \right\rangle \ll 1. \quad (325)$$

Here, angle brackets denote the fact that the values of functions $\mathfrak{D}$, $\mathfrak{n}$, and $\mathfrak{m}$ are defined by the regions of the phase space of process (231) yielding the primary contribution to the measured number of neutrino events.

11.4. Additional Methodological Remarks

It follows from the above analysis that the rather strong dependence of factor $S_0(t,t')$ on its arguments at $t \lesssim t'$ provides an opportunity to estimate function $\mathfrak{D}$ (or, more precisely, its mean values within the above-mentioned regions of the phase space) experimentally by measuring the count rate as a function of variables τ_d and τ_s (at fixed distance $\bar{L}$) and comparing the data obtained with the results of Monte Carlo modeling. It is evident that the optimum strategy of such an experiment should be the subject of a separate study and tailored to each particular experiment. We consider here only the most general technique without going deep into the features of experiments.

The following ratio is a convenient measured quantity for experiments with accelerator neutrino beams emitted in time window τ_s and detected in time τ_d:

$$W(\tau_d) = \frac{\sum_i N\left(y_i^0 \in \tau_d\right)}{\sum_i N\left(y_i^0 \in \tau_d^{\max}\right)}.$$

Here, $N\left(y_i^0 \in \tau_d\right)$ is the number of events detected at time y_i^0 within time window τ_d, and $\tau_d^{\max}$ is the time window expanded to the maximum[45]. Evidently, $W(\tau_d)$ grows linearly with τ_d as it increases from zero (at $\tau_d \lesssim \tau_s$) almost to unity (at $\tau_d \approx \tau_s$). The most intriguing region is the narrow interval near $\tau_d = \tau_s$, where linear growth ends with the $W \approx 1$ plateau at $\Delta\tau_d \geq \tau_d$. This transition is smooth rather than step-

[45] This should be a compromise value in the sense that is needs to exceed τ_s considerably to ensure reliable signal detection but needs not be too large so as to prevent the signal from being lost in the background.

wise, and the measurement of derivative $dW(\tau_d)/d\tau_d$ in this region should allow one to measure $\mathfrak{D}$, since

$$\left.\frac{dW(\tau_d)}{d\tau_d}\right|_{\tau_d=\tau_s} = \frac{1}{2\tau_s}\operatorname{erf}(2\tau_s\mathfrak{D}).$$

Such a measurement is very important, since function $\mathfrak{D}$ is included in the probability of flavor transitions (see below) and needs to be known to extract the parameters of neutrino oscillations (i.e., differences between the squares of masses and mixing angles) accurately. Since function $\mathfrak{D}$ depends on both the neutrino energy and the external momenta, quantity $dW(\tau_d)/d\tau_d$ should be measured at least within several experimentally accessible kinematic intervals.

We should recall that conditions (325) and formula (324) were obtained with the use of a number of simplifying assumptions and approximations. Their validity in real-life experiments is by no means always apparent. It follows from the above analysis (supplemented by the results detailed in Appendix F) that conditions (325) should be used in combination with data on the periods of operation of the source and the detector, their size and geometry, the explicit form of distribution functions of in- particles in the source and the detector, and other technical features in the processing and interpretation of measurements performed in real neutrino experiments.

12. DISCUSSION

12.1. How a Virtual Neutrino Becomes Real

A neutrino is characterized as a virtual particle in the macroscopic diagram corresponding to the production of charged leptons ℓ^+_α and ℓ^-_β in the source and the detector. On the other hand, it is expected intuitively that any virtual particle traveling over a sufficiently large distance should be "similar" to a real particle with a 4-momentum on the mass shell. For example, two approaches to the study of light emitted by a lamp and reaching sensitive cones in our eye are possible. In the first approach, the propagation of a real photon with a 4-momentum on the mass shell is considered. In the second approach, both the emission of light and its detection by the eye are characterized within the QFT formalism by a single macroscopic diagram with two vertices: the source (lamp) and the detector (eye). Naturally, these two descriptions do not contradict each other.

A virtual particle[46] with mass m is described in the configuration space by the causal Green's function [133]

$$D^c(x) = \frac{im}{4\pi^2}\frac{K_1(m\sqrt{-\lambda+i\epsilon})}{\sqrt{-\lambda+i\epsilon}},$$

where $\lambda = x^2 = x_0^2 - \mathbf{x}^2$ and $\sqrt{-\lambda+i\epsilon} = i\sqrt{\lambda}$ at $\lambda > 0$. $K_\nu(x)$ is the Hankel function (Bessel function of the third kind). Function $D^c(x)$ decreases at spatial infinity (in the causally unconnected region) as $|\lambda|^{-3/4}\, e^{-m\sqrt{|\lambda|}}$ and at temporal infinity (in the causally connected region) as $|\lambda|^{-3/4}$. $D^c(x)$ is concentrated near light cone $\lambda = 0$ and has singularities there.

The diagrammatic approach with the source and the detector characterized in the coordinate space by some functions $\psi_s(x - x_s)$ and $\psi_d(x - x_d)$, respectively, yields amplitude

$$\mathfrak{A}(x_d - x_s) \propto \int dxdy\psi_s(x - x_s) \times \psi_d(y - x_d)D^c(y - x),$$

where x_s, x_d are points at which $|\psi_s(x - x_s)|$ and $|\psi_d(x - x_d)|$ are maximized.

Thus, since $D^c(x)$ differs significantly from zero only in the vicinity of the light cone and functions $\psi_s(x - x_s)$ and $\psi_d(x - x_d)$ are concentrated near points x_s, x_d, amplitude $\mathfrak{A}(x_d - x_s)$ at sufficiently large[47] $|\mathbf{x}_d - \mathbf{x}_s|$ corresponds rather accurately to a WP characterizing a particle with mass m moving along classical trajectory $\mathbf{x} = \mathbf{x}_s + \mathbf{v}(t - t_s)$ from point $\mathbf{x}_s$ to point $\mathbf{x}_d$ with an exponentially small deviation from it. Velocity $\mathbf{v} = \mathbf{n}p/E$, where $\mathbf{n} = (\mathbf{x}_d - \mathbf{x}_s)/|(\mathbf{x}_d - \mathbf{x}_s)|$, and the modulus of momentum p is the effective momentum at which integral $\mathfrak{A}(p) \propto \int dk\mathfrak{A}(x)e^{-ikx}$ (corresponding to the amplitude in the momentum representation) is saturated.

Therefore, a virtual particle becomes almost real at macroscopic distances, thus resolving the apparent contradiction.

12.2. Neutrino Wave Function and Process Amplitude

Amplitude $\mathfrak{A}_{\alpha\beta}$ (282) allows for a natural interpretation in terms of the wave function of a virtual neutrino (see Section 8.4). The wave function of state ν_j, which was produced at point X_s in the source, at arbitrary point x is a WP in the SRGP approximation: $\psi^*(\mathbf{p}, x - X_s)/|\mathbf{x} - \mathbf{X}_s|$, where $\psi(\mathbf{p}, x) = e^{-\Omega_j(T,L)}$ and $\Omega_j(T, L)$ is given by (286). The momentum dispersion of neutrino ν_j produced in the source is defined by the 4-momenta and momenta dispersions of all in- and out-packets in the source (see σ_{sj} in (293)). The wave function of state ν_j interacting at point X_d in the

[46] For simplicity, we limit ourselves to scalar particles.

[47] Compared to the spatial dispersions of functions $\psi_{s,d}(x)$.

detector is also a WP $\psi(\mathbf{p}, X_d - x)$ with momentum dispersion σ_{dj} defined by the 4-momenta and dispersions of all in- and out-packets in the detector (293). The projection of state $|\mathbf{p}_j, X_s; \sigma_{sj}\rangle$ in the source onto state $|\mathbf{p}_j, X_d; \sigma_{dj}\rangle$ in the detector defines amplitude $\mathfrak{A}_{\alpha\beta} \propto \langle \mathbf{p}_j, X_d; \sigma_{dj} | \mathbf{p}_j, X_s; \sigma_{sj}\rangle$.

12.3. Ensemble Averaging and Role of Relativistic Covariance

In accordance with intuitive expectations, the interference of diagrams corresponding to external states with well-defined momenta is suppressed. Intermediate neutrinos with different masses m_i correspond in this case to external states with different momenta. In the limit of exactly determined momenta, such states are orthogonal, and, in accordance with the QFT rules, diagrams with different external states need to be summed at the level of squares of moduli of matrix elements. This eliminates their interference. The calculation with WPs corresponding to external states reproduces this rule. To achieve that, one should always sum amplitudes. Interference contributions in the square of the amplitude modulus vanish automatically in the plane-wave limit.

It is possible to determine the probability of neutrino oscillations in the QFT formalism correctly by factorizing expected number $N_{\alpha\beta}$ of events (with the production of charged leptons ℓ^+_α and ℓ^-_β in the source and the detector) into three factors $\Phi_\nu(E_\nu, L) \times \mathcal{P}_{\alpha\beta}(E_\nu, L; \mathfrak{D}) \times \sigma(E_\nu)$. The calculation of the expected number of events is, in turn, possible by the procedure of averaging over the ensemble of initial particles and integrating in coordinates and momenta of final particles. The Lorentz invariance of $N_{\alpha\beta}$ requires covariance of WPs corresponding to external particles. By construction, this requirement is fulfilled in our formalism. In addition, the WP covariance is of fundamental importance in the determination of impact 4-vectors. Nonzero impact 4-vectors of scattering WPs suppress the interaction probability. It would be very hard, if not impossible, to determine the correct form of suppression associated with nonzero impact 4-vectors in a model with a noncovariant WP $\propto e^{-(\mathbf{k}-\mathbf{p})^2/4\sigma_p^2}$, since the object σ_p is transformed in a very complex way under Lorentz transformations.

The Lorentz invariance of the neutrino oscillation probability follows directly from the covariance of the formalism. It is instructive in this context to discuss an apparent paradox related to the interference of neutrino states. Let there be two neutrino states with masses $m_i = 0$ and $m_j = m > 0$. Let us perform a boost to the rest frame of the heavy neutrino. The massless neutrino moves (with the speed of light) in this frame away from the massive neutrino at rest towards the target. Is it possible for these two mass states to be in a coherent superposition and induce neutrino oscillations? The massless neutrino reaches the detector well in advance of the heavy one and, it should seem, may cease to overlap with it, thus damping oscillations. The solution to this paradox is simple: under Lorentz boosts, the WP form is transformed in such a way that two WPs overlapping in a certain reference frame remain overlapping in any other. Thus, oscillations do not vanish in any reference frame, although their "pattern" may change dramatically. The formalism covariance ensures the reconstructibility of this pattern after the transition from one frame to another.

An important detail should be pointed out: since the ultrarelativistic approximation was introduced in calculations, the Lorentz invariance of the resulting formulas is, strictly speaking, an "approximate" one. This is still a fine approximation, since the velocity of even a moderately energetic (anti) neutrino is close to the speed of light:

$$1 - |\mathbf{v}_\mathbf{p}| \approx 0.5 \times 10^{-14} \left(\frac{m}{0.1\ \text{eV}}\right)^2 \left(\frac{1\ \text{MeV}}{E_\mathbf{p}}\right)^2.$$

However, the approximate Lorentz invariance, which holds under Lorentz boosts with gamma factors $\Gamma \ll E_\nu / \max(m_j)$, is certainly violated in the formal transition to the rest frame of a neutrino[48]. At the same time, the formalism itself does not require the ultrarelativistic approximation and may be applied to any process with an arbitrary (even the most exotic) configuration of momenta of external in- and out-packets[49]. The ultrarelativistic approximation (together with other simplifying assumptions) was used just to simplify calculations and for convenience of comparison of the obtained results with other approaches and experimental data.

12.4. Probability of Flavor Transitions

Function $\mathcal{P}_{\alpha\beta}(E_\nu, L; \mathfrak{D})$ is not the probability of neutrino oscillations in the quantum-mechanical sense. It depends on the neutrino energy, the source–detector distance, effective dispersion $\mathfrak{D}$ of a neutrino WP, and the widths of time intervals of operation of the source (τ_s) and the detector (τ_d). In the general case considered here, the neutrino emission and detection times are not necessarily synchronized.

12.4.1. Synchronized and nonsynchronized measurements. In the case of nonsynchronized production

[48] This is why the "proofs" of Lorentz invariance of the standard formula for the oscillation probability, which one may find in literature, are erroneous.

[49] We have prepared some "work pieces" for such potentially interesting problems (and with educational purposes); see Sections 8.2.2 and Appendix D.

and detection processes, $\mathcal{P}_{\alpha\beta}(E_\nu, L; \mathfrak{D})$ is, in accordance with intuitive expectations, suppressed exponentially. This fact alone explains why one should not expect unitarity conditions (19) to be satisfied. In the case of synchronized measurements, formula (315) (or (318)) predicts a number of intriguing phenomena stemming from the hierarchy of time scales τ_s, τ_d, and $\tau_\nu = 1/\min \mathfrak{D}$.

Stationary source. The case of a stationary source, which was discussed in Section 3.8, is obtained in the $\tau_s \to \infty$ limit (or the $\tau_s \gg \tau_d$ approximation). It differs significantly from the quantum-mechanical approach in that functions $\mathfrak{D}$ and $\mathcal{B}_{ij}^2$ depend on the event kinematics and, consequently, on the 4-momenta of ℓ_α^+ and ℓ_β^- (i.e., on indices α, β). Therefore, the unitarity conditions for $\mathcal{P}_{\alpha\beta}(E_\nu, L; \mathfrak{D})$ can be satisfied only if the dependence of functions $\mathfrak{D}$ and $\mathcal{B}_{ij}^2$ on their variables and parameters (i.e., on indices α, β) is weak. With the exception of these important factors, the quantum-field result is similar to the quantum-mechanical one (see (71)). In particular, the vanishing of interference terms at distances exceeding the coherence length is predicted. The exponential loss of coherence is compensated in part by the longitudinal neutrino WP spreading. The spreading effect is also manifested in the power suppression of interference terms.

Function $\mathcal{B}_{ij}^2$ gives rise to the exponential and distance-independent suppression of interference terms in $\mathcal{P}_{\alpha\beta}(E_\nu, L; \mathfrak{D})$. The lower the neutrino energy-momentum dispersion $\mathfrak{D}$, the stronger the suppression. Thus, the probability of flavor transitions becomes distance-independent in the plane-wave limit, $\mathfrak{D} \to 0$, and neutrino oscillations vanish. The formal reason for oscillation suppression is the above-mentioned rule of the squared amplitudes summation corresponding to diagrams with orthogonal external states. The quantum-mechanical experiment with two slits and an electron, which passes through them and reaches a screen inspected by the experimenter, provides a fine physical illustration of this effect. If the experimenter is able to determine the slit through which the electron passed, the interference pattern on the screen vanishes. The $\mathfrak{D} \to 0$ case is thus equivalent to identifying unambiguously the mass of an intermediate neutrino; the interference of diagrams with the exchange of ν_i and ν_j ($m_i \neq m_j$) is then destroyed. Function $\mathcal{B}_{ij}^2$ illustrates why charged leptons do not oscillate. The answer to this question was first provided in [134]; in the present study, we reproduced it by using a different technique.

The loss of neutrino coherence depends on $\mathfrak{D}$ or on relative dispersion $\sigma_{\text{rel}} = \mathfrak{D}/E_\nu$. The available estimates of its value for, e.g., reactor antineutrinos vary within several orders of magnitude. Thus, assuming $\sigma_x \sim 10^{-12}$ cm, which is equal to the size of the uranium nucleus, one obtains an upper bound: $\mathfrak{D} \sim 10$ MeV. Atomic or interatomic distances provide the following estimate: $\sigma_x \simeq (10^{-8}$–$10^{-7})$ cm and $\mathfrak{D} \sim (10^3$–$10^2)$ eV. The broadening of lines at a nonzero ambient temperature results in $\sigma_x \sim 10^{-4}$ cm and $\mathfrak{D} \sim 0.1$ eV. The decoherence in neutrino oscillations may manifest itself in future experiments with a large number of oscillation cycles (e.g., the JUNO reactor experiment [135]). Figure 24 shows the $\bar{\nu}_e$ survival probability for distance $L = 52$ km (the planned experimental baseline) as a function of the antineutrino energy. Calculations were performed in the standard (plane-wave) model of neutrino oscillations and in the model with a neutrino WP for two values of parameter $\sigma_{\text{rel}} = \sigma/p_\nu$, which are not exactly realistic, but are also not excluded by the current experimental constraints. It can be seen that the decoherence effect may play a significant part in the determination of the neutrino mass hierarchy at sufficiently large values of σ_{rel}. Note that the region of allowed σ_{rel} values, $10^{-16} \ll \sigma_{\text{rel}} \ll 10^{-1}$, identified in [135] corresponds to the case when the neutrino WP effects for distances $L \lesssim 52$ km are negligible and the formula for $\mathcal{P}_{\alpha\beta}(E_\nu, L; \mathfrak{D})$ becomes numerically equivalent to the formula for the flavor transition probability in the plane-wave approximation.

Nonstationary source. If condition $\tau_s \leq \tau_d$, which is typical for certain accelerator experiments, is fulfilled, it becomes possible to measure dispersion $\mathfrak{D}$ by comparing the count rate to the one obtained from the formula for $\mathcal{P}_{\alpha\beta}(E_\nu, L; \mathfrak{D})$. A new important factor should also be mentioned here. If τ_s and τ_d are finite, the suppression of interference terms (by factor $e^{-\mathcal{B}_{ij}^2}$) is somewhat weaker than that for a stationary source. The functional dependence of the corresponding suppression factor, which is independent of distance L, but depends on operating time intervals τ_s and τ_d of the source and the detector, was examined in detail in Section 11. Let us discuss the issue of why the $S(t, t, b)$ suppression at finite τ_s and τ_d is below the asymptotic $\exp(-b^2)$ limit, where $b = \mathcal{B}_{ij}$ depends on the neutrino energy dispersion, on a qualitative level. This effect may be interpreted by appealing to a quantum-mechanical analogy: the measurement of the energy-momentum at finite times is equivalent to introducing an additional uncertainty, which makes the neutrino states more coherent.

The proposed theory of flavor transitions conclusively resolves all the paradoxes of naïve plane-wave

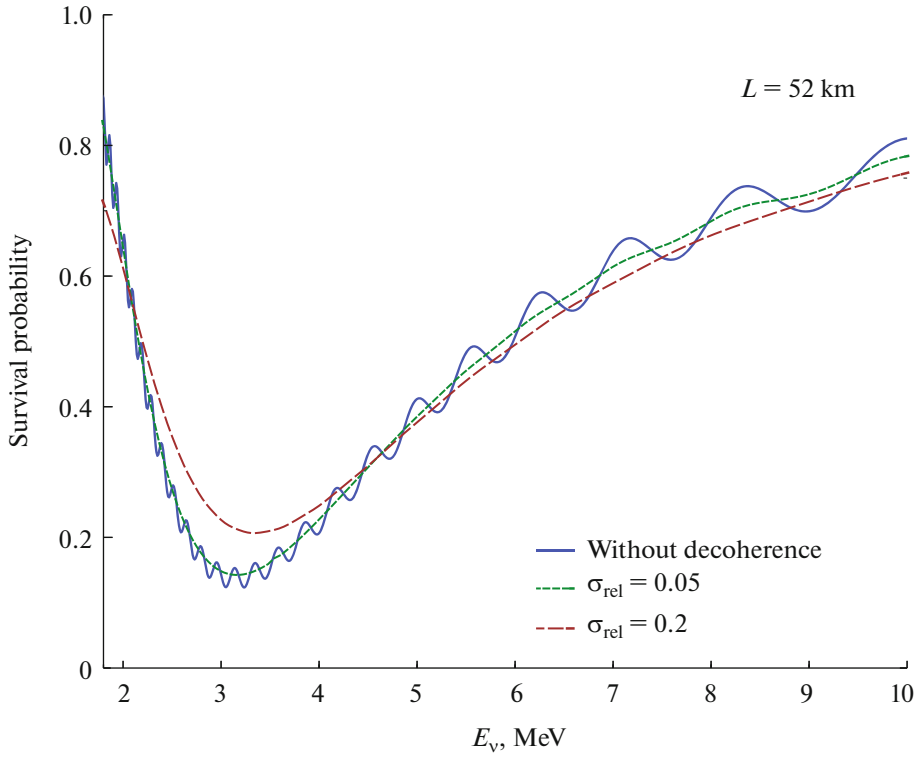

Fig. 24. $\bar{\nu}_e$ survival probability (at $L = 52$ km) as a function of the antineutrino energy in the plane-wave model and the model with a neutrino WP for two values of σ_{rel}.

approximation of the quantum-mechanical theory. In addition, it predicts a number of novel effects, which can be studied in experiments with accelerator, atmospheric, and reactor neutrinos and neutrinos emitted by artificial radioactive sources. The results of the first study of this kind were presented in [88]. The potential influence of decoherence effects on the accuracy of determination of mixing angle θ_{23} in accelerator experiments was examined in [91]. However, the possible loss of coherence is not associated here with the WP nature; instead, it is related to the potential effects of interaction with the environment.

12.5. Wave Packet Observability

Although the model with a WP is undeniably efficient in producing a theoretical description of neutrino oscillations, a reader familiar with classical studies (see, e.g., [98, 117]) on scattering theory can ask a legitimate question: "It is indeed demonstrated in textbooks on scattering theory that a consistent theoretical description of scattering processes cannot be constructed without a WP. However, no information on the WP properties is left in the cross section obtained by averaging the interaction cross section over an ensemble of scattering particles. At the same time, event number $N_{\alpha\beta}$ obtained after averaging over a particle ensemble in the theory of neutrino oscillations with a WP depends explicitly on the dispersions of all WPs via functions $\mathfrak{D}$, $\mathfrak{n}$, etc. Is there a contradiction?" Let us try to answer this interesting question. Let us retrace the key steps of Taylor's calculations [98] using our notation. WP scattering amplitude

$$\mathfrak{A} = \langle\{\mathbf{p}_f, x_f\}|\mathbb{S} - 1|\{\mathbf{p}_i, x_i\}\rangle$$

can be presented as (see Section 6)

$$\mathfrak{A} = \frac{i}{\mathcal{N}}\int d^4x\left[\prod_{i,f}\int\frac{d\mathbf{q}_i\phi(\mathbf{q}_i,\mathbf{p}_i)e^{iq_i(x_i-x)}}{(2\pi)^3 2E_{\mathbf{q}_i}}\right.$$
$$\left.\times\frac{d\mathbf{k}_f\phi^*(\mathbf{k}_f,\mathbf{p}_f)e^{-ik_f(x_f-x)}}{(2\pi)^3 2E_{\mathbf{k}_f}}\right]\mathcal{M}(\{\mathbf{q}_i,\mathbf{k}_f\}),$$

where $\mathcal{N} = \sqrt{\langle\{\mathbf{p}_f, x_f\}|\{\mathbf{p}_f, x_f\}\rangle\langle\{\mathbf{p}_i, x_i\}|\{\mathbf{p}_i, x_i\}\rangle}$ is the state norm, and $\mathcal{M}$ is the matrix element in the plane-wave approximation. The Taylor's calculation [98] (reproduced later by Peskin and Schroeder [117]) assumes that the dependence of matrix element $i\mathcal{M}(\{\mathbf{q}_i,\mathbf{k}_f\})$ of the process on momenta $(\{\mathbf{q}_i,\mathbf{k}_f\})$ is weaker than the momentum dependence of a WP $\phi(\mathbf{q}_i,\mathbf{p}_i)$. The following factorization is possible in this approximation:

$$\mathfrak{A} \simeq \frac{i}{\mathcal{N}}\left(\int d^4x\prod_{i,f}\psi(\mathbf{p}_i, x - x_i)\psi^*(\mathbf{p}_f, x - x_f)\right)$$
$$\times\,\mathcal{M}(\{\mathbf{p}_i,\mathbf{p}_f\}),$$

and macroscopically averaged $\langle|\mathfrak{M}|^2\rangle$ is indeed independent of the WP type [98].

However, the Taylor's approximation is not always valid. Let us list several counterexamples.

(1) The dependence of $i\mathcal{M}(\{\mathbf{p}_i, \mathbf{p}_f\})$ on momenta $(\{\mathbf{q}_i, \mathbf{k}_f\})$ may be strong (e.g., hadronic resonances).

(2) The possibility of measurement of the phase of a matrix element in the linear approximation to the plane-wave cross section is proposed in electron vortex beams (a variation of a WP) [136, 137]. The introduction of quadratic corrections to the Taylor's approximation also allows one to measure the phase of a matrix element [122]. Such measurements are not possible in the plane-wave approximation.

(3) The cross sections of certain processes (e.g., $e^+e^- \to e^+e^-\gamma$) calculated in the plane-wave approximation contradict experimental data [118]. As was noted in Section 6, the measured cross section turned out to be ~30% lower than the calculated one in the region of low photon energies. This is attributable to the fact that impact parameters ρ up to 5 cm produce a significant contribution to this cross section, whereas the transverse size of colliding beams was no larger than $a \simeq 10^{-3}$ cm. If impact parameters are limited to $\rho \le a$, the observed number of photons decreases. The theory with a finite size of colliding beams taken into account was developed in [120].

(4) If the matrix element is a sum of singular matrix elements, e.g.,

$$i\mathcal{M}(\{\mathbf{q}_i, \mathbf{k}_f\}) \sim \sum_k V_{\alpha k} V^*_{\beta k} \mathcal{M}'_d \frac{1}{q^2 - m_k^2} \mathcal{M}'_s,$$

it is not possible to "defactorize" the WP form at a single point in the transfer of 4-momentum q if masses m_k are different. Matrix elements of this type correspond to the interference of diagrams with virtual neutrinos in the quantum-field theory of neutrino oscillations (or, more correctly, flavor transitions). Thus, the analysis of neutrino oscillations in the quantum field theory with a WP is indeed an important exception that is not covered by the Taylor's approximation.

13. CONCLUSIONS

Let us summarize the results.

It has already been noted multiple times (starting from the 1970s) in the literature that the plane-wave quantum-mechanical theory of neutrino oscillations is incomplete and self-contradictory. We have discussed critically the hypotheses and approximations underlying this theory and tried to outline the domain of their applicability using one of the simplest extensions of the plane-wave theory based on the model of a neutrino WP. The general properties of a WP were studied within the noncovariant quantum-mechanical formalism. Several well-known features of a WP such as the quasi-classical nature of its trajectory and the general law of spreading in the configuration space were reproduced. One novel result is the proof that the WP spreading leads to inverse-square law $\sim 1/|\mathbf{x}|^2$ for the probability of finding a state at distance $\mathbf{x}$ from the source in a sufficiently long observation time. The theory of neutrino oscillations was constructed within the model of a noncovariant Gaussian WP. A correct derivation of the formula for the probabilities of flavor transitions via macroscopic averaging of the squared modulus of the transition amplitude was proposed. A general formula for the probabilities depending on oscillation length L_{ij}^{osc}, coherence length L_{ij}^{coh}, dispersion length L_{ij}^{d}, and effective spatial size σ_x of a neutrino WP (see the definitions in (73)) was obtained as a result. This formula predicts the following:

(1) Loss of coherence for a pair of states ν_i and ν_j at distances $L \gg L_{ij}^{\mathrm{coh}}$. The probability of oscillations at very large (astronomical) distances is then reduced to noncoherent sum $P_{\alpha\beta} = \sum_k |V_{\alpha k}|^2 |V_{\beta k}|^2$ that is independent of energy and distance[50].

(2) Noncoherent production (or detection) of neutrinos, which is governed by factor $\exp\left(-\mathcal{B}_{ij}^2\right) = \exp\left[-\Delta m_{kj}^2 / \left(8\sqrt{2} p \sigma_p\right)\right]$ (see (78)). This factor explains why charged leptons do not oscillate.

(3) Corrections to the oscillation phase associated with the neutrino WP dispersion effect.

(4) Partial compensation of the loss of coherence for a pair of states ν_i and ν_j due to packet spreading.

(5) Additional suppression of interference terms by factors of the $1/q_{kj}$ form (see (79)).

A covariant theory of relativistic wave packets, which are constructed as linear superpositions of single-particle Fock states with definite momenta and evolve into these states in the plane-wave limit, was proposed. The properties of such packets were studied. It was demonstrated, e.g., that mean 4-momentum $\langle P\rangle$ of a relativistic packet and its effective volume V are exact integrals of motion. At the same time, $\langle P\rangle^2 = \langle m\rangle^2$, where $\langle m\rangle$ is the effective mass of a WP, which always exceeds the mass of quanta of the corresponding free field. A relativistic packet moves, on the average, along a classical trajectory with velocity $\mathbf{v}_{\mathbf{p}} = \mathbf{p}/E_{\mathbf{p}}$ (where $\mathbf{p}$ and $E_{\mathbf{p}}$ are its most probable 3-momentum and energy, respectively), and quantum fluctuations about this trajectory decay at distances

[50] This result is also reproduced in the quantum-field theory and is the real reason (as opposed to the meaningless "averaging over sources" mentioned in many papers) why astrophysical neutrinos do not oscillate, with an important reservation that the interactions of neutrinos with matter in the astrophysical source are neglected.

that are large compared to the effective size of the packet. The suppression of fluctuations transverse to vector $\mathbf{v_p}$ is weaker than that of longitudinal fluctuations, and ultrarelativistic packets may have only transverse fluctuations (i.e., packets move within classical light cones). Multipacket states characterizing systems of n free identical bosons or fermions were studied. It was demonstrated that the effects of Bose–Einstein attraction and Fermi repulsion are significant only at distances comparable to the effective size of packets and become negligible at larger distances.

A relativistic Gaussian packet characterized by a single phenomenological parameter σ, which defines the scale of quantum 4-momentum fluctuations and the effective packet size, was examined thoroughly as the simplest working model of a "memoryless" relativistic wave packet satisfying all the requirements of the formalism. The regime in which the RGP spreading is negligible (SRGP model) was studied in detail. This regime provides an opportunity to use an RGP in the S-matrix QFT formalism to characterize asymptotically free states of stable and unstable (but relatively long-lived) particles. It was demonstrated that all unstable long-lived particles and atomic nuclei regarded as important decay sources of neutrino and antineutrino beams have fairly wide regions of allowed values of σ satisfying all the constraints of the SRGP model under which a wave packet does not spread within the particle lifetime.

The developed theory was used to describe the scattering of relativistic WPs. The amplitude of an arbitrary process of the form $a + b \to X$ in the S-matrix QFT formalism with WPs was calculated. The general formula for the *rate* of this process was obtained (see (180)):

$$dN = d\sigma L(|\mathbf{b}\times\mathbf{n}|) = d\sigma L(0)e^{-(\mathbf{b}\times\mathbf{n})^2/2\sigma_{x,ab}^2},$$

where $d\sigma$ is the standard plane-wave cross section, and $L(0) = 1/2\pi\sigma_{x,ab}^2$ is the luminosity of scattering of two WPs as defined in the scattering theory and accelerator physics. Factor $e^{-(\mathbf{b}\times\mathbf{n})^2/2\sigma_{x,ab}^2}$ introduces geometric suppression of the interaction probability of two WPs scattered with a nonzero impact parameter $|\mathbf{b}\times\mathbf{n}|$, where $\mathbf{b}$ is the impact vector and $\mathbf{n} = \mathbf{v}_{ab}/|\mathbf{v}_{ab}|$ is a unit vector codirectional with relative velocity $\mathbf{v}_{ab}$. $\sigma_{x,ab}^2 = \sigma_{x,a}^2 + \sigma_{x,b}^2$ is the effective spatial dispersion of the region of overlap of two Gaussian WPs with spatial dispersions $\sigma_{x,a}^2$ and $\sigma_{x,b}^2$ and impact parameter $|\mathbf{b}\times\mathbf{n}|$. This result has been obtained for the first time in [120] with the use of the Wigner function. In the present study, it was reproduced within the covariant WP formalism. Macroscopic averaging of the probability of interaction of colliding packets over the impact parameter yields standard formula $dN = d\sigma L$, where luminosity L is defined by the spatial dispersions of WPs and beams of particles a and b. The Lorentz invariance of impact parameter $|\mathbf{b}\times\mathbf{n}|$ was proven.

The technique of calculation of macroscopic Feynman diagrams with the exchange of massive neutrinos was developed. It is based on the covariant theory of wave packets, where the states of free fields (external legs of macrodiagrams) are constructed as linear superpositions of single-particle Fock states that pass into these states in the plane-wave limit. The overlap integrals of packets, which characterize the spatiotemporal overlap of in- and out-packets in the source and detector, were studied in detail. These integrals account for the key differences between our approach and the standard QFT formalism, which utilizes states with definite momenta smeared over the entire spacetime. It was demonstrated that the overlap integrals are small in absolute value if the classical world tubes of packets are located far away from impact points (4-vectors X_s and X_d, which define the position of effective regions of interaction of packets near the macrodiagram vertices). The conditions under which in- and out-packets may be considered asymptotically free were formulated.

The amplitude of process (231) of the general form with the production of two oppositely charged leptons ℓ_α and ℓ_β at macroscopically separated diagram vertices with an arbitrary number of other particles (all external legs are wave packets) was calculated. It was demonstrated that diagram blocks characterizing the interactions of hadrons may be presented as a product of two hadronic currents that are associated with the source and detector vertices and depend only on the corresponding sets of variables (momenta, spins, and coordinates of external packets). As a result, the amplitude was presented as a sum of products of matrix elements of the subprocesses of production and absorption of a real massless neutrino and factor ψ_j^*/L, which may be interpreted as a spherical wave of a neutrino with mass m_j with amplitude ψ_j^* having the form of a relativistic Gaussian packet with its "dispersion" being a relativistically invariant function of the effective neutrino energy as well as momenta, masses, and momenta dispersions of all external packets. The amplitude includes geometric suppression factors, which are associated with the incomplete overlap of external packets at the diagram vertices, and nonsingular factors, which ensure approximate energy-momentum conservation at these vertices, as common factors.

Since process (231) is, in the general case, lepton number violating, experimental studies of this process are an important source of information on the mixing parameters and the differences between squared neutrino masses. A Lorentz-invariant formula for the probability of process (231) was derived and subjected to statistical averaging, which led to an experimentally measurable quantity, the differential number of events

in the detector ($dN_{\alpha\beta}$). The terms "source" and "detector" are used here to denote mathematical models characterizing the conditions of an actual experiment. With a number of simplifying assumptions introduced, the formula for $dN_{\alpha\beta}$ can be presented as a multidimensional integral of the product of differential forms $d\Phi_\nu$ and $d\sigma_{\nu\mathfrak{D}}$, which characterize the flux (energy spectrum) of massless neutrinos and the differential cross section of their interaction with the detector, and factor $\mathcal{P}_{\alpha\beta}$, which is the generalization of the standard quantum-mechanical expression characterizing flavor transitions $\nu_\alpha \to \nu_\beta$. It was demonstrated that quantum-field function $\mathcal{P}_{\alpha\beta}$ did not have probability features, since it includes, in addition to the standard oscillation factor, decoherence factors that depend on neutrino energy E_ν and momenta $\mathbf{p}_\varkappa$ of external packets (variables of integration over the phase space of process (231)) and on masses $m_\varkappa$ and parameters $\sigma_\varkappa$ (uncertainties of momenta of external packets, including the packets of leptons $\ell_{\alpha,\beta}$).

The value of general decoherence factor S_0, which suppresses the mean event count rate in synchronized measurements, is defined within a simple model for the distribution functions of in-packets in the source and detector by the ratio of source operation time τ_s and detector exposure time τ_d and by space-time width $\tau_\nu \sim 1/\mathfrak{D}$ of the effective neutrino WP, where $\mathfrak{D}$ is a function of E_ν and $\mathbf{p}_\varkappa$. The suppression is weak if $\tau_s \gg \tau_d$ or $\tau_s \sim \tau_d \gg \tau_\nu$. The strong dependence of S_0 on parameters τ_s and τ_d provides an opportunity to measure the averaged value of function $\mathfrak{D}$ by varying these parameters (or one of them) in a specialized accelerator or reactor experiment[51]. Such measurements (even rough ones) would provide useful references for planning and processing the data of future precision experiments at neutrino factories and experiments with β-beams, "ultrabeams," etc. The behavior of nondiagonal decoherence factors S_{ij} $(i \neq j)$ is more complex, which is illustrated by analytical and numerical estimates given above. It was demonstrated that factor S_{ij} ceases to depend on τ_s and τ_d in the $\tau_s \gtrsim \tau_d \gg \tau_\nu$ asymptotic regime and may induce strong suppression of oscillatory contributions to $\mathcal{P}_{\alpha\beta}$. The conditions under which the decoherence effects are weak (and, consequently, the standard quantum-mechanical formula for the probability of flavor transitions is applicable) were formulated. It was shown that the decoherence effects need to be taken into account in current accelerator experiments utilizing short pulsed neutrino beams. These effects are also significant in astrophysical neutrino experiments (due to the spreading of a neutrino wave packet at large distances). The procedure for measurement of decoherence factors in future experiments was discussed.

To conclude, let us formulate the key results of this study.

(1) The covariant WP formalism, which eliminates artificial singular state normalizations typical of the standard S-matrix QFT approach, was developed.

(2) The new model of a relativistic Gaussian WP was proposed. The difficulties in generalizing the formalism with a WP of a more general form are technical rather than fundamental.

(3) The interaction points of in- and out-packets are arbitrary. This leads to a four-dimensional generalization of the impact parameter. A correct definition of points $\mathbf{x}_S$ and $\mathbf{x}_D$, which characterize the neutrino production and absorption, follows automatically from the formalism. These points are not set ad hoc, as is done in all the other approaches that we know of. In contrast, they emerge automatically as effective points contained in the phase of the complex-valued four-dimensional overlap volume of packets with arbitrary initial or final coordinates x_κ and velocities $\mathbf{v}_\kappa$, which define uniquely the classical world tubes of packets. The factors of geometric suppression of the WP interaction probability for noncollinear collisions and the overlap volumes (with nonzero impact parameters factored in) were calculated.

(4) The longitudinal dispersion of the effective neutrino WP is automatically taken into account in the formalism.

(5) A correct method for macroscopic averaging, where arbitrary (finite or infinite, synchronized or nonsynchronized) time intervals of operation of the source and detector are taken into account, was developed and applied. A formula for the number of events corresponding to a macroscopic Feynman diagram of a rather general form was derived. Its generalization to other types of macrodiagrams is fairly evident. An expression generalizing the probability of a flavor transition, $\mathcal{P}_{\alpha\beta}$, with consideration of all the above effects was obtained.

(6) In all physically reasonable limiting cases, the formulas for $\mathcal{P}_{\alpha\beta}$ either agree with the ones verified experimentally or predict novel nontrivial effects.

The following are examples of novel effects:

(1) Dependence of the probabilities of flavor transitions (more exactly, the count rate for events with violation of lepton numbers) on finite time intervals of operation of the source and detector. This is important, e.g., for experiments with accelerator neutrinos.

(2) Exponential suppression of the number of nonsynchronized events.

[51] Only one experiment of this kind, where our model (in its maximally simplified form) was used in the data analysis on vanishing of reactor $\bar{\nu}_e$, has been performed to date [88].

(3) Spreading of the effective neutrino WP at large distances.

(4) Dependence of the neutrino momentum dispersion on the event kinematics in the source and detector. Explicit formulas describing this dependence were derived in the most general case (i.e., for arbitrary reactions in the source and detector) and analyzed in detail for the simplest and the most important processes (two- and three-particle decay, quasi-elastic scattering) in the plane-wave limit.

APPENDIX A

PROPERTIES OF OVERLAP TENSORS

A.1. General Formulas for $\mathfrak{R}^{\mu\nu}_{s,d}$ and $\tilde{\mathfrak{R}}^{\mu\nu}_{s,d}$

Let us examine the general properties of overlap tensors

$$\mathfrak{R}^{\mu\nu}_{s,d} = \sum_{\varkappa} T^{\mu\nu}_{\varkappa} = \sum_{\varkappa} \sigma^2_{\varkappa} \left(u^{\mu}_{\varkappa} u^{\nu}_{\varkappa} - g^{\mu\nu}\right).$$

It is useful in this regard to write matrices $\mathfrak{R}_{s,d} = \left\|\mathfrak{R}^{\mu\nu}_{s,d}\right\|$ in the explicit form:

$$\mathfrak{R}_{s,d} = \sum_{\varkappa} \sigma^2_{\varkappa} \begin{pmatrix} \Gamma^2_{\varkappa} - 1 & -\Gamma_{\varkappa} u_{\varkappa 1} & -\Gamma_{\varkappa} u_{\varkappa -} & -\Gamma_{\varkappa} u_{\varkappa 3} \\ -\Gamma_{\varkappa} u_{x1} & 1 + u^2_{\varkappa 1} & u_{\varkappa 1} u_{\varkappa 2} & u_{\varkappa 1} u_{\varkappa 3} \\ -\Gamma_{\varkappa} u_{x2} & u_{\varkappa 2} u_{\varkappa 1} & 1 + u^2_{\varkappa 2} & u_{\varkappa 2} u_{\varkappa 3} \\ -\Gamma_{\varkappa} u_{x3} & u_{\varkappa 3} u_{\varkappa 1} & u_{\varkappa 3} u_{\varkappa 2} & 1 + u^2_{\varkappa 3} \end{pmatrix}$$

or, equivalently,

$$\mathfrak{R}_{s,d} = \sum_{\varkappa} (\sigma_{\varkappa} \Gamma_{\varkappa})^2 \times \begin{pmatrix} \mathbf{v}^2_{\varkappa} & -v_{\varkappa 1} & -v_{\varkappa 2} & -v_{\varkappa 3} \\ -v_{\varkappa 1} & 1 - v^2_{\varkappa 2} - v^2_{\varkappa 3} & v_{\varkappa 1} v_{\varkappa 2} & v_{\varkappa 1} v_{\varkappa 3} \\ -v_{\varkappa 2} & v_{\varkappa 2} v_{\varkappa 1} & 1 - v^2_{\varkappa 3} - v^2_{\varkappa 1} & v_{\varkappa 2} v_{\varkappa 3} \\ -v_{\varkappa 3} & v_{\varkappa 3} v_{\varkappa 1} & v_{\varkappa 3} v_{\varkappa 2} & 1 - v^2_{\varkappa 1} - v^2_{\varkappa 2} \end{pmatrix}.$$

Here and elsewhere, $u_{\varkappa i}$ and $v_{\varkappa i}$ $(i = 1, 2, 3)$ are the components of vectors $\mathbf{u}_{\varkappa} = \mathbf{p}_{\varkappa}/m_{\varkappa}$ and $\mathbf{v}_{\varkappa}$, respectively ($u_{\varkappa i} = v_{\varkappa i}$). As above, index $\varkappa$ designates packets from all four sets of initial ($I_{s,d}$) and final ($F_{s,d}$) states. It is evident that $|T_{\varkappa}| = |T_{\varkappa}|_{\mathbf{v}_{\varkappa}=0} = 0$, but $|\mathfrak{R}_{s,d}| > 0$. This follows from the positivity of quadratic forms $\mathfrak{R}^{\mu\nu}_{s,d} x_{\mu} x_{\nu}$ under the assumption that $\sigma_{\varkappa} > 0$ for at least two packets $\varkappa$. Note also that $\mathrm{Tr} T_{\varkappa} = T^{\mu}_{\mu} = -3\sigma^2_{\varkappa}$ and, consequently, $\mathrm{Tr}\mathfrak{R}_{s,d} = -3\sum_{\varkappa} \sigma^2_{\varkappa}$. The positivity of all principal minors is another important property of the determinant $|\mathfrak{R}_{s,d}|$. It then follows that the spatial parts of matrices $\mathfrak{R}_{s,d}$ (i.e., matrices $\left\|\mathfrak{R}^{ij}_{s,d}\right\|$ $(i, j = 1, 2, 3)$) are also positively defined; therefore, quadratic forms $\mathfrak{R}^{ij}_{s,d} x_i x_j$ are positive.

In what follows, the following definitions are used:

$$\begin{aligned} \omega_i &= \sum_{\varkappa} \sigma^2_{\varkappa} \left(1 + u^2_{\varkappa i}\right), \quad \omega = \sum_{\varkappa} \sigma^2_{\varkappa} \mathbf{u}^2_{\varkappa}, \\ \upsilon_i &= \sum_{\varkappa} \sigma^2_{\varkappa} \Gamma_{\varkappa} u_{\varkappa i}, \quad w_i = \sum_{\varkappa} \sigma^2_{\varkappa} u_{\varkappa j} u_{\varkappa k}. \end{aligned} \tag{A.1}$$

Here and elsewhere, indices s and d are omitted for simplicity. Spatial indices i, j, k assume the values of 1, 2, 3; it is assumed, unless stated otherwise, that $i \neq j \neq k$, and the (i, j, k) triad in each formula containing all three indices is a cyclic permutation of (1, 2, 3). The determinants of $\mathfrak{R}_s$ and $\mathfrak{R}_d$ may be written in this notational convention as

$$\begin{aligned} |\mathfrak{R}_{s,d}| &= \omega \prod_i \omega_i + 2\omega \prod_i w_i \\ &+ \sum_i \upsilon_i w_i \left(\upsilon_i w_i - \upsilon_j w_j - \upsilon_k w_k\right) \\ &+ \sum_i \left[w_i \omega_i \left(2\upsilon_j \upsilon_k - \omega w_i\right) - \upsilon^2_i \omega_j \omega_k\right]. \end{aligned} \tag{A.2}$$

A.2. Inverse Overlap Tensors $\tilde{\mathfrak{R}}^{\mu\nu}_{s,d}$

The matrices inverse to $\mathfrak{R}_{s,d}$ are defined in terms of algebraic cofactors $\mathfrak{N}^{\mu\nu}_{s,d}$ of the matrix elements of $\mathfrak{R}_{s,d}$:

$$\mathfrak{R}^{-1}_{s,d} = |\mathfrak{R}_{s,d}|^{-1} \left\|\mathfrak{N}^{\mu\nu}_{s,d}\right\|, \tag{A.3}$$

$$\begin{aligned} \mathfrak{N}^{00}_{s,d} &= \prod_i \omega_i - \sum_i w^2_i \omega_i + 2\prod_i w_i, \\ \mathfrak{N}^{0i}_{s,d} &= \upsilon_i \omega_j \omega_k - \upsilon_j w_k \omega_k - \upsilon_k w_j \omega_j \\ &+ w_i \left(\upsilon_j w_j + \upsilon_k w_k - \upsilon_i w_i\right), \\ \mathfrak{N}^{ii}_{s,d} &= \omega\left(\omega_j \omega_k - w^2_i\right) \\ &+ 2w_i \upsilon_j \upsilon_k - \upsilon^2_j \omega_k - \upsilon^2_k \omega_j, \\ \mathfrak{N}^{jk}_{s,d} &= \left(\upsilon_j \upsilon_k - \omega w_i\right) \omega_i \\ &+ \upsilon_i \left(\upsilon_i w_i - \upsilon_j w_j - \upsilon_k w_k\right) + \omega w_j w_k. \end{aligned} \tag{A.4}$$

The matrix elements of $\tilde{\mathfrak{R}}_{s,d}$ are then given by

$$\tilde{\mathfrak{R}}^{\mu\nu}_{s,d} = \left(\mathfrak{R}^{-1}_{s,d}\right)_{\mu\nu} = |\mathfrak{R}_{s,d}|^{-1} \tilde{\mathfrak{N}}^{\mu\nu}_{s,d},$$

where

$$\begin{gathered} \tilde{\mathfrak{N}}^{00}_{s,d} = \mathfrak{N}^{00}_{s,d}, \quad \tilde{\mathfrak{N}}^{0i}_{s,d} = \tilde{\mathfrak{N}}^{i0}_{s,d} = -\mathfrak{N}^{0i}_{s,d}, \\ \tilde{\mathfrak{N}}^{ij}_{s,d} = \tilde{\mathfrak{N}}^{ji}_{s,d} = \mathfrak{N}^{ij}_{s,d}. \end{gathered}$$

Explicit formulas for the components of inverse overlap tensors in terms of the most probable 4-velocities were obtained in [123]:

$$\tilde{\mathfrak{R}}^{\mu\nu}_{s,d} = \frac{1}{|\mathfrak{R}_{s,d}|} \sum_{a,b,c \in \mathcal{P},\mathcal{D}} \sigma^2_a \sigma^2_b \sigma^2_c \mathfrak{I}^{abc\mu\nu}_{s,d}. \tag{A.5}$$

The multiindex expressions (symmetric in Lorentz indices) appearing in (A.5) take the form

$$\mathfrak{I}^{abc00}_{s,d} = \left[\Gamma_a\Gamma_b - \frac{1}{3}(u_au_b)\right](u_bu_c)(u_cu_a) + \frac{1}{2}\Gamma_a^2\left[1-(u_bu_c)^2\right] + \frac{1}{3},$$

$$\mathfrak{I}^{abc0i}_{s,d} = \frac{1}{2}\Gamma_c\left[(u_au_b)^2u_{ci} - u_{ci} - 2(u_au_b)(u_bu_c)u_{ai} + 2(u_au_c)u_{ai}\right] - \Gamma_b(u_au_b)u_{ai},$$

$$\mathfrak{I}^{abcij}_{s,d} = \Gamma_a\Gamma_b\left[(u_cu_a)(u_cu_b) - (u_au_b)\right]\delta_{ij} + \frac{1}{2}\left(\Gamma_c^2-1\right)\times\left[1-(u_au_b)^2\right]\delta_{ij} + \left\{\Gamma_c\left[\Gamma_a(u_bu_c) + \Gamma_b(u_cu_a) - \Gamma_c(u_au_b)\right] - \Gamma_a\Gamma_b + (u_au_b)\right\}u_{ai}u_{bj} + \Gamma_b\left[\Gamma_b - \Gamma_a(u_au_b)\right]u_{ci}u_{cj};$$

$$\left|\mathfrak{R}_{s,d}\right| = \sum_{a,b,c,d\in\mathcal{S},\mathcal{D}}\sigma_a^2\sigma_b^2\sigma_c^2\sigma_d^2\{\Gamma_a\Gamma_b(u_cu_a)\times\left[(u_cu_d)(u_du_b) - (u_bu_c)\right] + \frac{1}{3}\left[(u_au_b)(u_bu_c)(u_cu_a) - 1\right] - \frac{1}{2}\Gamma_a\Gamma_b(u_au_b)\left[(u_cu_d)^2 - 1\right] + \frac{1}{6}\Gamma_d^2\times\left[3(u_bu_c)^2 - 2(u_au_b)(u_bu_c)(u_cu_a) - 1\right]\}.$$

This result was obtained without assuming energy-momentum conservation.

The positive definiteness of symmetric matrices $\mathfrak{R}_{s,d}$ (and, consequently, $\tilde{\mathfrak{R}}_{s,d}$) leads to a number of strict inequalities; in particular[52],

$$\tilde{\mathfrak{R}}^{\mu\mu}_{s,d} > 0,\quad \tilde{\mathfrak{R}}^{00}_{s,d}\tilde{\mathfrak{R}}^{ii}_{s,d} - \left(\tilde{\mathfrak{R}}^{0i}_{s,d}\right)^2 > 0,\quad \tilde{\mathfrak{R}}^{jj}_{s,d}\tilde{\mathfrak{R}}^{kk}_{s,d} - \left(\tilde{\mathfrak{R}}^{jk}_{s,d}\right)^2 > 0. \tag{A.6a}$$

Similar inequalities are valid for the cofactors $\mathfrak{N}^{\mu\nu}_{s,d}$ and $\tilde{\mathfrak{N}}^{\mu\nu}_{s,d}$ (since $\left|\tilde{\mathfrak{R}}_{s,d}\right| > 0$) and for the elements of matrix $\left\|R^{\mu\nu}\right\| = \left\|\tilde{\mathfrak{R}}^{\mu\nu}_s + \tilde{\mathfrak{R}}^{\mu\nu}_d\right\|$ (without summation over repeated indices):

$$R_{\mu\mu} > 0,\quad R_{00}R_{ii} - R_{0i}^2 > 0,\quad R_{jj}R_{kk} - R_{jk}^2 > 0. \tag{A.6b}$$

Inequalities (A.6b) have important corollaries such as the positivity of functions $\mathcal{R}$ and $\mathfrak{m} - \mathfrak{n}_0 - \mathfrak{n}_0^2$. Indeed, the following is true in the reference frame with axis z directed along unit vector $\mathbf{l}$:

$$\mathcal{R} = R_{33},\quad \mathfrak{m} - \mathfrak{n}_0 - \mathfrak{n}_0^2 = \frac{R_{00}\mathcal{R} - (\mathbf{Rl})^2}{R^2} = \frac{R_{00}R_{33} - R_{03}^2}{\left(R_{00} - 2R_{03} + R_{33}\right)^2}.$$

[52] The left-hand sides of inequalities (A.6a) are the principal minors of the first and the second orders. It is implied that summation over repeated indices is not performed in (A.6a) and (A.6b).

Since these quantities are rotationally invariant, it follows from (A.6b) that $\mathcal{R} > 0$ and $\mathfrak{m} - \mathfrak{n}_0 - \mathfrak{n}_0^2 > 0$. It is evident from the latter inequality that quantity (285) is positive. This results in the suppression of probability (297).

Functions n and $\bar{m}$ are constructed from the components of 4-vector $Y = Y_s + Y_d$, where

$$Y_s^\mu = \tilde{\mathfrak{R}}_s^{\mu\nu}q_{s\nu}\quad\text{and}\quad Y_d^\mu = -\tilde{\mathfrak{R}}_d^{\mu\nu}q_{d\nu},$$

and tensor components $R^{0i} = \tilde{\mathfrak{R}}_s^{0i} + \tilde{\mathfrak{R}}_d^{0i}$. Note that scalar product $Yl = (Y_s + Y_d)l = E_\nu R$ and zeroth component $Y^0 = Y_s^0 + Y_d^0$ are the only quantities actually needed to calculate function n. It is also sufficient to determine them in the PW_0 limit, where calculations are simplified considerably. In what follows, we use symbol $[\![f]\!]$ to denote that function f is calculated in the PW_0 limit. In these terms,

$$Y_{s,d}l \to \tilde{\mathfrak{R}}^{\mu\nu}_{s,d}q_\mu l_\nu\Big|_{q=E_\nu l} = E_\nu^{-1}\left[\!\left[\tilde{\mathfrak{R}}^{\mu\nu}_{s,d}q_\mu q_\nu\right]\!\right]$$
$$\text{and}\quad Y^0_{s,d} \to \left[\!\left[\tilde{\mathfrak{R}}^{0\mu}_{s,d}q_\mu\right]\!\right].$$

Let us examine several simple types of processes in the source and detector, which are relevant to real-life neutrino experiments, to clarify these general formulas.

A.3. Two-Particle Decay in the Source

Let us study the simplest process: lepton decay $a \to \ell\nu_*$ in the source ($a_{\ell 2}$). Here, a is a charged meson ($\pi^\pm$, $K^\pm$, $D_s^\pm$,...), ℓ is a charged lepton ($e^\pm,\mu^\pm,\tau^\pm$), and ν_* is a virtual neutrino or antineutrino. Since such decays are the primary sources of high-energy accelerator, atmospheric, and astrophysical neutrinos and antineutrinos, we examine this example in sufficient detail[53].

A.3.1. Formulas for arbitrary momenta. In the case under consideration, the determinant of matrix $\mathfrak{R}_s$ is easy to calculate using formula (A.2) written in the intrinsic frame of the meson packet[54]:

$$\left|\mathfrak{R}_s\right| = \sigma_a^2\sigma_\ell^2\sigma_2^4\left|\mathbf{u}_\ell^\bigstar\right|^2. \tag{A.7}$$

[53] Naturally, the formulas given in this section hold true for any two-particle decay (e.g., decays of relativistic ions via the capture of an orbit electron (such as $^{140}Pr^{57+} \to {}^{140}Ce^{57+}\nu_*$) in the thought experiment on detection of low-energy neutrinos from the EC decay. With certain reservations, the formulas are also applicable to the consecutive processes of emission and resonance absorption (induced by the electron capture) of a Mössbauer antineutrino (e.g., $^3H \to {}^3He + \bar{\nu}_*$, $\bar{\nu}_* + {}^3He \to {}^3H$).

[54] Subscript ★ denotes the intrinsic reference frame of a meson. Throughout the present section, indices a and ℓ denote the corresponding particles and should not be confused with Lorentz indices.

Here, $\sigma_2^2 = \sigma_a^2 + \sigma_\ell^2$ and $\mathbf{u}_\ell = \mathbf{p}_\ell/m_\ell = \Gamma_\ell \mathbf{v}_\ell$. Since determinant $|\mathfrak{R}_s|$ is Lorentz-invariant, it is transformed to the laboratory frame by substitution

$$\left|\mathbf{u}_\ell^\star\right| = \frac{1}{m_a m_\ell}\sqrt{(E_\ell \mathbf{p}_a - E_a \mathbf{p}_\ell)^2 - |\mathbf{p}_a \times \mathbf{p}_\ell|^2} = (u_a u_\ell)\mathrm{V}_{a\ell},$$

where

$$\mathrm{V}_{a\ell} = \frac{\sqrt{(\mathbf{v}_a - \mathbf{v}_\ell)^2 - |\mathbf{v}_a \times \mathbf{v}_\ell|^2}}{1 - \mathbf{v}_a \mathbf{v}_\ell}$$

is the invariant relative velocity of a meson and a lepton in the laboratory frame. Note that the kinematic variables corresponding to different particles are independent in this formula because they are not constrained by the energy-momentum conservation law. In the particular case with a virtual neutrino on the mass shell and the neutrino mass and the spreads of lepton and meson momenta being negligible, one may use the common relations of the two-particle decay kinematics, which state that

$$\left|\mathbf{v}_\ell^\star\right| = \mathrm{V}_{a\ell} = \frac{m_a^2 - m_\ell^2}{m_a^2 + m_\ell^2} \quad \text{and} \quad \left|\mathbf{u}_\ell^\star\right| = \frac{m_a^2 - m_\ell^2}{2m_a m_\ell}.$$

A somewhat more complex calculation involving general formulas (A.4) allows one to determine the explicit form of cofactors $\mathfrak{A}_s^{\mu\nu}$:

$$\begin{aligned}
\mathfrak{A}_s^{00} &= \sigma_2^2\left[\sigma_2^2\left(\sigma_a^2\Gamma_a^2 + \sigma_\ell^2\Gamma_\ell^2\right) + \sigma_a^2\sigma_\ell^2|\mathbf{u}_a \times \mathbf{u}_\ell|^2\right],\\
\mathfrak{A}_s^{0i} &= \sigma_2^2\left\{\sigma_a^2\left[\sigma_a^2\Gamma_a + \sigma_\ell^2\Gamma_\ell(u_a u_\ell)\right]u_{ai}\right.\\
&\quad \left. + \sigma_\ell^2\left[\sigma_\ell^2\Gamma_\ell + \sigma_a^2\Gamma_a(u_a u_\ell)\right]u_{\ell i}\right\},\\
\mathfrak{A}_s^{ii} &= \sigma_2^2\left\{\sigma_a^2\left[\sigma_a^2 u_{ai} + \sigma_\ell^2(u_a u_\ell)u_{\ell i}\right]u_{ai}\right.\\
&\quad + \sigma_\ell^2\left[\sigma_\ell^2 u_{\ell i} + \sigma_a^2(u_a u_\ell)u_{ai}\right]u_{\ell i}\\
&\quad \left. + \sigma_a^2\sigma_\ell^2\left[(\Gamma_\ell\mathbf{u}_a - \Gamma_a\mathbf{u}_\ell)^2 - |\mathbf{u}_a \times \mathbf{u}_\ell|^2\right]\right\},\\
\mathfrak{A}_s^{jk} &= \sigma_2^2\left[\sigma_a^4 u_{aj}u_{ak} + \sigma_\ell^4 u_{\ell j}u_{\ell k} + \sigma_a^2\sigma_\ell^2(u_a u_\ell)\right.\\
&\quad \left.\times\,(u_{aj}u_{\ell k} + u_{\ell j}u_{ak})\right],\ j \neq k.
\end{aligned} \tag{A.8}$$

An explicitly Lorentz-invariant formula for the components of the inverse tensor may be derived from (A.8) or (A.5):

$$\tilde{\mathfrak{R}}_s^{\mu\nu} = \frac{\sigma_a^4 u_a^\mu u_a^\nu + \sigma_\ell^4 u_\ell^\mu u_\ell^\nu - \sigma_a^2\sigma_\ell^2\left\{g^{\mu\nu}\left[(u_a u_\ell)^2 - 1\right] - (u_a u_\ell)(u_a^\mu u_\ell^\nu + u_\ell^\mu u_a^\nu)\right\}}{\sigma_a^2\sigma_\ell^2\left(\sigma_a^2 + \sigma_\ell^2\right)\left[(u_a u_\ell)^2 - 1\right]}.$$

It follows that

$$\tilde{\mathfrak{R}}_s^{\mu\nu}q_\mu q_\nu = \frac{\sigma_a^4(u_a q)^2 + \sigma_\ell^4(u_\ell q)^2 + 2\sigma_a^2\sigma_\ell^2(u_a u_\ell)(u_a q)(u_\ell q)}{\sigma_a^2\sigma_\ell^2\sigma_2^2\left|\mathbf{u}_\ell^\star\right|^2} - \frac{q^2}{\sigma_2^2}. \tag{A.9}$$

Let us now find the explicit form of 4-vector Y_s with its components defined as

$$Y_s^0 = \tilde{\mathfrak{R}}_s^{0\nu}q_{s\nu} = \frac{1}{|\mathfrak{R}_s|}\left[\mathfrak{A}^{00}(E_a - E_\ell) - \mathfrak{A}^{0i}(p_a - p_\ell)_i\right],$$

$$Y_s^i = \tilde{\mathfrak{R}}_s^{i\nu}q_{s\nu} = \frac{1}{|\mathfrak{R}_s|}\left[\mathfrak{A}^{ij}(p_a - p_\ell)_j - \mathfrak{A}^{i0}(E_a - E_\ell)\right].$$

With elementary transformations, the following is derived from (A.8):

$$Y_s^\mu = \frac{1}{\left|\mathbf{u}_\ell^\star\right|^2}\left\{\left[\frac{(p_a p_\ell)}{m_a^2} - 1\right]\frac{p_a^\mu}{\sigma_\ell^2} - \left[\frac{(p_a p_\ell)}{m_\ell^2} - 1\right]\frac{p_\ell^\mu}{\sigma_a^2}\right\}. \tag{A.10}$$

Useful identities:

$$\begin{aligned}
&(u_a q)(u_\ell q) = \Gamma_a\Gamma_\ell q_0^2\\
&- \left[\Gamma_a(\mathbf{u}_\ell\mathbf{q}) + \Gamma_\ell(\mathbf{u}_a\mathbf{q})\right]q_0 + (\mathbf{u}_a\mathbf{q})(\mathbf{u}_\ell\mathbf{q}),\\
&(\mathbf{u}_a\mathbf{q})(\mathbf{u}_\ell\mathbf{q})\\
&= \sum_i\left[(u_{ai}q_i)(u_{\ell i}q_i) + (u_{aj}q_j)(u_{\ell k}q_k) + (u_{ak}q_k)(u_{\ell j}q_j)\right].
\end{aligned}$$

A.3.2. PW_0 limit. Since kinematic constraints were not applied in the derivation of formulas in the previous section, they hold true for an arbitrary 4-vector q. Let us now introduce the exact conservation laws (i.e., pass to the PW_0 limit, which implies in this special case that $q = p_a - p_\ell = p_\nu = E_\nu l$ and $p_\nu^2 = 0$):

$$u_a u_\ell = \frac{E_\ell^\star}{m_\ell},\quad u_a q = E_\nu^\star,\quad u_\ell q = \frac{m_a E_\nu^\star}{m_\ell},$$

where

$$E_\ell^\star = \frac{m_a^2 + m_\ell^2}{2m_a} \quad \text{and} \quad E_\nu^\star = \frac{m_a^2 - m_\ell^2}{2m_a}$$

are the energies of a lepton and a neutrino in the intrinsic reference frame of a meson. Inserting these relations into (A.9), we find the PW_0 limit for quadratic form $\tilde{\mathfrak{R}}_s^{\mu\nu}q_\mu q_\nu$:

$$\left[\!\left[\tilde{\mathfrak{R}}_s^{\mu\nu}q_\mu q_\nu\right]\!\right] = \frac{m_\ell^2}{\sigma_\ell^2} + \frac{m_a^2}{\sigma_a^2} \gg 1. \tag{A.11}$$

Estimation of the parameters of an effective neutrino packet. In order to illustrate the result, we consider a special (although fairly realistic) case when the contribution from the reaction in the detector to complete function $\mathfrak{D}$ may be neglected (i.e., it is assumed that

parameters $\sigma_\varkappa$ for all $\in D$ are sufficiently large compared to σ_a and σ_ℓ). This assumption is valid in experiments with accelerator and atmospheric muon neutrinos and antineutrinos. The interactions of mesons and muons in the source (decay channel, atmosphere) with each other and the medium are normally negligible in such experiments; therefore, the values of σ_a and σ_μ are very small (close to the limiting ones in the SRGP model). The values of parameters $\sigma_\varkappa$ for long-lived in- and out-particles $\varkappa$ (nuclei, hadrons, leptons) in a typical detector are defined by their mean free paths in the detector medium rather than by their decay widths[55]; thus, $\sigma_\varkappa \gg \sigma_{a,\mu}$. At the very least, the $\sigma_\varkappa \gg \sigma_\mu$ condition is satisfied for short-lived particles and resonances that are produced in the detector and decay prior to interacting with the medium.

Thus, using (A.11), we find

$$\mathfrak{D}^2 \approx E_\nu^2\left[2\left(\frac{m_\ell^2}{\sigma_\ell^2}+\frac{m_a^2}{\sigma_a^2}\right)\right]^{-1} \ll E_\nu^2, \qquad \text{(A.12)}$$

and, consequently,

$$\sigma_j^2 \approx \frac{m_j^2}{2}\left(\frac{m_\ell^2}{\sigma_\ell^2}+\frac{m_a^2}{\sigma_a^2}\right)^{-1} \ll m_j^2. \qquad \text{(A.13)}$$

It is evident that the effective wave packet of a virtual neutrino with a given mass is defined completely in this simplest case by the masses and momentum spreads of packets a and ℓ, and the values of σ_j for all three known neutrinos are exceptionally small at any σ_a and σ_ℓ allowed by the SRGP approximation. In addition, since all the other (known) elementary particles with a nonzero mass are many orders of magnitude lower than the three known neutrinos, we conclude that $\sigma_j^2 \lll \sigma_{a,\ell}^2$. Although these estimates were obtained without including the contributions of the reaction in the detector, they explain qualitatively the relevance of the standard quantum-mechanical assumption that light neutrinos have definite momenta in spite of the fact that they are produced in processes involving particles with relatively large momentum spreads. It follows from (A.12) that $\sigma_j = 0$ at $m_j = 0$; i.e., massless neutrinos may be regarded as plane waves. With obvious reservations, this remarkable fact may be used in the analysis of processes similar to those depicted in Fig. 8, where light massive neutrinos act as external wave packets.

The conditions of applicability of the SRGP approximation for unstable particles

$$\left(\sigma_\varkappa/\sigma_\varkappa^{\max}\right)^4 \ll 1, \quad \sigma_\varkappa^{\max} = \sqrt{m_\varkappa\Gamma_\varkappa}$$

($\Gamma_\varkappa = 1/\tau_\varkappa$ is the total decay width of particle $\varkappa$) yield the following important constraint:

$$\sigma_j^2 \ll \frac{m_j^2}{2}\left(\frac{m_\ell}{\Gamma_\ell}+\frac{m_a}{\Gamma_a}\right)^{-1}.$$

Thus, two-particle decays of any mesons with a muon in the final state ($\pi_{\mu 2}$, $K_{\mu 2}$, etc.) are constrained from the above:

$$\frac{\sigma_j^2}{m_j^2} \ll \frac{\Gamma_\mu}{2m_\mu} \approx 1.4\times 10^{-18};$$

therefore, $\sigma_j^{\max}/\sigma_\mu^{\max} \approx m_j/m_\mu \lll 1$. This yields the following lower bounds for the effective sizes of a neutrino packet transverse and longitudinal with respect to the neutrino momentum[56]:

$$d_j^\perp \gg 2.6\left(\frac{0.1\text{ eV}}{m_j}\right)\text{km}$$

$$\text{and} \quad d_j^\parallel = \frac{d_j^\perp}{\Gamma_j} \gg 2.6\times 10^{-5}\left(\frac{1\text{ GeV}}{E_\nu}\right)\left(\frac{0.1\text{ eV}}{m_j}\right)\text{cm}.$$

The constraints on the characteristics of neutrino packets emerging in $a_{\tau 2}$ decays depend on the type of the decaying particle. For example, $\sigma_j^2/m_j^2 \ll 2.2\times 10^{-13}$ in the decay of a D_s meson. At $m_j = 0.1$ eV, this corresponds to a limiting effective transverse size of a neutrino packet of "just" 6.6 m.

Effective sizes $d_j^\perp$ and $d_j^\parallel$ define (in the order of magnitude) the allowed transverse and longitudinal quantum deviations of the center of the neutrino wave packet from "classical trajectory" $\bar{\mathbf{L}}_j = \mathbf{v}_j T$. Evidently, transverse deviations $\delta\mathbf{L}_j^\perp \sim d_j^\perp/2$ may be huge and exceed in magnitude the size of current neutrino detectors and the natural accelerator neutrino beam divergence (all over distances of several hundred or thousand kilometers from the source). This should come as no surprise if one remembers that the standard quantum-mechanical description of a massive neutrino as a state with definite momentum implies (as a direct consequence of the uncertainty principle) that its transverse and longitudinal "sizes" are infinite. When data from common experiments on neutrino oscillations are interpreted, this description does not yield nonphysical results because neither the transverse size of a neutrino packet nor transverse quantum

[55] Wave packets form anew in each (inelastic or elastic) interaction of a particle with the medium and external fields.

[56] It should be noted that $d_j^\perp$ is by no means the size of a neutrino packet at rest, since all estimates were obtained in the ultrarelativistic approximation and remain true only in those reference frames where a neutrino is ultrarelativistic. The same important reservation applies to the Lorentz invariance of neutrino wave function $\Psi_y^j(\mathbf{p}_j, x)$. The explicit form of the effective wave packet of a nonrelativistic neutrino requires separate consideration, which is beyond the bounds of the present study.

fluctuations are found in the expression for the count rate of neutrino events averaged properly over spatial coordinates $\mathbf{x}_\varkappa$ of external packets. This averaging also eliminates automatically the dependence on time components $x_\varkappa^0$; only the dependence of the count rate on external ("instrumental") space-time variables set by the experimental conditions[57] remains. Large transverse sizes of a neutrino packet may manifest themselves in specialized neutrino experiments, where both the source–detector distance and the time interval between the neutrino production and its interaction are monitored. Such experiments will be discussed in a separate study.

The effects of noncollinearity of momentum transfers in the source and detector are contained in functions $\mathfrak{n}$ and . The properties of these functions are discussed below.

Contributions to functions $\mathfrak{n}$ and $\mathfrak{m}$. Using general formula (A.10), we find 4-vector Y_s in the PW_0 approximation:

$$[\![Y_s]\!] = \frac{1}{m_a E_\nu^\star}\left[\left(\frac{m_\ell^2}{\sigma_\ell^2}+\frac{m_a^2}{\sigma_a^2}\right)p_a - \frac{m_a^2}{\sigma_a^2}p_\nu\right]$$
$$= \frac{1}{m_a E_\nu^\star}\left[\left(\frac{m_\ell^2}{\sigma_\ell^2}+\frac{m_a^2}{\sigma_a^2}\right)p_\ell - \frac{m_\ell^2}{\sigma_\ell^2}p_\nu\right].$$

Scalar products needed to calculate the $a_{\ell 2}$ contributions to function n take the form

$$[\![Y_s l]\!] = \left[\!\left[\tilde{\mathfrak{R}}_s^{\mu\nu}q_\mu q_\nu\right]\!\right]\frac{1}{E_\nu} = \left(\frac{m_\ell^2}{\sigma_\ell^2}+\frac{m_a^2}{\sigma_a^2}\right)\frac{1}{E_\nu}$$

$$[\![Y_s\mathbf{l}]\!] = [\![Y_s^0 - Y_s l]\!] = \frac{\Gamma_a}{E_\nu^\star}$$
$$\times\left[\left(\frac{m_\ell^2}{\sigma_\ell^2}+\frac{m_a^2}{\sigma_a^2}\right)\left(1-\frac{m_a E_\nu^\star}{E_a E_\nu}\right) - \frac{m_a^2}{\sigma_a^2}\frac{E_\nu}{E_a}\right].$$

This yields the following:

$$\left[\!\left[\frac{\mathbf{Y}_S\mathbf{l}}{Y_S l}\right]\!\right] = \left[\Gamma_a - \left(\frac{m_a^2\sigma_\ell^2}{m_a^2\sigma_\ell^2+m_\ell^2\sigma_a^2}\right)\frac{E_\nu}{m_a}\right]$$
$$\times\frac{E_\nu}{E_\nu^\star} - 1 \equiv \mathfrak{n}_s(E_a, E_\nu).$$

Function $\mathfrak{n}_s$ may serve as an estimate for complete function $\mathfrak{n}$ if, just as with function $\mathfrak{D}$, we neglect the contribution to $\mathfrak{n}$ from the detector part of the diagram (in the present case, from Y_d^0 and $Y_d l$) assuming that parameters $\sigma_\varkappa$ ($\varkappa \in D$) are sufficiently large compared to σ_a and σ_ℓ. Since function $\mathfrak{n}_s$ depends linearly on E_a at a fixed value of E_ν, the following inequality holds true:

$$\mathfrak{n}_s \geq \mathfrak{n}_s\left(E_a^{\min}, E_\nu\right),$$

where

$$E_a^{\min} = \frac{m_a}{2}\left(\frac{E_\nu}{E_\nu^\star}+\frac{E_\nu^\star}{E_\nu}\right)$$

is the minimum energy of particle a needed to produce a massless neutrino with energy E_ν in an $a_{\ell 2}$ decay. Thus, the absolute minimum of function $\mathfrak{n}_s$ is negative:

$$\mathfrak{n}_s^{\min} = \mathfrak{n}_s(m_a, E_\nu^\star) = -\frac{\left(m_a^2-m_\ell^2\right)\sigma_\ell^2}{2\left(m_a^2\sigma_\ell^2+m_\ell^2\sigma_a^2\right)},$$
$$\left|\mathfrak{n}_s^{\min}\right| < \frac{1}{2}\left(1-\frac{m_\ell^2}{m_a^2}\right).$$

Function n_s increases with neutrino energy and may be arbitrarily large at $E_\nu \gg E_\nu^\star$:

$$\mathfrak{n}_s \geq \mathfrak{n}_s\left(E_a^{\min}, E_\nu\right) = \frac{1}{2}\left(1-2\left|\mathfrak{n}_s^{\min}\right|\right)$$
$$\times\left(\frac{E_\nu}{E_\nu^\star}\right)^2\left[1+\mathbb{O}\left(\frac{E_\nu^\star}{E_\nu}\right)\right].$$

As is well known, the neutrino energy distribution in an $a_{\ell 2}$ decay is uniform (i.e., independent of E_ν) within the following kinematic bounds:

$$E_\nu^\star\Gamma_a(1-|\mathbf{v}_a|) \leq E_\nu \leq E_\nu^\star\Gamma_a(1+|\mathbf{v}_a|).$$

It follows that the mean energy of a decay neutrino is $\bar{E}_\nu = \Gamma_a E_\nu^\star$. Therefore, the following is true to within $\mathbb{O}(\Gamma_a^{-2})$ at high energies of decaying mesons, $\Gamma_a \gg 1$:

$$\mathfrak{n}_s\left(E_a, \bar{E}_\nu\right) \approx \Gamma_a^2\left(1-\left|\mathfrak{n}_s^{\min}\right|\right)$$
$$= \left(1-\left|\mathfrak{n}_s^{\min}\right|\right)\left(\frac{\bar{E}_\nu}{E_\nu^\star}\right)^2.$$

Consequently,

$$\mathfrak{n}_s r_j\big|_{E_\nu=\bar{E}_\nu} \approx \frac{1}{2}\left(1-\left|\mathfrak{n}_s^{\min}\right|\right)\left(\frac{m_j}{E_\nu^\star}\right)^2 \ll 1.$$

Under the same assumptions, retaining only the leading terms in Γ_a and $E_\nu/E_\nu^\star$, one may estimate the $a_{\ell 2}$-decay contribution to function $\mathfrak{m}$:

$$\mathfrak{m}_s \approx \Gamma_a^2\left\{1+\frac{\sigma_\ell^4 m_a^4}{\left(m_\ell^2\sigma_a^2+m_a^2\sigma_\ell^2\right)^2}\left[1+\frac{2\sigma_a^2 E_\nu^\star}{m_a\left(\sigma_a^2+\sigma_\ell^2\right)}\right]\right.$$
$$\left.\times\left(\frac{E_\nu}{E_a}\right)^2\right\}\left(\frac{E_\nu}{E_\nu^\star}\right)^2.$$

[57] However, it should be kept in mind that the applicability conditions of the mathematical averaging procedure are rather restrictive and are by no means guaranteed to be fulfilled in all neutrino experiments. For example, they are definitely violated in accelerator experiments with a baseline shorter than the effective transverse sizes of neutrino packets.

It can be seen that $\mathfrak{m}_s \gg \mathfrak{n}_s$; however, inequalities (284) assumed in Section 8.2.1 remain valid at $E_\nu \sim \bar{E}_\nu$.

A.4. Quasi-elastic Scattering in the Detector

Let us consider the quasi-elastic scattering of a virtual neutrino $\nu_* a \to b\ell$, where target particle a may be an electron, a nucleon, or a nucleus and ℓ is a charged lepton, as the simplest (and the most important) example of a reaction at the detector vertex. Since the velocities of target particles in the laboratory frame are very low (thermal) in a typical neutrino experiment, we assume that the laboratory frame coincides with the intrinsic frame of a wave packet describing the state of particle a. If necessary, all formulas may be rewritten in any other reference frame, since we are concerned just with vectors and tensors, and the laws of their transformations are well known.

A.4.1. Formulas for arbitrary momenta. The determinant of matrix $\mathfrak{R}_d$ in the intrinsic reference frame of packet a takes the form

$$|\mathfrak{R}_d| = \sigma_3^2\{(\sigma_3^2+\sigma_a^2)\sigma_b^2\sigma_\ell^2(u_b u_\ell)^2 \mathrm{V}_{b\ell}^2 + 2\sigma_a^2\sigma_b^2\sigma_\ell^2(u_b u_\ell)(\mathbf{u}_b\mathbf{u}_\ell) + \sigma_a^2[\sigma_b^2(\sigma_a^2+\sigma_b^2)\mathbf{u}_b^2 + \sigma_\ell^2(\sigma_a^2+\sigma_\ell^2)\mathbf{u}_\ell^2]\}. \quad (A.14)$$

Here, $\mathrm{V}_{b\ell}$ is the relative velocity of particles b and ℓ, and $\sigma_3^2 \equiv \sigma_a^2+\sigma_b^2+\sigma_\ell^2$. One important implication of this formula is that determinant $|\mathfrak{R}_d|$ remains nonnegative even if one (but only one) of the particles (a, b, or ℓ) is described by a plane wave. If, e.g., one neglects the terms proportional to σ_ℓ^2, formula (A.14) takes the form coinciding with that of (A.7):

$$|\mathfrak{R}_d| \approx \sigma_a^2\sigma_b^2(\sigma_a^2+\sigma_b^2)^2|\mathbf{u}_b|^2. \quad (A.15)$$

This important feature provides an opportunity to simplify the analysis of multipacket in- and out-states by neglecting the contributions of packets with very large spatial sizes (characterized by very small values of parameters $\sigma_\varkappa$). However, it should be kept in mind that approximate formula (A.15) is applicable only if $|\mathbf{u}_b| \neq 0$[58]. The same is true in the general case; i.e., when omitting the contributions of packets with very small values of $\sigma_\varkappa$, the phase-space regions within which determinants $|\mathfrak{R}_s|$ and $|\mathfrak{R}_d|$ calculated in this approximation vanish, should be cut-off. Such regions are typically located near the kinematic boundaries of the phase space and do not contribute to experimentally measureable characteristics.

According to (A.4), cofactors $\mathfrak{N}_d^{\mu\nu}$ are written as follows:

$$\begin{aligned}
\mathfrak{N}_d^{00} &= \sigma_3^2[\sigma_3^2(\sigma_a^2+\sigma_b^2\Gamma_b^2+\sigma_\ell^2\Gamma_\ell^2) + \sigma_b^2\sigma_\ell^2|\mathbf{u}_b\times\mathbf{u}_\ell|^2],\\
\mathfrak{N}_d^{0i} &= \sigma_3^2\{\sigma_b^2[(\sigma_a^2+\sigma_b^2)\Gamma_b + \sigma_\ell^2(u_b u_\ell)]u_{bi} + \sigma_\ell^2[(\sigma_a^2+\sigma_\ell^2)\Gamma_\ell + \sigma_b^2(u_b u_\ell)]u_{\ell i}\},\\
\mathfrak{N}_d^{ii} &= \sigma_b^2(\sigma_3^2\sigma_b^2 - \sigma_a^2\sigma_\ell^2\mathbf{u}_\ell^2)u_{bi}^2 + \sigma_\ell^2(\sigma_3^2\sigma_\ell^2 - \sigma_a^2\sigma_b^2\mathbf{u}_b^2)u_{\ell i}^2 + 2\sigma_b^2\sigma_\ell^2\\
&\times[\sigma_a^2\Gamma_b\Gamma_\ell + (\sigma_b^2+\sigma_\ell^2)(u_b u_\ell)]u_{bi}u_{\ell i} + \sigma_3^{-2}|\mathfrak{R}_d|,\\
\mathfrak{N}_d^{jk} &= \sigma_b^2(\sigma_3^2\sigma_b^2 - \sigma_a^2\sigma_\ell^2\mathbf{u}_\ell^2)u_{bj}u_{bk} + \sigma_\ell^2(\sigma_3^2\sigma_\ell^2 - \sigma_a^2\sigma_b^2\mathbf{u}_b^2)u_{\ell j}u_{\ell k} + \sigma_b^2\sigma_\ell^2\\
&\times[\sigma_a^2\Gamma_b\Gamma_\ell + (\sigma_b^2+\sigma_\ell^2)(u_b u_\ell)](u_{bj}u_{\ell k} + u_{bk}u_{\ell j}),\\
&j \neq k.
\end{aligned} \quad (A.16)$$

The following is then obtained for an arbitrary 4-vector q:

$$\begin{aligned}
|\mathfrak{R}_d|\tilde{\mathfrak{R}}_d^{\mu\nu}q_\mu q_\nu &= \mathfrak{N}_d^{00}q_0^2 + \sum_i(-2\mathfrak{N}_d^{0i}q_0 + \mathfrak{N}_d^{ii}q_i)q_i + 2\sum_{j<k}\mathfrak{N}_d^{jk}q_j q_k\\
&= \sigma_3^2[\sigma_3^2(\sigma_a^2+\sigma_b^2\Gamma_b^2+\sigma_\ell^2\Gamma_\ell^2) + \sigma_b^2\sigma_\ell^2|\mathbf{u}_b\times\mathbf{u}_\ell|^2]q_0^2\\
&- 2\sigma_3^2\sigma_b^2[(\sigma_a^2+\sigma_b^2)\Gamma_b + \sigma_\ell^2\Gamma_\ell(u_b u_\ell)](\mathbf{u}_b\mathbf{q})q_0\\
&- 2\sigma_3^2\sigma_\ell^2[(\sigma_a^2+\sigma_\ell^2)\Gamma_\ell + \sigma_b^2\Gamma_b(u_b u_\ell)](\mathbf{u}_\ell\mathbf{q})q_0\\
&+ \sigma_3^2[\sigma_b^4(\mathbf{u}_b\mathbf{q})^2 + \sigma_\ell^4(\mathbf{u}_\ell\mathbf{q})^2 + 2\sigma_b^2\sigma_\ell^2(u_b u_\ell)(\mathbf{u}_b\mathbf{q})(\mathbf{u}_\ell\mathbf{q})]\\
&+ \sigma_a^2\sigma_b^2\sigma_\ell^2\{[(\mathbf{u}_b\times\mathbf{u}_\ell)\mathbf{q}]^2 - (\mathbf{u}_b\times\mathbf{u}_\ell)^2\mathbf{q}^2\} + \sigma_3^{-2}|\mathfrak{R}_d|\mathbf{q}^2.
\end{aligned}$$

Using (A.16), we determine the components of 4-momentum Y_d:

$$Y_d^0 = \frac{\sigma_3^2}{|\mathfrak{R}_d|}(c_a^0 m_a - c_b^0 E_b - c_\ell^0 E_\ell),$$

$$\mathbf{Y}_d = \frac{\sigma_3^2}{|\mathfrak{R}_d|}(c_b\mathbf{u}_b + c_\ell\mathbf{u}_\ell).$$

The coefficient functions found here are given by

$$\begin{aligned}
c_a^0 &= \sigma_a^2(\sigma_3^2+\sigma_b^2\Gamma_b^2+\sigma_\ell^2\Gamma_\ell^2) + \sigma_b^2\sigma_\ell^2\\
&\times[(\Gamma_b\Gamma_\ell - 1)^2 - (\mathbf{u}_b\mathbf{u}_\ell)^2] + (\sigma_b^2\Gamma_b + \sigma_\ell^2\Gamma_\ell)^2,\\
c_b^0 &= \sigma_3^2[\sigma_a^2+\sigma_b^2+\sigma_\ell^2\Gamma_\ell^2(1-\mathbf{v}_b\mathbf{v}_\ell)],\\
c_\ell^0 &= \sigma_3^2[\sigma_a^2+\sigma_\ell^2+\sigma_b^2\Gamma_b^2(1-\mathbf{v}_b\mathbf{v}_\ell)],\\
c_b &= \sigma_b^2\{[m_a\sigma_\ell^2\Gamma_\ell - m_\ell(\sigma_b^2+\sigma_\ell^2)](u_b u_\ell) + m_a\sigma_b^2\Gamma_b - m_b(\sigma_b^2+\sigma_\ell^2)\}\\
&+ \sigma_a^2\{m_b\sigma_\ell^2\mathbf{u}_\ell^2 + \sigma_b^2[\Gamma_b(m_a - m_\ell\Gamma_\ell) - m_b]\},\\
c_\ell &= \sigma_\ell^2\{[m_a\sigma_b^2\Gamma_b - m_b(\sigma_b^2+\sigma_\ell^2)]\\
&\times(u_b u_\ell) + m_a\sigma_\ell^2\Gamma_\ell - m_\ell(\sigma_b^2+\sigma_\ell^2)\}\\
&+ \sigma_a^2\{m_\ell\sigma_b^2\mathbf{u}_b^2 + \sigma_\ell^2[\Gamma_\ell(m_a - m_b\Gamma_b) - m_\ell]\}.
\end{aligned}$$

[58] We should recall that $|\mathbf{u}_\ell^\star|$ in (A.7) is always nonzero.

As it should be, the above expressions are symmetric with respect to index interchange $b \leftrightarrow \ell$, and their explicitly noncovariant form is attributable to the use of a special reference frame.

A.4.2. PW_0 limit. The kinematics of reaction $2 \to 2$ in the PW_0 limit allows one to write quantities $|\Re_d|$, $\tilde{\Re}_d^{\mu\nu} q_\mu q_\nu$, and $\mathbf{Y}_d\mathbf{l}$ in terms of two arbitrary independent invariant variables; we used the standard pair of variables

$$s = (p_a + p_\nu)^2 = m_a(2E_\nu + m_a)$$
$$\text{and} \quad Q^2 = -(p_\nu - p_\ell)^2.$$

In order to rewrite the expressions from the previous section in terms of these variables, we use the following exact kinematic relations:

$$E_b = \frac{1}{m_a}\left(E_b^* E_a^* - E_\nu^* P_\ell^* \cos\theta_*\right),$$
$$\mathbf{p}_b\mathbf{p}_\nu = \frac{E_\nu}{m_a}\left(E_b^* E_\nu^* - E_a^* P_\ell^* \cos\theta_*\right),$$
$$E_\ell = \frac{1}{m_a}\left(E_\ell^* E_a^* + E_\nu^* P_\ell^* \cos\theta_*\right),$$
$$\mathbf{p}_\ell\mathbf{p}_\nu = \frac{E_\nu}{m_a}\left(E_\ell^* E_\nu^* + E_a^* P_\ell^* \cos\theta_*\right),$$
$$|\mathbf{u}_b \times \mathbf{u}_\ell| = \frac{E_\nu P_\ell^* \sin\theta_*}{m_b m_\ell}, \quad (\mathbf{u}_b \times \mathbf{u}_\ell)\,\mathbf{p}_\nu = 0,$$
$$u_b u_\ell = \frac{s - m_b^2 - m_\ell^2}{2m_b m_\ell}, \quad \mathrm{V}_{b\ell} = \frac{2\sqrt{s}P_\ell^*}{s - m_b^2 - m_\ell^2},$$

where $E_\nu = |\mathbf{p}_\nu| = (s - m_a^2)/2m_a$ and $\mathbf{p}_\nu = E_\nu\mathbf{l}$ are the energy and the momentum of a massless neutrino in the laboratory frame;

$$E_\nu^* = \frac{s - m_a^2}{2\sqrt{s}}, \quad E_\ell^* = \frac{s + m_\ell^2 - m_b^2}{2\sqrt{s}},$$
$$E_a^* = \frac{s + m_a^2}{2\sqrt{s}} \quad \text{and} \quad E_b^* = \frac{s - m_\ell^2 + m_b^2}{2\sqrt{s}},$$

are the energies of particles ν^*, ℓ, a, and b in the center-of-mass system of colliding particles ν^* and a, which is determined by

$$E_\nu^* + E_a^* = E_b^* + E_\ell^*, \quad \mathbf{p}_\nu^* + \mathbf{p}_a^* = \mathbf{p}_\ell^* + \mathbf{p}_b^* = 0;$$

and $P_\ell^* = |\mathbf{p}_\ell^*|$. Lepton scattering angle θ_* in the center-of-mass system is related to Q^2:

$$Q^2 = 2E_\nu^*\left(E_\ell^* - P_\ell^* \cos\theta_*\right) - m_\ell^2.$$

The kinematically allowed region of the phase space is defined by the following inequalities:

$$s \geq s_{\mathrm{th}} = \max\left[m_a^2, (m_b + m_\ell)^2\right], \tag{A.17}$$

$$Q_-^2 \leq Q^2 \leq Q_+^2, \quad Q_\pm^2 = 2E_\nu^*\left(E_\ell^* \pm P_\ell^*\right) - m_\ell^2. \tag{A.18}$$

Performing elementary (although rather cumbersome) algebraic transformations, we find

$$[\![|\Re_d|]\!] = \frac{\sigma_3^2}{4m_a^2 m_b^2 m_\ell^2}\sum_{k,l=0}^{2} A_{kl} s^k Q^{2l},$$
$$\left[\!\left[|\Re_d|\tilde{\Re}_d^{\mu\nu} q_\mu q_\nu\right]\!\right] = \frac{\sigma_3^2}{4m_a^2 m_b^2 m_\ell^2}\sum_{k,l=0}^{2} B_{kl} s^k Q^{2l},$$
$$[\![|\Re_d|\,\mathbf{Y}_d\mathbf{q}]\!] = \frac{\sigma_3^2}{8m_a^2 m_b^2 m_\ell^2}\sum_{k,l=0}^{3} C_{kl} s^k Q^{2l}.$$

Nonzero coefficients A_{kl}, B_{kl} $(0 \leq k,l \leq 2)$, and C_{kl} $(0 \leq k,l \leq 3)$ have the form

$$A_{00} = \sigma_b^2 m_a^2 m_\ell^2\left[\sigma_a^2(\sigma_a^2 + \sigma_b^2)(m_a^2 - 2m_b^2) + \sigma_\ell^2(\sigma_b^2 + \sigma_\ell^2)(m_\ell^2 - 2m_b^2) - 3\sigma_a^2\sigma_\ell^2 m_b^2\right] + \sigma_3^2 m_b^2\left[\sigma_b^2 m_b^2(\sigma_a^2 m_\ell^2 + \sigma_\ell^2 m_a^2) + \sigma_a^2\sigma_\ell^2(m_b^4 - 4m_a^2 m_\ell^2)\right],$$
$$A_{01} = \sigma_a^2\{\sigma_b^2[2\sigma_a^2 m_\ell^2(m_a^2 + m_b^2) + \sigma_\ell^2(m_b^2 + m_\ell^2)(m_a^2 + 2m_b^2)] + 2[\sigma_b^4 m_\ell^2(m_a^2 + m_b^2) + \sigma_\ell^2 m_b^4(\sigma_a^2 + \sigma_\ell^2)]\},$$
$$A_{02} = \sigma_3^2\sigma_a^2(\sigma_b^2 m_\ell^2 + \sigma_\ell^2 m_b^2),$$

$$A_{10} = -\sigma_\ell^2\{\sigma_b^2[\sigma_a^2(m_a^2 + m_b^2)(2m_b^2 + m_\ell^2) + 2\sigma_\ell^2 m_a^2(m_b^2 + m_\ell^2)] + 2[\sigma_b^4 m_a^2(m_b^2 + m_\ell^2) + \sigma_a^2 m_b^4(\sigma_a^2 + \sigma_\ell^2)]\},$$
$$A_{11} = -\sigma_a^2\sigma_\ell^2[\sigma_b^2(m_a^2 + m_b^2 + m_\ell^2) + 2\sigma_3^2 m_b^2],$$
$$A_{12} = -\sigma_a^2\sigma_b^2\sigma_\ell^2,$$
$$A_{20} = \sigma_3^2\sigma_\ell^2(\sigma_a^2 m_b^2 + \sigma_b^2 m_a^2),$$
$$A_{21} = \sigma_a^2\sigma_b^2\sigma_\ell^2;$$

$$B_{00} = m_a^2 m_\ell^2\{\sigma_b^2(m_a^2 + m_\ell^2)[\sigma_a^2(m_a^2 + m_b^2) + \sigma_b^2(m_a^2 + m_\ell^2) + \sigma_\ell^2(m_b^2 + m_\ell^2)] + m_b^2(\sigma_a^4 m_a^2 + \sigma_\ell^4 m_\ell^2 + \sigma_a^2\sigma_\ell^2 m_b^2)\},$$
$$B_{01} = m_a^2\{2\sigma_\ell^4 m_b^2 m_\ell^2 + \sigma_\ell^2(m_b^2 + m_\ell^2) \times [\sigma_b^2(m_a^2 + 2m_\ell^2) + \sigma_a^2 m_b^2] + \sigma_b^2 m_\ell^2 \times [\sigma_a^2(2m_a^2 + m_b^2 + m_\ell^2) + 2\sigma_b^2(m_\ell^2 + m_a^2)]\},$$
$$B_{02} = \sigma_3^2 m_a^2(\sigma_b^2 m_\ell^2 + \sigma_\ell^2 m_b^2),$$

$$B_{10} = -m_\ell^2\{\sigma_\ell^2[\sigma_b^2 m_a^2(m_a^2+m_b^2+2m_\ell^2) + \sigma_a^2 m_b^2(m_a^2+m_b^2)] + \sigma_a^2\sigma_b^2(m_a^2+m_b^2)(m_\ell^2+2m_a^2) + 2m_a^2[\sigma_a^4 m_b^2 + \sigma_b^4(m_\ell^2+m_a^2)]\},$$
$$B_{11} = -[2\sigma_3^2\sigma_b^2 m_a^2 m_\ell^2 + (m_a^2+m_b^2+m_\ell^2) \times (\sigma_a^2\sigma_b^2 m_\ell^2 + \sigma_b^2\sigma_\ell^2 m_a^2 + \sigma_\ell^2\sigma_a^2 m_b^2)],$$
$$B_{12} = -(\sigma_a^2\sigma_b^2 m_\ell^2 + \sigma_b^2\sigma_\ell^2 m_a^2 + \sigma_\ell^2\sigma_a^2 m_b^2),$$
$$B_{20} = \sigma_3^2 m_\ell^2(\sigma_a^2 m_b^2 + \sigma_b^2 m_a^2),$$
$$B_{21} = \sigma_a^2\sigma_b^2 m_\ell^2 + \sigma_b^2\sigma_\ell^2 m_a^2 + \sigma_\ell^2\sigma_a^2 m_b^2;$$

$$C_{00} = m_a^2 m_\ell^2\{\sigma_a^2[\sigma_b^2(m_a^4 + m_a^2 m_\ell^2 - m_a^2 m_b^2 + m_\ell^2 m_b^2) + \sigma_\ell^2 m_b^2(m_b^2-2m_a^2)] + (\sigma_b^2 m_a^2 + \sigma_\ell^2 m_b^2 + \sigma_b^2 m_\ell^2) \times [\sigma_b^2 m_a^2 + (2m_\ell^2 - m_b^2)(\sigma_\ell^2+\sigma_b^2)]\},$$
$$C_{01} = m_a^2\{\sigma_a^2[\sigma_b^2(2m_a^2 m_\ell^2 + m_b^2 m_\ell^2 + m_\ell^4) + \sigma_\ell^2 m_b^2(m_\ell^2+m_b^2)] + \sigma_\ell^4 m_b^2(3m_\ell^2 - m_b^2) + \sigma_b^4 m_\ell^2(2m_a^2 - m_b^2 + 3m_\ell^2) + \sigma_b^2\sigma_\ell^2(m_b^2+m_\ell^2)(m_a^2 - m_b^2 + 3m_\ell^2)\},$$
$$C_{02} = m_a^2\sigma_3^2(m_b^2\sigma_\ell^2 + \sigma_b^2 m_\ell^2),$$
$$C_{10} = -m_\ell^2\{\sigma_a^2[\sigma_b^2(2m_a^4 - 2m_a^2 m_b^2 + m_a^2 m_\ell^2 + m_b^2 m_\ell^2) + \sigma_\ell^2 m_b^2(m_b^2 - 3m_a^2)] + \sigma_b^4[2m_a^2(m_a^2 - m_b^2) + m_\ell^2(3m_a^2 - m_b^2)] - \sigma_\ell^4 m_b^2(m_a^2+m_b^2) + \sigma_b^2\sigma_\ell^2 \times [m_a^2(2m_a^2 + 4m_\ell^2 - 3m_b^2) - m_b^2(m_b^2+m_\ell^2)]\},$$

$$C_{11} = -\sigma_a^2[\sigma_b^2 m_\ell^2(3m_a^2 + m_b^2 + m_\ell^2) + \sigma_\ell^2 m_b^2(m_a^2+m_b^2+m_\ell^2)] - \sigma_b^4 m_\ell^2(m_a^2 - m_b^2 - m_\ell^2) + \sigma_\ell^4 m_b^2(m_a^2+m_b^2+m_\ell^2) + \sigma_b^2\sigma_\ell^2 \left[(m_b^2+m_\ell^2)^2 - m_a^2(m_a^2 - m_b^2 + 3m_\ell^2)\right],$$
$$C_{12} = -\sigma_a^2(\sigma_b^2 m_\ell^2 + \sigma_\ell^2 m_b^2) - \sigma_b^2\sigma_\ell^2(m_a^2 - m_b^2 - m_\ell^2) + \sigma_b^4 m_\ell^2 + \sigma_\ell^4 m_b^2,$$

$$C_{20} = m_\ell^2\{\sigma_a^2[\sigma_b^2(m_a^2 - m_b^2) - \sigma_\ell^2 m_b^2] + \sigma_b^4(m_a^2 - m_b^2) - \sigma_\ell^2 m_b^2(\sigma_b^2+\sigma_\ell^2) + 2\sigma_b^2(\sigma_\ell^2 m_a^2 - \sigma_\ell^2 m_b^2)\},$$
$$C_{21} = \sigma_a^2(\sigma_b^2 m_\ell^2 + \sigma_\ell^2 m_b^2) - 2\sigma_b^2\sigma_\ell^2(m_b^2+m_\ell^2) - \sigma_b^4 m_\ell^2 - \sigma_\ell^4 m_b^2,$$
$$C_{22} = -\sigma_b^2\sigma_\ell^2,$$
$$C_{31} = \sigma_b^2\sigma_\ell^2.$$

Thus, quadratic form $\tilde{\mathfrak{R}}_d^{\mu\nu} q_\mu q_\nu$ and scalar product $\mathbf{Y}_d\mathbf{q}$ are rational functions of variables s and Q^2:

$$[\![\tilde{\mathfrak{R}}_d^{\mu\nu} q_\mu q_\nu]\!] = \frac{\sum_{k,l} B_{kl} s^k Q^{2l}}{\sum_{k,l} A_{kl} s^k Q^{2l}} \equiv \tilde{\mathfrak{F}}_d(s, Q^2),$$
$$[\![\mathbf{Y}_d\mathbf{q}]\!] = \frac{1}{2}\frac{\sum_{k,l} C_{kl} s^k Q^{2l}}{\sum_{k,l} A_{kl} s^k Q^{2l}} \equiv \mathfrak{n}_d(s, Q^2)\tilde{\mathfrak{F}}_d(s, Q^2).$$

The following function was introduced here[59]:

$$\mathfrak{n}_d = \frac{[\![\mathbf{Y}_d\mathbf{l}]\!]}{[\![Y_d l]\!]} = \frac{1}{2}\frac{\sum_{k,l} C_{kl} s^k Q^{2l}}{\sum_{k,l} B_{kl} s^k Q^{2l}}.$$

It is also expedient to introduce function $\mathfrak{D}_d$ defined in the following way:

$$\frac{\mathfrak{D}_d^2}{E_\nu^2} = \frac{1}{2\tilde{\mathfrak{F}}_d} = \frac{1}{2}\frac{\sum_{k,l} A_{kl} s^k Q^{2l}}{\sum_{k,l} B_{kl} s^k Q^{2l}}.$$

Although neither $\mathfrak{D}_d$ nor $\mathfrak{n}_d$ have a clear physical meaning, they help illustrate the behavior of functions $\mathfrak{D}$ and $\mathfrak{n}$, which are of interest to us, in the special case when the contributions to $\mathfrak{D}$ and $\mathfrak{n}$ from the reaction in the source can be neglected[60]. This case is defined by the following conditions:

$$[\![\tilde{\mathfrak{R}}_d^{\mu\nu} q_\mu q_\nu]\!] \gg [\![\tilde{\mathfrak{R}}_s^{\mu\nu} q_\mu q_\nu]\!] \quad \text{and} \quad [\![|\mathbf{Y}_d\mathbf{l}|]\!] \gg [\![|\mathbf{Y}_s\mathbf{l}|]\!].$$

In the simplest particular case with $\sigma_a/m_a = \sigma_b/m_b = \sigma_\ell/m_\ell = \lambda = \text{const}$ (these relations characterize the scaling of effective sizes of packets), one can demonstrate that functions $\lambda^2\tilde{\mathfrak{F}}_d$ (and, consequently, $\mathfrak{D}_d/\lambda$) and $\mathfrak{n}_d$ are independent of parameter λ and are defined by the kinematics only. The domains of functions $\tilde{\mathfrak{F}}_d$ and $\mathfrak{n}_d$ are bounded by kinematic conditions (A.17) and (A.18), and the shape variations of surfaces shown in different panels are attributable primarily to the differences in reaction thresholds (A.17) (essentially, the differences in masses of final leptons). Therefore, these variations are smoothed out at sufficiently high energies (i.e., $s \gg \max(s_{\text{th}})$). The fact that function $\tilde{\mathfrak{F}}_d$ turns to zero at $E_\nu \to 0$ for thresholdless reaction $\nu n \to pe^-$ is irrelevant to our analysis limited to ultrarelativistic neutrinos[61].

[59] It is worth noting that, in contrast to $\tilde{\mathfrak{F}}_d$, function $\mathfrak{n}_d$ is not a relativistic invariant, although it is expressed (in the laboratory frame) in terms of two invariants.

[60] This case is exactly the opposite of the one discussed as an example in Section A.3.2.

[61] We should recall that the formulas for dispersion are modified greatly at $E_\nu \sim m_j$; see Section 8.2.2.

In the general case, the behavior of functions $\mathfrak{F}_d$ and $\mathfrak{n}_d$ is much more complex. Naturally, this assumption, which was adopted for purely illustrative purposes, is completely arbitrary and unrealistic. In a more realistic case, $\sigma_\varkappa/m_\varkappa \lll 1$, even function $\log(\mathfrak{F}_d)$ varies strongly within its domain, and the features of its behavior are hard to reproduce in a two-dimensional plot. Let us consider the most important limiting cases, asymptotics, and inequalities to gain a better understanding of the properties of functions $\mathfrak{F}_d$ and $\mathfrak{n}_d$.

A.4.3. Low-energy limits of functions $\mathfrak{F}_d$ and $\mathfrak{n}_d$. The limits of functions $\mathfrak{F}_d$ and $\mathfrak{n}_d$ at the kinematic threshold of quasi-elastic reaction $\nu + b \to b + \ell$ in the detector are as follows[62]:

$$\mathfrak{F}_d(s_{\text{th}}, Q^2_{\text{th}}) = \frac{(m_b + m_\ell)^2}{\sigma_b^2 + \sigma_\ell^2} + \frac{m_a^2}{\sigma_a^2},$$

$$\mathfrak{n}_d(s_{\text{th}}, Q^2_{\text{th}}) = \frac{\left(\sigma_b^2 + \sigma_\ell^2\right)\left[m_a^2 - (m_b + m_\ell)^2\right]}{2\left[\sigma_a^2 (m_b + m_\ell)^2 + \sigma_b^2 m_a^2 + \sigma_\ell^2 m_a^2\right]}.$$

It is assumed here that $m_a < m_b + m_\ell$. The threshold values of s and Q^2 are

$$s_{\text{th}} = (m_b + m_\ell)^2 \quad \text{and} \quad Q^2_{\text{th}} = m_\ell\left(m_b - \frac{m_a^2}{m_b + m_\ell}\right).$$

The following is then obtained for the thresholdless reaction ($m_a > m_b + m_\ell$, $s_{\text{th}} = m_a^2$, $Q^2_{\text{th}} = -m_\ell^2$):

$$\mathfrak{F}_d(s_{\text{th}}, Q^2_{\text{th}}) = 0, \quad \mathfrak{n}_d(s_{\text{th}}, Q^2_{\text{th}}) = 1 - \frac{\sigma_3^2\left[2\sigma_a^2 m_b^2 + \sigma_b^2\left(m_a^2 + m_b^2 - m_\ell^2\right)\right]}{2\left[\sigma_a^2\sigma_b^2\left(m_a^2 + m_b^2 - m_\ell^2\right) + \sigma_a^4 m_b^2 + \sigma_b^4 m_a^2\right]}.$$

Thus, function $\mathfrak{F}_d$ may assume a value of exactly zero only in a thresholdless reaction (e.g., $\nu n \to pe$) at $E_\nu = 0$. Naturally, this formal limit goes well beyond the bounds of ultrarelativistic approximation $E_\nu^2 \gg \max(m_j^2)$, which was used in derivation of the formulas for functions $\mathfrak{F}_d$ and $\mathfrak{n}_d$, and is of no practical importance, because ultrarelativistic neutrino and antineutrino beams[63] only are used in all current neutrino experiments. It is of interest to note that the limit of $\mathfrak{F}_d$ at $E_\nu = \max(m_j) \equiv m_\nu$ and $Q^2 = -m_\ell^2$ (for a thresholdless reaction), which is given by

$$\frac{4m_a^2 m_\ell^2 m_\nu^2}{\sigma_3^2\sigma_a^2\sigma_b^2\sigma_\ell^2}\left[\frac{\sigma_a^2\sigma_b^2\left(m_a^2 + m_b^2 - m_\ell^2\right) + \sigma_b^4 m_a^2 + \sigma_a^4 m_b^2}{\left(m_a^2 - m_b^2\right)^2 - 2m_\ell^2\left(m_a^2 + m_b^2\right) + m_\ell^4}\right]\left(\frac{m_a^2}{\sigma_a^2} + \frac{m_b^2}{\sigma_b^2} + \frac{m_\ell^2}{\sigma_\ell^2}\right)^{-1},$$

may still be large in magnitude if at least two out of three parameters σ_a, σ_b, and σ_ℓ are small compared to m_ν.

A.4.4. High-energy asymptotics of functions $\mathfrak{F}_d$ and $\mathfrak{n}_d$. Under the assumption that $\sigma_{a,b,\ell} \neq 0$ and $Q^2 < \infty$, the asymptotic behavior of functions $\mathfrak{F}_d(s, Q^2)$ and $\mathfrak{n}_d(s, Q^2)/s$ at high energies is independent of s:

$$\mathfrak{F}_d(s, Q^2) \underset{s\to\infty}{\sim} \frac{m_a^2}{\sigma_a^2} + \frac{m_b^2}{\sigma_b^2} + \frac{m_\ell^2}{\sigma_\ell^2} - \left(\frac{m_a^2}{\sigma_a^2} + \frac{m_b^2}{\sigma_b^2}\right)^2\left(\frac{Q^2}{\sigma_3^2} + \frac{m_a^2}{\sigma_a^2} + \frac{m_b^2}{\sigma_b^2}\right)^{-1},$$

$$n_d(s, Q^2) \underset{s\to\infty}{\sim} \frac{s}{2\sigma_a^2}\left[\frac{m_a^2}{\sigma_a^2} + \frac{m_b^2}{\sigma_b^2} + \frac{m_\ell^2}{\sigma_\ell^2} + \frac{\sigma_3^2 m_\ell^2}{\sigma_\ell^2 Q^2}\left(\frac{m_a^2}{\sigma_a^2} + \frac{m_b^2}{\sigma_b^2}\right)\right]^{-1}.$$

These asymptotics satisfy the following inequalities:

$$\frac{m_\ell^2}{\sigma_\ell^2} < \mathfrak{F}_d(s, Q^2) < \frac{m_a^2}{\sigma_a^2} + \frac{m_b^2}{\sigma_b^2} + \frac{m_\ell^2}{\sigma_\ell^2}, \quad \frac{\sigma_b^2\sigma_l^2\left(m_b^2 - m_a^2\right)}{2\sigma_3^2\left(\sigma_a^2 m_b^2 + \sigma_b^2 m_a^2\right)} < \mathfrak{n}_d(s, Q^2) < \frac{s}{2m_a^2}\left[1 + \frac{\sigma_a^2}{m_a^2}\left(\frac{m_b^2}{\sigma_b^2} + \frac{m_\ell^2}{\sigma_\ell^2}\right)\right]^{-1},$$

($s \to \infty$, $Q^2 < \infty$), and their limiting values at kinematic boundaries are

$$\lim_{s\to\infty}\mathfrak{F}_d(s, Q_-^2) = \frac{m_\ell^2}{\sigma_\ell^2}, \quad \lim_{s\to\infty}\mathfrak{n}_d(s, Q_-^2) = \frac{\sigma_b^2\left(m_a^2 - m_b^2\right) - \sigma_\ell^2 m_b^2}{2\left(\sigma_a^2 m_b^2 + \sigma_b^2 m_a^2\right)},$$

$$\lim_{s\to\infty}\mathfrak{F}_d(s, Q_+^2) = \frac{m_b^2}{\sigma_b^2}, \quad \lim_{s\to\infty}\mathfrak{n}_d(s, Q_+^2) = \frac{\sigma_\ell^2\left(m_a^2 - m_\ell^2\right) - \sigma_b^2 m_\ell^2}{2\left(\sigma_a^2 m_\ell^2 + \sigma_\ell^2 m_a^2\right)}.$$

[62] All formulas are written in the PW_0 limit, which implies the exact energy-momentum conservation in reaction $2 \to 2$ plus $m_j = 0, \forall j$. It is also assumed (unless stated otherwise) that all parameters $\sigma_\varkappa$ are nonzero.

[63] It appropriate at this point to note that a more general analysis covering the nonrelativistic case is of potential interest in the context of studies into the possibility of detecting relic neutrinos and for accelerator and astrophysical experiments in the search for hypothetical superheavy neutrinos and sterile neutrinos of keV-scale masses.

It is evident that these quantities are symmetric with respect to index interchange $b \leftrightarrow \ell$. The $\mathfrak{n}_d(s, Q_\pm^2)$ threshold values vanish at specific relations between parameters $\sigma_\varkappa$ and masses. The next ($\sim 1/s$) corrections need to be taken into account in these exotic cases.

In the particular case when target particle a is a nucleon, it follows from dynamic considerations that, at high neutrino energies, the mean scattering angle in the center-of-mass system, $\langle\theta_*\rangle$, is equal in order of magnitude to the inverse Lorentz factor of a lepton $\Gamma_\ell^* = E_\ell^*/m_\ell$. Therefore, $\langle Q^2\rangle \sim m_\ell^2$ and $\langle\theta\rangle \sim m_\ell/\sqrt{s}$, where θ is the scattering angle of a lepton in the laboratory frame (coinciding with the intrinsic frame of a nucleon). It can be demonstrated that the corresponding asymptotics of functions $\mathfrak{F}_d$ and $\mathfrak{n}_d$ take the form

$$\mathfrak{F}_d\left(s, m_\ell^2\right) \underset{s\to\infty}{\sim} \frac{m_\ell^2}{\sigma_\ell^2}\left[1 + \frac{\sigma_\ell^2}{\sigma_3^2}\left(\frac{m_a^2}{\sigma_a^2} + \frac{m_b^2}{\sigma_b^2}\right)\left(\frac{m_a^2}{\sigma_a^2} + \frac{m_b^2}{\sigma_b^2} + \frac{m_\ell^2}{\sigma_3^2}\right)^{-1}\right] < 2\frac{m_\ell^2}{\sigma_\ell^2},$$

$$\mathfrak{n}_d\left(s, m_\ell^2\right) \underset{s\to\infty}{\sim} \frac{\sigma_b^2\sigma_\ell^2 s}{2\left[\left(\sigma_b^2 m_a^2 + \sigma_a^2 m_b^2\right)\left(\sigma_a^2 + \sigma_b^2 + 2\sigma_\ell^2\right) + \sigma_a^2\sigma_b^2 m_\ell^2\right]} < \frac{E_\nu}{2m_a}.$$

Since only a narrow region of angles close to $\theta = \langle\theta\rangle$ produces a significant contribution to the count rate for quasi-elastic events at high energies, one may conclude that effective asymptotic value $\mathfrak{F}_d$ is almost constant and is defined primarily by momentum dispersion σ_ℓ of the lepton WP. Arbitrary[64] variations of parameters σ_a and σ_b may change the asymptotics only within a factor of two.

The asymptotic behavior of $\mathfrak{F}_d(s, Q^2)$ changes drastically if one (and only one) of the $\sigma_\varkappa$ parameters turns to zero. If $\sigma_a = 0$ or $\sigma_b = 0$, the asymptotics is independent of s:

$$\mathfrak{F}_d(s, Q^2) \xrightarrow[s\to\infty]{} \begin{cases} \dfrac{Q^2}{\sigma_b^2 + \sigma_\ell^2} + \dfrac{m_\ell^2}{\sigma_\ell^2}, & \text{at} \quad \sigma_a = 0, \\ \dfrac{Q^2}{\sigma_a^2 + \sigma_\ell^2} + \dfrac{m_\ell^2}{\sigma_\ell^2}, & \text{at} \quad \sigma_b = 0, \end{cases}$$

and if $\sigma_\ell = 0$, increases quadratically with s:

$$\mathfrak{F}_d(s, Q^2) \underset{s\to\infty}{\sim} \frac{\left(\dfrac{Q^2}{\sigma_a^2 + \sigma_b^2} + \dfrac{m_a^2}{\sigma_a^2} + \dfrac{m_b^2}{\sigma_b^2}\right)s^2}{\left(Q^2 + m_a^2 + m_b^2\right)^2 - 4m_a^2 m_b^2}, \quad \text{at} \quad \sigma_\ell = 0.$$

Other variables. Certain properties of function $\mathfrak{F}_d$ become more evident if it is rewritten in terms of variables E_ν and θ_*. Let us consider the asymptotic expansion of $\mathfrak{F}_d$ at $E_\nu \to \infty$ and a fixed value of θ_*. If the values of $\sin\theta_*$ are not too small, it can be written as

$$\mathfrak{F}_d(E_\nu, \theta_*) = \frac{m_a^2}{\sigma_a^2} + \frac{m_b^2}{\sigma_b^2} + \frac{m_\ell^2}{\sigma_\ell^2} - \frac{a_1\sigma_3^2}{2m_a E_\nu \sin^2\theta_*}\left\{\left[\left(\frac{m_b^2}{\sigma_b^2} + \frac{m_\ell^2}{\sigma_\ell^2}\right)\cos\theta_* + \left(\frac{m_b^2\sigma_\ell^2 - m_\ell^2\sigma_b^2}{m_\ell^2\sigma_b^2 + m_b^2\sigma_\ell^2}\right)\right.\right.$$
$$\left.\left.\times\left(\frac{2m_a^2}{\sigma_a^2} + \frac{m_b^2}{\sigma_b^2} + \frac{m_\ell^2}{\sigma_\ell^2}\right)\right]^{-2} + \left(\frac{4m_a m_b m_\ell}{\sigma_a\sigma_b\sigma_\ell}\right)^2\left(\frac{m_b^2}{\sigma_b^2} + \frac{m_\ell^2}{\sigma_\ell^2}\right)^2\left(\frac{m_a^2}{\sigma_a^2} + \frac{m_b^2}{\sigma_b^2} + \frac{m_\ell^2}{\sigma_\ell^2}\right)\right\} + \frac{1}{\sin^4\theta_*}\mathbb{O}\left(\frac{m_a^2}{E_\nu^2}\right).$$

At $\sin\theta_* = 0$, one finds

$$\mathfrak{F}_d(E_\nu, 0) = \frac{m_\ell^2}{\sigma_\ell^2}\left[1 - \frac{m_a^2 - m_b^2}{m_a E_\nu} + \mathbb{O}\left(\frac{m_a^2}{E_\nu^2}\right)\right], \quad \mathfrak{F}_d(E_\nu, \pi) = \frac{m_b^2}{\sigma_b^2}\left[1 - \frac{m_a^2 - m_\ell^2}{m_a E_\nu} + \mathbb{O}\left(\frac{m_a^2}{E_\nu^2}\right)\right].$$

As was already noted, $\langle\theta_*\rangle \sim \Gamma_\ell^* = E_\ell^*/m_\ell$ at high energies. It can be demonstrated that the corresponding asymptotic expansion takes the form

$$\mathfrak{F}_d(E_\nu, \theta_* = 1/\Gamma_\ell^*) = \frac{m_\ell^2}{\sigma_\ell^2}\left[b_0 - \frac{b_1\sigma_3^2}{m_a(b_0 - 1)^2 E_\nu} + \mathbb{O}\left(\frac{m_a^2}{E_\nu^2}\right)\right],$$

[64] Naturally, these variations should not violate the conditions of applicability of the SRGP model.

where

$$b_0 = 1 + \frac{\sigma_\ell^2\left(m_b^2\sigma_a^2 + m_a^2\sigma_b^2\right)}{\sigma_3^2\left(m_b^2\sigma_a^2 + m_a^2\sigma_b^2\right) + m_\ell^2\sigma_a^2\sigma_b^2},$$

$$b_1 = 8\sigma_\ell^2\left(m_b^2\sigma_a^2 + m_a^2\sigma_b^2\right)^3\left[m_b^2\left(m_a^2 - m_b^2 + \frac{m_\ell^2}{3}\right)\sigma_a^2 + m_a^2\left(m_a^2 - m_b^2 + \frac{4m_\ell^2}{3}\right)\sigma_b^2\right]$$
$$+ 2\sigma_\ell^2\left(m_b^2\sigma_a^2 + m_a^2\sigma_b^2\right)\left[m_b^2\sigma_a^4 + \left(m_a^2 + m_b^2 + m_\ell^2\right)\sigma_a^2\sigma_b^2 + m_a^2\sigma_b^4\right]$$
$$\times\left[m_b^2\left(m_a^2 - m_b^2 - m_\ell^2\right)\sigma_a^2 + m_a^2\left(m_a^2 - m_b^2 + m_\ell^2\right)\sigma_b^2\right].$$

It is evident that the effective asymptotic $\tilde{\mathfrak{F}}_d(E_\nu, \theta_*)$ value is almost constant and, since $1 < b_0 < 2$, is defined primarily by the momentum dispersion of the lepton packet.

The case of strong hierarchy. Function $\tilde{\mathfrak{F}}_d(s, Q^2)$ is simplified considerably in the case of a strong hierarchy of parameters σ_a, σ_b, and σ_ℓ. Calculating the corresponding sequential limits, we obtain the following:

$$\tilde{\mathfrak{F}}_d(s,Q^2) \approx \begin{cases} \dfrac{\left(Q^2 + m_\ell^2\right)^2}{\left(s - Q^2 - m_b^2\right)^2 - 4m_a^2m_\ell^2}\left(\dfrac{m_a}{\sigma_a}\right)^2, & \text{for} \quad \sigma_\ell \gg \sigma_a \gg \sigma_b, \\ \dfrac{\left(Q^2 + m_\ell^2\right)^2}{\left(s - m_b^2 - m_\ell^2\right)^2 - 4m_b^2m_\ell^2}\left(\dfrac{m_a}{\sigma_a}\right)^2, & \text{for} \quad \sigma_\ell \gg \sigma_b \gg \sigma_a, \\ \dfrac{\left(s - m_a^2\right)^2}{\left(Q^2 + m_a^2 + m_b^2\right)^2 - 4m_a^2m_b^2}\left(\dfrac{m_b}{\sigma_b}\right)^2, & \text{for} \quad \sigma_a \gg \sigma_b \gg \sigma_\ell, \\ \dfrac{\left(s - m_a^2\right)^2}{\left(s - Q^2 - m_b^2\right)^2 - 4m_a^2m_\ell^2}\left(\dfrac{m_\ell}{\sigma_\ell}\right)^2, & \text{for} \quad \sigma_a \gg \sigma_\ell \gg \sigma_b, \\ \dfrac{\left(s - Q^2 - m_a^2 - m_\ell^2\right)^2}{\left(s - m_b^2 - m_\ell^2\right)^2 - 4m_b^2m_\ell^2}\left(\dfrac{m_\ell}{\sigma_\ell}\right)^2, & \text{for} \quad \sigma_b \gg \sigma_\ell \gg \sigma_a, \\ \dfrac{\left(s - Q^2 - m_a^2 - m_\ell^2\right)^2}{\left(Q^2 + m_a^2 + m_b^2\right)^2 - 4m_a^2m_b^2}\left(\dfrac{m_a}{\sigma_a}\right)^2, & \text{for} \quad \sigma_b \gg \sigma_a \gg \sigma_\ell. \end{cases}$$

It can be seen that[65] the shape and the value of function $\tilde{\mathfrak{F}}_d(s, Q^2)$ are not affected by the smallest and the largest of parameters σ. This nontrivial property may be generalized to the case of processes with an arbitrary number of particles in the final state. In the strong hierarchy scenario, the only significant parameter is the second-largest dispersion. This is useful in the analysis of multiparticle processes (with more than two external packets), since one may then treat packets with (comparatively) very small $\sigma_\varkappa$ as plane waves. In particular, the calculation of radiative corrections with plane-wave photons in the external legs of Feynman diagrams is simplified significantly, since the standard QFT calculation methods become available. We should recall that loop electroweak corrections do not introduce additional computational complications associated with the WP formalism, since all of them are formally included in the corresponding matrix elements and are in no way related to the characteristics of external in- and out-states. Under the convention adopted in the main text, the external legs of diagrams do not feature gauge bosons.

[65] In the case of strong hierarchy of scales of momenta dispersions of external packets, but not in the general case.

A.5. Three-Particle Decay in the Source

The general formulas characterizing three-particle decay $a \to b + \ell + \nu_*$ agree formally with the ones for the $2 \to 2$ scattering (if they are considered in the intrinsic reference frame of particle a). The primary difference is of kinematic origin. Therefore, we discuss this case in brief. Just as in the case of the $2 \to 2$ scattering, functions $|\mathfrak{R}_s|$ and $\tilde{\mathfrak{R}}_s^{\mu\nu}q_\mu q_\nu$ may be written in terms of two independent invariant variables. One may use, e.g., any pair of invariants

$$s_1 = (p_b + p_\ell)^2 = (p_a - p_\nu)^2,$$
$$s_2 = (p_\nu + p_\ell)^2 = (p_a - p_b)^2,$$
$$s_3 = (p_\nu + p_b)^2 = (p_a - p_\ell)^2,$$

which are related by identity $s_1 + s_2 + s_3 = m_a^2 + m_b^2 + m_\ell^2$, as these variables. The physical domain for them is defined by conditions

$$(m_b + m_\ell)^2 \le s_1 \le m_a^2, \quad m_\ell^2 \le s_2 \le (m_a - m_\ell)^2,$$
$$m_b^2 \le s_3 \le (m_a - m_b)^2.$$

For definiteness, we use the (s_1, s_2) pair. The domain of definition for this pair is the Dalitz diagram

$$s_1^- \le s_1 \le s_1^+, \quad m_\ell^2 \le s_2 \le (m_a - m_\ell)^2,$$

where

$$s_1^\pm = m_b^2 + m_\ell^2 - \frac{(s_2 + m_b^2)(s_2 - m_a^2 + m_\ell^2) \mp (s_2 - m_b^2)\sqrt{(s_2 - m_a^2 - m_\ell^2)^2 - 4m_a^2 m_\ell^2}}{2s_2}.$$

Using the results obtained in the previous section, we find

$$[\![|\Re_s|]\!] = \frac{\sigma_3^2}{4m_a^2 m_b^2 m_\ell^2} \sum_{k,l=0}^{2} A'_{kl} s_1^k s_2^l,$$
$$\left[\!\left[|\Re_s|\tilde{\Re}_d^{\mu\nu} q_\mu q_\nu\right]\!\right] = \frac{\sigma_3^2}{4m_a^2 m_b^2 m_\ell^2} \sum_{k,l=0}^{2} B'_{kl} s_1^k s_2^l.$$

Therefore, quadratic form $\tilde{\Re}_s^{\mu\nu} q_\mu q_\nu$ is a rational function of variables s_1 and s_2,

$$\left[\!\left[\tilde{\Re}_s^{\mu\nu} q_\mu q_\nu\right]\!\right] = \frac{\sum_{k,l} B'_{kl} s_1^k s_2^l}{\sum_{k,l} A'_{kl} s_1^k s_2^l} \equiv \tilde{\mathfrak{S}}_s(s_1, s_2).$$

Nonzero coefficients A'_{kl} and B'_{kl} $(0 \le k, l \le 2)$ take the form

$$A'_{00} = \sigma_\ell^2\left[\sigma_a^2 m_b^2(\sigma_a^2 + \sigma_\ell^2)(m_a^2 - m_\ell^2)^2 + \sigma_b^2 m_a^2(\sigma_b^2 + \sigma_\ell^2)(m_b^2 - m_\ell^2)^2\right] + \sigma_a^2\sigma_b^2 m_\ell^2$$
$$\times\left\{\sigma_\ell^2\left[m_\ell^2(m_a^2 + m_b^2 + m_\ell^2) - 7m_a^2 m_b^2\right] + (\sigma_a^2 + \sigma_b^2)(m_\ell^4 - 4m_a^2 m_b^2)\right\},$$
$$A'_{01} = -\sigma_a^2\left\{\sigma_b^2\left[\sigma_\ell^2(m_b^2 + m_\ell^2)(m_a^2 + 2m_\ell^2) + 2m_\ell^4(\sigma_a^2 + \sigma_b^2)\right] + 2\sigma_\ell^2 m_b^2(m_\ell^2 + m_a^2)(\sigma_a^2 + \sigma_\ell^2)\right\},$$
$$A'_{02} = \sigma_3^2\sigma_a^2(\sigma_b^2 m_\ell^2 + \sigma_\ell^2 m_b^2),$$
$$A'_{10} = -\sigma_b^2\left\{\sigma_a^2\left[\sigma_\ell^2(m_\ell^2 + m_a^2)(2m_\ell^2 + m_b^2) + 2m_\ell^4(\sigma_a^2 + \sigma_b^2)\right] + 2\sigma_\ell^2 m_a^2(\sigma_b^2 + \sigma_\ell^2)(m_\ell^2 + m_b^2)\right\},$$
$$A'_{11} = \sigma_a^2\sigma_b^2\left[\sigma_\ell^2(m_a^2 + m_b^2 + m_\ell^2) + 2\sigma_3^2 m_\ell^2\right], \quad A'_{12} = -\sigma_a^2\sigma_b^2\sigma_\ell^2,$$
$$A'_{20} = \sigma_3^2\sigma_b^2(\sigma_a^2 m_\ell^2 + \sigma_\ell^2 m_a^2), \quad A'_{21} = -\sigma_a^2\sigma_b^2\sigma_\ell^2;$$
$$B'_{00} = m_a^2 m_b^2\left\{\sigma_\ell^2(m_a^2 + m_b^2)\left[\sigma_a^2(m_a^2 + m_\ell^2) + \sigma_b^2(m_b^2 + m_\ell^2) + \sigma_\ell^2(m_a^2 + m_b^2)\right]\right.$$
$$\left. + m_\ell^2(\sigma_a^4 m_a^2 + \sigma_b^4 m_b^2 + \sigma_a^2\sigma_b^2 m_b^2)\right\},$$
$$B'_{01} = -m_a^2\left\{\sigma_a^2\left[\sigma_b^2 m_\ell^2(m_b^2 + m_\ell^2) + \sigma_\ell^2 m_b^2(2m_a^2 + m_b^2 + m_\ell^2)\right] + 2m_b^2\left[\sigma_b^4 m_\ell^2 + \sigma_\ell^4(m_a^2 + m_b^2)\right]\right.$$
$$\left. + \sigma_b^2\sigma_\ell^2(m_b^2 + m_\ell^2)(m_a^2 + 2m_b^2)\right\}, \quad B'_{02} = \sigma_3^2 m_a^2(\sigma_b^2 m_\ell^2 + \sigma_\ell^2 m_b^2),$$
$$B'_{10} = -m_b^2\left\{2\sigma_a^4 m_a^2 m_\ell^2 + \sigma_a^2(m_a^2 + m_\ell^2)\left[\sigma_b^2 m_\ell^2 + \sigma_\ell^2(2m_a^2 + m_b^2)\right] + \sigma_\ell^2 m_a^2\right.$$
$$\left.\times\left[2\sigma_\ell^2(m_a^2 + m_b^2) + \sigma_b^2(m_a^2 + 2m_b^2 + m_\ell^2)\right]\right\},$$
$$B'_{11} = 2\sigma_3\sigma_\ell^2 m_a^2 m_b^2 + (m_a^2 + m_b^2 + m_\ell^2)(\sigma_a^2\sigma_b^2 m_\ell^2 + \sigma_b^2\sigma_\ell^2 m_a^2 + \sigma_\ell^2\sigma_a^2 m_b^2),$$
$$B'_{12} = -(\sigma_a^2\sigma_b^2 m_\ell^2 + \sigma_b^2\sigma_\ell^2 m_a^2 + \sigma_\ell^2\sigma_a^2 m_b^2),$$
$$B'_{20} = \sigma_3^2 m_b^2(\sigma_a^2 m_\ell^2 + \sigma_\ell^2 m_a^2),$$
$$B'_{21} = \sigma_a^2\sigma_b^2 m_\ell^2 + \sigma_b^2\sigma_\ell^2 m_a^2 + \sigma_\ell^2\sigma_a^2 m_b^2.$$

We will not study the limiting cases and asymptotics in detail, because they may be obtained from the formulas for quasi-elastic scattering in the detector. As an example, we consider the case of a strong hierarchy of parameters σ_a, σ_b, and σ_ℓ, where, as in the case of the $2 \to 2$ scattering, function $\tilde{\mathfrak{S}}_s(s_1, s_2)$ is especially simple:

$$\tilde{\mathcal{S}}_s(s_1,s_2)\approx\begin{cases}\dfrac{\left(s_1+s_2-m_a^2-m_b^2\right)^2}{\left(s_2-m_a^2-m_\ell^2\right)^2-4m_a^2m_\ell^2}\left(\dfrac{m_a}{\sigma_a}\right)^2, & \text{for } \sigma_\ell\gg\sigma_a\gg\sigma_b,\\ \dfrac{\left(s_1+s_2-m_a^2-m_b^2\right)^2}{\left(s_1-m_b^2-m_\ell^2\right)^2-4m_b^2m_\ell^2}\left(\dfrac{m_b}{\sigma_b}\right)^2, & \text{for } \sigma_\ell\gg\sigma_b\gg\sigma_a,\\ \dfrac{\left(s_1-m_a^2\right)^2}{\left(s_1+s_2-m_\ell^2\right)^2-4m_a^2m_b^2}\left(\dfrac{m_b}{\sigma_b}\right)^2, & \text{for } \sigma_a\gg\sigma_b\gg\sigma_\ell,\\ \dfrac{\left(s_1-m_a^2\right)^2}{\left(s_2-m_a^2-m_\ell^2\right)^2-4m_a^2m_\ell^2}\left(\dfrac{m_\ell}{\sigma_\ell}\right)^2, & \text{for } \sigma_a\gg\sigma_\ell\gg\sigma_b,\\ \dfrac{\left(s_2-m_b^2\right)^2}{\left(s_1-m_b^2-m_\ell^2\right)^2-4m_b^2m_\ell^2}\left(\dfrac{m_\ell}{\sigma_\ell}\right)^2, & \text{for } \sigma_b\gg\sigma_\ell\gg\sigma_a,\\ \dfrac{\left(s_2-m_b^2\right)^2}{\left(s_1+s_2-m_\ell^2\right)^2-4m_a^2m_b^2}\left(\dfrac{m_a}{\sigma_a}\right)^2, & \text{for } \sigma_b\gg\sigma_a\gg\sigma_\ell.\end{cases}$$

It can be seen that, under strong hierarchy, the shape and the value of function $\tilde{\mathcal{S}}_s(s_1,s_2)$ are not affected by the smallest and the largest of parameters.

APPENDIX B

MULTIDIMENSIONAL GAUSSIAN QUADRATURES

Integrals

$$\mathcal{G}(A,B)=\int dx\exp\left(-A_{\mu\nu}x^\mu x^\nu+B_\mu x^\mu\right), \qquad \text{(B.1)}$$

where $A=\|A_{\mu\nu}\|$ is a symmetric positively defined matrix and B_μ are arbitrary complex constants[66], are used often in the main text. Although such integrals are well known (see, e.g., [138]), we detail here a simple calculation of (B.1), since the published papers suffer from a certain confusion (or, to put it better, lack of agreement) regarding the definition of the matrix inverse to A in the Minkowski space. Symmetric matrix A can always be diagonalized with orthogonal transformation $O=\|O_{\mu\nu}\|$ (see, e.g., [139]):

$$A_{\mu\nu}=\sum_\alpha a_\alpha O_{\mu\alpha}O_{\nu\alpha},\quad \sum_\alpha O_{\mu\alpha}O_{\nu\alpha}=\delta_{\mu\nu}, \qquad \text{(B.2)}$$

where a_α are (positive) eigenvalues of matrix A. Therefore, the quadratic form in the exponent of the integrand in (B.1) may be rewritten as

$$-\sum_\alpha a_\alpha\left(O_{\mu\alpha}x^\mu\right)\left(O_{\nu\alpha}x^\nu\right)+B_\mu x^\mu=\sum_\alpha\left(-a_\alpha y_\alpha^2+\sum_\mu B_\mu O_{\mu\alpha}y_\alpha\right), \qquad \text{(B.3)}$$

where $y_\alpha=O_{\mu\alpha}x^\mu$ and, consequently, $x^\mu=\sum_\alpha O_{\mu\alpha}y_\alpha$. The Jacobian of this transform is $|O|=1$, so $dx=dy$. Inserting (B.3) into (B.1), we reduce the integral to a product of standard Gaussian quadratures:

$$\mathcal{G}(A,B)=\prod_\alpha\sqrt{\frac{\pi}{a_\alpha}}\exp\left[\frac{1}{4a_\alpha}\left(\sum_\mu B_\mu O_{\mu\alpha}\right)^2\right]. \qquad \text{(B.4)}$$

According to (B.2),

$$\sum_\alpha a_\alpha^{-1}O_{\mu\alpha}O_{\nu\alpha}=\left(A^{-1}\right)_{\mu\nu}\overset{\text{def}}{=}\tilde{A}^{\mu\nu}\quad\text{and}\quad\prod_\alpha a_\alpha=|A|.$$

The following is then obtained for the 3-dimensional Euclidean space:

$$\mathcal{G}(A,B)=\sqrt{\frac{\pi^3}{|A|}}\exp\left(\frac{1}{4}\tilde{A}_{kn}B_kB_n\right),\quad \tilde{A}=A^{-1}. \qquad \text{(B.5)}$$

In the 4-dimensional Minkowski space,

$$\mathcal{G}(A,B)=\frac{\pi^2}{\sqrt{|A|}}\exp\left(\frac{1}{4}\tilde{A}^{\mu\nu}B_\mu B_\nu\right),\quad \tilde{A}=gA^{-1}g. \qquad \text{(B.6)}$$

Note that $\tilde{A}\neq A^{-1}$ in the latter case, because $\tilde{A}_{0k}=\tilde{A}_{k0}=-(A^{-1})_{0k}$, $k=1,2,3$. It is evident that the eigenvalues of matrix $\tilde{A}$ are $1/a_\alpha>0$; therefore, it is positively defined. Naturally, $|\tilde{A}|=1/|A|$. In the case of most importance to us (with quantities $A^{\mu\nu}$ and B^μ constituting a tensor and a 4-vector, respectively), $\tilde{A}^{\mu\nu}B_\mu B_\nu$ is a Lorentz scalar, since integral (B.1) is also a Lorentz scalar.

[66] In this study, quantities $A_{\mu\nu}$ and B_μ are the components of a tensor and a 4-vector, respectively, but this is not significant for subsequent analysis. In addition, (B.4) is independent of the dimensionality and signature of spacetime.

APPENDIX C

FACTORIZATION OF HADRON BLOCKS

Let us demonstrate that, under certain reasonable assumptions formulated below, hadronic matrix element (233) may be reduced to form (235).

To this end, we express the matrix element at the right-hand side of (234), which includes elementary quark currents j_q and $j_q^\dagger$, in terms of hadronic currents. Using the definition of a chronological product of local operators, we write[67]

$$\begin{aligned} &T\left[j_q(x)j_q^\dagger(y)\mathbb{S}_h\right] \\ &= \theta(x_0 - y_0)A(x,y) + \theta(y_0 - x_0)B(x,y), \end{aligned} \tag{C.1}$$

where

$$A(x,y) = \mathbb{U}(\infty, x_0)j_q(x)\mathbb{U}(x_0, y_0)j_q^\dagger(y)\mathbb{U}(y_0, -\infty), \tag{C.2a}$$

$$B(y,x) = \mathbb{U}(\infty, y_0)j_q^\dagger(y)\mathbb{U}(y_0, x_0)j_q(x)\mathbb{U}(x_0, -\infty), \tag{C.2b}$$

and

$$\mathbb{U}(\tau_2, \tau_1) = \exp\left[i\int_{\tau_1}^{\tau_2} dx_0 \int d\mathbf{x}\mathscr{L}_\mathrm{h}(x)\right] \tag{C.3}$$

is the evolution operator for the hadronic part of the Lagrangian. Utilizing the well-known properties of this operator

$$\begin{aligned} &\mathbb{U}(\tau_2, \tau_1) = \mathbb{U}(\tau_2, \tau)\mathbb{U}(\tau, \tau_1), \quad \mathbb{U}(\tau_2, \tau_1)\mathbb{U}(\tau_1, \tau_2) = 1, \\ &\mathbb{U}(\infty, -\infty) = S_h, \quad \mathbb{U}(\pm\infty, \pm\infty) = 1, \end{aligned}$$

we rewrite expression (C.2a) in the following way:

$$\begin{aligned} A(x,y) &= \mathbb{U}(\infty, \tau)\mathbb{U}(\tau, x_0)j_q(x)\mathbb{U}(x_0, \tau)\mathbb{U}(\tau, x_0) \\ &\times \mathbb{U}(x_0, y_0)j_q^\dagger(y)\mathbb{U}(y_0, \tau)\mathbb{U}(\tau, y_0)\mathbb{U}(y_0, -\infty) \\ &= \mathbb{U}(\infty, \tau)\mathbb{U}(\tau, x_0)j_q(x)\mathbb{U}(x_0, \tau) \\ &\times \mathbb{U}(\tau, y_0)j_q^\dagger(y)\mathbb{U}(y_0, \tau)\mathbb{U}(\tau, -\infty). \end{aligned} \tag{C.4}$$

Here, τ is an arbitrary parameter. Let us now define the hadronic current operator (in the Heisenberg representation) as

$$J(x) = \lim_{\tau\to-\infty} \mathbb{U}(\tau, x_0)j_q(x)\mathbb{U}(x_0, \tau). \tag{C.5}$$

Equation (C.4) may then be rewritten as

$$A(x,y) = \mathbb{S}_h J(x)J^\dagger(y). \tag{C.6a}$$

In a similar fashion, the following is derived from (C.2b):

$$B(y,x) = \mathbb{S}_h J^\dagger(y)J(x). \tag{C.6b}$$

Inserting (C.6) into (C.1), we find

$$T\left[j_q(x)j_q^\dagger(y)\mathbb{S}_h\right] = \mathbb{S}_h T\left[J(x)J^\dagger(y)\right]. \tag{C.7}$$

[67] Lorentz indices and normal ordering symbols are omitted for brevity in this section (when it can be done without ambiguity).

As is known, single-particle hadronic states do not change under the effect of a hadronic S-matrix. Since our states $|\{k_b\}\rangle$ are direct products of single-particle hadronic states, it may be assumed that $\mathbb{S}_h^\dagger|\{k_b\}\rangle = |\{k_b\}\rangle$ to within an insignificant phase factor. Therefore, the following expression derived from (C.7) is true to within this factor:

$$\begin{aligned} &\langle\{k_b\}|T\left[j_q(x)j_q^\dagger(y)\mathbb{S}_h\right]|\{k_a\}\rangle \\ &= \langle\{k_b\}|\left|T\left[J(x)J^\dagger(y)\right]\right|\{k_a\}\rangle \equiv \left\langle J(x)J^\dagger(y)\right\rangle_T. \end{aligned} \tag{C.8}$$

Let us now discuss matrix element

$$\left\langle J(x)J^\dagger(y)\right\rangle = \langle\{k_b\}|J(x)J^\dagger(y)|\{k_a\}\rangle.$$

Owing to the translational invariance, current $J(x)$ satisfies equation

$$i\partial_\mu J(x) = [J(x), P^\mu], \tag{C.9}$$

where P^μ is the complete 4-momentum operator corresponding to the hadronic part of the Lagrangian (see, e.g., [140]). Using (C.9), one obtains

$$\begin{aligned} i\left(\frac{\partial}{\partial x_\mu} + \frac{\partial}{\partial y_\mu}\right)\left\langle J(x)J^\dagger(y)\right\rangle &= \left\langle [J(x)J^\dagger(y), P^\mu]\right\rangle \\ &= \left(K - K'\right)^\mu \left\langle J(x)J^\dagger(y)\right\rangle, \end{aligned} \tag{C.10}$$

where

$$\begin{aligned} K &= K_s + K_d = \sum_{a\in I_s} k_a + \sum_{a\in I_d} k_a, \\ K' &= K_s + K_d = \sum_{b\in F_s'} k_b + \sum_{b\in F_d'} k_b. \end{aligned}$$

The formal solution of differential equations (C.10) takes the form

$$\begin{aligned} \left\langle J_\mu(x)J_\nu^\dagger(y)\right\rangle &= e^{i\left[\left(K_s' - K_s\right)(x - x_s) + \left(K_d' - K_d\right)(y - x_d)\right]} \\ &\times \left\langle J_\mu(x_s)J_\nu^\dagger(x_d)\right\rangle + C_{\mu\nu}(x - y), \end{aligned} \tag{C.11}$$

where x_s and x_d are arbitrary space-time 4-vectors, and $C_{\mu\nu}(x)$ are the components of a certain tensor[68] such that $C_{\mu\nu}(x_s - x_d) = 0$.

A similar result may also be obtained for matrix element (C.8). Indeed, rewriting (C.8) in the explicit form

$$\begin{aligned} \left\langle J(x)J^\dagger(y)\right\rangle_T &= \theta(x_0 - y_0)\left\langle J(x)J^\dagger(y)\right\rangle \\ &+ \theta(y_0 - x_0)\left\langle J^\dagger(y)J(x)\right\rangle, \end{aligned}$$

[68] In the general case, this tensor may depend parametrically on the momenta and spins of the initial and final single-particle Fock states of hadrons.

and taking relation $(\partial/\partial x_\mu + \partial/\partial y_\mu)\theta(x_0 - y_0) = 0$ and (C.10) into account, we obtain the following equations:

$$i\left(\frac{\partial}{\partial x_\mu} + \frac{\partial}{\partial y_\mu}\right)\langle J(x)J^\dagger(y)\rangle_T = (K - K')^\mu \langle J(x)J^\dagger(y)\rangle_T. \quad \text{(C.12)}$$

Their solution coincides with (C.11), where $\langle\cdots\rangle$ is substituted by $\langle\cdots\rangle_T$. It is convenient for our purpose to choose the impact points for in- and out-packets in the source and detector as 4-vectors x_s and x_d, respectively. Since points X_s and X_d are macroscopically separated, currents $J(X_s)$ and $J^\dagger(X_d)$ are mutually commuting: $[J_\mu(X_s), J^\dagger_\nu(X_d)] = 0$. As a result, matrix element $\langle J_\mu(X_s)J^\dagger_\nu(X_d)\rangle_T$ is factorized into two cofactors that are associated with the source and detector vertices and depend on the corresponding variables only. Thus, having introduced 4-vectors (c-number hadronic currents)

$$\mathcal{J}_s(X_s;\{k_a,k_b\}) = e^{i(K_s-K_s)X_s}\langle\{k_b\}|J(X_s)|\{k_a\}\rangle, \quad a\in I_s,\ b\in F_s',$$

$$\mathcal{J}^*_d(X_d;\{k_a,k_b\}) = e^{i(K_d-K_d)X_d}\langle\{k_b\}|J^\dagger(X_d)|\{k_a\}\rangle, \quad a\in I_d,\ b\in F_d,$$

one obtains

$$\langle J_\mu(x)J^\dagger_\nu(y)\rangle_T = \exp\{i[(K_s - K_s)x + (K_d - K_d)y]\} \times J^\mu_s(X_s;\{k_a,k_b\})J^{\nu*}_d(X_d;\{k_a,k_b\}) + C_{\mu\nu}(x-y). \quad \text{(C.13)}$$

Tensor components $C_{\mu\nu}(x-y)$, which satisfy conditions

$$C_{\mu\nu}(X_s - X_d) = 0, \quad \text{(C.14)}$$

may feature a singularity (no stronger than a δ function or its derivatives) only at point $x = y$. At the same time, by virtue of condition (C.14), they should vanish after integration over x and y performed over sufficiently small space-time volumes surrounding the impact points. Functions $C_{\mu\nu}(x-y)$ enter the amplitude only via integral

$$\propto \int dxdy e^{iq(x-y)}C_{\mu\nu}(x-y) \times \psi^*_\alpha(\mathbf{p}_\alpha, x_\alpha - x)\psi^*_\beta(\mathbf{p}_\beta, x_\beta - y), \quad \text{(C.15)}$$

where ψ^*_α and ψ^*_β are ψ functions describing the WPs of final leptons ℓ^+_α and ℓ^-_β with momenta $\mathbf{p}_\alpha$ and $\mathbf{p}_\beta$, respectively. The contribution of product $\psi^*_\alpha\psi^*_\beta$ to the integrand in (C.15) is significant only within the classical world tubes located near the corresponding impact points. Therefore, the integrand in (C.15) is not negligible only if they have a considerable overlap region (in the limiting case, if the axes of lepton tubes coincide). However, this configuration is strongly suppressed by virtue of the approximate energy-momentum conservation. This is evident from the analysis of the simplest case with $C_{\mu\nu}(x-y) \propto \delta(x-y)$. Integral (C.15) is then proportional to the smeared δ function $\tilde{\delta}(p_\alpha + p_\beta)$ and is negligible, since $p^0_\alpha + p^0_\beta \geq m_\alpha + m_\beta$. These qualitative arguments enable one to ignore nonphysical long-range correlations induced by term $C_{\mu\nu}(x-y)$ in (C.13). By virtue of (C.8), one can rewrite the right-hand side of (233) as

$$\int\left[\prod_a \frac{d\mathbf{k}_a\phi_a(\mathbf{k}_a,\mathbf{p}_a)}{(2\pi)^3 2E_{\mathbf{k}_a}}e^{i[(k_a-p_a)x_a - k_a x]}\right] \times \int\left[\prod_b \frac{d\mathbf{k}_b\phi^*_b(\mathbf{k}_b,\mathbf{p}_b)}{(2\pi)^3 2E_{\mathbf{k}_b}}e^{-i[(k_b-p_b)x_b - k_b y]}\right] \times \mathcal{J}^\mu_s(X_s;\{k_a,k_b\})\mathcal{J}^{\nu*}_d(X_d;\{k_a,k_b\}).$$

Taking the properties of the form factor in $\phi_a(\mathbf{k}_a,\mathbf{p}_a)$ and $\phi_b(\mathbf{k}_b,\mathbf{p}_b)$ into account, one can substitute variables $\mathbf{k}_a$ and $\mathbf{k}_b$ in functions $\mathcal{J}_s$ and $\mathcal{J}_d$ by the corresponding external momenta $\mathbf{p}_a$ and $\mathbf{p}_b$. Having introduced this (last) approximation, we arrive at (235), thus completing the proof.

APPENDIX D

STATIONARY POINT FOR AN ARBITRARY CONFIGURATION OF MOMENTA OF EXTERNAL WAVE PACKETS

Let us detail the algorithm for solving Eq. (249) in the general case (i.e., for an arbitrary configuration of external momenta). The general solution is of interest both in the methodological context and for purposes of data processing in neutrino experiments at intermediate (subrelativistic) energies. Although the proposed algorithm is rather cumbersome, it is easy to implement in the form of a computer program and is thus convenient primarily for numerical analysis.

Form (267) of Eq. (249), where the velocity of a virtual neutrino is the unknown quantity, is more convenient to work with. Raising both parts of (267) to the second power, we arrive at algebraic equation of the fourth order

$$v^4 + c_3v^3 + c_2v^2 + c_1v + c_0 = 0, \quad \text{(D.1)}$$

with coefficients

$$c_0 = \frac{(\mathbf{Rl})^2 - (\boldsymbol{\eta}\mathbf{l})^2}{(\mathbf{Rl})^2 + \eta_0^2},$$
$$c_1 = -2\frac{R(\mathbf{Rl}) + 2(\mathbf{Rl})^2 - \eta_0(\boldsymbol{\eta}\mathbf{l})}{(\mathbf{Rl})^2 + \eta_0^2},$$
$$c_2 = \frac{R^2 + 6(\mathbf{Rl})^2 + 4R(\mathbf{Rl}) + (\boldsymbol{\eta}\mathbf{l})^2 - \eta_0^2}{(\mathbf{Rl})^2 + \eta_0^2},$$
$$c_3 = -2\frac{R(\mathbf{Rl}) + 2(\mathbf{Rl})^2 + \eta_0(\boldsymbol{\eta}\mathbf{l})}{(\mathbf{Rl})^2 + \eta_0^2}.$$

Here, $\eta_\mu = Y_\mu/m_j$; it is assumed from now on that $m_j > 0$ (the case of a massless neutrino is trivial), and index "j" numbering neutrinos is omitted to simplify the formulas, which are already cumbersome enough. The other designations are the same as in the main text. Equation (D.1) can be solved using the Descartes–Euler method (see, e.g., [141]). Following the corresponding algorithm, we write Eq. (D.1) in the "incomplete" form

$$\left(v + \frac{c_3}{4}\right)^4 + \tilde{c}_2\left(v + \frac{c_3}{4}\right)^2 + \tilde{c}_1\left(v + \frac{c_3}{4}\right) + \tilde{c}_0 = 0. \quad \text{(D.2)}$$

The solutions of this equation are constructed from the roots of cubic equation

$$z^3 + a_2 z^2 + a_1 z + a_0 = 0, \quad \text{(D.3)}$$

where

$$a_0 = -\frac{\tilde{c}_1^2}{64}, \quad a_1 = \frac{\tilde{c}_2^2 - 4\tilde{c}_0}{16}, \quad a_2 = \frac{\tilde{c}_2}{2}.$$

Equation (D.3) may also be reduced to the incomplete (Cardano) form:

$$\left(z + \frac{a_2}{3}\right)^3 + \mathfrak{p}\left(z + \frac{a_2}{3}\right) + \mathfrak{q} = 0.$$

Here,

$$\mathfrak{p} = a_1 - \frac{a_2^2}{3} = -\frac{\left[R^2 + 4R(\mathbf{Rl}) - \eta_0^2 + (\boldsymbol{\eta}\mathbf{l})^2\right]^2}{48\left[(\mathbf{Rl})^2 + \eta_0^2\right]^2},$$
$$\mathfrak{q} = a_0 - \frac{a_1 a_2}{3} + 2\left(\frac{a_2}{3}\right)^3 = -\frac{A}{864\left[(\mathbf{Rl})^2 + \eta_0^2\right]^3},$$
$$A = A_0 + A_1(\mathbf{Rl}) + A_2(\mathbf{Rl})^2 + A_3(\mathbf{Rl})^3,$$
$$A_0 = R^6 - 3\left[\eta_0^2 - (\boldsymbol{\eta}\mathbf{l})^2\right]R^4$$
$$+ 3\left[\eta_0^4 + 16\eta_0^2(\boldsymbol{\eta}\mathbf{l})^2 + (\boldsymbol{\eta}\mathbf{l})^4\right]R^2 - \left[\eta_0^2 - (\boldsymbol{\eta}\mathbf{l})^2\right]^3,$$
$$A_1 = 12R\left\{R^4 - 2\left[\eta_0^2 - (\boldsymbol{\eta}\mathbf{l})^2\right]R^2\right.$$
$$\left. + \left[\eta_0^2 - 7\eta_0(\boldsymbol{\eta}\mathbf{l}) + (\boldsymbol{\eta}\mathbf{l})^2\right](\eta l)^2\right\},$$
$$A_2 = 48R^2\left[R^2 - \eta_0^2 + (\boldsymbol{\eta}\mathbf{l})^2\right] + 54(\eta l)^4,$$
$$A_3 = 64R^3.$$

The number of real roots is defined by the sign of function

$$\mathfrak{V} = \frac{\mathfrak{q}^2}{4} + \frac{\mathfrak{p}^3}{27} = \frac{\left[\eta_0(\boldsymbol{\eta}\mathbf{l})R - (\eta l)^2(\mathbf{Rl})\right]^2 B}{27\,648\left[(\mathbf{Rl})^2 + \eta_0^2\right]^6},$$

which coincides with the sign of polynomial $B = B_0 + B_1(\mathbf{Rl}) + B_2(\mathbf{Rl})^2 + B_3(\mathbf{Rl})^3$ with coefficients

$$B_0 = R^6 - 3\left[\eta_0^2 - (\boldsymbol{\eta}\mathbf{l})^2\right]R^4$$
$$+ 3\left[\eta_0^4 + 7\eta_0^2(\boldsymbol{\eta}\mathbf{l})^2 + (\boldsymbol{\eta}\mathbf{l})^4\right]R^2 - \left[\eta_0^2 - (\boldsymbol{\eta}\mathbf{l})^2\right]^3,$$
$$B_1 = 6R\left\{2R^4 - 4\left[\eta_0^2 - (\boldsymbol{\eta}\mathbf{l})^2\right]R^2\right.$$
$$\left. + \left[2\eta_0 - (\boldsymbol{\eta}\mathbf{l})\right]\left[\eta_0 - 2(\boldsymbol{\eta}\mathbf{l})\right](\eta l)^2\right\},$$
$$B_2 = 48R^2\left[R^2 - \eta_0^2 + (\boldsymbol{\eta}\mathbf{l})^2\right] + 27(\eta l)^4,$$
$$B_3 = 64R^3.$$

Three different real roots are found at $B < 0$; at $B > 0$, one real root and two mutually conjugate complex roots are present; at $B = 0$, two (or all three) real roots may coincide. The validity of the following useful identity may be proven:

$$A = B + 27\left[\eta_0(\boldsymbol{\eta}\mathbf{l})R - (\eta l)^2(\mathbf{Rl})\right]^2. \quad \text{(D.4)}$$

Del Ferro–Tartaglia–Cardano solution in radicals. The roots of incomplete cubic equation (D.3) are

$$z_0 = a + (A_+ + A_-),$$
$$z_\pm = a - \frac{1}{2}(A_+ + A_-) \pm i\frac{\sqrt{3}}{2}(A_+ - A_-),$$

where

$$a = \frac{a_2}{3} = -\frac{C_0 + C_1(\mathbf{Rl}) + C_2(\mathbf{Rl})^2 + C_3(\mathbf{Rl})^3}{12\left[(\mathbf{Rl})^2 + \eta_0^2\right]^2},$$
$$A_\pm^3 = -\frac{q}{2} \pm \sqrt{\mathfrak{V}} = \frac{\frac{A}{18} \pm i^\delta\left|\eta_0(\boldsymbol{\eta}\mathbf{l})R - (\eta l)^2(\mathbf{Rl})\right|\sqrt{\frac{|B|}{3}}}{96\left[(\mathbf{Rl})^2 + \eta_0^2\right]^3};$$
$$C_0 = -\eta_0^2\left[2R^2 - 2\eta_0^2 - (\boldsymbol{\eta}\mathbf{l})^2\right],$$
$$C_1 = -2\eta_0\left[4\eta_0 - 3(\boldsymbol{\eta}\mathbf{l})\right]R,$$
$$C_2 = R^2 - 2(\eta l)\left[5\eta_0 - (\boldsymbol{\eta}\mathbf{l})\right],$$
$$C_3 = 4R;$$

$\delta = 0$ at $B \geq 0$ and $\delta = 1$ at $B < 0$. The expression for $A_\pm$ is simplified if identity (D.4) is taken into account:

$$A_\pm = \frac{\left[3\sqrt{3}\left|\eta_0(\boldsymbol{\eta}\mathbf{l})R - (\eta l)^2(\mathbf{Rl})\right| \pm i^\delta\sqrt{|B|}\right]^{2/3}}{12\left[(\mathbf{Rl})^2 + \eta_0^2\right]}.$$

Solution in the Vieta's trigonometric representation. For completeness, we also present the more compact trigonometric solution (Vieta's representation), which may turn out to be more convenient for numerical cal-

culations. If nothing else, it is useful for monitoring the accuracy of calculations by means of comparison with the canonical solution. The explicit form of the trigonometric solution depends on the sign of function B.

$B < 0$. As was already noted, Eq. (D.3) has three real roots in this case (sometimes called the irreducible case):

$$z_0 = a + \zeta_0 \cos\frac{\alpha}{3},$$
$$z_\pm = a - \zeta_0 \cos\left(\frac{\alpha \pm \pi}{3}\right),$$

where

$$\zeta_0 = \frac{\left|R^2 + 4R(\mathbf{Rl}) - \eta_0^2 + (\eta\mathbf{l})^2\right|}{6\left[(\mathbf{Rl})^2 + \eta_0^2\right]},$$
$$\cos\alpha = -\frac{A}{\left|R^2 + 4R(\mathbf{Rl}) - \eta_0^2 + (\eta\mathbf{l})^2\right|}.$$

$B \geq 0$. Equation (D.3) has one real and two complex roots. Let us introduce the following notation[69]:

$$\tan\alpha' = \sqrt[3]{\tan\frac{\beta}{2}}, \quad \sin\beta = -\frac{4}{\cos\alpha}$$
$$= \frac{4}{A}\left|R^2 + 4R(\mathbf{Rl}) - \eta_0^2 + (\eta\mathbf{l})^2\right|^3.$$

Then, the roots are

$$z_0 = a - \zeta_0 \mathrm{cosec} 2\alpha',$$
$$z_\pm = a + \frac{1}{2}\zeta_0\left(\mathrm{cosec} 2\alpha' \pm i\sqrt{3}\cot 2\alpha'\right).$$

Roots of Eq. (D.1). The roots of incomplete equation of the fourth order (D.2) are given by combinations

$$\Xi_n = \pm\sqrt{z_-} \pm \sqrt{z_0} \pm \sqrt{z_+},$$

where four out of the possible eight combinations of signs are chosen so that condition

$$-\sqrt{z_-}\sqrt{z_0}\sqrt{z_+} = \frac{\tilde{c}_1}{8}$$
$$= \frac{D_0 + D_1(\mathbf{Rl}) + D_2(\mathbf{Rl})^2 + D_3(\mathbf{Rl})^3 + D_4(\mathbf{Rl})^4}{8\left[(\mathbf{Rl})^2 + \eta_0^2\right]^3}$$

is satisfied. Here,

$$D_0 = \eta_0^3(\eta\mathbf{l})\left(R^2 + \eta_0^2\right),$$
$$D_1 = \eta_0^2\left[R^2 - 3\eta_0^2 + 4\eta_0(\eta\mathbf{l}) - 2(\eta\mathbf{l})^2\right]R,$$
$$D_2 = \eta_0\left\{2\left[3\eta_0 - (\eta\mathbf{l})\right]R^2 - (\eta l)\right.$$
$$\left.\times\left[6\eta_0^2 - 3\eta_0(\eta\mathbf{l}) + (\eta\mathbf{l})^2\right]\right\},$$
$$D_3 = \left[9\eta_0^2 - 8\eta_0(\eta\mathbf{l}) + (\eta\mathbf{l})^2\right]R,$$
$$D_4 = 2(\eta l)^2.$$

[69] Note that $|\alpha'| \leq \pi/4$ and $|\beta| \leq \pi/2$; the real value of the cubic root is taken in all cases.

All four roots of Eq. (D.1) can then be derived using formula

$$v_n = \Xi_n - c_3/4 \quad (n = 1, 2, 3, 4).$$

The real nonnegative root of interest to us, which corresponds to the stationary point, should satisfy the condition of positivity of the second derivative (251). The solutions found in the main text for two opposite limiting cases ($1 - v \ll 1$ and $v \sim 1$) may serve as additional criteria of uniqueness of the solution of the general form based on the algorithm described here, since they should "join" the correct numerical solution smoothly under the corresponding variations of momenta of the external WPs and discrete parameters defining the effective velocity of a virtual neutrino.

APPENDIX E

SPREADING OF A NEUTRINO WAVE PACKET AT EXTREMELY LONG DISTANCES

Let us consider the generalization of some results from the main text to the case with spreading of an effective neutrino packet at astronomical distances. This generalization can apply in the processing of data from neutrino telescopes (Baikal GVD, IceCube, KM3Net ARCA, etc.), various experiments on radio detection of ultrahigh-energy neutrinos, and future orbital experiments that are aimed, among other things, at measuring the flavor composition of neutrino and antineutrino fluxes from remote astrophysical sources.

The integration over x^0 in (302) yields the following expression for the decoherence factor:

$$S_{ij} = \frac{\sqrt{\pi}}{4\tilde{\mathfrak{D}}_{ij}}\exp(\Phi_{ij})\int_{y_1^0}^{y_2^0} dy^0$$
$$\times\left\{\mathrm{erf}\left[2\tilde{\mathfrak{D}}_{ij}\left(y^0 - x_1^0 - \frac{L}{v_{ij}}\right) + \frac{i\Delta E_{ij}}{4\tilde{\mathfrak{D}}_{ij}}\right]\right. \quad \text{(E.1)}$$
$$\left. - \mathrm{erf}\left[2\tilde{\mathfrak{D}}_{ij}\left(y^0 - x_2^0 - \frac{L}{v_{ij}}\right) + \frac{i\Delta E_{ij}}{4\tilde{\mathfrak{D}}_{ij}}\right]\right\},$$

$$\Phi_{ij} = -\left(\frac{1}{v_i} - \frac{1}{v_j}\right)^2\left(\frac{\tilde{\mathfrak{D}}_i^*\tilde{\mathfrak{D}}_j}{\tilde{\mathfrak{D}}_{ij}}\right)^2 L^2$$
$$- \left(\frac{\Delta E_{ij}}{4\tilde{\mathfrak{D}}_{ij}}\right)^2 + i\left(\frac{\Delta E_{ij}}{v_{ij}} - \Delta P_{ij}\right)L. \quad \text{(E.2)}$$

Here,

$$\Delta P_{ij} = P_i - P_j, \quad \Delta E_{ij} = E_i - E_j,$$
$$\frac{1}{v_{ij}} = \frac{1}{2\tilde{\mathfrak{D}}_{ij}^2}\left[\frac{\left(\tilde{\mathfrak{D}}_i^*\right)^2}{v_i} + \frac{\tilde{\mathfrak{D}}_j^2}{v_j}\right],$$
$$\tilde{\mathfrak{D}}_{ij}^2 = \frac{1}{2}\left[\left(\tilde{\mathfrak{D}}_i^*\right)^2 + \mathfrak{D}_j^2\right],$$

and the other notations are the same as in the main text. Using the primitive of error function (306) introduced in the main text and integrating over y^0 in (E.1), we find the generalization of formula (303):

$$S_{ij} = \frac{\sqrt{\pi}}{8\tilde{\mathfrak{D}}_{ij}^2}\exp(\Phi_{ij})\sum_{l,l'=1}^{2}(-1)^{l+l'+1} \times \mathrm{Ierf}\left[2\tilde{\mathfrak{D}}_{ij}\left(x_l^0 - y_{l'}^0 + \frac{L}{v_{ij}}\right) - i\frac{\Delta E_{ij}}{4\tilde{\mathfrak{D}}_{ij}}\right]. \quad \text{(E.3)}$$

Although this expression is much more complex than (303), there are no difficulties in analyzing the decoherence effects numerically. In the present section, we examine only the key properties of complex-valued phase Φ_{ij}. To this end, we need to isolate real and imaginary parts of the phase and determine the length scales governing its behavior.

Using the definitions introduced above and dropping evidently small corrections, we find[70]

$$v_{ij} = \frac{(\tau_i - \tau_j)\left(\frac{\tau_i}{v_j} - \frac{\tau_j}{v_i}\right) + 2\left(\frac{1}{v_i} + \frac{1}{v_j}\right) - i(\tau_i + \tau_j)\left(\frac{1}{v_i} - \frac{1}{v_j}\right)}{\left(\frac{1}{v_i} + \frac{1}{v_j}\right)^2 + \left(\frac{\tau_i}{v_j} - \frac{\tau_j}{v_i}\right)^2},$$

$$\tilde{\mathfrak{D}}_{ij}^2 = \frac{D^2\left[2 + \tau_i^2 + \tau_j^2 + i(1 - \tau_i\tau_j)(\tau_i - \tau_j)\right]}{2(1+\tau_i^2)(1+\tau_j^2)}, \quad \left(\frac{\tilde{\mathfrak{D}}_i^*\tilde{\mathfrak{D}}_j}{\tilde{\mathfrak{D}}_{ij}}\right)^2 = \frac{\mathfrak{D}^2}{1 - i\tau_{ij}}.$$

Inserting these expressions into (E.2), one obtains

$$\Phi_{ij} = -\frac{1}{1+\mathfrak{r}_{ij}^2}\left[\frac{\Delta E_{ij}}{4\mathfrak{D}_{ij}} + \frac{\mathfrak{r}_i + \mathfrak{r}_j}{2}\left(\frac{1}{v_i} - \frac{1}{v_j}\right)\mathfrak{D}_{ij}L\right]^2 - \left(\frac{1}{v_i} - \frac{1}{v_j}\right)^2\mathfrak{D}_{ij}^2L^2 + i\left\{\left[\frac{1}{2}\left(\frac{1}{v_i} + \frac{1}{v_j}\right) - \frac{\mathfrak{r}_{ij}(\mathfrak{r}_i + \mathfrak{r}_j)}{4(1+\mathfrak{r}_{ij}^2)}\left(\frac{1}{v_i} - \frac{1}{v_j}\right)\right]\Delta E_{ij} - \Delta P_{ij}\right\}L + \frac{i\mathfrak{r}_{ij}}{1+r_{ij}}\left[(1 - \mathfrak{r}_i\mathfrak{r}_j)\left(\frac{\Delta E_{ij}}{4\mathfrak{D}}\right)^2 - \left(\frac{1}{v_i} - \frac{1}{v_j}\right)^2\mathfrak{D}^2L^2\right], \quad \text{(E.4)}$$

where

$$\mathfrak{D}_{ij} = \mathfrak{D}\left(1 + \frac{\mathfrak{r}_i^2 + \mathfrak{r}_j^2}{2}\right)^{-1/2}, \quad \mathfrak{r}_{ij} = \frac{\mathfrak{r}_i - \mathfrak{r}_j}{2} \approx \frac{2\Delta m_{ij}^2\mathfrak{D}^2L}{E_\nu^3}. \quad \text{(E.5)}$$

It follows from the analysis of (E.4) that the real part of phase Φ_{ij} becomes independent of L within two (strongly) spatially separated regions defined by the following conditions:

$$L \ll \mathfrak{L} = \frac{\mathfrak{n}E_\nu}{4\mathfrak{D}^2},$$

and

$$L \gg \mathfrak{L}_{ij} = \begin{cases} \dfrac{E_\nu}{2(m_i^2 + m_j^2)}\left(\dfrac{E_\nu}{\mathfrak{D}}\right)^2 \\ \text{if} \quad m_i \gg m_j \quad \text{or} \quad m_i \gg m_j, \\ \dfrac{E_\nu}{2|m_i^2 - m_j^2|}\left(\dfrac{E_\nu}{\mathfrak{D}}\right)^2 \\ \text{if} \quad |m_i - m_j| \ll m_i + m_j. \end{cases}$$

The corresponding asymptotic values of $\mathrm{Re}\Phi_{ij}$ calculated to an accuracy of $\mathbb{O}(r_{i,j})$ take the form

$$\mathrm{Re}\Phi_{ij}\big|_{L\ll\mathfrak{L}} \approx \mathrm{Re}\Phi_{ij}^0 = -\left(\frac{\pi\mathfrak{n}}{2\mathfrak{D}L_{ij}}\right)^2\left[1 + \frac{\mathfrak{m}}{\mathfrak{n}}(r_i + r_j)\right], \quad \text{(E.6a)}$$

$$\mathrm{Re}\Phi_{ij}\big|_{L\gg\mathfrak{L}_{ij}} \approx \mathrm{Re}\Phi_{ij}^\infty = -\left(\frac{E_\nu}{4\mathfrak{D}}\right)^2[1 - 4(\mathfrak{n}+1)(r_i + r_j)]. \quad \text{(E.6b)}$$

Here and elsewhere, the common definitions for oscillation lengths and differences between the neutrino masses squared are used:

$$L_{ij} = \frac{4\pi E_\nu}{\Delta m_{ij}^2}, \quad \Delta m_{ij}^2 = m_i^2 - m_j^2 \quad (i \neq j).$$

It can be seen that the asymptotics at large L, $\mathrm{Re}\Phi_{ij}^\infty$, is almost independent of neutrino masses and factor $\mathfrak{n}$; both $\mathrm{Re}\Phi_{ij}^0$ and $\mathrm{Re}\Phi_{ij}^\infty$ become arbitrarily large if $\mathfrak{D}$ tends to zero. In addition, obvious relations

$$\mathfrak{L}_{ij} = \frac{\mathfrak{L}}{\mathfrak{n}|r_i \pm r_j|} \quad \text{and} \quad \mathrm{Re}\Phi_{ij}^0 = \mathfrak{n}(r_i - r_j)\mathrm{Re}\Phi_{ij}^\infty[1 + \mathbb{O}(r_{i,j})]$$

[70] Note that $v_{jj} = v_j$, $\tilde{\mathfrak{D}}_{jj}^2 = \mathfrak{D}^2/(1+r_j^2)$, and $|\tilde{\mathfrak{D}}_j|^2/\tilde{\mathfrak{D}}_{jj} = \mathfrak{D}$.

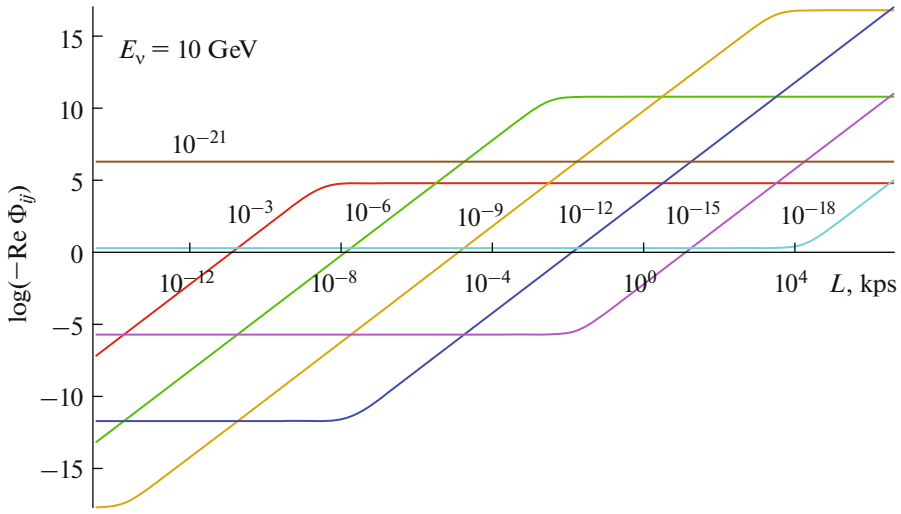

Fig. 25. Variation of function $\log|\mathrm{Re}\Phi_{ij}|$ with L (in kiloparsecs) calculated at $m_i = 0.1$ eV, $m_j = 0.01$ eV, and $E_\nu = 10$ GeV for seven values of ratio $\mathfrak{D}/E_\nu$ (indicated next to the curves). Function n was estimated under the assumption that the dominant contribution to it is produced by the $\pi_{\mu 2}$ decay in the source.

lead to model-independent inequalities

$$\mathfrak{L} \ll \mathfrak{L}_{ij} \quad \text{and} \quad \left|\mathrm{Re}\Phi_{ij}^{0}\right| \ll \left|\mathrm{Re}\Phi_{ij}^{\infty}\right|.$$

Therefore, as is seen from (E.4), a wide interval of distances $\mathfrak{L} \ll L \ll \mathfrak{L}_{ij}$, where $|\mathrm{Re}\Phi_{ij}|$ increases quadratically with L, exists for any pair of neutrinos ν_i, ν_j:

$$\mathrm{Re}\Phi_{ij} \approx -\left(\frac{1}{v_i} - \frac{1}{v_j}\right)^2 \mathfrak{D}^2 L^2 \approx -(r_i - r_j)^2 \mathfrak{D}^2 L^2.$$

All these features of behavior of the real part of phase are illustrated by Fig. 25, which presents function $\log|\mathrm{Re}\Phi_{ij}|$ within a wide range of L values, which vary from terrestrial ($\gtrsim 100$ km) to cosmological ($\sim 10^4$ Mpc) distances, at several arbitrary values of dimensionless ratio $\mathfrak{D}/E_\nu$. The curves in this figure were calculated for $m_i = 0.1$ eV, $m_j = 0.01$ eV, and $E_\nu = 10$ GeV. In order to estimate the value of important factor $\mathfrak{n}$, we assumed, for illustrative purposes, that it is saturated by the contribution from pion decays (the typical source of accelerator, atmospheric, and astrophysical neutrinos) and that the contribution of reactions in the detector is negligible. It was also assumed that the pion WP in the momentum space is much wider than the muon packet; i.e., $\sigma_\mu \ll \sigma_\pi$. It is then easy to demonstrate that factor n has the following approximate form at ultrarelativistic energies, $\Gamma_\pi \gg 1$:

$$\mathfrak{n} \approx (E_\nu/E_\nu^\star)^2 \approx (E_\nu/29.8\ \mathrm{MeV})^2 \approx 1.1\times 10^5.$$

The results of a similar analysis for the imaginary part of phase (E.4) reveal that this part increases linearly (although with different coefficients) with L in regions $L \ll \mathfrak{L}_{ij}$ and $L \gg \mathfrak{L}_{ij}$. In particular,

$$\mathrm{Im}\Phi_{ij}\big|_{L\ll\mathfrak{L}_{ij}} \approx \mathrm{Im}\Phi_{ij}^{\mathrm{st}} = \frac{2\pi L}{L_{ij}}\left[1 + n\mathfrak{n}(r_i + r_j)\right], \quad \text{(E.7a)}$$

$$\mathrm{Im}\Phi_{ij}\big|_{L\gg\mathfrak{L}_{ij}} \approx \mathrm{Im}\Phi_{ij}^{\infty} = \frac{3\pi L}{2L_{ij}}\left[1 + \frac{1}{3}(\mathfrak{n}+1)(r_i + r_j)\right]. \quad \text{(E.7b)}$$

These two regimes are separated by a relatively narrow transition region near $L = \mathfrak{L}_{ij}$. Nothing unexpected occurs in the $L \lesssim \mathfrak{L}$ region. This behavior of $\mathrm{Im}\Phi_{ij}$ is illustrated by Fig. 26, which shows the $\mathrm{Im}\Phi_{ij}/\mathrm{Im}\Phi_{ij}^{\mathrm{st}}$ ratio calculated with the same approximations that were used for the real part of the phase. The unconventional behavior of function $\mathrm{Im}\Phi_{ij}$ at $L \gtrsim \mathfrak{L}_{ij}$ is of a purely academic interest, since it is rendered unmeasurable by an enormous suppression factor

$$\propto \left(1 + \mathfrak{r}_{ij}^2\right)^{-1/4} \exp\left[-E_\nu^2/(16\mathfrak{D}^2)\right],$$

which eliminates interference terms ($i \neq j$) found in the expression for the event count rate. Thus, the oscillatory behavior of the count rate is encountered only at $L \ll \min(\mathfrak{L}_{ij})$. This is exactly the region that was examined thoroughly in the main text.

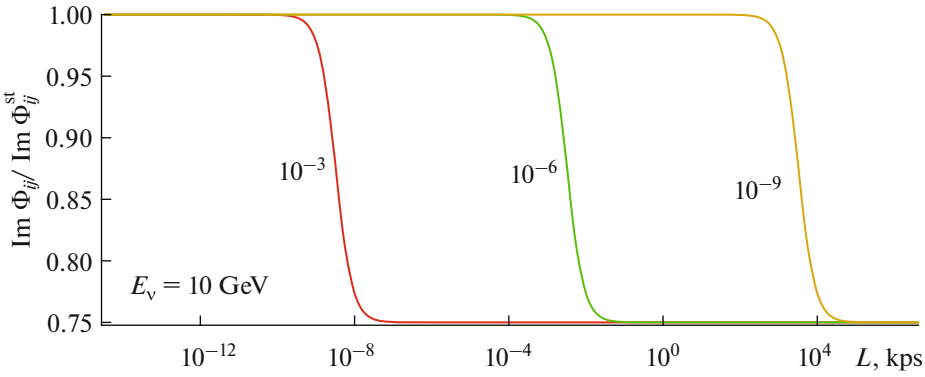

Fig. 26. Ratio $\mathrm{Im}_{ij}\big/\mathrm{Im}\Phi_{ij}^{\mathrm{st}}$ as a function of L calculated with the same parameters as those used for the real part of the phase (see the caption of Fig. 25) for three values of ratio $\mathcal{D}\big/E_\nu$ (indicated next to the curves).

APPENDIX F

SPATIAL AVERAGING

In realistic scenarios, the sizes of the source and detector are not always negligible compared to the distance between them. If this is the case, one needs to perform accurate spatial averaging of the count rate over the effective volumes of the source and detector. The plausible spatial inhomogeneities of the neutrino beam and the detector medium need to be taken into account. In the present section, we limit ourselves to the simple (but methodologically interesting) case when such inhomogeneities are negligible. This implies that density functions $\overline{f}_a(\mathbf{p}_a, s_a; \mathbf{x})$ are independent of $\mathbf{x}$ within the source and detector volumes and turn to zero outside the bounds of these volumes. Within these approximations, we are interested only in L-dependent factor $e^{\Phi_{ij}(L)}\big/L^2$ (with $\Phi_{ij}(L) = i\varphi_{ij}(L) - \mathscr{A}_{ij}(L)^2$) in the complete expression for the count rate; it is worth reminding that $\mathscr{B}_{ij}^2$ and Θ_{ij} do not depend on L.

The following simplification is also adopted below: the linear size of the detector in the direction of the neutrino beam is assumed to be negligible compared to the size of the source in the same direction, which, in turn, is small compared to the average source–detector distance. The origin of coordinates is located within the detector (point O_d in Fig. 27), and axis z is codirectional with unit vector $-\mathbf{l}$ (i.e., directed toward a certain inner point O_s of the source). Let $\mathbf{x} = L\mathbf{l}$ and $L = O_sO_d$; the sought-for integral over the spatial volume of the source may then be written as follows:

$$\mathscr{J}_{ij} \equiv \int\limits_{\mathrm{V}_s} \frac{d\mathbf{x}}{L^2} e^{\Phi_{ij}(L)} = \int\limits_{\Omega_s} d\boldsymbol{\Omega} \int\limits_{L_\Omega^N}^{L_\Omega^F} dL e^{\Phi_{ij}(L)}. \qquad \text{(F.1)}$$

Here, V_s is the working volume of the source, Ω_s is the solid angle under which this volume is seen from point O_d, and L_Ω^N and L_Ω^F are the distances from O_d to the near and far boundaries of the source (for simplicity, it is assumed to be convex) along unit vector $\boldsymbol{\Omega} = (\sin\phi\sin\theta, \cos\varphi\sin\theta, \cos\theta)$. It is convenient to introduce the following measure of distance between the source and detector:

$$\overline{L} = \frac{1}{2\Omega_s} \int\limits_{\Omega_s} d\boldsymbol{\Omega} \left(L_\Omega^F + L_\Omega^N\right).$$

To avoid any misunderstanding, we note that, depending on the angular resolution of the detector and features of the experimental setup, solid angle Ω_s may turn out to be smaller than the full solid angle under which the source is seen. Figure 27 illustrates this possibility schematically, while equality (F.1) holds true in the general case. Note also that the smallness of angle Ω_s is not equivalent to the smallness of the source itself; a well-collimated meson beam from an accelerator (neutrino factory) in a long decay channel is an important counterexample. Elementary integration over L yields

$$\mathscr{J}_{ij} = \frac{E_\nu L_{ij}}{4\sqrt{\pi}D} \int\limits_{\Omega_s} d\boldsymbol{\Omega} \times \left[\mathrm{erf}\left(\frac{2\pi D L_\Omega^F}{E_\nu L_{ij}} - \frac{iE_\nu}{2D}\right) - \mathrm{erf}\left(\frac{2\pi D L_\Omega^N}{E_\nu L_{ij}} - \frac{iE_\nu}{2D}\right)\right] \times \exp\left[-\frac{2E_\nu^2 + (\Delta E_{ij})^2}{8D^2}\right] \quad (i \neq j), \qquad \text{(F.2a)}$$

and

$$\mathscr{J}_{jj} = \int\limits_{\mathrm{V}_s} \frac{d\mathbf{x}}{L^2} = \int\limits_{\Omega_s} d\boldsymbol{\Omega} \left(L_\Omega^F - L_\Omega^N\right). \qquad \text{(F.2b)}$$

These general formulas may be used in processing the data of short-baseline neutrino experiments, where the distance from the source (e.g., a decay channel) to the detector is comparable to the longitudinal size of the source.

In an ideal experiment with

$$r_N = \max_{\Omega\in\Omega_s}\left(\bar{L} - L^N_\Omega\right) \ll \bar{L}$$
$$\text{and} \quad r_F = \max_{\Omega\in\Omega_s}\left(L^F_\Omega - \bar{L}\right) \ll \bar{L}, \tag{F.3}$$

one can use the following expansion of the error function:

$$\operatorname{erf}(z+\delta) \approx \operatorname{erf}(z) + \frac{2\delta}{\sqrt{\pi}} e^{-z^2}\left[1 - z\delta + \frac{2}{3}(2z^2-1)\delta^2 + \ldots\right]. \tag{F.4}$$

The contributions of order $\mathbb{O}(\delta^2)$ and $\mathbb{O}(z^2\delta^2)$ in this expansion may be neglected under the assumption that $|\delta| \ll 1$ and $|z\delta| \ll 1$. In the case under consideration, the first condition implies that

$$\frac{2\pi D r_{N,F}}{E_\nu L_{ij}} \ll 1, \tag{F.5}$$

while the second one is not necessary due to the approximate cancellation of terms of second order. Using (F.4), we indeed find that

$$\mathcal{J}_{ij} \approx \int_{\Omega_s} d\boldsymbol{\Omega}\left(L^F_\Omega - L^N_\Omega\right) e^{\Phi_{ij}(\bar{L})} \times\left\{1 - \Delta_\Omega\left[\frac{2i\pi\bar{L}}{L_{ij}} - \left(\frac{2\pi D\bar{L}}{E_\nu L_{ij}}\right)^2\right]\right\},$$

where

$$\Delta_\Omega = 2\left(1 - \frac{L^N_\Omega + L^F_\Omega}{2\bar{L}}\right) = \frac{L^F_\Omega - \bar{L}}{\bar{L}} - \frac{\bar{L} - L^N_\Omega}{\bar{L}}.$$

Evidently, $|\Delta_\Omega| \ll 1$. Assuming that

$$\max_{\Omega\in\Omega_s}\Delta_\Omega\left[\left(\frac{2\pi D\bar{L}}{E_\nu L_{ij}}\right)^4 + \left(\frac{2\pi\bar{L}}{L_{ij}}\right)^2\right]^{1/2} \ll 1, \tag{F.6}$$

we arrive at the following result (valid for any i and j):

$$\mathcal{J}_{ij} \approx e^{\Phi_{ij}(\bar{L})}\int_{\Omega_s} d\boldsymbol{\Omega}\left(L^F_\Omega - L^N_\Omega\right) \approx \mathrm{V}_s\frac{e^{\Phi_{ij}(\bar{L})}}{\bar{L}^2}, \tag{F.7}$$

which could be deduced from the mean-value theorem. Our result, however, is supplemented by fairly nontrivial sufficient conditions (F.3), (F.5), and (F.6), which are impossible to obtain from the mean-value theorem alone. Volume V_s in (F.7) is estimated (with the same accuracy) as

$$\mathrm{V}_s = \int_{\mathrm{V}_s} d\mathbf{x} = \frac{1}{3}\int_{\Omega_s} d\boldsymbol{\Omega}\left[\left(L^F_\Omega\right)^3 - \left(L^N_\Omega\right)^3\right] \approx \bar{L}^2\int_{\Omega_s} d\boldsymbol{\Omega}\left(L^F_\Omega - L^N_\Omega\right).$$

If we now assume that working (reference) detector volume V_d is sufficiently small compared to V_s (this condition is satisfied in a typical neutrino experiment) and that the detector geometry is not too fancy, the integration over $\mathbf{y}$ becomes trivial and yields

$$\int_{\mathrm{V}_d} d\mathbf{y}\int_{\mathrm{V}_s} d\mathbf{x}\frac{e^{\Phi_{ij}(L)}}{L^2} \approx \mathrm{V}_s\mathrm{V}_d\frac{e^{\Phi_{ij}(\bar{L})}}{\bar{L}^2}, \tag{F.8}$$

where $\bar{L}$ still denotes the conventional measure of distance between the source and detector.

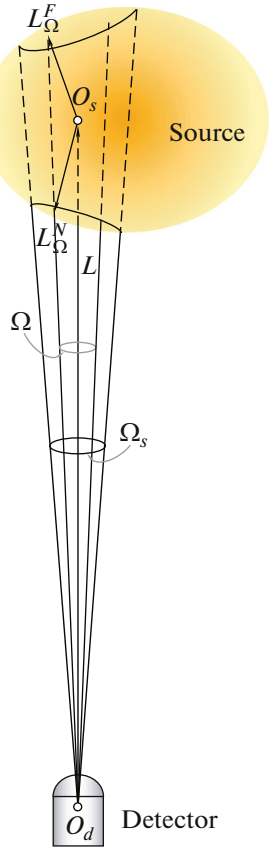

Fig. 27. Schematic illustration of spatial averaging.

In order to illustrate the importance and nontrivial nature of conditions (F.3), (F.5), and (F.6), we consider the simplest case of a spheroidal source with radius r. Its angular size θ_s does not exceed the angular resolution of the detector. It follows from simple geometric considerations that $\Delta_\Omega = 2(1-\cos\theta)$ and, naturally, $r_N = r_F = r$. Therefore,

$$\max_{\Omega\in\Omega_s}\Delta_\Omega = \Delta_{\Omega_s} = 2(1-\cos\theta_s) \approx \theta_s^2 \approx \left(r/\bar{L}\right)^2. \tag{F.9}$$

To simplify the scenario further, we assume that $2\pi\bar{L} \gg |L_{ij}|$ (this inequality is always fulfilled for solar and astrophysical neutrinos detected on the Earth) and $2\pi\bar{L} \lesssim |L_{ij}|E_\nu/D$ (this is not always true for remote astrophysical sources, but is valid for the Sun).

Condition (F.5) is then satisfied automatically, while condition (F.6) takes the form

$$\frac{2\pi r^2}{\bar{L}|L_{ij}|} \ll 1. \quad \text{(F.10)}$$

This inequality is definitely not fulfilled for the Sun and the currently adopted value of Δm^2_{12}. The regions of efficient neutrino production in the solar core are relatively thin concentric layers with typical radii varying from $0.1R_\odot$ for ^{8}B, ^{7}Be, and CNO neutrinos to $0.3R_\odot$ for *pp*, *pep*, and *hep* neutrinos[71] ($R_\odot$ is the solar radius). The left-hand side of (F.10) may then be estimated as

$$\frac{2\pi r^2}{\bar{L}|L_{12}|} \approx 26\left(\frac{r}{0.2R_\odot}\right)^2\left(\frac{|\Delta m^2_{12}|}{8\times10^{-5}\ \text{eV}^2}\right)\left(\frac{1\ \text{MeV}}{E_\nu}\right),$$

which demonstrates (and this is no news) that approximation (F.8) is definitely not applicable in the analysis of oscillations of solar neutrinos.

Summarizing the results, we note the following: although the above analysis was simplified in many respects[72], it demonstrates that the finite size of the source needs to be taken into account to process data correctly in both short-baseline oscillation experiments and very-long-baseline experiments (including the ones with L on the order of an astronomical unit, which is the case with experiments involving solar neutrinos).

APPENDIX G

COMPLEX ERROR FUNCTION AND ASSOCIATED FORMULAS

The error function and the complementary error function of complex argument have already been studied extensively (see, e.g., [146–150] and references therein). Let us list here some results that were used in Section 11 to analyze the decoherence function. For convenience, we first write the following well-known formulas [103]:

$$\text{erf}(z) = \frac{2}{\sqrt{\pi}}\sum_{n=0}^{\infty}\frac{(-1)^n z^{2n+1}}{(2n+1)n!} = \frac{2}{\sqrt{\pi}}e^{-z^2}\sum_{n=0}^{\infty}\frac{2^n z^{2n+1}}{(2n+1)!!}, \quad \text{(G.1)}$$

$$\text{erfc}(z) \sim \frac{e^{-z^2}}{\sqrt{\pi}z}\left[1+\sum_{n=1}^{\infty}\frac{(-1)^n(2n-1)!!}{(2z^2)^n}\right] \quad \text{(G.2)}$$
$$\left(z\to\infty, |\arg z| < \frac{3\pi}{4}\right).$$

[71] See [142, 143] for details.

[72] A more accurate analysis should cover the spatial distributions of colliding and/or decaying particles in the source and the effects of interaction of virtual neutrinos with the source medium (namely, coherent scattering of neutrinos off electrons in the medium, or the MSW effect [144, 145]), which are crucial for astrophysical applications such as experiments with solar neutrinos.

The following expansions for function $\text{Ierf}(z)$, which was introduced in the main text, are derived from (306) and (G.1):

$$\text{Ierf}(z) = \frac{1}{\sqrt{\pi}}\left[1+z^2-\frac{z^4}{6}+\frac{z^6}{30}-\frac{z^8}{168}+\mathbb{O}(z^{10})\right], \quad \text{(G.3a)}$$

$$= \frac{e^{-z^2}}{\sqrt{\pi}}\left[1+2z^2+\frac{4z^4}{3}+\frac{8z^6}{15}+\frac{16z^8}{105}+\mathbb{O}(z^{10})\right]. \quad \text{(G.3b)}$$

These expansions are useful for small and intermediate values of $|z|$[73], respectively. In order to determine the asymptotics of functions $\text{erfc}(z)$ and $\text{Ierf}(z)$ at large $|z|$, one needs to use (G.2) for $\text{erfc}(-z)$ and then apply the following rule:

$$\text{erfc}(z) = 2 - \text{erfc}(-z).$$

The result derived from (306) and (G.2) is

$$\text{Ierf}(z) \sim \pm z + \frac{e^{-z^2}}{2\sqrt{\pi}z^2} \times\left[1-\frac{3}{2z^2}+\frac{15}{4z^4}-\frac{105}{8z^6}+\mathbb{O}\left(\frac{1}{z^8}\right)\right] \quad (z\to\infty), \quad \text{(G.4)}$$

where the upper (lower) sign should be taken for $|\arg z| < 3\pi/4$ ($|\arg z| > 3\pi/4$).

The formulas given below are helpful in high-accuracy numerical calculations of the error function. They are based on the following integral representation of the complementary error function (see, e.g., [146, 149]):

$$\text{erfc}(z) = \frac{2z}{\pi}\int_0^\infty \frac{dte^{-(t^2+z^2)}}{t^2+z^2}.$$

From this it follows that (cf. the result in [147])

$$\text{Re}\left[\text{erfc}(a+ib)\right] = +\frac{r}{\pi}\exp\left[-r^2\cos(2\omega)\right] \times\left[r^2\cos(w_+)\mathcal{J}_0(a,b)+\cos(w_-)\mathcal{J}_2(a,b)\right],$$

$$\text{Im}\left[\text{erfc}(a+ib)\right] = -\frac{r}{\pi}\exp\left[-r^2\cos(2\omega)\right] \times\left[r^2\sin(w_+)\mathcal{J}_0(a,b)+\sin(w_-)\mathcal{J}_2(a,b)\right],$$

where

$$\mathcal{J}_n(a,b) = \int_{-\infty}^{\infty}\frac{dtt^n e^{-t^2}}{(t^2+a^2-b^2)^2+4a^2b^2} = \int_{-\infty}^{\infty}\frac{dtt^n e^{-t^2}}{\left[t^2+r^2\cos(2\omega)\right]^2+\left[r^2\sin(2\omega)\right]^2},$$

$$w_\pm = 2ab+\omega,\quad r=\sqrt{a^2+b^2},$$

$$\cos\omega = a/r,\ \sin\omega = b/r.$$

[73] In practice, (G.3a) and (G.3b) work fine at $|z| \lesssim 1$ and $1 \lesssim |z| \lesssim 4.5$, respectively.

All the quantities found here are real. Note that the integrands in integrals $\mathcal{J}_n(a, b)$ are positive, nonsingular (with the exception of the trivial case of $a = b = 0$), and decrease rapidly at large $|t|$. These properties are helpful in numerical integration based on the standard quadrature formulas.

ACKNOWLEDGMENTS

We would like to thank E.K. Akhmedov, V.A. Bednyakov, S.M. Bilenky, Z.G. Berezhiani, F. Vissani, M.I. Vysotsky, A.Z. Gazizov, M.O. Gonchar, D.S. Gorbunov, C. Giunti, I.P. Ivanov, I.D. Kakorin, A.E. Kaloshin, D.I. Kazakov, S.E. Korenblit, K.S. Kuzmin, V.A. Li, W. Potzel, V.A. Rubakov, D.V. Taichenachev, O.V. Teryaev, K.A. Treskov, A.I. Frank, A.S. Sheshukov, M.I. Shirokov, and D.S. Shkirmanov for stimulating discussions.

REFERENCES

1. E. Fermi, "Versuch einer Theorie der β-Strahlen. I," Z. Phys. **88**, 161–177 (1934).
2. J. Steinberger, "The history of neutrinos, 1930–1985. What have we learned about neutrinos? What have we learned using neutrinos?" Ann. Phys. **327**, 3182–3205 (2012).
3. E. Fermi, "Tentativo di una teoria dei raggi β," Ric. Sci. **4**, 491–495 (1933).
4. B. Pontecorvo, "Mesonium and antimesonium," Sov. Phys. JETP **6**, 429 (1957).
5. B. Pontecorvo, "Inverse β processes and nonconservation of lepton charge," Sov. Phys. JETP **7**, 172 (1957).
6. B. T. Cleveland et al., "Measurement of the solar electron neutrino flux with the Homestake chlorine detector," Astrophys. J. **496**, 505–526 (1998).
7. F. Kaether, W. Hampel, G. Heusser, J. Kiko, and T. Kirsten, "Reanalysis of the GALLEX solar neutrino flux and source experiments," Phys. Lett. B **685**, 47–54 (2010).
8. J. N. Abdurashitov et al., "Measurement of the solar neutrino capture rate with gallium metal. III: Results for the 2002–2007 data-taking period," Phys. Rev. C **80**, 015807 (2009).
9. Y. Fukuda et al., "Evidence for oscillation of atmospheric neutrinos," Phys. Rev. Lett. **81**, 1562–1567 (1998).
10. P. Adamson et al., "Combined analysis of ν_μ disappearance and $\nu_\mu \to \nu_e$ appearance in MINOS using accelerator and atmospheric neutrinos," Phys. Rev. Lett. **112**, 191801 (2014).
11. M. H. Ahn et al., "Indications of neutrino oscillation in a 250 km long baseline experiment," Phys. Rev. Lett. **90**, 041801 (2003).
12. S. Abe et al., "Precision measurement of neutrino oscillation parameters with KamLAND," Phys. Rev. Lett. **100**, 221803 (2008).
13. F. P. An et al., "Observation of electron-antineutrino disappearance at Daya Bay," Phys. Rev. Lett. **108**, 171803 (2012).
14. J. K. Ahn et al., "Observation of reactor electron antineutrino disappearance in the RENO experiment," Phys. Rev. Lett. **108**, 191802 (2012).
15. Y. Abe et al., "Reactor electron antineutrino disappearance in the Double Chooz experiment," Phys. Rev. D **86**, 052008 (2012).
16. Z. Maki, M. Nakagawa, and S. Sakata, "Remarks on the unified model of elementary particles," Prog. Theor. Phys. **28**, 870–880 (1962).
17. V. Gribov and B. Pontecorvo, "Neutrino astronomy and lepton charge," Phys. Lett. B **28**, 493–496 (1969).
18. Sh. Eliezer and A. R. Swift, "Experimental consequences of ν_e–ν_μ mixing in neutrino beams," Nucl. Phys. B **105**, 45–51 (1976).
19. H. Fritzsch and P. Minkowski, "Vector-like weak currents, massive neutrinos, and neutrino beam oscillations," Phys. Lett. B **62**, 72–76 (1976).
20. S. M. Bilenky and B. Pontecorvo, "Again on neutrino oscillations," Lett. Nuovo Cimento **17**, 569–574 (1976).
21. S. M. Bilenky and B. Pontecorvo, "Lepton mixing and neutrino oscillations," Phys. Rep. **41**, 225–261 (1978).
22. S. M. Bilenky, C. Giunti, and W. Grimus, "Phenomenology of neutrino oscillations," Prog. Part. Nucl. Phys. **43**, 1–86 (1999).
23. P. Fisher, B. Kayser, and K. S. McFarland, "Neutrino mass and oscillation," Annu. Rev. Nucl. Part. Sci. **49**, 481–528 (1999).
24. S. M. Bilenky, "Neutrino masses, mixing and oscillations," Proc. R. Soc. London A **460**, 403–444 (2004).
25. R. N. Mohapatra et al., "Theory of neutrinos: A white paper," Rep. Prog. Phys. **70**, 1757–1867 (2007).
26. M. C. Gonzalez-Garcia and M. Maltoni, "Phenomenology with massive neutrinos," Phys. Rep. **460**, 1–129 (2008).
27. S. Bilenky, "Introduction to the physics of massive and mixed neutrinos," Lect. Notes Phys. **817**, 1–255 (2010).
28. S. F. King, A. Merle, S. Morisi, Y. Shimizu, and M. Tanimoto, "Neutrino mass and mixing: From theory to experiment," New J. Phys. **16**, 045018 (2014).
29. S. F. King, "Models of neutrino mass, mixing and CP violation," J. Phys. G **42**, 123001 (2015).
30. S. Bilenky, "Introduction to the physics of massive and mixed neutrinos," Lect. Notes Phys. **947**, 1–273 (2018).
31. Yu. G. Kudenko, "Neutrino oscillations: Recent results and future prospects," Phys.-Usp. **61**, 739–747 (2018).
32. C. Giunti, C. W. Kim, J. A. Lee, and U. W. Lee, "On the treatment of neutrino oscillations without resort to weak eigenstates," Phys. Rev. D **48**, 4310–4317 (1993).
33. W. Grimus and P. Stockinger, "Real oscillations of virtual neutrinos," Phys. Rev. D **54**, 3414–3419 (1996).
34. C. Giunti, C. W. Kim, and U. W. Lee, "When do neutrinos cease to oscillate?" Phys. Lett. B **421**, 237–244 (1998).
35. J.-E. Campagne, "Neutrino oscillations from pion decay in flight," Phys. Lett. B **400**, 135–144 (1997).

36. K. Kiers and N. Weiss, "Neutrino oscillations in a model with a source and detector," Phys. Rev. D **57**, 3091–3105 (1998).
37. M. Zralek, "From kaons to neutrinos: Quantum mechanics of particle oscillations," Acta Phys. Pol., B **29**, 3925–3956 (1998).
38. A. Ioannisian and A. Pilaftsis, "Neutrino oscillations in space within a solvable model," Phys. Rev. D **59**, 053003 (1999).
39. W. Grimus, P. Stockinger, and S. Mohanty, "The field theoretical approach to coherence in neutrino oscillations," Phys. Rev. D **59**, 013011 (1999).
40. W. Grimus, S. Mohanty, and P. Stockinger, "Neutrino oscillations and the effect of the finite lifetime of the neutrino source," Phys. Rev. D **61**, 033001 (2000).
41. Ch. Y. Cardall and D. J. H. Chung, "The MSW effect in quantum field theory," Phys. Rev. D **60**, 073012 (1999).
42. Ch. Y. Cardall, "Coherence of neutrino flavor mixing in quantum field theory," Phys. Rev. D **61**, 073006 (2000).
43. M. Beuthe, "Propagation et oscillations en theorie des champs," arXiv:hep-ph/0010054 (2000).
44. P. Stockinger, "Introduction to a field-theoretical treatment of neutrino oscillation," Pramana **54**, 203–214 (2000).
45. M. Beuthe, "Oscillations of neutrinos and mesons in quantum field theory," Phys. Rep. **375**, 105–218 (2003).
46. M. Beuthe, "Towards a unique formula for neutrino oscillations in vacuum," Phys. Rev. D **66**, 013003 (2002).
47. C. Giunti, "Neutrino wave packets in quantum field theory," J. High Energy Phys. **2002** (11), 017 (2002).
48. M. Garbutt and B. H. J. McKellar, "Neutrino production, oscillation and detection in the presence of general four-fermion interactions," arXiv:hep-ph/0308111 (2003).
49. C. Giunti, "Coherence and wave packets in neutrino oscillations," Found. Phys. Lett. **17**, 103–124 (2004).
50. A. E. Bernardini and S. De Leo, "An analytic approach to the wave packet formalism in oscillation phenomena," Phys. Rev. D **70**, 053010 (2004).
51. A. Asahara, K. Ishikawa, T. Shimomura, and T. Yabuki, "Neutrino oscillations in intermediate states. II. Wave packets," Prog. Theor. Phys. **113**, 385–411 (2005).
52. A. D. Dolgov, O. V. Lychkovskiy, A. A. Mamonov, L. B. Okun, M. V. Rotaev, et al., "Oscillations of neutrinos produced and detected in crystals," Nucl. Phys. B **729**, 79–94 (2005).
53. C. C. Nishi, "First quantized approaches to neutrino oscillations and second quantization," Phys. Rev. D **73**, 053013 (2006).
54. J. Kopp, "Mössbauer neutrinos in quantum mechanics and quantum field theory," J. High Energy Phys. **2009** (06), 049 (2009).
55. E. Kh. Akhmedov and A. Yu. Smirnov, "Paradoxes of neutrino oscillations," Phys. At. Nucl. **72**, 1363–1381 (2009).
56. B. D. Keister and W. N. Polyzou, "Relativistic quantum theories and neutrino oscillations," Phys. Scr. **81**, 055102 (2010).
57. V. A. Naumov and D. V. Naumov, "Relativistic wave packets in a field theoretical approach to neutrino oscillations," Russ. Phys. J. **53**, 549–574 (2010).
58. D. V. Naumov and V. A. Naumov, "A diagrammatic treatment of neutrino oscillations," J. Phys. G **37**, 105014 (2010).
59. B. Kayser, J. Kopp, R. G. H. Robertson, and P. Vogel, "On a theory of neutrino oscillations with entanglement," Phys. Rev. D **82**, 093003 (2010).
60. E. Kh. Akhmedov and J. Kopp, "Neutrino oscillations: Quantum mechanics vs. quantum field theory," J. High Energy Phys. **2010** (04), 008 (2010).
61. E. Kh. Akhmedov and A. Yu. Smirnov, "Neutrino oscillations: Entanglement, energy-momentum conservation and QFT," Found. Phys. **41**, 1279–1306 (2011).
62. A. E. Bernardini, M. M. Guzzo, and C. C. Nishi, "Quantum flavor oscillations extended to the Dirac theory," Fortschr. Phys. **59**, 372–453 (2011).
63. E. Akhmedov, D. Hernandez, and A. Smirnov, "Neutrino production coherence and oscillation experiments," J. High Energy Phys. **2012** (04), 052 (2012).
64. E. Kh. Akhmedov and A. Wilhelm, "Quantum field theoretic approach to neutrino oscillations in matter," J. High Energy Phys. **2013** (01), 165 (2013).
65. T. R. Morris, "Superluminal velocity through near-maximal neutrino oscillations or by being off shell," J. Phys. G **39**, 045010 (2012).
66. C. Giunti and Ch. W. Kim, *Fundamentals of Neutrino Physics and Astrophysics* (Oxford Univ. Press, New York, 2007).
67. Sh. Nussinov, "Solar neutrinos and neutrino mixing," Phys. Lett. B **63**, 201–203 (1976).
68. B. Kayser, "On the quantum mechanics of neutrino oscillation," Phys. Rev. D **24**, 110 (1981).
69. C. Giunti, C. W. Kim, and U. W. Lee, "When do neutrinos really oscillate? Quantum mechanics of neutrino oscillations," Phys. Rev. D **44**, 3635–3640 (1991).
70. C. Giunti, C. W. Kim, and U. W. Lee, "Coherence of neutrino oscillations in vacuum and matter in the wave packet treatment," Phys. Lett. B **274**, 87–94 (1992).
71. J. Rich, "The quantum mechanics of neutrino oscillations," Phys. Rev. D **48**, 4318–4325 (1993).
72. K. Kiers, Sh. Nussinov, and N. Weiss, "Coherence effects in neutrino oscillations," Phys. Rev. D **53**, 537–547 (1996).
73. C. Giunti and C. W. Kim, "Coherence of neutrino oscillations in the wave packet approach," Phys. Rev. D **58**, 017301 (1998).
74. L. Stodolsky, "The unnecessary wave packet," Phys. Rev. D **58**, 036006 (1998).
75. M. Nauenberg, "Correlated wave packet treatment of neutrino and neutral meson oscillations," Phys. Lett. B **447**, 23–30 (1999).
76. M. I. Shirokov and V. A. Naumov, "Time-to-space conversion in neutrino oscillations," Concepts Phys. **4**, 121–138 (2007).
77. A. E. Bernardini, M. M. Guzzo, and F. R. Torres, "Second-order corrections to neutrino two-flavor os-

cillation parameters in the wave packet approach," Eur. Phys. J. C **48**, 613–623 (2006).

78. Y. F. Pérez and C. J. Quimbay, "Spreading of wave packets for neutrino oscillations," Int. J. Mod. Phys. A **29**, 1450007 (2014).
79. Y. Takeuchi, Y. Tazaki, S. Y. Tsai, and T. Yamazaki, "Wave packet approach to the equal-energy/momentum/velocity prescriptions of neutrino oscillation," Mod. Phys. Lett. A **14**, 2329–2339 (1999).
80. B. Kayser and J. Kopp, "Testing the wave packet approach to neutrino oscillations in future experiments," arXiv:1005.4081 [hep-ph] (2010).
81. D. Bruss and L. M. Sehgal, "Distinguishing a coherent from an incoherent mixture of neutrino flavor," Phys. Lett. B **216**, 426–430 (1989).
82. E. Lisi, A. Marrone, and D. Montanino, "Probing possible decoherence effects in atmospheric neutrino oscillations," Phys. Rev. Lett. **85**, 1166–1169 (2000).
83. T. Araki et al., "Measurement of neutrino oscillation with KamLAND: Evidence of spectral distortion," Phys. Rev. Lett. **94**, 081801 (2005).
84. M. Blennow, T. Ohlsson, and W. Winter, "Damping signatures in future neutrino oscillation experiments," J. High Energy Phys. **2005** (06), 049 (2005).
85. G. Barenboim, N. E. Mavromatos, S. Sarkar, and A. Waldron-Lauda, "Quantum decoherence and neutrino data," Nucl. Phys. B **758**, 90–111 (2006).
86. P. Adamson et al., "Measurement of neutrino oscillations with the MINOS detectors in the NuMI beam," Phys. Rev. Lett. **101**, 131802 (2008).
87. B. J. P. Jones, "Dynamical pion collapse and the coherence of conventional neutrino beams," Phys. Rev. D **91**, 053002 (2015).
88. F. P. An et al., "Study of the wave packet treatment of neutrino oscillation at Daya Bay," Eur. Phys. J. C **77**, 606 (2017).
89. A. Kobach, A. V. Manohar, and J. McGreevy, "Neutrino oscillation measurements computed in quantum field theory," Phys. Lett. B **783**, 59–75 (2018).
90. J. A. B. Coelho and W. A. Mann, "Decoherence, matter effect, and neutrino hierarchy signature in long-baseline experiments," Phys. Rev. D **96**, 093009 (2017).
91. J. A. B. Coelho, W. A. Mann, and S. S. Bashar, "Non-maximal θ_{23} mixing at NOvA from neutrino decoherence," Phys. Rev. Lett. **118**, 221801 (2017).
92. P. Coloma, J. Lopez-Pavon, I. Martinez-Soler, and H. Nunokawa, "Decoherence in neutrino propagation through matter, and bounds from IceCube/DeepCore," Eur. Phys. J. C **78**, 614 (2018).
93. G. Balieiro Gomes, D. V. Forero, M. M. Guzzo, P. C. de Holanda, and R. L. N. Oliveira, "Quantum decoherence effects in neutrino oscillations at DUNE," Phys. Rev. D **100**, 055023 (2019).
94. J. C. Carrasco, F. N. Díaz, and A. M. Gago, "Probing CPT breaking induced by quantum decoherence at DUNE," Phys. Rev. D **99**, 075022 (2019).
95. A. Capolupo, S. M. Giampaolo, and G. Lambiase, "Decoherence in neutrino oscillations, neutrino nature and CPT violation," Phys. Lett. B **792**, 298–303 (2019).
96. D. V. Naumov, "On the theory of wave packets," Phys. Part. Nucl. Lett. **10**, 642–650 (2013).
97. C. Almeida and A. Jabs, "Spreading of a relativistic wave packet," Am. J. Phys. **52**, 921–925 (1984).
98. J. R. Taylor, *Scattering Theory: The Quantum Theory of Nonrelativistic Collisions* (Wiley, 1972).
99. M. L. Goldberger and K. M. Watson, *Collision Theory* (Wiley, 1964).
100. V. A. Naumov and D. S. Shkirmanov, "Covariant asymmetric wave packet for a field-theoretical description of neutrino oscillations," Mod. Phys. Lett. A **30**, 1550110 (2015).
101. S. E. Korenblit and D. V. Taychenachev, "Interpolating wave packets in QFT and neutrino oscillation problem," arXiv:1712.06641 [hep-th] (2017).
102. I. Bialynicki-Birula and Z. Bialynicka-Birula, "Twisted localized solutions of the Dirac equation: Hopfion-like states of relativistic electrons," Phys. Rev. A **100**, 012108 (2019).
103. *NIST Handbook of Mathematical Functions*, Ed. by F. W. J. Olver, D. W. Lozier, R. F. Boisvert, and Ch. W. Clark (National Inst. of Standards and Technology & Cambridge Univ. Press, 2010).
104. M. F. Fedoryuk, *Saddle-Point Method* (Nauka, Moscow, 1977).
105. A. P. Prudnikov, Yu. A. Brychkov, and O. I. Marichev, *Integrals and Series* (Nauka, Moscow, 1981), Vol. 1.
106. M. Tanabashi et al., "Review of particle physics," Phys. Rev. D **98**, 030001 (2018).
107. V. A. Naumov, "Atmospheric muons and neutrinos," arXiv:hep-ph/0201310 (2002).
108. P.-O. Lagage, "Accélération et propagation des rayons cosmiques. Production, oscillations et détection de neutrinos," PhD Thesis (Univ. of Paris VI–VII, Paris, 1987).
109. M. Lindroos and M. Mezzetto, *Beta Beams: Neutrino Beams* (Imperial College Press, London, 2010).
110. M. Goodman, "Planned reactor and beam experiments on neutrino oscillations," Nucl. Phys. A **827**, 518c–523c (2009).
111. *Proceedings of the 11th International Workshop on Neutrino Factories, Superbeams and Beta Beams, Chicago, IL, July 20–25, 2009*, Ed. by M. C. Goodman, D. M. Kaplan, and Z. Sullivan, AIP Conf. Proc. 1222 (2010).
112. J. Sato, "Monoenergetic neutrino beam for long baseline experiments," Phys. Rev. Lett. **95**, 131804 (2005).
113. M. Yoshimura and N. Sasao, "Neutrino pair and gamma beams from circulating excited ions," Phys. Rev. D **92**, 073015 (2015).
114. M. Yoshimura and N. Sasao, "Photon and neutrino-pair emission from circulating quantum ions," Phys. Rev. D **93**, 113018 (2016).
115. K. Bradler, "Relativistically invariant photonic wave packets," J. Opt. Soc. Am. B **28**, 113018 (2011).
116. B. J. Smith and M. G. Raymer, "Photon wave functions, wave-packet quantization of light, and coherence theory," New J. Phys. **9**, 414 (2007).
117. M. E. Peskin and D. V. Schroeder, *An Introduction To Quantum Field Theory* (Addison-Wesley, 1995).

118. A. E. Blinov et al., "Large impact parameters cutoff in bremsstrahlung at colliding beams," Phys. Lett. B **113**, 423 (1982).

119. Yu. A. Tikhonov, Candidate's Dissertation in Mathematics and Physics (Inst. Nucl. Phys., Novosibirsk, 1982).

120. G. L. Kotkin, V. G. Serbo, and A. Schiller, "Processes with large impact parameters at colliding beams," Int. J. Mod. Phys. A **7**, 4707–4745 (1992).

121. W. B. Case, "Wigner functions and Weyl transforms for pedestrians," Am. J. Phys. **76**, 937–946 (2008).

122. D. V. Karlovets, "Probing phase of a scattering amplitude beyond the plane-wave approximation," Europhys. Lett. **116**, 31001 (2016).

123. V. A. Naumov and D. S. Shkirmanov, "Extended Grimus–Stockinger theorem and inverse-square law violation in quantum field theory," Eur. Phys. J. C **73**, 2627 (2013).

124. S. E. Korenblit and D. V. Taychenachev, "Higher order corrections to the Grimus–Stockinger formula," Phys. Part. Nucl. Lett. **10**, 610–614 (2013).

125. S. E. Korenblit and D. V. Taychenachev, "Extension of Grimus–Stockinger formula from operator expansion of free Green function," Mod. Phys. Lett. A **30**, 1550074 (2015).

126. D. V. Naumov, V. A. Naumov, and D. S. Shkirmanov, "Inverse-square law violation and reactor antineutrino anomaly," Phys. Part. Nucl. **48**, 12–20 (2017).

127. D. V. Naumov, V. A. Naumov, and D. S. Shkirmanov, "Quantum field theoretical description of neutrino oscillations and reactor antineutrino anomaly," Phys. Part. Nucl. **48**, 1007–1010 (2017).

128. S. E. Korenblit and A. V. Sinitskaya, "The role of short distance power corrections to differential and total cross-section and the optical theorem for potential scattering," Mod. Phys. Lett. A **32**, 1750066 (2017).

129. M. Faizal, S. E. Korenblit, A. V. Sinitskaya, and S. Upadhyay, "Corrections to scattering processes due to minimal measurable length," Phys. Lett. B **794**, 1–6 (2019).

130. M. Nowakowski and A. Pilaftsis, "On gauge invariance of Breit–Wigner propagators," Z. Phys. C **60**, 121–126 (1993).

131. G. Lopez Castro, J. L. Lucio, and J. Pestieau, "Remarks on the W propagator at the resonance," Int. J. Mod. Phys. A **11**, 563–570 (1996).

132. N. Aghanim et al., "Planck 2018 results. VI. Cosmological parameters," arXiv:1807.06209 [astro-ph.CO] (2018).

133. N. N. Bogolyubov and D. V. Shirkov, *Introduction to Quantum Field Theory* (Nauka, Moscow, 1984).

134. E. Kh. Akhmedov, "Do charged leptons oscillate?" J. High Energy Phys. **2007** (09), 116 (2007).

135. F. P. An et al., "Neutrino physics with JUNO," J. Phys. G **43**, 030401 (2016).

136. I. P. Ivanov, D. Seipt, A. Surzhykov, and S. Fritzsche, "Elastic scattering of vortex electrons provides direct access to the Coulomb phase," Phys. Rev. D **94**, 076001 (2016).

137. I. P. Ivanov and V. G. Serbo, "Scattering of twisted particles: Extension to wave packets and orbital helicity," Phys. Rev. A **84**, 033804 (2011).

138. P. Ramond, *Field Theory: A Modern Primer*, 2nd ed. (Addison-Wesley, Redwood City, 2007).

139. R. Bellman, *Introduction to Matrix Analysis* (McGraw-Hill, New York, 1960).

140. S. M. Bilenky, *Introduction to the Feynman Diagram Technique* (Atomizdat, Moscow, 1971).

141. G. A. Korn and T. M. Korn, *Mathematical Handbook for Scientists and Engineers* (McGraw-Hill, 1968).

142. J. N. Bahcall, A. M. Serenelli, and S. Basu, "10,000 standard solar models: A Monte Carlo simulation," Astrophys. J. Suppl. Ser. **165**, 400–431 (2006).

143. V. Antonelli, L. Miramonti, C. Pena Garay, and A. Serenelli, "Solar neutrinos," Adv. High Energy Phys. **2013**, 351926 (2013).

144. L. Wolfenstein, "Neutrino oscillations in matter," Phys. Rev. D **17**, 2369–2374 (1978).

145. S. P. Mikheev and A. Yu. Smirnov, "Resonance amplification of oscillations in matter and spectroscopy of solar neutrinos," Sov. J. Nucl. Phys. **42**, 913–917 (1985).

146. *Handbook of Mathematical Functions with Formulas, Graphs and Mathematical Tables*, 10th ed., Ed. by M. Abramowitz and I. A. Stegun (Dover, National Bureau of Standards, Washington, 1972).

147. J. Kestin and L. N. Persen, "On the error function of a complex argument," Z. Angew. Math. Phys. **7**, 33–40 (1956).

148. T. A. Zaker, "Calculation of the complementary error function of complex argument," J. Comput. Phys. **4**, 427–430 (1969).

149. M. Mori, "A method for evaluation of the error function of real and complex variable with high relative accuracy," Publ. Res. Inst. Math. Sci., Kyoto Univ. **19**, 1081 (1983).

150. H. O. Di Rocco and M. Aguirre Téllez, "Evaluation of the asymmetric Voigt profile and complex error functions in terms of the Kummer functions," Acta Phys. Pol., A **106**, 817–826 (2004).

Translated by D. Safin